AD NUMBER

AD905026

NEW LIMITATION CHANGE

TO

Approved for public release, distribution unlimited

FROM

Distribution authorized to U.S. Gov't. agencies only; Test and Evaluation; 22 NOV 1972. Other requests shall be referred to Office of Naval Research, 875 North Randolph ST, Arlington, VA 22203.

AUTHORITY

ONR ltr, 8 Oct 1975

UILU-ENG-72-2551

AUTOMATIC TRIPLE INTERFEROMETER DIRECTION OF ARRIVAL CALCULATION TECHNIQUES

by

Keith Eugene Hoover
Edward W. Ernst

RRL Publication No. 414

September 1972

Technical Report No. 36

Contract: N00014-67-A-0305-0002

Supported by:

Office of Naval Research

and the

Naval Electronics Systems Command

Albert D. Bailey
Principal Investigator
Radiolocation Research Laboratory
Department of Electrical Engineering
Engineering Experiment Station
University of Illinois
Urbana, Illinois

ABSTRACT

The work reported here presents the principles of operation of a non-display-oriented triple interferometer RDF system. Particular attention was paid to the ambiguity resolving portion of the system. It was found that phase ambiguity resolution (ambiguity resolution using the differential phase information from a smaller aperture interferometer system) has distinct advantages over direction ambiguity resolution (ambiguity resolution on the basis of knowledge of the approximate direction of arrival). The use of only the approximate azimuthal angle of arrival in the direction ambiguity resolving process appears to be insufficient. Furthermore it was found that the use of averaged values of the small interferometer differential phases appears to be more reliable than the use of instantaneous values of these phases. Finally, a new method of processing erroneous (ideally "redundant") interferometer differential phase data was presented. It was found to be roughly equivalent, and yet much faster, than the old "angle averaging" method.

ACKNOWLEDGMENT

Special thanks must go to Dr. Edward W. Ernst for his ideas and advice which shaped the direction and scope of this research. Several others gave much help which is greatly appreciated: Dr. Eric K. Walton, for his encouragement and contributions to this thesis; Bill Little, for the self-scaling polar plotting routines; and Jim Driscoll, for the analytical work found in Appendix K. This thesis was typed by Helen Thornburgh. The figures were drawn by Richard Calliger. The support of the United States Army Electronics Command, Fort Monmouth, New Jersey, under contract number DAAB07-72-C-0146 and the Office of Naval Research, Washington, D.C., under contract number N00014-67-A-0305-0002 is gratefully acknowledged.

TABLE OF CONTENTS

LIST OF TABLES

Page

LIST OF FIGURES

I. INTRODUCTION

The concept of the radio interferometer direction finding system has been known for over 20 years. It was first used successfully by radio astronomers to determine the direction of arrival of steeply downcoming celestial radio waves at a fixed high frequency. However, problems were encountered when this technique was applied to a general high frequency wide-band radio direction finding system.[1] Because it could no longer be assumed that the radio waves were steeply downcoming, it was found that the interferometer system could not determine a unique direction of arrival. It indicated several directions, only one of which was the approximate, actual direction of arrival The others were called "ambiguities." Moreover, it was found that the more "accurate" an interferometer system was made, the more ambiguities it would yield Recently a fairly dependable method of eliminating these ambiguous answers (or "resolving the ambiguities") was developed,[2] and much work has been done in developing a general computer-radio-interferometer RDF system.[3] However, work still needs to be done in improving the accuracy, speed, and ambiguity resolving capability of the system. It is the goal of the work that follows to present a unified overview of the state of the art of the triple radio interferometer, as well as to investigate other possible methods of ambiguity resolution, and enhancement of system speed and accuracy.

A common type of radio-interferometer antenna array consists of three isotropic antennas positioned on the vertices of an isosceles triangle which lies on the earth's surface as in figure 1. For convenience it will be assumed that one of the equal legs of the triangle lies along

3 Dimensional View =

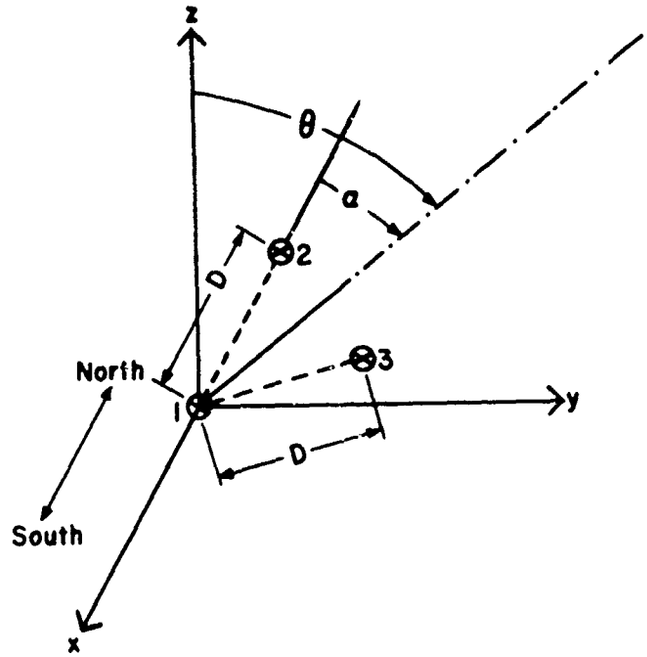

Overhead View =

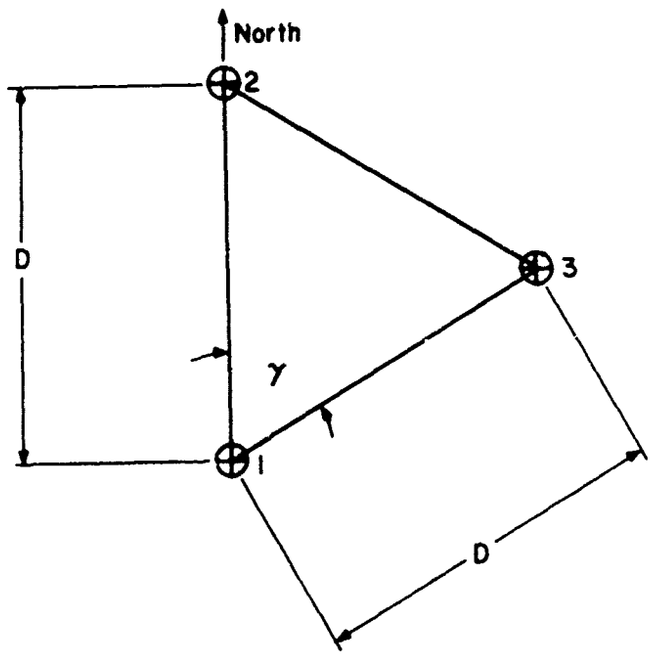

Figure 1. Isosceles Triple Interferometer Array Geometry

a north-south line, and the antennas are numbered as in the figure. Because the interferometer principle assumes the case of locally plane radio waves, the direction of arrival may be thought of as a single vector pointing along the direction of propagation. The orientation of this vector is often specified by 2 angles, the azimuth or bearing, and the vertical angle of incidence. The azimuth, denoted here by "α," is the angle that the projection of this vector upon the surface of the earth makes with a north - south line. Like a compass bearing, it is measured from the north in the clock wise direction, as in figure 1. Notice that α may take on values from 0 to 360 degrees. The vertical incidence angle, denoted by "θ," is the angle that this direction of arrival vector makes with a line normal to the earth's surface. Notice that θ may take on values from 0 to 90 degrees. From simple geometrical considerations, it may be shown[4] that Φ_{ij}, the phase of the voltage induced in the i^{th} antenna measured with respect to the phase of the voltage induced in the j^{th} antenna caused by an incident plane radio wave of wavelength λ propagating in the direction specified by (α,θ), is given by:

$$\Phi_{21} = \frac{2\pi D}{\lambda} \cos \alpha \sin \theta$$

$$\Phi_{13} = \frac{-2\pi D}{\lambda} \cos (\alpha-\gamma) \sin \theta \qquad \text{(I-1)}$$

$$\Phi_{32} = \frac{2\pi D}{\lambda} [\cos (\alpha-\gamma) - \cos \alpha] \sin \theta$$

Here D is the length of the equal sides of the isosceles triangle (called the array baseline), and γ is the angle that the two equal sides make with each other. (See figure 1.) The above expressions may be solved (two at a time) for α and θ, resulting in:[5]

$$(a)\qquad \alpha_{21-13} = \tan^{-1}\left[\frac{-\phi_{13} - \phi_{21}\cos\gamma}{\phi_{21}\sin\gamma}\right]$$

$$\theta_{21-13} = \sin^{-1}\frac{\sqrt{\phi_{21}^2 + \phi_{13} + \phi_{21}\,\phi_{13}}}{\frac{2\pi D}{\lambda}\left\{\begin{matrix}\cos^2(\alpha_{21-13}) + \cos^2(\alpha_{21-13} - \gamma) \\ -\cos(\alpha_{21-13})\cos(\alpha_{21-13} - \gamma)\end{matrix}\right\}}$$

$$(b)\qquad \alpha_{21-32} = \tan^{-1}\frac{-\phi_{31} + \phi_{32}\cos\gamma + \phi_{31}\cos\gamma}{-\phi_{31}\sin\gamma - \phi_{32}\sin\gamma} \qquad (I\text{-}2)$$

$$\theta_{21-32} = \sin^{-1}\frac{\sqrt{\phi_{21}^2 + \phi_{32}^2 + \phi_{21}\,\phi_{32}}}{\frac{2\pi D}{\lambda}\left\{\begin{matrix}\cos^2(\alpha_{21-32}) + \cos^2(\alpha_{21-32} - \gamma) \\ -\cos(\alpha_{21-32})\cos(\alpha_{21-32} - \gamma)\end{matrix}\right\}}$$

$$(c)\qquad \alpha_{32-13} = \tan^{-1}\frac{\phi_{32} + \phi_{21} - \phi_{21}\cos\gamma}{\phi_{21}\sin\gamma}$$

$$\theta_{32-13} = \sin^{-1}\frac{\sqrt{\phi_{32}^2 + \phi_{13}^2 + \phi_{32}\,\phi_{13}}}{\frac{2\pi D}{\lambda}\left\{\begin{matrix}\cos^2(\alpha_{32-13}) + \cos^2(\alpha_{32-13} - \gamma) \\ -\cos(\alpha_{21-32})\cos(\alpha_{21-32} - \gamma)\end{matrix}\right\}}.$$

Note that the expressions for α and θ are all mathematically equivalent if it is realized that $\phi_{21} + \phi_{13} + \phi_{32} = 0$. This is easily shown if ϕ_{ij} is written as $\phi_i - \phi_j$ where ϕ_i and ϕ_j are the phases of the voltages induced in the i^{th} and j^{th} interferometer antennas measured with respect to the induced voltage in some arbitrary reference antenna. Then we see:

$$\phi_{21} + \phi_{13} + \phi_{32} = (\phi_2 - \phi_1) + (\phi_1 - \phi_3) + (\phi_3 - \phi_2) = 0. \qquad (I\text{-}3)$$

The above equations I-2 become less burdensome if the special case for which $\gamma = 60$ degrees is considered. Now the isosceles array becomes symmetrical and the equations I-1 and I-2 reduce to:

$$\text{(a)} \quad \phi_{21} = \frac{2\pi D}{\lambda} \cos \alpha \sin \theta$$

$$\text{(b)} \quad \phi_{13} = \frac{2\pi D}{\lambda} \cos (\alpha - 240^\circ) \sin \theta$$

$$\text{(c)} \quad \phi_{32} = \frac{2\pi D}{\lambda} \cos (\alpha - 120^\circ) \sin \theta$$

$$\text{(d)} \quad \alpha_{21-13} = \tan^{-1} \frac{-2\phi_{13} - \phi_{21}}{\sqrt{3}\,\phi_{21}}$$

$$\text{(e)} \quad \alpha_{21-32} = \tan^{-1} \frac{2\phi_{32} + \phi_{21}}{\sqrt{3}\,\phi_{21}} \qquad \text{(I-4)}$$

$$\text{(f)} \quad \alpha_{32-13} = \tan^{-1} \frac{\phi_{32} - \phi_{13}}{-\sqrt{3}\,(\phi_{32} + \phi_{13})}$$

$$\text{(g)} \quad \theta_{21-13} = \sin^{-1} \frac{\sqrt{\phi_{21}^2 + \phi_{13}^2 + \phi_{21}\phi_{13}}}{\frac{2\pi D}{\lambda}\ \sqrt{3}/2}$$

$$\text{(h)} \quad \theta_{21-32} = \sin^{-1} \frac{\sqrt{\phi_{21}^2 + \phi_{32}^2 + \phi_{21}\phi_{32}}}{\frac{2\pi D}{\lambda}\ \sqrt{3}/2}$$

$$\text{(i)} \quad \theta_{32-13} = \sin^{-1} \frac{\sqrt{\phi_{32}^2 + \phi_{13}^2 + \phi_{32}\phi_{13}}}{\frac{2\pi D}{\lambda}\ \sqrt{3}/2}\ .$$

It is now evident how such an interferometer array might be used to determine the direction of arrival of a plane radio wave in a simple radio direction finding (RDF) system. (See figure 2.) It must

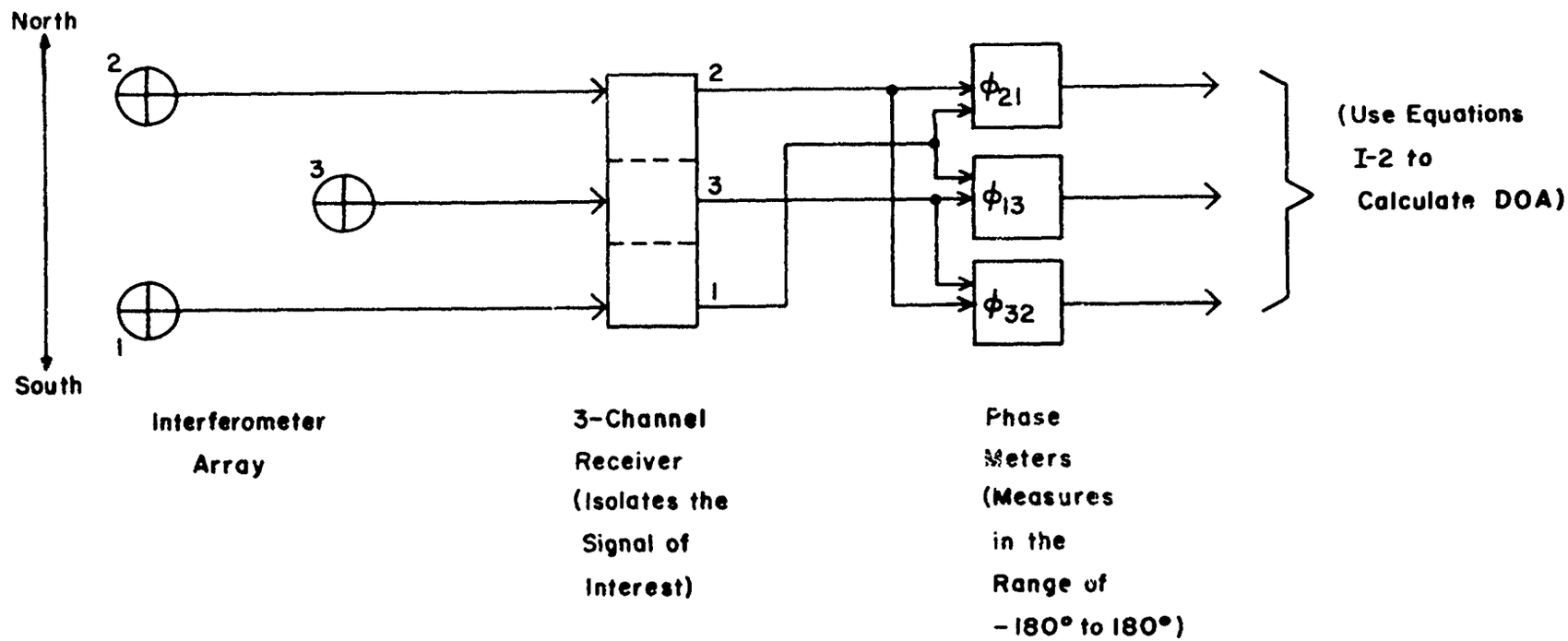

Figure 2. Simple RDF Interferometer System (No Ambiguity Resolution)

be kept in mind that the actual voltage induced in an interferometer array antenna is a superposition of many voltages induced in it by the myriads of radio waves (each of unique wavelength) which are incident upon the array. Hence a multi-channel receiver is tuned to isolate the voltages induced in the array by the particular signal of interest. (The receiver also performs the important function of heterodyning the signal voltage to a lower fixed intermediate frequency. This greatly facilitates phase measurements.) It is important that the antenna transmission lines and receiver channels be of the same effective electrical "length." This way the same phase relationships that existed between the voltages induced in the interferometer array by the radio wave still exist at the outputs of the receiver. These phase relationships are measured using electronic phase meters. From these phase meter readings, one can use equations I-2 (or I-4) to determine the direction of arrival of the signal.

The above process is foolproof providing the baseline of the interferometer array is not longer than one-half the wavelength of the radio wave. For shorter wavelengths the ubiquitous problem of phase measurement ambiguity arises. It is easy to see that one can measure the phase relationship (the "lag" or "lead" of one periodic voltage waveform with respect to another) between two sinusoidal voltages of a given frequency only to within an additive integral multiple of 360 degrees. That is, if there were no a priori restrictions on a phase measurement, who is to say that a measurement of 30 degrees does not actually represent a measurement of 390°, 750°, or -330°, etc? For this reason phase meters may be calibrated to read any electrical phase difference, $\phi_{ij}^{\text{actual}}$, with $(-\infty < \phi_{ij}^{\text{actual}} < \infty)$, such that the phase

meter reading, ϕ_{ij}^{meas}, is given by:

$$k(\text{degrees}) \leq \phi_{ij}^{meas} \leq k(\text{degrees}) + 360^{o}. \qquad \text{(I-5)}$$

The selection of k is often referred to as the selection of the "branch cut."[6,7] Electrical phase meters are commonly calibrated such that k = 0; however, for purposes of interferometry, it becomes much more convenient (as will be seen later) to select $k = -180^{o}$, such that (I-5) becomes:

$$-180^{o} \leq \phi_{ij}^{meas} \leq 180^{o}. \qquad \text{(I-5a)}$$

It must be kept in mind that:

$$\phi_{ij}^{actual} \in \{\phi_{ij}^{(N)AMB}\} = \{\phi_{ij}^{meas} + N(360^{o})\}; \qquad \text{(I-6)}$$

for $N = N_{min}, \ldots, -1, 0, 1, \ldots N_{max}$, where all elements of the above set, $\{\phi_{ij}^{(N)AMB}\}$, are called phase ambiguities. If there are no a priori restrictions on the range of ϕ_{ij}^{actual}, then $N_{min} = -\infty$ and $N_{max} = +\infty$. There are an infinite number of elements in $\{\phi_{ij}^{(N)AMB}\}$. But for the case of an interferometer system, we <u>do</u> have a restriction on the range of values that ϕ_{ij}^{actual} can take on. From equations I-1, it is evident that:

$$\frac{-360^{o}D}{\lambda} < \phi_{ij}^{actual} < \frac{360^{o}D}{\lambda}. \qquad \text{(I-7)}$$

For a given D and λ; N_{max} and N_{min} are fixed such that:

$$N_{min} = -\text{ INTEGER } (D/\lambda)$$
$$N_{max} = \text{INTEGER } (D/\lambda). \qquad \text{(I-8)}$$

(Where the INTEGER function simply rounds off its argument to the nearest integer.) The above holds only if we assume the phase meter reads in the range specified by equation I-5a. It should be noted that when $D < \frac{1}{2}\lambda$, equation I-8 implies that:

$$N_{min} = N_{max} = 0,$$

and there is only one element in $\{\phi^{(N)AMB}\}$. This means that

$$\phi_{ij}^{(N)AMB} = \phi_{ij}^{meas} = \phi_{ij}^{actual}.$$

The phase measurement becomes non-ambiguous, and hence there is no ambiguity problem to contend with (as mentioned previously). When $D > \frac{1}{2}\lambda$, there is more than one element in $\{\phi^{(N)AMB}\}$. Because there is no way of telling which value of N satisfies:

$$\phi_{ij}^{(N)AMB} = \phi_{ij}^{actual}, \qquad \text{(I-9)}$$

we may compute <u>all possible</u> directions of arrival using various combinations of elements in $\{\phi_{ij}^{(N)AMB}\}$. Thus the ambiguities in phase measurements have been "carried through" the direction of arrival calculation to yield ambiguities in direction of arrival as well. In essence, this simple interferometer system will generally give a number of answers to the direction finding problem -- only one of which is correct. Note that equations I-6 and I-8 indicate that the larger D becomes, the more elements (phase ambiguities) exist in $\{\phi_{ij}^{(N)AMB}\}$. Here the greater number of ambiguous directions will be indicated by the system.

One solution to the problem is obvious. All that need be done is to keep the array baseline shorter than one-half of the wavelength of the desired signal. Under these conditions there are no ambiguities, as

shown previously. However, it will be shown in Chapter VI that under real conditions interferometer accuracy varies with D/λ. Hence it is desirable to use as large a baseline as possible, certainly greater than $\frac{1}{2}\lambda$. Thus one must contend with the problem of deciding which of the ambiguous directions of arrival indicated by the interferometer is the actual one.

FOOTNOTES

1. A. D. Bailey and W. C. McClurg, "A Sum- and-Difference Interferometer System for HF Radio Direction Finding," IEEE Transactions on Aerospace and Navigational Electronics, March 1963, pp. 65-72.

2. J. B. Church, "A Digital Bearing Computer for an Interferometer RDF System," Master's Thesis, University of Illinois, Urbana, Illinois, January 1967, Chapter 2.

3. K. D. Stenzel, "An Interferometer RDF System with an On-Line Computer," Master's Thesis, University of Illinois, Urbana, Illinois, September 1971.

4. J. Creasy, "Digital Techniques for Radio Direction Finding with Interferometer Arrays," Master's Thesis, University of Illinois, Urbana, Illinois, June 1966, p. 3. (RRL Publication No. 309.)

5. Ibid., p. 5.

6. H. L. Grush, "An Investigation of a Digital Bearing Computer for a Small Aperture Radio Direction Finding System," Ph.D. Thesis, University of Illinois, Urbana, Illinois, June 1965, p. 16. (RRL Publication No. 280.)

7. L. C. Allen, "Improved Digital Bearing Computer Techniques," Master's Thesis, University of Illinois, Urbana, Illinois, June 1966, p. 4. (RRL Publication No. 314.)

II. PHASE AMBIGUITY RESOLUTION

There are at least two different strategies that one may use in attacking the ambiguity resolution problem. On the basis of some approximate outside phase information, one may choose from all possible values of an ambiguous phase measurement, $\{\phi_{ij}^{(N)AMB}\}$, the measurement most likely to be the actual one, ϕ_{ij}^{actual}. Then the true direction of arrival may be unambiguously calculated. Alternatively, one may calculate all of the possible ambiguous directions of arrival from all of the possible phase ambiguities, then the most likely true direction of arrival may be chosen on the basis of some outside approximate directional information. The former stratagem (called phase ambiguity resolution) keeps the weeds ($\{\phi_{ij}^{(N)AMB}\}$) around the flower (ϕ_{ij}^{actual}) from germinating; the latter (called direction ambiguity resolution) lets the weeds grow, then pulls them. Note that the former method requires only one direction-of-arrival calculation. As the latter method requires many direction-of-arrival calculations (equation I-2), it is inherently more time consuming. Thus the former method has become more popular and will be discussed first.

Notice that after the approximate interferometer phases (ϕ_{ij}^{approx}) are known, it is a simple matter to choose ϕ_{ij}^{actual} from $\{\phi_{ij}^{(N)AMB}\}$. Because the values of $\phi_{ij}^{(N)AMB}$ are spaced 360° apart, ϕ_{ij}^{approx} need only be accurate to within $\pm 180^{\circ}$. Obviously, if ϕ_{ij}^{approx} is off by more than 180°, the wrong choice of ϕ_{ij}^{actual} from $\{\phi_{ij}^{(N)AMB}\}$ may be made, and the method breaks down.

ϕ_{ij}^{approx} may be determined from a separate small baseline interferometer array. As mentioned previously, if the small array baseline

is less than $\lambda/2$, it will yield a unique, but only approximate, direction of arrival. Furthermore, the small and large arrays have been constructed such that they form triangles which are similar, with their corresponding sides parallel, as in figure 3. Assuming an incident plane wave, it can be seen that:[1]

$$\frac{D_L}{D_S} \phi_{ij}^{\text{small}} = \varphi_{ij}^{\text{actual}}, \qquad \text{(II-1)}$$

where D_L and D_S are the large and small array baselines, respectively In practice equation II-1 is only an approximation. Hence we let $\phi_{ij}^{\text{approx}} = \frac{D_L}{D_S} \phi_{ij}^{\text{small}}$. This is consistent with the previous statement that the large array will be more accurate than the small one. There are two reasons for this. One is that the incident wave may not be perfectly plane (this will be discussed in Chapter VI); the other is the inaccuracy in the phase measurement process. Assume that a "real world" phase meter can measure to only within $\pm$ e degrees. Then, even for a perfectly plane incident wave, the two sides of equation II-1 may differ by as much as e $(\frac{D_L}{D_S} + 1)$ degrees. Nevertheless, equation II-1 is often a fair approximation. As long as the effects of non-planar incident waves and phase measurement inaccuracies do not cause the right- and left-hand sides of equation II-1 to differ by more than 180°, the proper value of $\theta_{ij}^{\text{actual}}$ will be determined.

The ambiguity resolution scheme as outlined above may be put into use in the simple RDF system of figure 2. For economy, the small and large baseline arrays share a common antenna. (See figure 4.) Note that the steps the operator must take to calculate the direction of arrival (DOA) may easily be performed by a properly interfaced general-purpose on-line digital minicomputer. This greatly enhances system

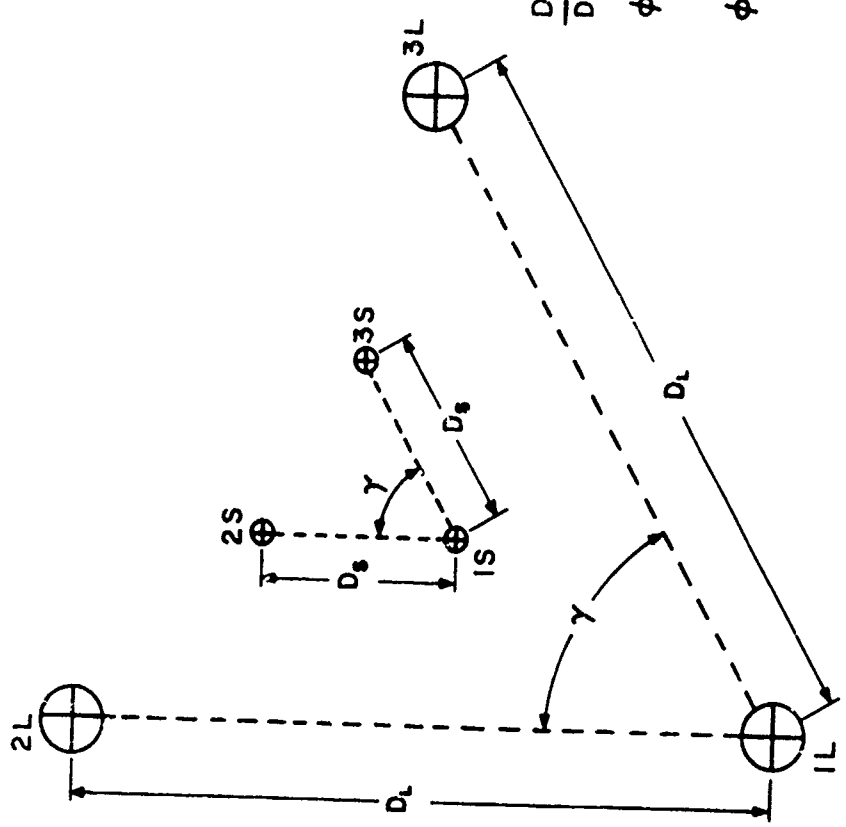

Figure 3. Large/Small Baseline Interferometer Ambiguity Resolution Array (Top View)

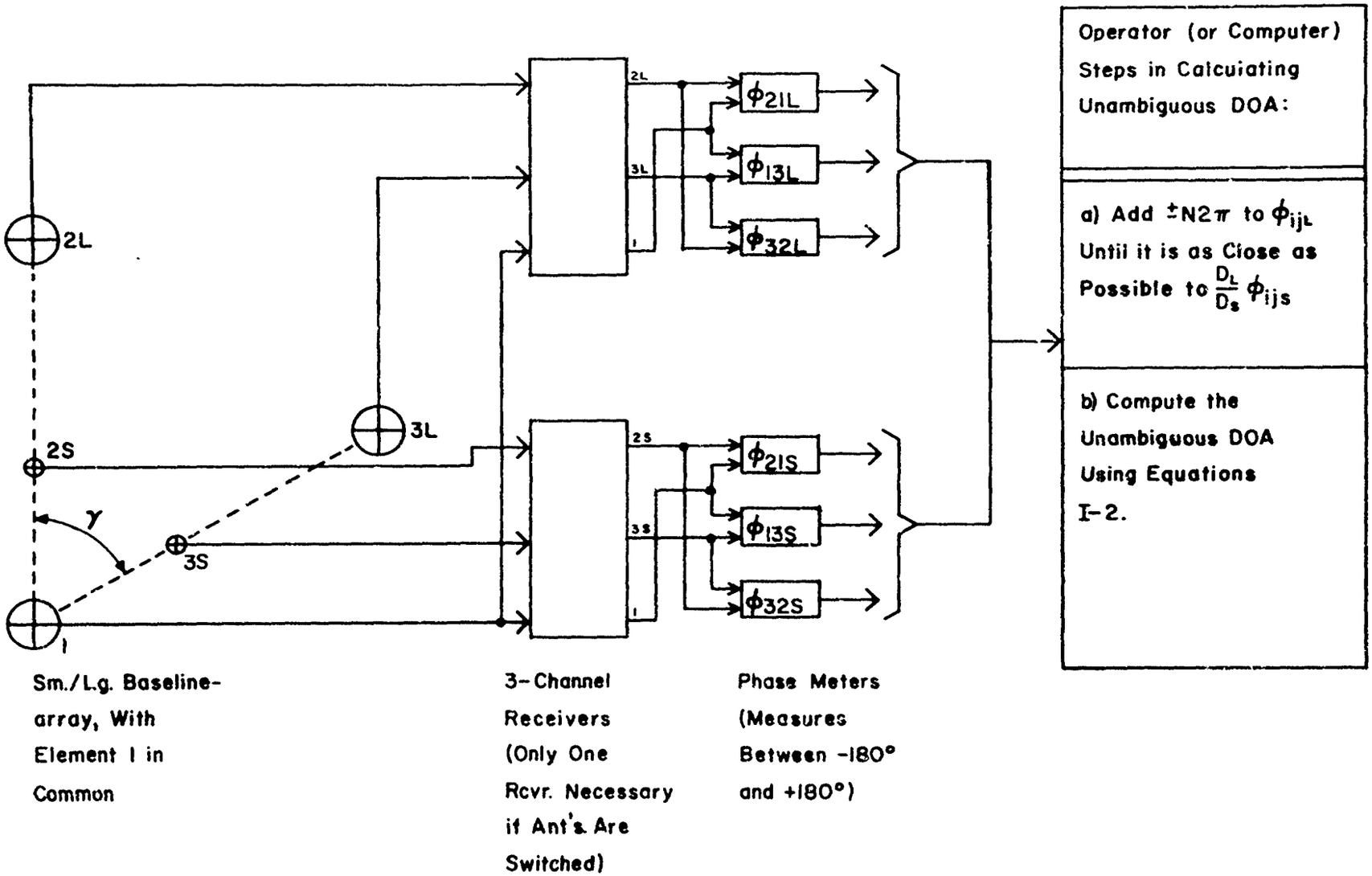

Figure 4. Ambiguity Resolving Interferometer System (Large/Small Baseline System)

data processing speed and flexibility. The implementation of such a system is currently underway at the University of Illinois' Monticello Road Field Station.[2]

FOOTNOTES

1. J. Creasy, "Digital Techniques for Radio Direction Finding with Interferometer Arrays," Master's Thesis, University of Illinois, Urbana, Illinois, June 1966, p. 42.

2. K. D. Stenzel, "An Interferometer RDF System with an On-Line Computer," Master's Thesis, University of Illinois, Urbana, Illinois, September 1971.

III. DIRECTION AMBIGUITY RESOLUTION

With the advent of a computer-interferometer RDF system, it is helpful to reconsider the use of the second ambiguity resolving stratagem: the elimination of all but one of the ambiguous DOA's on the basis of some outside directional information. Its drawback was that many DOA calculations had to be made before a unique DOA could be chosen. This is not such a serious problem if the high-speed computational capability of an on-line computer is available.

One advantage of such an approach is immediately evident. Often outside direction information may more easily be obtained than outside phase information. For example, the approximate location of the source of the signal, and hence its approximate direction of arrival may be known. In radio-astronomy or satellite tracking, both the azimuth and angle of incidence are known to lie in a certain range. In land communication, usually more information about propagation conditions must be obtained before an accurate prediction of incidence angle range can be made. However, the approximate source location information should restrict the azimuth range.

Other sources of outside directional information include similar interferometer RDF systems and small aperture azimuth-finding systems such as the Adcock, crossed-loop, or Yagi arrays. By now, it is clear that, depending on the source of information, this directional information may be of two types. It may consist of an approximate range of azimuthal angles (azimuthal sector of arrival) and an approximate range of vertical incidence angles, or it may consist solely of an azimuthal sector of arrival. Several questions arise. How accurate must this

approximate directional information be if all ambiguous directions are to be eliminated? Also, is a knowledge of the azimuthal sector of arrival alone sufficient to resolve all ambiguities? And finally, what is the relationship between the array baseline and the highest frequency at which all ambiguities can be resolved using the approximate directional information? To answer these questions, one must look further into the nature of interferometer direction ambiguities.

IV. INTERFEROMETER DIRECTION AMBIGUITIES

Given the three phase meter readings, ϕ_{21}^{meas}, ϕ_{13}^{meas}, ϕ_{32}^{meas}; the wavelength of the signal, λ, and information regarding the array geometry (D and γ), all possible ambiguous DOA's may be calculated using equations I-2, I-6, and I-8. The case of the symmetrical array ($\gamma = 60^{o}$) is of particular interest, because this is the array currently in operation at the University of Illinois' Monticello Road Field Station. For this reason, it has been assumed that $\gamma = 60^{o}$. Equations I-4 may be used in place of the more laborious equations I-2. Assuming errorless phase meters, it has been shown that equations I-4d,e,f and I-4g,h,i are equivalent. Note that under these conditions $\phi_{13}^{actual} = -(\phi_{21}^{actual} + \phi_{32}^{actual})$. This implies that after two phases are known, the remaining phase is necessarily determined. Using this fact, equations I-4d,e,f and I-4g,h,i are identical expressions. Hence, in the work that follows, only equations I-4e and h will be used:

$$\alpha(\phi_{21}, \phi_{32}) = \tan^{-1} \frac{2\phi_{32} + \phi_{21}}{\sqrt{3}\ \phi_{21}}. \qquad \text{(IV-1)}$$

$$\theta(\phi_{21}, \phi_{32}) = \sin^{-1} \frac{\sqrt{\phi_{21}^2 + \phi_{32}^2 + \phi_{21}\phi_{32}}}{\frac{2\pi D}{\lambda}\sqrt{3}/2}$$

Upon examining equations I-5 and I-8, it may appear that all one need do is "plug" all possible combinations of the elements of $\{\phi_{21}^{(N)AMB}\}$ and $\{\phi_{32}^{(N)AMB}\}$ into equations I-4e and h. $(1 + N_{max} - N_{min})^2$ ambiguous DOA's would be computed. But some of these ambiguous values could never occur, such as $\alpha(\phi_{21}^{(N_{max})AMB}, \phi_{32}^{(N_{max})AMB})$, as illustrated geometrically by figure 5.

a) Case for Maximum ϕ_{21} Reading $\left(=\phi_{21}^{(N\,max)AMB}\right)$:

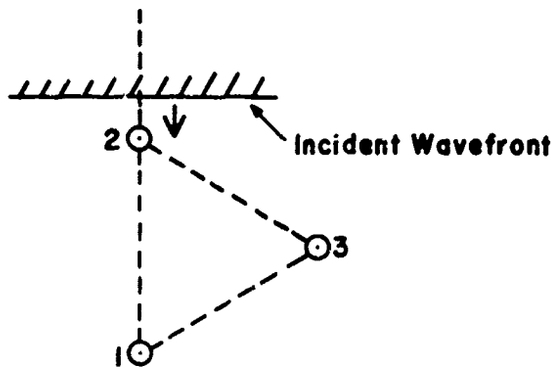

b) Case for Maximum ϕ_{32} Reading $\left(=\phi_{32}^{(N\,max)AMB}\right)$:

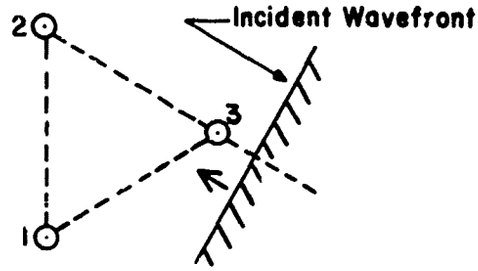

c) Case for the Largest Possible Simultaneous Values of $|\phi_{21}|$ and $|\phi_{32}|$ $\left(=\sqrt{3}/2\ \phi_{21}^{(N\,max)AMB},\ \sqrt{3}/2\ \phi_{32}^{(N\,max)AMB}\right)$:

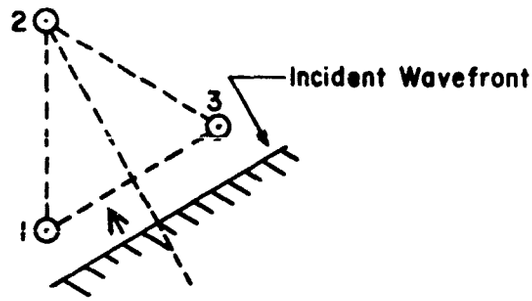

Figure 5. Illustration of Why the Individual Interferometer Phase Differences Can Never be Simultaneously at their Maximum Values.

The reason why some combinations of phase ambiguities $\phi_{21}^{(I)AMB}$ and $\phi_{32}^{(J)AMB}$ (for all integral values of I and J between N_{min} and N_{max}) are not valid interferometer phases becomes apparent when the expression for θ ($\phi_{21}^{(I)AMB}$, $\phi_{32}^{(J)AMB}$) is examined. For certain values of I and J (say, $I = I_0$, $J = J_0$) it is possible that the argument of $\sin^{-1}$ becomes > 1. Equation IV-1 implies that this will occur when:

$$\phi_{21}^2 + \phi_{32}^2 + \phi_{21}\phi_{32} > \frac{3\pi^2 D^2}{\lambda^2}. \qquad \text{(IV-2)}$$

In this case, a real value of θ does not exist. Then there exists no real direction from which a wave can arrive that will cause $\phi_{21}^{actual} = \phi_{21}^{(I_o)AMB}$ and $\phi_{32}^{actual} = \phi_{32}^{(J_o)AMB}$. Because the interferometer antenna voltages must, in fact, be caused by a wave arriving from a real direction, then it is obvious the ϕ_{21}^{actual} and ϕ_{32}^{actual} could never equal $\phi_{21}^{(I_o)AMB}$ and $\phi_{32}^{(J_o)AMB}$, respectively. Only the combination of phase ambiguities which do not satisfy equation IV-2 may be used to calculate all possible direction ambiguities. There will not be $(1 + N_{max} - N_{min})^2$ direction ambiguities, but only $(1 + N_{max} - N_{min})^2 - N_{reject}$ ambiguities, where N_{reject} is the number of phase ambiguity combinations rejected because they satisfied equation IV-2, thus yielding imaginary incidence angles.

A computer program was written that would calculate all possible direction ambiguities for a given true direction of arrival and a given value of D/λ. The flow diagram appears in figure 6. Sample runs appear in Appendix A. As expected, it appears that the number of ambiguities depends on the D/λ ratio. (See Tables A-1 through A-4.) However, the number of ambiguities also depends on the true direction of arrival, as

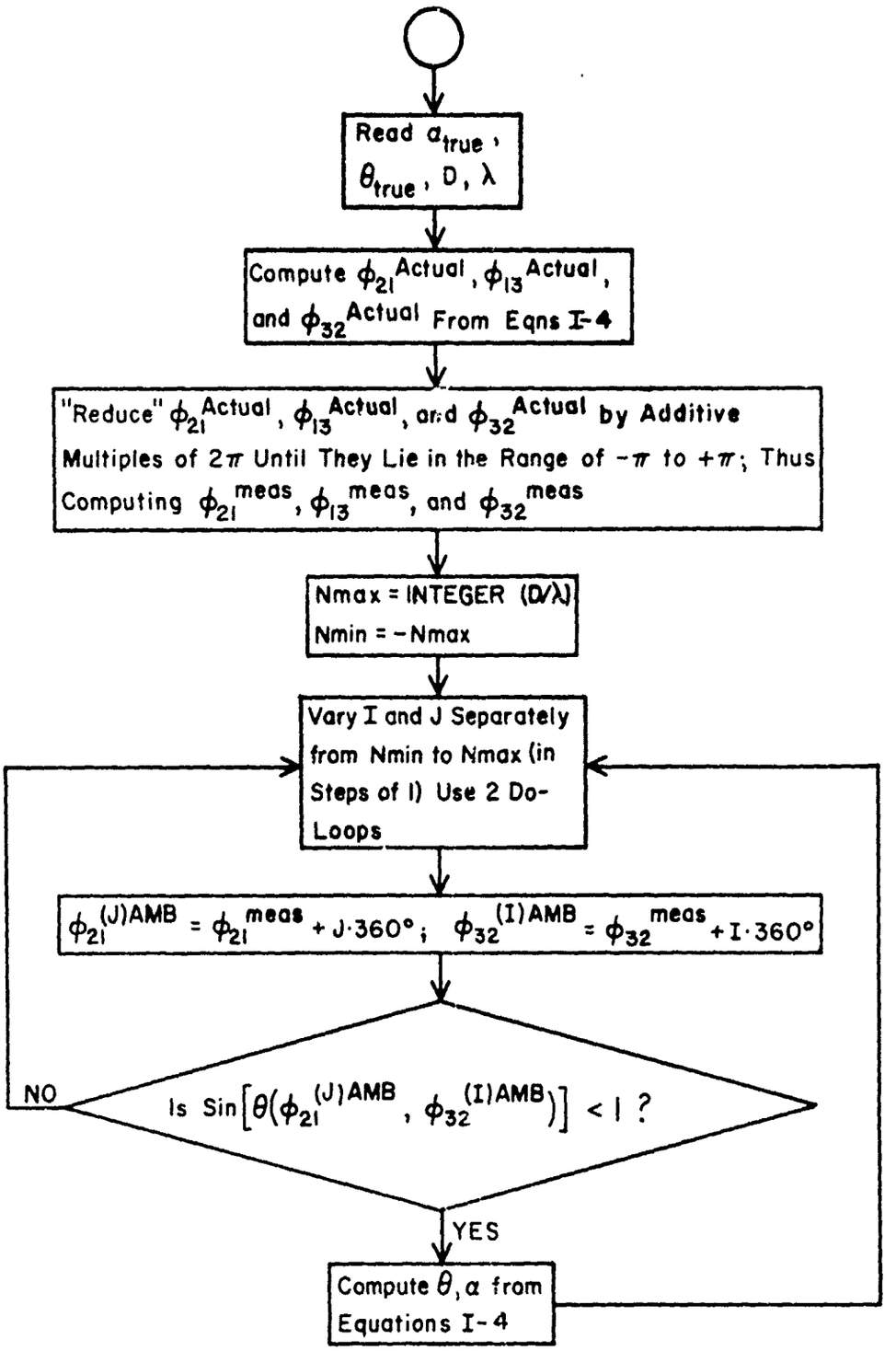

Figure 6. Flow Diagram of an Ambiguity Locating Program for a Symmetric Array

illustrated by Tables A-5 through A-8. These values were calculated with a fixed D/λ value, but with different true DOA's. The number of ambiguities varies slightly. Obviously N_{reject} must depend on the true DOA as well as the D/λ value.

For purposes of studying the feasibility of direction ambiguity resolution, it is useful to present this ambiguity location information graphically. Assume that the interferometer array has a large hemispherical "bowl" placed over it such that the center (reference origin) of the array and the center of the circle formed by the lip of the bowl coincide. (See figure 7.) The direction of arrival of a wave is then represented by the point on the hemispherical bowl where an incident plane wave first touches it. Alternatively, this point may be thought of as the intersection of the bowl and the ray of the incident plane wave that passes through the array center. Because there is a unique point on this hemisphere corresponding to any direction of arrival, a direction of arrival may be represented by a point on this hemisphere. All ambiguous directions of arrival may be plotted on one hemisphere in this manner. A man could stand at the center of such a hemisphere and point his finger at each plotted point on the hemisphere. He would then be pointing in all of the possible directions of arrival, or DOA's, indicated by the interferometer system. Since such a three-dimensional plot would be difficult to make, all points on the hemisphere are projected into the horizontal plane of the array. Still there exists a one-to-one correspondence between any direction of arrival and a corresponding point on this hemispherical projection, but now the plot is two dimensional and is easily drawn.

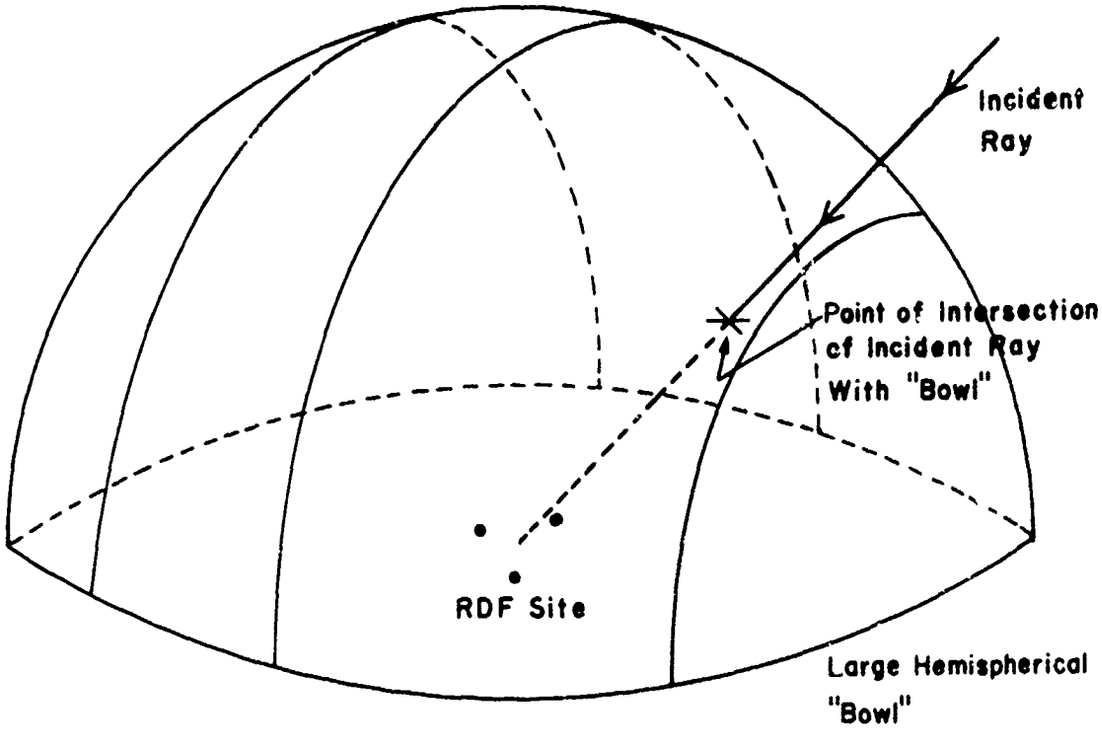

a) 3-Dimensional Hemispherical Plot of DOA

b) Top View of Hemispherical Plot (Hemispherical Projection)

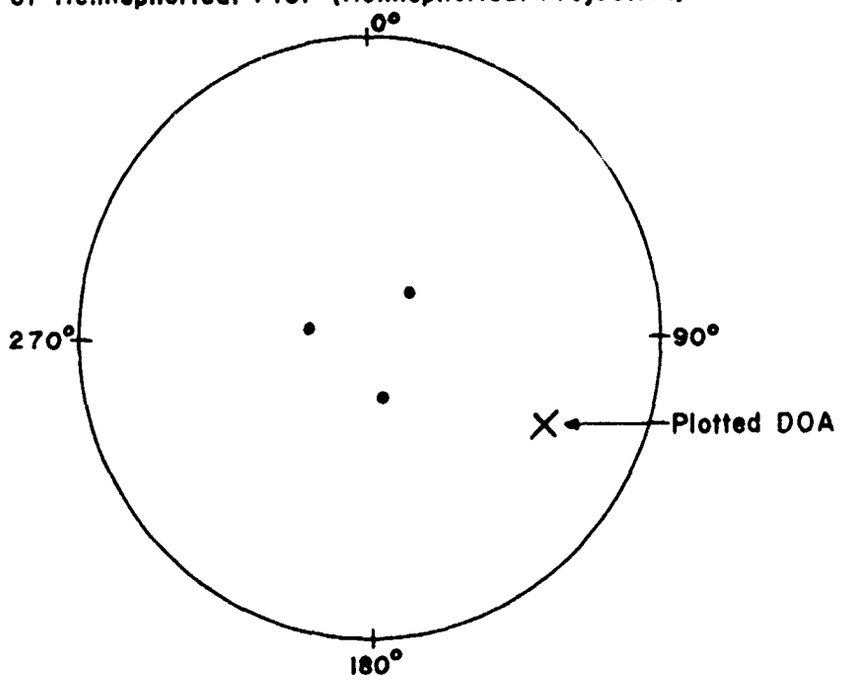

Figure 7. Hemispherical DOA Plot Geometry

These hemispherical projection plots may be thought of as what would be seen if one were to look down on the large hemispherical bowl from an airplane.

Such hemispherical projection plots for the ambiguity calculations of Appendix A are shown in Appendix B. Note the perimeter of the hemisphere projection is linearly calibrated in azimuthal degrees, as on a compass. The azimuth of any ambiguity may be determined by drawing a line out from the center of the projection (zenith) and through the ambiguity point. The incidence angle is sinusoidally calibrated as tick marks on the Cartesian north-south or east-west axes of the projection. The origin (zenith) represents 0° incidence, the next mark out from the origin represents 10°, etc. The distance that an ambiguity lies out from the zenith, measured according to this sinusoidal scale, determined its incidence angle.

In all ambiguity plots (for the symmetric interferometer array) there exists a high degree of symmetry. One ambiguity, called the prime ambiguity, is closest to the zenith. It represents the direction of arrival calculated from $\alpha(\phi_{21}^{meas}, \phi_{32}^{meas})$ and $\theta(\phi_{21}^{meas}, \phi_{32}^{meas})$. This makes sense geometrically, since if the wave is arriving from the direction indicated by the prime ambiguity, it must be the most "steeply downcoming" of all the possibilities. The more steeply downcoming the wave, the smaller will be the magnitudes of the phase differences of the voltage induced in the interferometer elements, as dictated by the sin θ factor in equations I-1. Hence the most steeply downcoming wave, as indicated by the prime ambiguity, must have been calculated from the combination of phase ambiguities of the smallest

magnitude, which is, of course, $(\phi_{21}^{meas}, \phi_{32}^{meas})$.

Centered on this prime ambiguity lie concentric hexagonal patterns of ambiguities. These hexagons have their sides parallel, and the outer hexagons may not be fully formed if the prime ambiguity is not very close to the zenith. (See Appendix B.) It should further be noted that the ambiguities lie in straight lines extending to the east and west, and that adjacent ambiguities are equidistant from each other.

The symmetry of these plots suggests that there exists a simple expression for the Cartesian coordinates (x,y) of the ambiguous directions of arrival as plotted on the hemispherical projection plot. A Cartesian coordinate system is constructed on the hemispherical projection such that the x axis bisects the projection and extends in an east-west direction. Likewise, the y axis bisects the projection, but extends in a north-south direction. A unit hemisphere is assumed in the following derivation, hence the Cartesian axes are scaled on the basis of a unit circle hemispherical projection. The Cartesian coordinates (x,y) for any point on the projection given by (α,θ) must be:

$$x = \sin\alpha \sin\theta \qquad y = \cos\alpha \sin\theta. \tag{IV-3}$$

Substituting equation I-4b into equation IV-3, yields:

$$x = \sin\left[\tan^{-1}\left(\frac{2\phi_{32} + \phi_{21}}{\sqrt{3}\,\phi_{21}}\right)\right] \sin\left[\sin^{-1}\frac{\sqrt{2\phi_{21}^2 + 2\phi_{32}^2 + 2\phi_{21}\phi_{32}}}{\frac{2\pi D}{x}\sqrt{3/2}}\right]$$

$$y = \cos\left[\tan^{-1}\left(\frac{2\phi_{32} + \phi_{21}}{\sqrt{3}\,\phi_{21}}\right)\right] \sin\left[\sin^{-1}\frac{\sqrt{2\phi_{21}^2 + 2\phi_{32}^2 + 2\phi_{21}\phi_{32}}}{\frac{2\pi D}{x}\sqrt{3/2}}\right]. \tag{IV-4}$$

After some manipulation, equations IV-4 become:

$$x = \frac{2\phi_{32} + \phi_{21}}{\frac{2\pi D}{\lambda}\sqrt{3}} \qquad y = \frac{\phi_{21}}{(\frac{2\pi D}{\lambda})} \quad . \tag{IV-5}$$

Equations IV-5 should enable one to sketch an ambiguity plot with little effort. Using these equations, the above symmetry observations may be substantiated. Notice that y depends only on ϕ_{21}. For combinations of phase ambiguities with $\phi_{21}^{(I)AMB}$ fixed, y is a constant and x varies. The direction ambiguities lie on a straight line parallel to the x axis. The spacing between the ambiguities that lie in the straight lines must be given by:

$$\text{Horiz spacing} = x\ (\phi_{21},\ \phi_{32} + 2\pi) - x\ (\phi_{21},\ \phi_{32}) = \frac{2}{\sqrt{3}} \cdot \frac{\lambda}{D}. \tag{IV-6}$$

Because ϕ_{21} and ϕ_{32} are arbitrary values of the phase ambiguities, the spacing between adjacent ambiguity points in the horizontal lines is uniform and equal to $\frac{2}{\sqrt{3}} \cdot \frac{\lambda}{D}$. Likewise, the vertical spacing between horizontal rows is given by:

$$\text{Vert spacing} = y\ (\phi_{21} + 2\pi) - y\ (\phi_{21}) = \lambda/D. \tag{IV-7}$$

Hence the row spacing is also uniform, since ϕ_{21} is any value in $\{\phi_{21}^{(N)AMB}\}$. Furthermore, it may be shown that the abscissae of the ambiguity points in one horizontal row must fall halfway between the abscissae of the points in adjacent rows. This may be shown by realizing that the difference in abscissae of 2 adjacent ambiguity points in adjacent horizontal rows is given by:

$$x(\phi_{21} + 2\pi,\ \phi_{32}) - x\ (\phi_{21},\ \phi_{32}) = \frac{1}{\sqrt{3}} \cdot \frac{\lambda}{D}. \qquad \text{(IV-8)}$$

But this abscissa difference is exactly one half that of the horizontal ambiguity spacing. Now the ambiguity locations are completely specified. To sketch such a plot, the only point that need actually be computed is the location of the prime ambiguity. This is found by substituting $\phi_{12} = \phi_{12}^{meas}$ and $\phi_{32} = \phi_{32}^{meas}$ into equation IV-5. The horizontal row and vertical distance spacings may be determined from equations IV-6 and IV-7. Adjacent rows must be positioned such that their ambiguity points precisely "interlace." The points that fall outside the circle must be rejected, as they correspond to values of $(\phi_{21}^{(I)AMB},\ \phi_{32}^{(J)AMB})$ which give rise to imaginary incidence angles ($\sin\theta > 1$).

The preceding discussion applies equally well to the general isosceles interferometer array. From equations I-2b, it is apparent that the incidence angle becomes imaginary when the argument of the arcsine function becomes greater than one. This will occur when:

$$\frac{\phi_{21}^2 + \phi_{13}^2 + \phi_{32}^2}{2\cos^2(\alpha) + 2\cos^2(\alpha-\gamma) - 2\cos\alpha\cos(\alpha-\gamma)} > \frac{2\pi D}{\lambda}. \qquad \text{(IV-9)}$$

The ambiguity locating program was rewritten using the general array equations and the new phase ambiguity rejection criterion IV-9. Various general interferometer ambiguity plots appear in Appendix C.

As before, a number of general statements may be made concerning these plots. The ambiguities tend to lie along uniformly spaced lines which are parallel to the x axis. No longer do adjacent points form equilateral triangles, instead they form congruent isosceles triangles. Furthermore, the angle formed by the intersection of the two sides of

equal length of these isosceles triangels is equal to γ, the interferometer array vertex angle. These triangles are in fact similar to the triangle formed by the interferometer antenna elements.

The symmetry of these plots once again suggests that there may exist a simple relationship between the ambiguity locations and the x-y coordinates of the unit hemispherical projection. Substituting equation I-2 into equation IV-2 (after some algebra) yields:

$$x = \frac{\lambda}{D} \left(\frac{\phi_{32} + \phi_{21} (1 - \cos \gamma)}{2\pi \sin \gamma} \right)$$

$$y = \frac{\lambda}{D} \frac{\phi_{21}}{2\pi} . \qquad \text{(IV-10)}$$

Equations IV-10 may be used to authenticate the generality of the preceding observations, as done previously for the case of the symmetric array. It can also be shown that, in general, equations IV-6 and IV-7 become:

$$\text{Horiz spacing} = \frac{\lambda}{D \sin \gamma} \qquad \text{(IV-11)}$$

$$\text{Vert spacing} = \frac{\lambda}{D} . \qquad \text{(IV-12)}$$

Likewise, it may also be shown that each successive row (going from south to north) is horizontally displaced by this amount:

$$\text{Horiz displacement} = \frac{\lambda}{D} \left(\frac{1 - \cos \gamma}{\sin \gamma} \right) . \qquad \text{(IV-13)}$$

It is interesting to note from Appendix C that the number of possible ambiguities appears to decrease as the array angle γ decreases. This result can also be obtained analytically from equation IV-13. Unfortunately, the effects of wave interference become more noticeable as γ decreases (explained in Chapter 7), thus making even a larger

baseline array relatively inaccurate for very small values of γ. In essence we have decreased the aperture of the array. Obviously, for a given array baseline, a compromise between the ambiguity resolution capability (optimum at $\gamma = 0^{o}$) and the system accuracy (optimum at $\gamma = 90^{o}$) must be made when one is choosing the value of γ for a general interferometer array.

V. LIMITATIONS OF A DIRECTION AMBIGUITY RESOLUTION SYSTEM

Now that the nature of the interferometer ambiguity problem is better understood, the limitations of a direction ambiguity resolving scheme become more apparent. A resolution scheme based on the foreknowledge of an azimuthal sector of arrival only will first be considered. The success of such a scheme can be predicted by examining the ambiguity tables of Appendix B (assuming a symmetric array). If the ambiguity plot is regarded as a pie, the known, approximate sector of arrival may be sketched in on the plot as a slice of pie; a typical case is shown in figure 8. It is obvious that the true direction of arrival will lie somewhere on this slice of the pie. Unfortunately, there are still several other answers to choose from. In this case, the ambiguities cannot be totally resolved on the basis of the available directional information. Note (from Appendix B) that this situation becomes more and more likely as D/λ is increased. Moreover, if the prime ambiguity is very close to the origin, the ambiguities will line up radially. Under this condition, even for relatively small ($D/\lambda < 2$), complete resolution of ambiguities becomes hopeless. (See figure 9.)

To get a better feel for the limitations of such an approximate azimuth resolution scheme, a fairly comprehensive study was made of the number of interferometer direction ambiguities that fall within approximate azimuthal sectors of arrival of various angular widths. This study was made using a modified version of the ambiguity locating program of figure 6. A listing of this program appears at the beginning of Appendix D. The approximate sector was assumed to be a range of azimuths centered about the specified "true" direction of arrival. The number of ambiguities that fell within this sector were then counted.

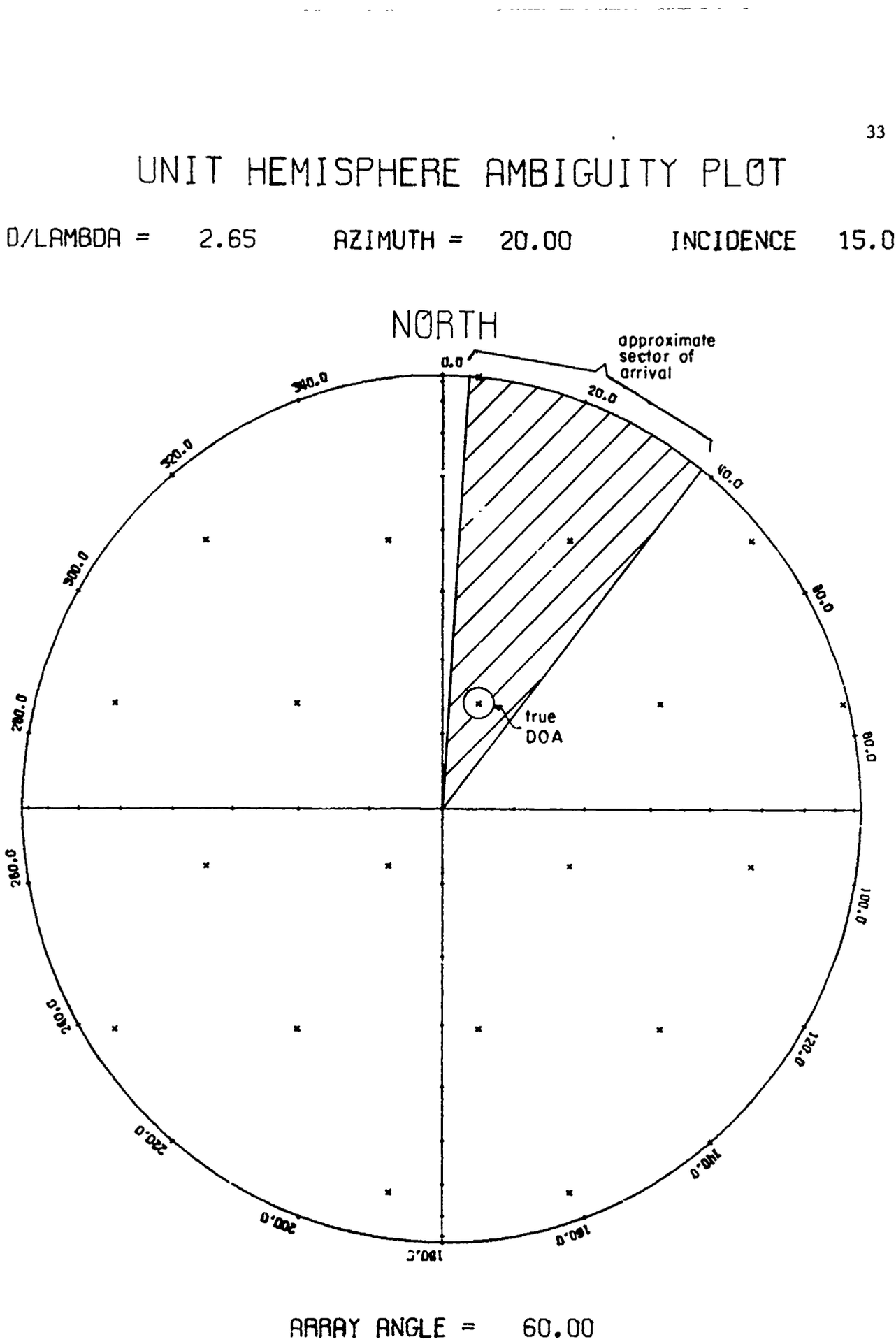

Figure 8. Limitations of an Approximate Azimuth Ambiguity Resolution System

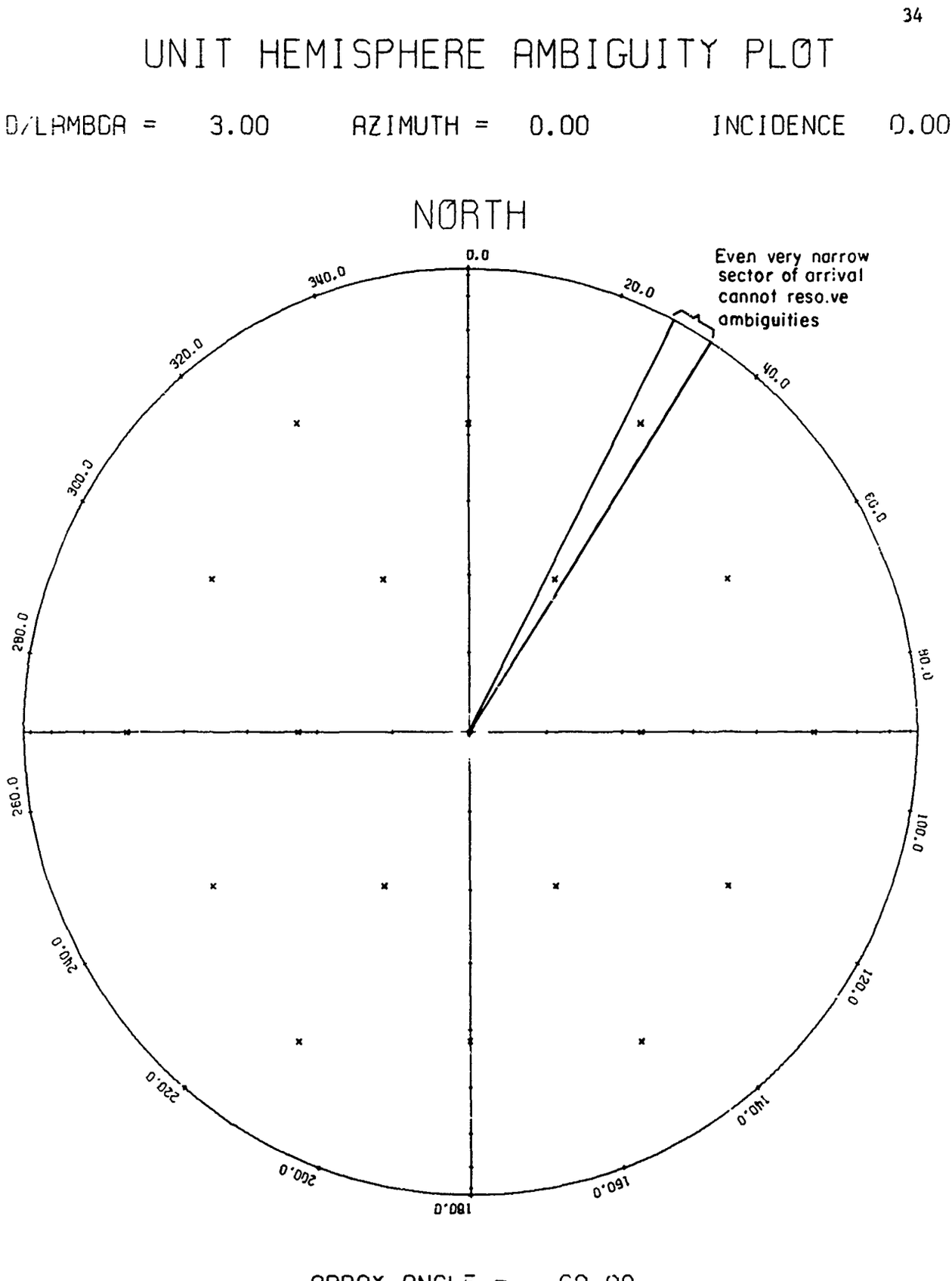

Figure 9. Radial Lines of Ambiguities Formed When the Prime Ambiguity Lies Near the Zenith

These calculations were made for various values of D/λ, azimuthal sector of arrival "widths," and directions of arrival. The results were tabulated in a number of tables; a typical one appears in Appendix D, Table D-1. Note the D/λ value is varied from 1 to 6 in steps of 1/3. The sector width (+ error, in degrees) is varied from 0 to 20 degrees. Ninety-six of these tables were made, varying α from 0 to 360 degrees in increments of 22 degrees, and θ was varied from 0 to 90 degrees in increments of 15 degrees. From these tables it becomes apparent that successful direction ambiguity resolution is a function of D/λ as well as the particular direction of arrival. For some directions of arrival, ($\alpha = 44^{\circ}$, $\theta = 45^{\circ}$) ambiguities may be resolved using a 20 degree sector of arrival for values of D/λ as high as 3.67. (See Appendix D, Table D-2.) On the other hand, for other directions of arrival, ($\alpha = 330^{\circ}$, $\theta = 75^{\circ}$) ambiguities may be resolved only for values of D/λ less than 1.33, assuming a 20° sector of arrival. (See Appendix D, Table D-3.)

An attempt was made to reduce the number of direction ambiguities that must be contended with. It is assumed that the true azimuth lies within a known azimuthal sector of arrival. This restriction on the azimuth can be reflected back through the DOA equations I-4, thus yielding a more stringent phase ambiguity combination rejection criterion (assuming theta can take on any value from 0° to 90°). Unfortunately, it has been determined that this criterion simply cuts out ambiguities with azimuths out of the range of the assumed azimuthal sector of arrival. This conclusion was arrived at by performing a computer simulation of the operations outlined above. To accomplish this task, the program described in the preceding paragraph was modified to take the known, appropriate sector of arrival into consideration. In the simulation

run presented in Appendix D, Table D-4, it was assumed that the known sector of arrival extended from 320 to 340 degrees. (The true DOA was at $\alpha = 330^{\circ}$, $\theta = 75^{\circ}$.) This restriction on the azimuth was then reflected back through the DOA equations. Table D-4 lists all possible ambiguities for various values of D/λ for the given true DOA. The starred ambiguities are the ones that were rejected due to consideration of the known azimuthal sector of arrival. As can be seen, the only ambiguities rejected are those whose azimuth lies outside of the assumed azimuthal sector of arrival. Nothing has been gained, as is further illustrated by the striking similarity of Tables D-5 and D-6, which are found in Appendix D.

The results of this section indicate that an approximate azimuth ambiguity resolution system may not be practical under even very low ambiguity conditions (small values of D/λ). If the prime ambiguity is near the zenith, the ambiguities will line up radially making ambiguity resolution impossible, no matter how "narrow" the known sector of arrival may be. Such a system may be greatly improved if knowledge of the approximate incidence angle is available as well. The locus of possible DOA's on the hemispherical projection is no longer a pie, but the intersection of a pie (approximate azimuth range) and an annulus centered about the zenith (approximate incidence range). (See figure 10.)

From the geographical standpoint, it is considerably more difficult to obtain the approximate range of incidence angles. For example, in addition to knowing the distance from the source, it is necessary to know (approximately) the path by which the signal is arriving at the interferometer site. However, under low ambiguity conditions (i.e.,

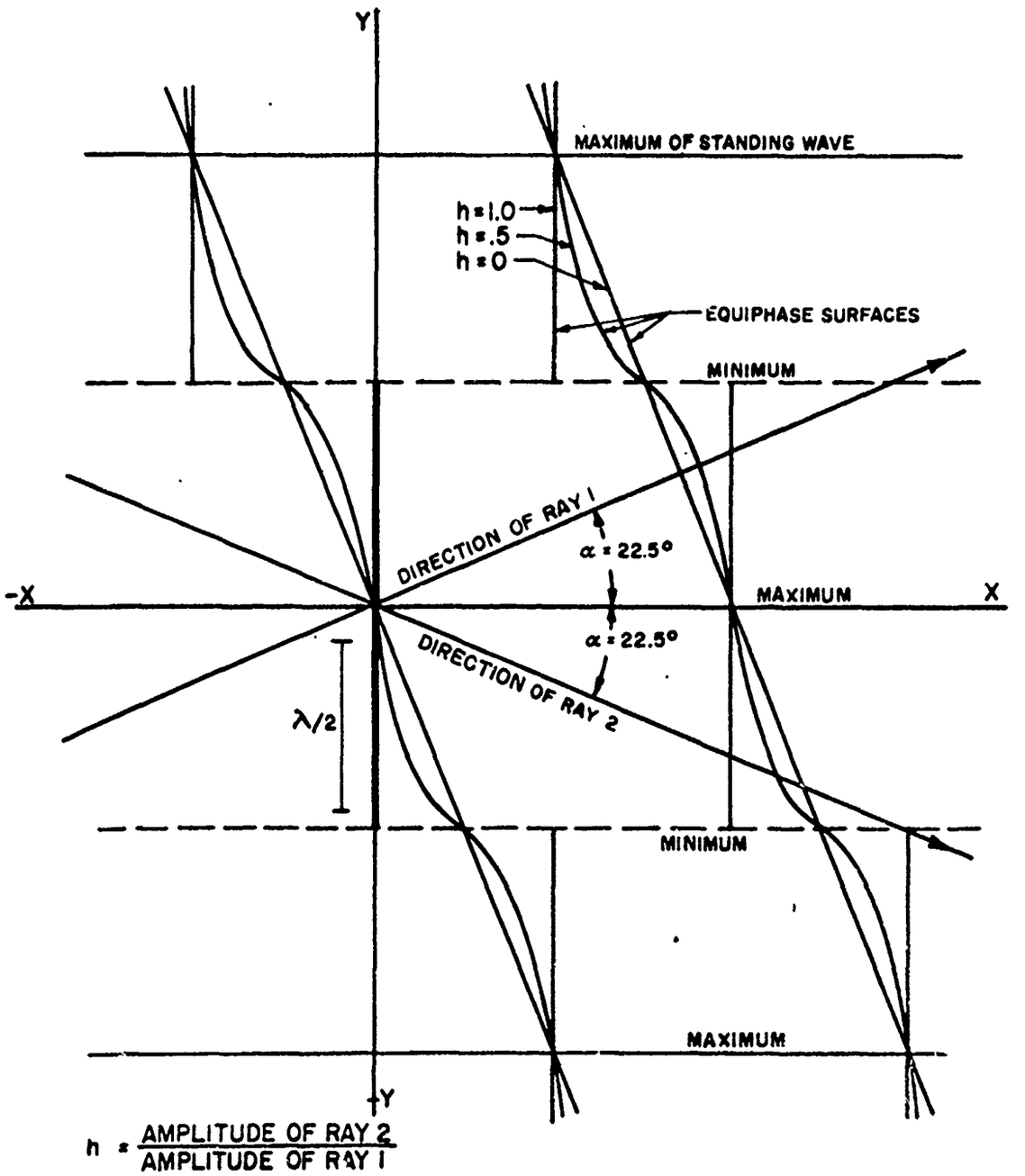

Figure 11. Wave Corrugation as a Result of Two Interfering Plane Waves (From Hayden's Thesis)

only one hexagonal ring centered about the prime ambiguity) it is necessary only to be able to accept or reject the prime ambiguity as the true DOA. Ambiguity resolution is then completed by utilizing the approximate azimuth information.

If the interferometer is used in conjunction with a device that gives both approximate azimuth and incidence angle information, directional ambiguity resolution becomes quite practical. If this peripheral device is a small baseline interferometer, we have exactly the type of interferometer RDF system studied by Creasy.[1] The system might be set up to operate in the following manner (as viewed on a three-dimensional hemisphere plot): The approximate unambiguous DOA, as indicated by the small baseline interferometer, is plotted on a hemisphere onto which all possible ambiguities indicated by the large baseline interferometer have already been plotted. The ambiguity closest in path length to this plotted approximate DOA (along the surface of this hemisphere) must be the true DOA. However, it can be shown inductively that this method of ambiguity resolution is essentially equivalent to the phase ambiguity resolution system of Chapter IV. (See Appendix E.) Because the method of Chapter IV requires much less computation, the above scheme is not particularly useful.

It should be emphasized that the approximate azimuth angle and incidence angle direction ambiguity resolution process must be carried out on the three-dimensional hemisphere plot, and <u>not</u> on the hemispherical projection plot. This raises a point that should be kept in mind. Although the interferometer direction ambiguities are evenly distributed when plotted on the hemispherical projection, the actual ambiguous directions of arrival may not appear to be uniformly distributed to an

observer. This is best understood by recalling the example of the last chapter in which an observer was located at the center of a large hemisphere onto which all ambiguous DOA's (indicated by a large baseline interferometer) have been plotted. As the hemispherical projection plot of the ambiguities is uniform, the observer will generally find that most of the ambiguities are clustered directly over his head. Only a very few will lie near the horizon. One must bear in mind that the hemispherical projection plots have no direct physical interpretation. To relate these plots to the physical situation, it is necessary to mentally picture the corresponding three-dimensional hemisphere plot. One may then imagine himself standing at the center of the hemisphere, pointing at the various plotted points on the hemispherical surface.

FOOTNOTES

1. J. Creasy, "Digital Techniques for Radio Direction Finding with Interferometer Arrays," Master's Thesis, University of Illinois, Urbana, Illinois, June 1966, pp. 33-37.

VI. LIMITATIONS OF THE SMALL/LARGE BASELINE PHASE AMBIGUITY RESOLUTION SYSTEM

From the preceding work it appears that the conventional small/large baseline phase ambiguity resolution system may be the most practical. The limitations of this system will be examined further. The discussion of Chapter II suggests that this system will work if:

$$\left| \frac{D_L}{D_S} \phi_{ij}^{\text{small}} - \phi_{ij}^{\text{actual}} \right| < 180^\circ. \qquad \text{(VI-1)}$$

It is desired to determine the range of signal wavelengths over which such an ambiguity resolution system will work (called the system operating wavelength range).

Due to the effects of wave corrugation (to be discussed in Chapter VII) and phase measurement inaccuracies (see Chapter II), the large array is generally not operated at wavelengths greater than twice the large array baseline. (This implies that D_L is always greater than $\lambda/2$.) This establishes an upper bound on the range of operating wavelengths of the interferometer system.

An expression for the lower bound on the range of operating wavelengths of the system will be derived in the following paragraphs. Let it be assumed that the maximum error of the small baseline interferometer system, in the range of wavelengths over which it is operated, is "K_{err}" degrees, such that:

$$\left| \phi_{ij}^{\text{small}} - \phi_{ij}^{\text{small, ideal}} \right| \leq \left| K_{err} \right|, \qquad \text{(VI-2)}$$

where ϕ_{ij}^{small} designates the measured small array phase angle, and $\phi_{ij}^{\text{small, ideal}}$ designates the small array phases that would correspond precisely to the direction of arrival of the signal wave. (As

before, the "ij" subscripting signifies that equation VI-1 must hold for all of the three interferometer phase measurements.) K_{err} describes the small baseline system error. It has two components. One component is due to the effects of wave corrugation. (See Chapter VII.) This causes the actual voltage phase differences which appear across the array elements, $\phi_{ij}^{\text{small, actual}}$, to differ from those corresponding to the precise direction of arrival of the signal wave, $\phi_{ij}^{\text{small, ideal}}$. The second component is due to phase measurement error. (See Chapter II.) This second component is not dependent upon the operating wavelength of the array. It depends only upon the design of the instrumentation in the interferometer system.

For a given large array baseline, D_L, and a given value of K_{err}, the minimum useable small array baseline length, D_S, may be computed from equation VI-1. It follows from the discussion of Chapter II that:

$$\phi_{ij}^{\text{small, ideal}} = \frac{D_S}{D_L} \phi_{ij}^{\text{actual}}, \qquad \text{(VI-3)}$$

where $\phi_{ij}^{\text{actual}}$ denotes the unambiguous large array phases, as in Chapter I. This equation holds providing that the large baseline array is assumed to be errorless in comparison with the error of the small baseline array. Equation VI-2 suggests that at the operating wavelength at which the error is maximum (normally the longest operating wavelength);

$$\phi_{ij}^{\text{small}} = \phi_{ij}^{\text{small, ideal}} + K_{err}. \qquad \text{(VI-4)}$$

Substitution of equations VI-3 and VI-4 into equation VI-1 yields:

$$\left| \phi_{ij}^{\text{actual}} \pm \frac{D_L}{D_S} K_{err} - \phi_{ij}^{\text{actual}} \right| < 180^{\circ}$$

or,

$$D_L < \left(\frac{180}{K_{err}}\right) D_S. \qquad \text{(VI-5)}$$

The above inequality holds at the operating wavelength of maximum error, hence it must hold at all other operating wavelengths as well. This is because of the inverse relation between the system error and the length of the array baseline.

The lower bound on the range of operating wavelengths is reached when the small baseline array becomes ambiguous. This occurs when the operating wavelength becomes less than twice the small array baseline, that is, when $D_S > \lambda/2$. Hence, the range of operating wavelengths, λ_{op}, is given by:

$$2D_S < \lambda_{op} < 2D_L. \qquad \text{(VI-6)}$$

Alternatively this can be expressed as a ratio of the longest useable operating wavelength ($\lambda_{Longest}$) to the shortest useable operating wavelength ($\lambda_{Shortest}$):

$$\frac{\lambda_{Longest}}{\lambda_{Shortest}} = \frac{D_L}{D_S}. \qquad \text{(VI-7)}$$

D_L is chosen to ensure satisfactory operation at the longest desired operating wavelength; D_S must be chosen so as to satisfy equation VI-5. At the same time it is often desirable to make D_S as small as possible, thus maximizing the range of useable wavelengths for the system. It is evident from equation VI-5 that the minimum useable value of D_S is $(K_{err})(D_L)/180^{\circ}$. Substituting this value of D_S into equation VI-7 yields an equation for the optimum operating wavelength ratio of a small/large baseline interferometer system:

$$\frac{\lambda_{Longest}}{\lambda_{Shortest}} = \frac{180^{o}}{K_{err}} , \qquad \text{(VI-8)}$$

Two practical conclusions can be drawn from the preceding discussion. If a small/large baseline interferometer system satisfies equation VI-5 almost as an equality, the operating wavelength ratio will be maximized. The maximum possible operating wavelength ratio is given by equation VI-8. Unfortunately, the apparent simplicity of VI-5 is misleading. The component of K_{err} due to wave corrugation appears to vary with D_S (assuming the operating wavelength is held constant). This dependence of K_{err} on the small array baseline complicates the design of a system with an optimum operating wavelength ratio. Finally, it should be pointed out that the system may conceivably be operated at wavelengths greater than $\lambda_{Longest}$. There will be no ambiguities to resolve in this case; however system accuracy will suffer. On the other hand, the system cannot operate at wavelengths shorter than $\lambda_{Shortest}$, as the small array becomes ambiguous.

Equation VI-8 indicates that the operating wavelength ratio increases as K_{err} decreases. To minimize K_{err}, it is necessary to study the sources of inaccuracy in an interferometer system. It should be noted that these sources of inaccuracy affect both the large and small baseline arrays to different extents. The "corrective measures" suggested in the work that follows may be applied to both systems. Application of these corrective techniques to the small array system will result in a wider operating wavelength range of the ambiguity resolution system. Applying them to the large array system will result in greater system accuracy.

The errors in an interferometer array are primarily due to the invalidity (in practice) of two assumptions that were made in the derivation of the DOA equations I-2. The first faulty assumption was that the incident wave has an essentially uniform, plane phase front across the array aperture. Usually this is only an approximation, due primarily to the effects of wave interference. As was pointed out in Chapter I, many plane waves of various amplitudes might arrive from different directions at the interferometer array simultaneously. The waves superimpose (add algebraically) to form very irregular phase and amplitude patterns across the array aperture. Fortunately the components of the voltages induced in the array elements by all waves not at (or very near) the signal wavelength are rejected in the receiver. Hence the apparent wavefront across the array aperture is formed only by those waves at or very near the signal wavelength. Up until this time it has been assumed that there existed only one plane wave at the signal wavelength. More often than not, there exists more than one such plane wave incident upon the array at the signal wavelength. These waves are usually of different amplitudes and DOA's. They will superimpose to form a resultant wave which is <u>neither</u> uniform nor plane. Figure 11 (taken from a thesis by Hayden[1]) shows in two dimensions the resultant "corrugated" wavefront that is produced by two interfering waves.[2] As shown in the figure, the incident waves are arriving from different directions such that an angle of 45^{o} is made by the intersection of lines normal to the plane wavefronts. The figure has been drawn for various values of relative wave amplitude, h. The value of h indicates the relative strength of one interfering wave with respect to the other. It should be noted that the averaged wavefronts (see the dashed lines)

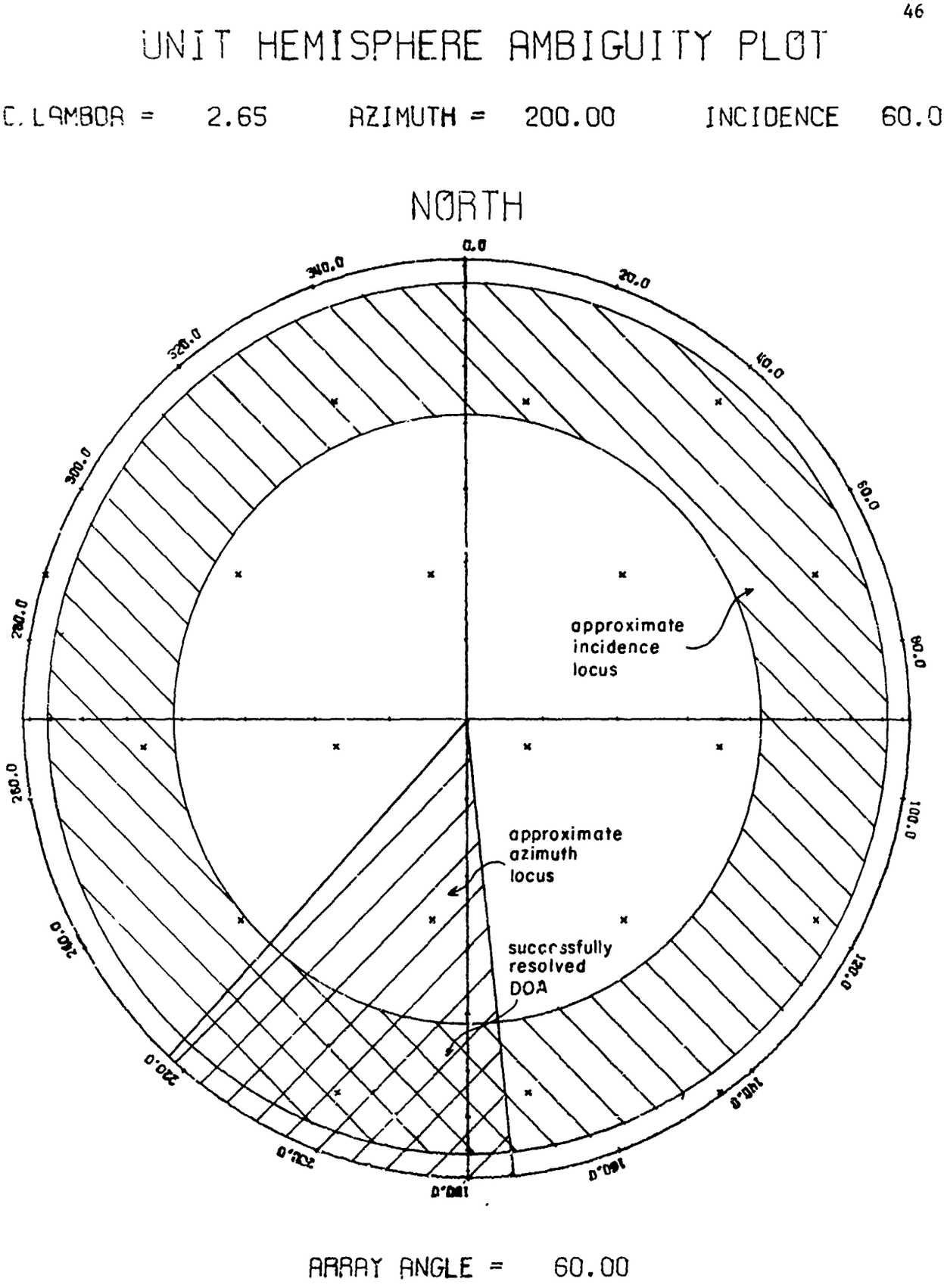

Figure 10. Approximate Azimuth and Incidence Ambiguity Resolution Procedure as Depicted on a Hemispherical Projection

appear to travel in the direction of the stronger incident plane wave.

In the HF range the most prevalent cause of wave interference (which results in wave corrugation) is the phenomenon of multimode propagation. Multimode propagation may be thought of as the transmission of a radio wave from its source to the receiving site via several different paths. A typical situation which might occur over a 200 km distance is shown in figure 12. Here, part of the transmitted signal travels via a "two-hop" path, whereas the other travels via a "one-hop" path. There are two separate plane waves arriving at the receiving site from different elevation angles. The waves may be arriving from slightly different azimuthal angles as well. This will occur if there exists any lateral gradient in the ionization (free electron density) of the refracting portion of the ionosphere. Under these conditions the ionosphere is said to be "tilted." It will act as a tilted reflecting surface instead of the more commonly postulated plane horizontal reflector. Waves that are refracted twice by the tilted ionosphere will certainly be laterally deflected to a greater extent than those that were refracted only once. Thus, the waves may arrive from slightly different azimuthal directions.[3]

A further observation concerning multimode propagation may be made. Because the plane waves have travelled over different path lengths, there must exist a phase difference, ϕ_d, between these interfering waves, even though both waves have originated from the same source. Furthermore, if the refracting layer of the ionosphere is moving either further away from or closer to the surface of the earth, as is often the case,[4] it is clear that the difference in the lengths of the two propagation paths will vary. Likewise ϕ_d must vary. The velocity of the refracting

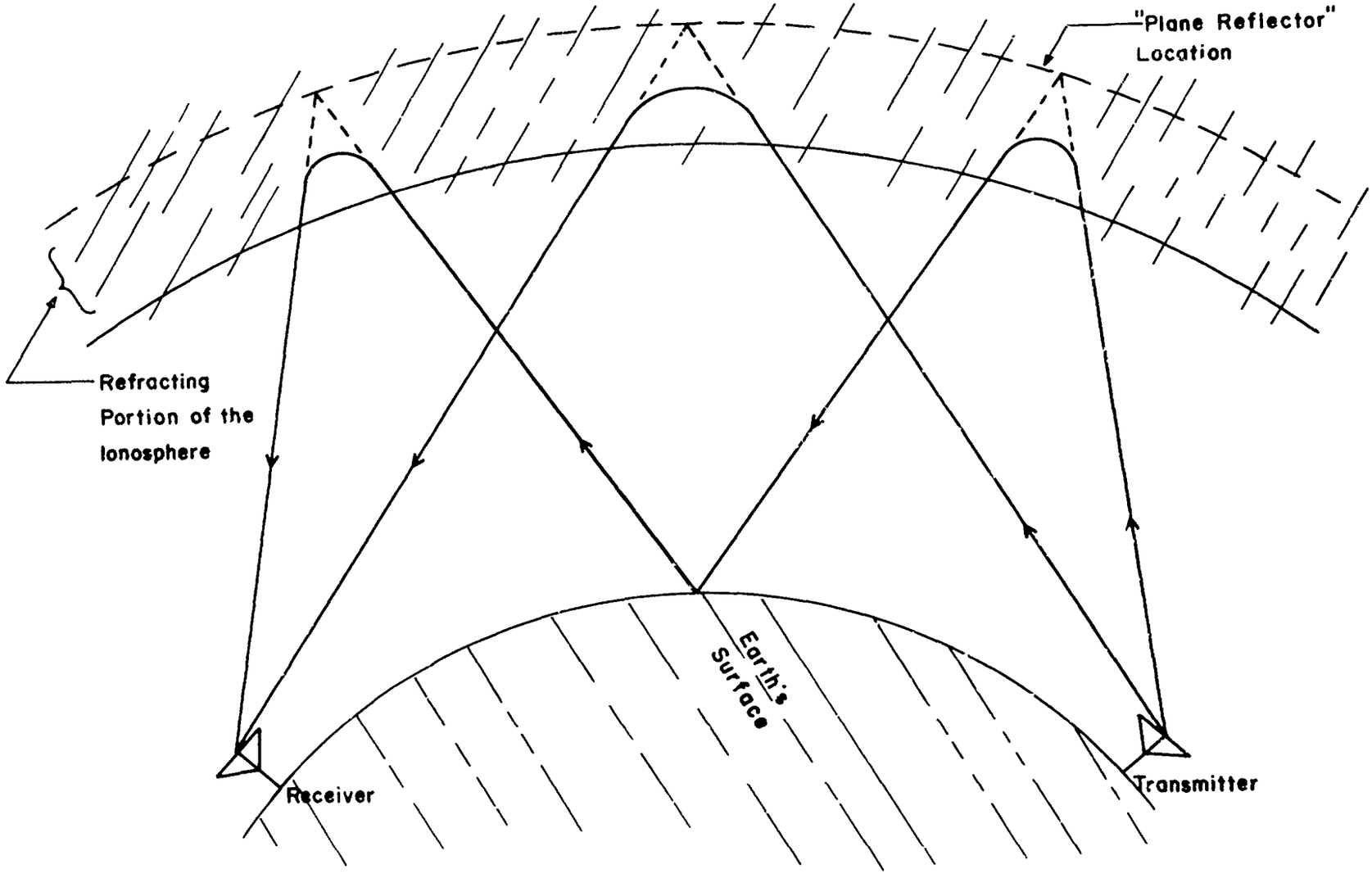

Figure 12. Multimode Propagation over a Medium-Length Path

portion of the ionosphere is somewhat constant; hence ϕ_d will vary in an approximately linear fashion with respect to time.

Another cause of wave interference is the reflection (or reradiation) of the signal from an object relatively near the array. This again results in a deformation in the incident uniform plane wave due to the superposition of the scattered radiation field and the incident wave. Generally this reradiated field is quite low in amplitude compared to the incident wave amplitude, and the amount of wave corrugation due to this effect may be quite small compared to the wave corrugation due to multimode propagation. In this case the path difference between the two interfering waves is not time variant (unless the reradiating object is in motion) and the phase difference between the two waves does not vary with time. Errors due to this effect are commonly called siting errors.

In the preceding discussion it has been assumed that there exist only two interfering waves. There may be several. The resultant wavefront will be further corrugated by the contributions from these additional interfering waves. However, in practice, the assumption of only two interfering waves may not be such a bad approximation. This is because it is likely that the other interfering waves are smaller in amplitude and thus they affect the wave corrugation pattern to a lesser extent. To simplify the analysis, this assumption shall be maintained throughout the remaining sections of this work.

It has been stated that wave interference results in a corrugated wavefront. It can be further asserted that these corrugations may be abrupt enough to make themselves "felt" across the aperture of the interferometer array. If they are not abrupt enough, the corrugated

wave will still appear as a "locally plane" wave. However, it is highly probable that this "plane wave" that the array "sees" is not arriving from the DOA of either of the two interfering waves. Hayden has shown that the distance between corrugation maxima, S, (see figure 11) is given by:

$$S = \frac{\lambda}{2 \sin (\theta/2)}, \qquad \text{(VI-9)}$$

where θ is the angle made by the intersection of the 2 interfering wavefront normals. Because the interferometer system may have an aperture of several wavelengths or more, several corrugations of the resultant wave may appear across the aperture (depending on the value of θ), thus invalidating the DOA equations.

Wave corrugation may also be caused by signals of similar wavelength arriving from different sources. Such interference is known as "co-channel interference" if the wavelengths of the two signals are coincident. If the signals are on adjacent wavelengths but both are within the receiver passband, the situation is again analogous to that of receiving a corrugated wave formed by the superposition of these two waves. Such interference is known as "adjacent channel interference." It should be noted that the relative phase between such interfering waves is time-variant, as the waves are rarely of precisely the same wavelength.

Wave interference may not be the only cause of deformation of the incident plane wave. Any inhomogeneities in the ionosphere or ground at the points of "reflection" of the propagating wave will cause such deformations. These inhomogeneities may take the form of changes in the density of free electrons in the ionosphere due to atmospheric turbulences, or changes in elevation, at the point of reflection on the

ground.[5] Of course, these inhomogeneities must be of sufficient abruptness to be "felt" by the interferometer array if they are to cause any problems.

The second faulty assumption made in the derivation of the DOA equations was that the phase differences of the signal voltages induced in the interferometer elements could be measured precisely. Electronic phasemeters are generally only accurate to within one half of a degree. Further system instrumentation errors result from the fact that the effective electrical lengths of the three transmission paths between the interferometer elements and the phase meters may not be exactly equal. It is assumed that the transmission lines between the array elements and receivers have been made of equal length. Unequal lengths of transmission line would cause the electrical phase differences measured at the receiving ends of the transmission lines to differ from those that would be measured at the array elements. A more serious probl[illegible]es in the multichannel receiver. The receiver channels must exhibit identical phase delay characteristics. This ensures that each channel will be of the same effective electrical length. Unfortunately, identical phase characteristics are hard to maintain in a practical multichannel receiver. Each channel's phase delay characteristics tend to drift as component values change due to thermal effects and component ageing. If the receiver channels drift independently, the receiver channels will no longer be of identical effective electrical lengths. The phase measurements made at the receiver IF frequency are no longer accurate indications of the interferometer phase differences.

Another type of phase measurement error (which is, in reality, due to transient wave interference) results if there are transient noise

spikes present on the received signal. If the phase measurement is made at the instant that the noise transient is occurring, the noise signal will interfere with the signal wave, causing a momentary wavefront corrugation across the array aperture. The phase measurements will not correspond to the DOA of the signal. Such transient noise spikes, due both to natural phenomena such as thunderstorms and man-made sources such as automobile ignition systems, are not uncommon comparions of a radio signal. Because these noise transients occur at random time intervals, it seems that it would be desirable to make the phase measurements as rapidly as possible, thus decreasing the chance of phase measurement error due to the occurrence of a noise transient during the measurement period. For this reason, systems employing an antenna-switched, two-channel receiver might be more susceptible to this type of interference. Such a system can measure only one interferometer phase at a time. The three phase measurements are made in rapid succession, as fast as the antenna switching times will allow. The likelihood of encountering a noise spike in this sequence of three individual phase measurement periods can be greater than that of encountering a noise spike in one phase measurement period. This depends on the expected duration of a noise spike relative to the length of the switching time interval between the three successive phase measurements. If the former is substantially greater than the latter, it is clear that the two-channel receiver system would work almost as reliably as the three-channel receiver system.

By taking many phase readings as rapidly as possible in a transient-noise environment, it seems probable that the ratio of "accurate" phase measurements to "erroneous" phase measurements will be increased over that which is realizable with a slower (two-channel) system. Averaging

these phase readings taken at the faster rate should result in averaged values which are substantially more accurate than those obtained from the slower system. It may be added that there exist analog phase measurement techniques which will permit continuous (analog) averaging of the phase measurements. This method should yield the most accuracy of all, providing that the analog measuring and averaging systems can be made sufficiently precise. A three-channel receiver must be used if such analog averaging techniques are to be employed. This enables continuous monitoring of all three array element voltages. It will be shown in Chapter VII that interferometer phase measurement averaging has other benefits as well as the averaging out of the effects of this transient noise wave interference.

Another source of phase measurement error is signal fading. The signal may drop below a threshold level under which noise dominates the phase measurement, not the signal. This fading problem is largely akin to the noise spike problem in that both result in degradation of the signal-to-noise ratio. Signal fading is almost always present on ionospherically propagated signals.[6] It is a result of several different propagation phenomena. Among them are multimode wave interference and time variations in ionospheric absorption or focusing.

The nature of various causes of interferometer inaccuracy has been discussed. Now it is time to investigate various methods of reducing these sources of error in the interferometer system.

FOOTNOTES

1. E. C. Hayden, "Some Basic Problems in the Determination of the Direction of Arrival of Radio Waves," Ph.D. Thesis, University of Illinois, Urbana, Illinois, September 1958, p. 12. (RRL Publication No. 158.)

2. See also: H. A. Whale, Effects of Ionospheric Scattering on Very-Long-Distance Radio Communication, Plenum Press, New York, 1969, p. 15.

3. Ibid., p. 102

4. K. Davies, Ionospheric Radio Propagation, Government Printing Office, Washington, D. C., 1965, p. 416.

5. Whale, op. cit., pp. 90, 98.

6. Davies, op. cit., p. 242.

VII. REDUCTION OF WAVE INTERFERENCE EFFECTS

In the previous chapter it was demonstrated that interferometer errors were due primarily to the violation of two assumptions used in the derivation of the DOA equations (equations 1-2). In this chapter the reduction of error due to the violation of the first assumption (that the incidence signal wave is locally plane) will be discussed.

It has been stated that multimode propagation results in a corrugated wavefront across the interferometer aperture. Furthermore, because the relative phase difference between the two interfering waves varies in a somewhat linear fashion with respect to time, the corrugation pattern will shift its position across the array aperture. As the corrugation pattern is spatially periodic, the interferometer phases must likewise vary with time in a periodic manner. This phenomenon is illustrated in figure 13. The observation made in connection with figure 11 (that the averaged corrugation pattern taken over an integral number of corrugation periods appears to be a plane wave travelling in the same direction as the stronger of the two interfering waves) suggests that time averaging over one or more of these corresponding interferometer phase variation periods may result in averaged interferometer phases which indicate the direction of arrival of the stronger wave. It has been shown by Glick[1] and Church[2] that this is indeed the case.

Central to Glick's proof is the consideration of the voltages induced in the interferometer antenna elements. In a case in which there are two waves incident upon the array arriving from different directions, each wave will induce a sinusoidally varying voltage in each interferometer element. The total voltage induced in each array element

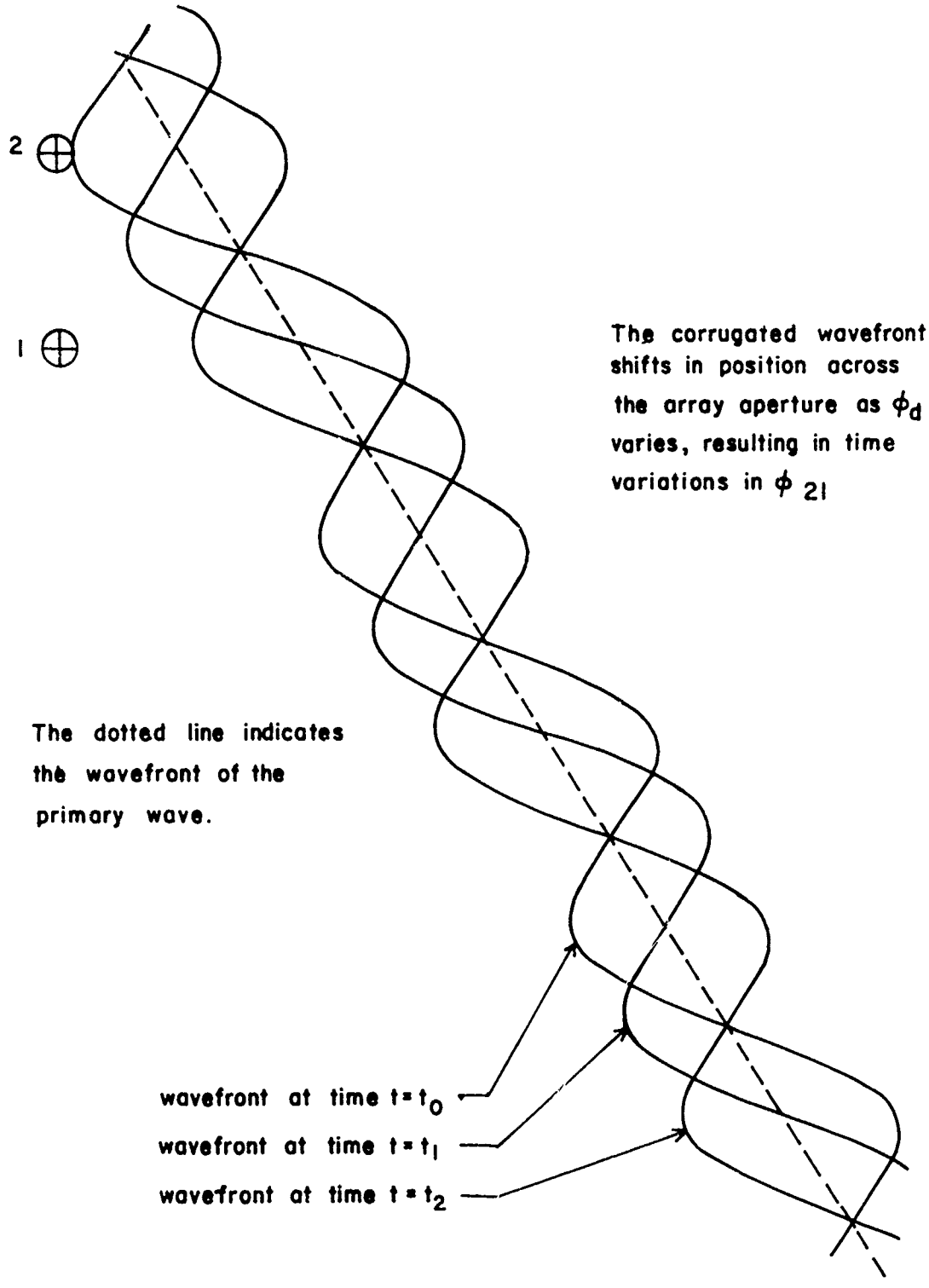

Figure 13. Interferometer Phase Variation Due to Wave Interference (With Time-Variant ϕ_d)

may be expressed as a sum of the two phasors that correspond to the voltages induced in that element by the incident (interfering) waves. Because all phase measurements must be made relative to some reference voltage, it will be assumed that the reference voltage is the voltage component induced by the stronger of the two incident waves in array element number 1. (See figure 1.) Let it be assumed that the stronger, or primary wave, induces a voltage of unity magnitude in the interferometer elements. The weaker wave induces a voltage of magnitude "h" in the elements. The value of h may be interpreted as the relative magnitude of the weaker (secondary) wave measured with respect to the stronger (primary) wave. The phase relationships existing between the two voltage components induced in each of the array elements may be determined from a knowledge of the relative phase difference (ϕ_d) between the two interfering waves and the use of the interferometer phase difference equations (see equations I-1). ϕ_d is identical to the phase difference between the two induced voltages in the array reference element (element number 1). The phasor diagram for the voltages induced in element number 1 is given in figure 14a. Here the phase representing the voltage induced by the primary and secondary wave phasors is given as ϕ_d. The phasor diagram for the voltages induced in antenna element number 2 may likewise be drawn (see figure 14b), where ϕ_{21p} and ϕ_{21s} are the phases of the voltage components induced in element number 2 with respect to element number 1 by the primary and secondary waves, respectively. These phases may be individually calculated from the interferometer phase equations I-1. ϕ_{21p} is calculated using the direction of arrival of the stronger of the two interfering waves, and ϕ_{21s} is calculated using the DOA of the weaker one. Here the phase of the primary wave is

(a) Element No. 1

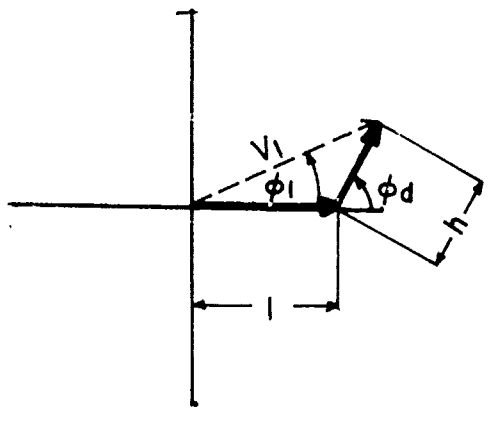

$$|V_1| = \sqrt{1+h^2+2h\cos\phi_d}$$

$$\phi_1 = \tan^{-1}\frac{h\sin\phi_d}{1+h\cos\phi_d}$$

(b) Element No. 2

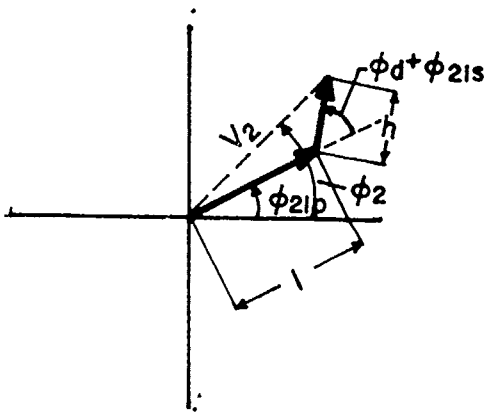

$$|V_2| = \sqrt{1+h^2+2h\cos(\phi_d+\phi_{21s}-\phi_{21p})}$$

$$\phi_2 = \tan^{-1}\frac{\sin\phi_{21p}+h\sin(\phi_d+\phi_{21s})}{\cos\phi_{21p}+h\cos(\phi_d+\phi_{21s})}$$

(c) Element No. 3

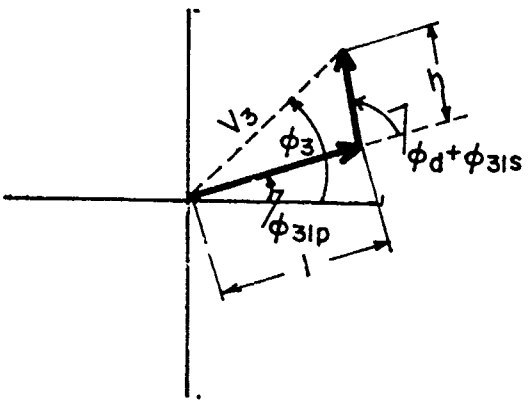

$$|V_3| = \sqrt{1+h^2+2h\cos(\phi_d+\phi_{31s}-\phi_{31p})}$$

$$\phi_3 = \tan^{-1}\frac{\sin\phi_{31p}+h\sin(\phi_d+\phi_{31s})}{\cos\phi_{31p}+h\cos(\phi_d+\phi_{31s})}$$

Figure 14. Interferometer Element Voltages Under Wave Interference Conditions

given as ϕ_{21p}, while the phase of the secondary wave is given by $\phi_d + \phi_{21s}$. ϕ_d appears in this expression in order to make this phase value relative to the induced primary wave voltage in antenna number 1. Using analogous reasoning and notation, the phasor diagram for the third element may be drawn as in figure 14c. The actual phase of the resultant voltage induced in each of the antenna elements (as measured with respect to the previously defined reference voltage) may be derived geometrically from these phasor diagrams and are given in figure 14. The interferometer phase differences are easily calculated by subtracting these various element phases as shown below:

$$\phi_{21} = \tan^{-1} \frac{\sin \phi_{21p} + h \sin (\phi_d + \phi_{21s})}{\cos \phi_{21p} + h \cos (\phi_d + \phi_{21s})} - \tan^{-1} \frac{h \sin \phi_d}{1 + h \cos \phi_d}$$

$$\phi_{13} = \tan^{-1} \frac{h \sin \phi_d}{1 + h \cos \phi_d} - \tan^{-1} \frac{\sin \phi_{31p} + h \sin (\phi_d + \phi_{31s})}{\cos \phi_{31p} + h \cos (\phi_d + \phi_{31s})}$$

$$\phi_{32} = \tan^{-1} \frac{\sin \phi_{31p} + h \sin (\phi_d + \phi_{31s})}{\cos \phi_{31p} + h \cos (\phi_d + \phi_{31s})}$$

$$- \tan^{-1} \frac{\sin \phi_{21p} + h \sin (\phi_d + \phi_{21s})}{\cos \phi_{21p} + h \cos (\phi_d + \phi_{21s})}. \qquad \text{(VII-1)}$$

If it is assumed that ϕ_d varies with time, as in the case of multimode propagation, it may be concluded by studying the phase diagrams of figure 14 that the voltages induced in the array elements will vary in amplitude resulting in fluctuation of the received signal amplitude. The phasor representing the voltage induced in an element by the secondary wave simply pivots about its "tail," which is tacked down to

the "head" of the primary voltage phasor. Because the resultant element voltage phasor is drawn from the "tail" of the primary voltage phasor to the "head" of the secondary voltage phasor, the resultant voltage likewise fluctuates in amplitude and in phase as ϕ_d varies. This is one cause of signal fading. The severity of the signal fading depends upon the value of h. If the two waves are of equal amplitude (h = 1), it is apparent that the signal will fade away completely for some values of ϕ_d. Furthermore, as ϕ_d varies, it can be seen from the diagram that it is possible that as the value of h approaches unity, the phase of the resultant element voltage may deviate from the phase of the component of the element voltage induced by the primary wave by as much as $\pm 90^{\circ}$. This analytical result is in agreement with what was predicted heuristically from the consideration of the corrugated wavefront picture at the beginning of this chapter.

Appendix F contains computer-generated plots of all three interferometer phases under wave interference conditions, plotted as a function of relative phase difference (ϕ_d). The first three plots illustrate the increased severity of interferometer phase deviation with increasing values of h. (See figures F-1, F-2, and F-3.) Another set of three plots (see figures F-2, F-4, and F-5) illustrates how the extent of interferometer phase variation changes with increasing angles between the interfering signals. These observations will be elaborated upon later in this chapter. As illustrated, the average of these readings (taken over one period of these fluctuations) appears to be equal to ϕ_{ijp}, the interferometer phase difference induced in the array by the primary wave alone. Glick has shown analytically[3] that averaging the equations with respect to ϕ_d over a period (or integral number of periods)

of interferometer phase difference variation (from $\phi_d = -180^o$ to 180^o) does indeed yield averaged phase values which are identical to the phases of the voltage components induced by the primary wave. This indicates that if the interferometer phase difference measurements are time averaged over an integral number of periods of phase variation (under time variant ϕ_d wave interference conditions), the DOA corresponding to these averaged phases is that of the stronger of the two interfering waves.

At first glance, it might appear that ϕ_d must vary in a strictly linear fashion with respect to time for the above conclusion to be valid. If this is the case, the time variations of the interferometer phases will follow their ϕ_d variations, and Glick's result directly applies to time averaging as well as to averaging with respect to ϕ_d. However, it is also permissible that ϕ_d vary with time in a random fashion, providing that it is uniformly distributed in an interval of ϕ_d which corresponds to an integral number (N) of periods of interferometer phase variation (T). This easily follows from the fact that the average (expected) value of $\phi_{ij}(t)$ is given as:

$$\phi_{ij}\,[\phi_d(t)] = \int_0^{NT} f_{\phi_d}\,[\phi_d(t)]\;\phi_{ij}\,[\phi_d(t)]\;d\phi_d \qquad \text{(VII-2)}$$

where f_{ϕ_d} is the probability density of $\phi_d(t)$. Because ϕ_d is taken to be uniformly distributed in the interval [0, NT],

$$\{\phi_{ij}\,[\phi_d(t)]\} = \int_0^{NT} \left(\frac{1}{NT}\right)\;\phi_{ij}\,[\phi_d(t)]\;d\phi_d. \qquad \text{(VII-3)}$$

But this is simply an interferometer phase difference average taken with respect to ϕ_d. This establishes the validity of time averaging the

interferometer phase differences instead of averaging directly with respect to ϕ_d, provided that ϕ_d is uniformly distributed over an integral number of phase variation periods.

From a study of experimental data,[4] Crush has determined that ϕ_d does vary in a semirandon fashion under multimode propagation conditions. Under such conditions, th ϕ_d variation is commonly observed to behave as:

$$\phi_d = w_\phi t + P. \qquad \text{(VII-4)}$$

Here P is a random phase perturbation with a Gaussian probability density function and a mean value of zero. w_ϕ is the rate at which the phase is changing. The standard deviation of P is observed to be small compared to w_ϕ. This gives ϕ_d a probability density function that is uniformly distributed over an interval of ϕ_d whose length is roughly proportional to the observation time. In essence, ϕ_d varies in an approximately linear fashion, with small random perturbations to either side of the linear path, as suggested in the discussion of Chapter VI. Hence the interferometer phases will vary in a somewhat periodic manner with respect to time. (If ϕ_d varied in a perfectly linear fashion with respect to time, the interferometer phase variation would be exactly periodic in time.) Because these approximately periodic time variations of ϕ_{ij} correspond somewhat to the periodic ϕ_d variations of ϕ_{ij}, it would be desirable to time average ϕ_{ij} over an integral number of these coarse periodic variations. ϕ_d would then be uniformly distributed over an approximately integral number of periods of ϕ_{ij}.

Alternatively, it may be found easier to average the phase measurements over an arbitrary length of time that is substantially greater than several periods of phase variation. It is likely that the error

introduced by averaging over the fractional phase variation period is negligible, since the average has been taken over a number of integral phase variation periods as well. This conclusion may be expressed mathematically. The average of $\phi_{ij}(t)$ taken with respect to time over an arbitrarily long time interval, T, is given as:

$$\frac{1}{T}\int_0^T \phi_{ij}(t)dt, \qquad \text{(VII-5)}$$

Suppose now that there exists a maximum of N periods of ϕ_{ij} variation within [0, T], each of approximate length τ. Then the average may be written as:

$$\frac{1}{T}\int_0^T \phi_{ij}(t)dt = \frac{1}{T}\int_0^{N\tau} \phi_{ij}(t)dt + \frac{1}{T}\int_{N\tau}^T \phi_{ij}(t)dt. \qquad \text{(VII-6)}$$

The right-most term in the above expression represents the error introduced due to averaging over the fractional wavelength. It obviously tends to zero as T is increased, since $T - N\tau$ must always be less than τ, and $\phi_{ij}(t)$ remains finite.

The actual time-averaging operation is not carried out in an analog sense even though analog averaging is implied by the above equation. Instead, these averages are approximated digitally. This is done by taking a number of successive phase measurements, and then averaging these. Thus a "sample mean" is obtained which can be made arbitrarily close to the true time-averaged value of the interferometer phases, providing that a sufficient number of samples are taken. This implies that the interferometer system should have a sufficiently high sampling rate. It should again be noted that a three-channel receiver allows a

much faster sampling rate, as all phases are available simultaneously. In the three-channel system, all three phases may be read at the same time instead of in succession, as in a two-channel receiver system. Another way to take advantage of the simultaneous availability of the three-interferometer phases in a three-channel system is the combination of analog and digital averaging techniques. Between samples, the phase variations may be averaged in an analog sense. (This is equivalent to inserting low-pass filters between the phase meter outputs and the inputs to the digital sampling circuitry.) This procedure improves the accuracy of the sample mean without requiring that more samples per period be taken. It may be concluded that under rapidly changing multimode propagation conditions, a three-channel system can yield more accurate DOA's.

Insight into a second technique by which wave interference effects may be reduced can be gained by examining the effect of array baseline length on the extent of interferometer phase fluctuation caused by wave interference phenomena. This effect can best be visualized by again referring to the corrugated wavefront pattern formed by two interfering plane waves as shown in figure 15. This figure is drawn such that the direction of arrival of the primary wave is orthogonal to a line drawn through the antenna elements. (The primary wavefront can be recovered by "averaging" the corrugated wavefront.) It is apparent that the greater the separation between a pair of interferometer elements, the more closely the induced voltage phase difference will correspond to the DOA of the primary wave. For example, in figure 15, antenna elements 1 and 2 will indicate an azimuth of about 40°; antenna elements 1 and 3 will indicate an azimuth of about 73°. Finally, elements 1 and 4 will

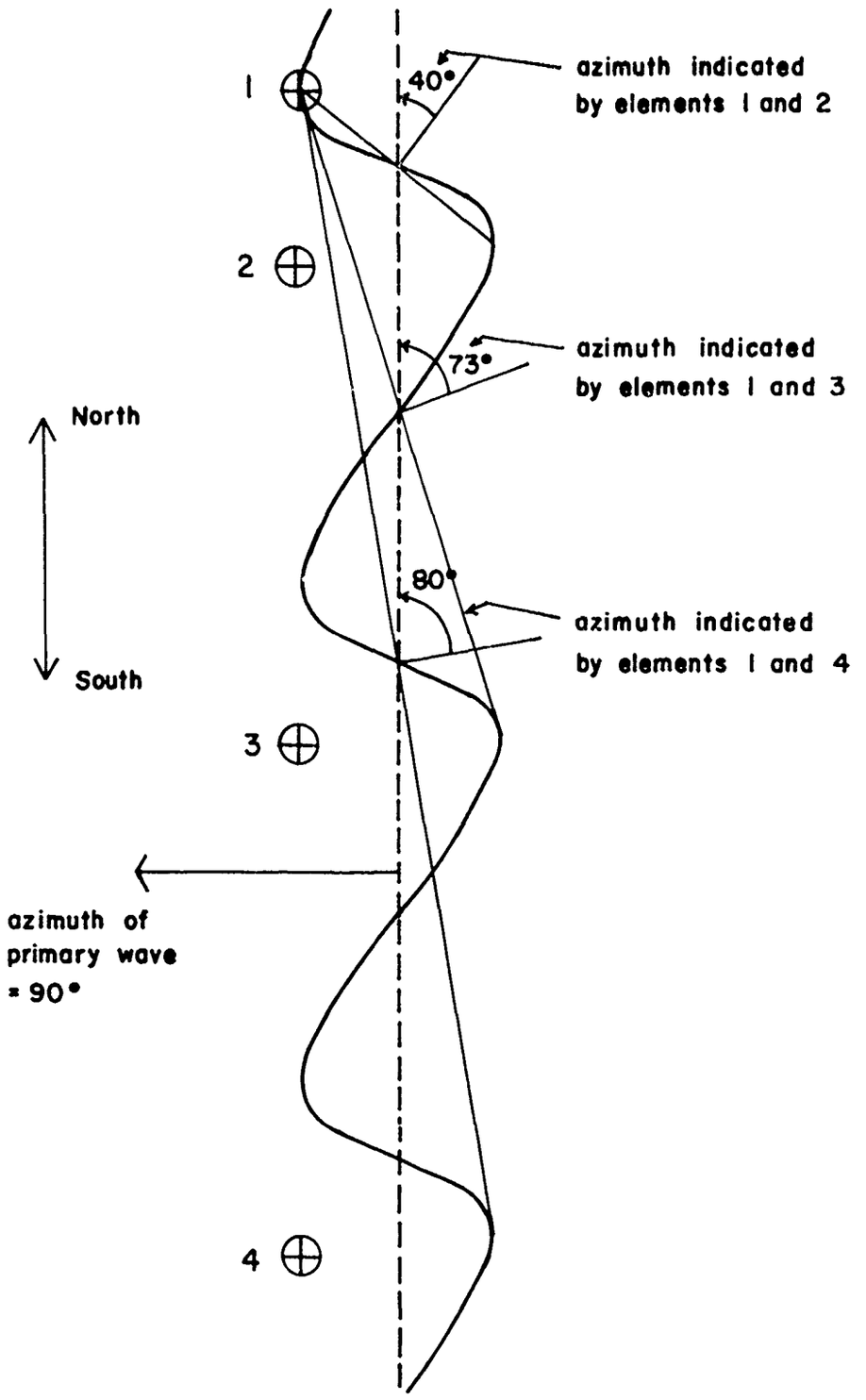

Figure 15. Increasing Accuracy of an Interferometer Array by Increasing the Array Baseline

indicate an azimuth of 80°, very close to the azimuth of the primary wave (90°). Note that the antenna elements have deliberately been positioned at "worst-case" points on the corrugated waveform. That is, they are positioned such that one element is at a crest of the corrugated wavefront while the other is at a trough. The deviation of the indicated DOA from the DOA of the primary wave must be at a maximum under these conditions. Evidently the greater the array baseline, the less will be the deviation of the indicated DOA from that of the primary wave. As previously mentioned, it is therefore desirable to keep the interferometer baseline as long as possible, thus reducing the deviation of indicated DOA due to wave interference. It should be realized that although the above paragraph has considered a two-dimensional (2-element) interferometer system, the results should hold equally well for the triple interferometer.

The effects of multimode wave interference on a triple interferometer system can be studied with the aid of a hemispherical projection plot. In Appendix G are shown a number of such wave interference plots. The computer program listing that performed this simulation appears at the beginning of Appendix G. Because the DOA fluctuations are confined to a small area on the hemispherical projection, only the appropriate section of the plot is drawn. The orientation of this section is maintained relative to the total plot such that the azimuth indicated by any point on the plot is readily identifiable. Furthermore, the coaxial, dotted, semicircular lines in the plot represent vertical incidence angles, and are labelled in degrees. The orientation of these sections and the vertical incidence angle lines completely specify the position that the section of the hemispherical projection plot occupies in the

total hemispherical projection. The DOA trajectories are formed by computing the DOA under wave interference conditions using the equations presented earlier in this chapter. A number of DOA's are plotted, each corresponding to different values of ϕ_d, while all other parameters are held constant. ϕ_d is varied incrementally in steps of about 11.5° from 0° to 360°. This is the path of DOA variation as indicated by a triple interferometer under ϕ_d-variant (multimode) wave interference conditions. Two trajectories are drawn per plot. The trajectory that indicates the smaller DOA fluctuation corresponds to an interferometer with a baseline-to-wavelength ratio of 1. The other trajectory corresponds to an interferometer with a baseline-to-wavelength ratio of 1/2. The DOA of the primary wave is denoted in each plot by the large X.

The first three plots (figures G-1 through G-3) show the various shapes of the DOA trajectories for three different angles between the two interfering waves. The next three plots (figures G-3 through G-5) illustrate the effect that increasing the relative amplitude of the interfering (secondary) wave has on the DOA variation. Finally, the latter 4 plots (figures G-6 through G-9) demonstrate the relationship between the isosceles triple interferometer array angle (γ) and the extent of DOA variation. In examining these plots, it is important to note the scale at which they are drawn. Even very small sections of the hemispherical projection plot will be drawn so as to fill the whole page.

Several general conclusions can be drawn from these (and other) plots concerning the effects of wave interference on an interferometer system. First of all, it is obvious that, as the relative phase difference between the interfering waves (ϕ_d) varies, the indicated DOA will vary. It will follow a closed trajectory that is repeated as ϕ_d

varies through multiples of 360^{o}. These trajectories generally "encircle" the DOA of the primary wave. They are not of any specific shape. The extent to which the indicated DOA's will vary increases with the angle between the DOA's of the two interfering waves and the relative amplitude of the two interfering waves. It decreases as the array angle is increased. This latter observation is not surprising if it is realized that decreasing the array angle greatly decreases the effective aperture of the system. The distance between two of the array elements is reduced, thus making the system more susceptible to the effects of wave interference. This observation is pertinent because it shows that though a small array angle interferometer system may be attractive from the ambiguity resolution standpoint (see Appendix C), it is even more unattractive from the standpoint of wave interference susceptibility. Finally, it is evident that the extent of DOA fluctuation decreases as the array baseline is increased. A more thorough treatment of the effect of array baseline length on interferometer wave interference errors is presented by Talbott.[5]

An examination of Table 1, tabulated from data generated by the aforementioned plotting program, indicates that a sample mean of the 32 computed azimuth and incidence angles yielded an average DOA that was somewhat close to the DOA of the primary wave. On the other hand, a similar sample mean of each of the three interferometer phases yielded a DOA that was very close to that of the primary wave. This is in agreement with Glick's results.

As suggested at the end of Chapter VI, it is necessary to make both the small and large interferometer arrays as accurate as possible. The small array must be made as accurate as possible in order that it can

Table 1

Data Tabulated from Wave Interference Simulation Program

Concerning Averaged DOA's and DOA's Calculated from

Averaged Phases. (D/L = .5)

	Pri Wave		Sec Wave		REL	ARRAY	AVG DOA		DOA FRM AVG PHASES	
	AZ	INC	AZ	INC	AMP	ANGLE	AZ	INC	AZ	INC
Plot 6-2	310°	20°	315°	30°	.5	90°	309.4°	20.16°	310.0°	20.06°
Plot 6-3	310°	20°	315°	45°	.5	90°	308.9°	20.96°	310.0°	20.12°
Plot 6-4	310°	20°	315°	45°	.25	90°	309.7°	20.20°	310.0°	20.08°
Plot 6-5	310°	20°	315°	45°	.75	90°	268.1°	24.57°	310.0°	20.17°
Plot 6-6	310°	20°	315°	45°	.5	60°	305.8°	20.52°	310.0°	20.13°
Plot 6-7	310°	20°	315°	45°	.5	45°	305.1°	20.47°	310.0°	20.13°
Plot 6-8	310°	20°	315°	45°	.5	25°	306.8°	20.55°	310.0°	20.13°
Plot 6-9	310°	20°	310°	50°	.45	5°	300.9°	20.60°	310.0°	20.14°

be used to correctly resolve ambiguities over the widest possible range of operating wavelengths. It therefore makes sense that the small array phases should be time averaged, just as the large array phase should be averaged to enhance the system accuracy. After these two sets of phases have been averaged over a period of time that is long enough to "remove" the wave interference effects, the phase ambiguity resolution procedure may be carried out using these averaged values. An alternative approach that has been suggested is to take instantaneous phase readings from the two arrays and carry out the phase ambiguity resolution procedure immediately. Many of these "phase ambiguity resolved" (large interferometer) phases may then be averaged to remove the wave interference error.

With some thought it can be seen that this second technique is not completely reliable. The problem with this method stems from the fact that the effects of wave interference will change the value of each small interferometer phase by a certain amount in one direction from the proper (primary wave) value, while the corresponding large interferometer phase may be changed to a much lesser extent. In fact, the large array phase may be changed in the other direction entirely. This case is illustrated in two dimensions in figure 16. Because these small and large array phase measurements are no longer proportional, there is a strong possibility that the phase ambiguity resolution procedure will fail. If there is no way to determine when the resolution fails and when it succeeds, the failures will decrease the accuracy of the final averaged interferometer phase values.

There also exists a problem with the first method, but this one is surmountable. Averaging the measured large baseline interferometer

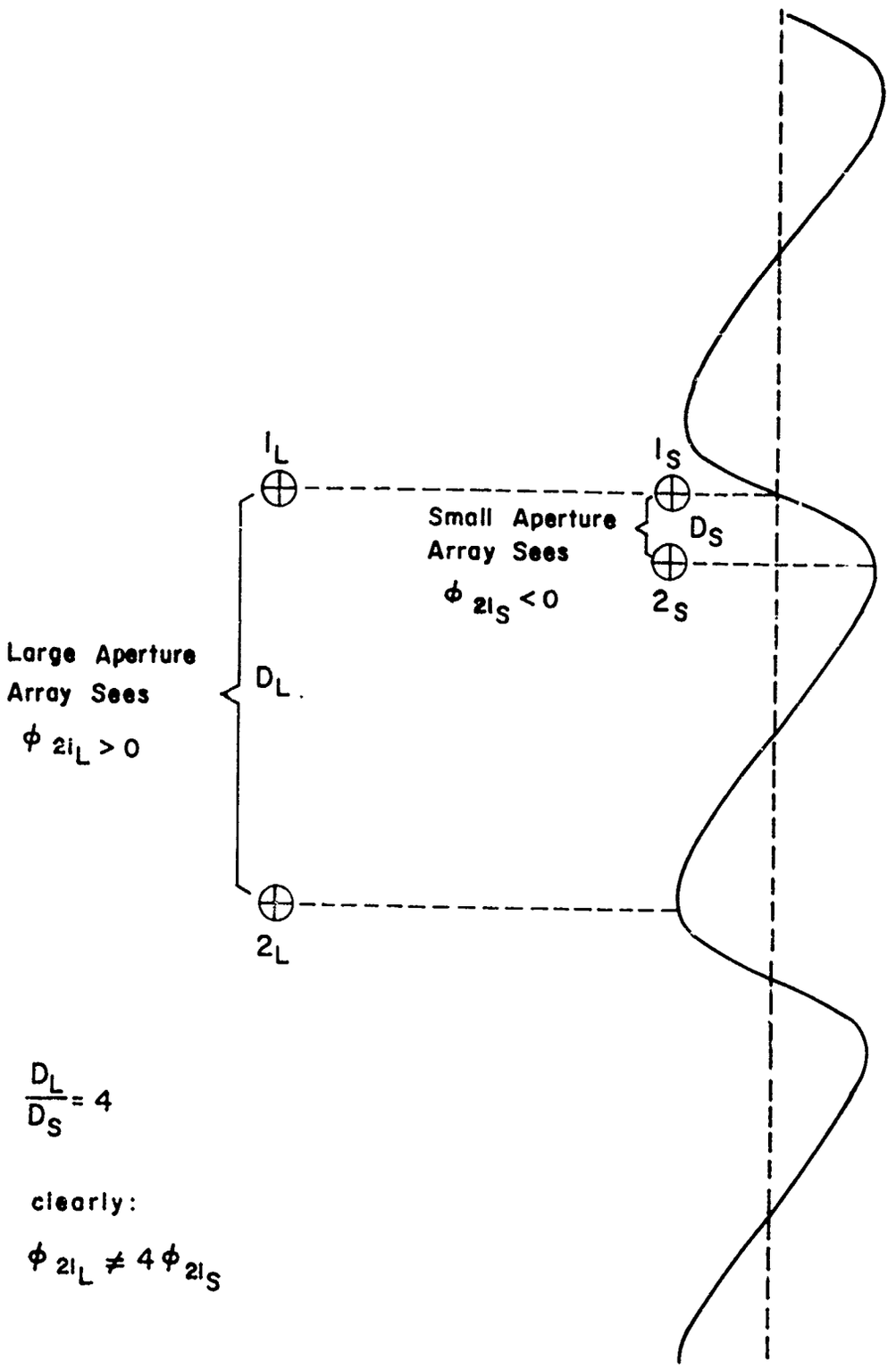

Figure 16. Disproportionate Effects of Wave Interference on a Small/Large Baseline Interferometer System

phases directly (as measured in the range of - 180° to + 180°) is quite useless. A proper "branch cut" must be chosen. To understand what is meant by this, one must go back to the discussion of Chapter 1, which demonstrates that any phase difference of two sinusoids can be expressed by an angle that lies within any arbitrarily selected 360° range. (See equation I-4.) This 360° range of angles (or branch cut) must be chosen so as to permit averaging of a continuous interferometer phase versus time curve.[6] Such a branch cut will always exist, since, as shown at the beginning of this chapter, the interferometer phase variation is confined to a 360° interval. A solution to the problem of suitable branch cut selection was proposed by Grush in 1965.[7] A faster and more dependable branch cut selection algorithm was introduced by Allen in 1966.[8] Both methods are iterative procedures which require the use of a digital computer.

The temptation to use the "instantaneous phase resolution method" (ambiguity resolution before averaging the interferometer phases) has been great. No branch cut problem exists in this case, as the interferometer phase measurement samples are automatically made continuous after phase ambiguity resolution, assuming the resolution has been carried out successfully for each sample. Unfortunately, the phase ambiguity resolution is not always successful.

To further illustrate this problem, and hence the desirability of using the "average phase resolution method" (phase ambiguity after averaging both the interferometer phases), both methods were simulated on the G-20 digital computer. The wave interference simulation program used in Appendix G was modified to perform this task. The modified program listing and two sample runs are included in Appendix H. In the

first sample run, Table H-1, the relative amplitude of the secondary wave with respect to the primary wave was chosen such that the wave interference effects were not too severe. (See figures F-1 and G-4.) Both methods yielded the correct primary DOA. In the second run, Table H-2, the effects of the wave interference were more severe. (See figures F-3 and G-5.) The instantaneous phase resolution method fails to indicate the correct primary DOA. This is due, as hypothesized, to the occasional failure of the instantaneous phase ambiguity resolution procedure. Such failures can be discerned in the second sample run by noticing the occasional discontinuities in the interferometer phases in the column labelled "RESULTS INST PHASE AMBIGUITY RESOLUTION."

To determine how often the instantaneous phase resolution method might be expected to fail, the program of Appendix H was modified to run for many different combinations of interference conditions and system parameters. A listing of the modified program as well as the program output appears in Appendix I. The first 5 columns in the Tables (program output) describe the wave interference conditions. It should be noted that the secondary wave DOA is expressed in terms of its deviation from that of the primary wave DOA. The next 3 columns describe the system parameters. "SM D/L" denotes the value of D_S/λ, the small array baseline-to-wavelength ratio. Likewise, "LG D/L" denotes the large array baseline-to-wavelength ratio. The remaining 4 columns in the program output contain the results of the two different methods of phase ambiguity resolution. It should be emphasized that the two phase ambiguity resolution procedures are carried out in exactly the same manner as in Appendix H (using 36 phase measurement samples distributed over one period of ϕ_d variation), except that the intermediate steps are

not printed in order to conserve space.

In Table I-1, the primary DOA is varied while all other parameters are held constant. As expected, the average phase resolution method was always successful; however, the instantaneous resolution method failed over 50 percent of the time! It should be noted that the failures are not very severe. Often the indicated DOA differs from the actual primary DOA by not more than a few degrees. This is because only a few of the 36 phase measurements have been erroneously ambiguity resolved. For this reason, it is likely that one who has chosen to use the instantaneous phase resolution method may not realize that there is anything wrong with the results obtained.

In Table I-2, the primary DOA has been held constant, but the secondary DOA has been varied. Once again the instantaneous resolution method fails occasionally. It appears to fail for the cases where the deviation between the DOA's of the interfering waves is relatively large.

In Table I-3, the relative amplitude between the interfering DOA's (h) has been varied. As would be expected, the instantaneous resolution method fails for the larger values of the relative amplitude.

In Table I-4, the small and large array baseline-to-wavelength ratios have been varied. As would be expected from the discussion at the beginning of Chapter VI, the instantaneous resolution method is more successful for smaller ratios of large array baseline to small array baseline (D_L/D_S). A further generalization that is not so obvious may be drawn from this tabulation. It appears that for a given value of L_L/D_S, the instantaneous phase resolution method is more likely to succeed for larger wavelengths. Look, for example, at how the instantaneous resolution method succeeds for a small D/λ of .1 and a large D/λ

of 1, but not for a small D/λ of .3 and a large D/λ of 3, etc. However, previous work has indicated that the effects of wave interference are greater for larger wavelengths. This is because increasing the wavelength for a given D_L/D_S value results in lower values of both D_L/λ and D_S/λ. Hence both the small and large array are more subject to the effects of wave interference for larger wavelengths.

In a like manner, it is interesting to note from Table I-5 that the instantaneous phase resolution process becomes more successful for smaller array angles. (Of course, both the small and large isosceles arrays must be of the same angle.) This is again contrary to what might be expected, as it has been shown earlier in this chapter that the effects of wave interference increase as the array angle decreases.

The observations of the preceding two paragraphs lead to an interesting conclusion which can be further verified geometrically. Either increasing the operating wavelength or decreasing the array angle results in a proportionate decrease in the effective aperture of both the small and large arrays. Consequently, the results of Tables I-4 and I-5 indicate that decreasing the effective array apertures in a small/large baseline interferometer system results in greater phase deviations of both arrays due to wave interference; however, these relatively large deviations are more closely proportional than they are in larger aperture systems. Hence (with regard to instantaneous phase measurements), equation VI-3 becomes less of an approximation and more of an equality as the small and large array apertures are proportionately decreased. (Of course the overall system accuracy will suffer with the decrease in array aperture.) The general validity of these results can be investigated geometrically by reconsidering the case of a two-dimensional, two-

element interferometer system as in figure 16. In figure 17 it is seen that because the corrugated phase pattern "looks" somewhat plane to the small aperture system, while the large system sees a corrugated wavefront, the small system's corresponding small and large array phases are more nearly proportional. It should be noted that this conclusion is only valid if the portion of the corrugated wavefront intercepted by the small aperture system is a small fraction of a period of wave corrugation variation. To further illustrate this fact, Tables I-4 and I-5 were regenerated (see Tables I-6 and I-7), using interfering waves that arrived from more diverse directions of arrival. This implies that the wave corrugation pattern will be much finer, as predicted by equation VI-9. (See figure 18.) Now the small aperture system sees a corrugated wavefront as well, and the above conclusion is no longer valid; in fact, the originally expected conclusion now appears more valid.

It should be pointed out that the preceding simulation studies have been based on the assumption of uniform sampling of the interferometer phases throughout one period of ϕ_d variation. In practice, sampling is not uniform with respect to ϕ_d, but rather with respect to time. Hence the approximate assumption of ϕ_d variation that is linear with respect to time has been tacitly implied. Of course, even if ϕ_d is not varying in a strictly linear fashion with respect to time, the instantaneous phase resolution method will fail in exactly the same manner.

All of the preceding discussion in this chapter has dealt with the removal of the effects of wave interference in which the relative phase between the interfering signals is time-variant (such as under multimode propagation conditions or under conditions of adjacent channel interference). In cases in which the relative phase between the interfering

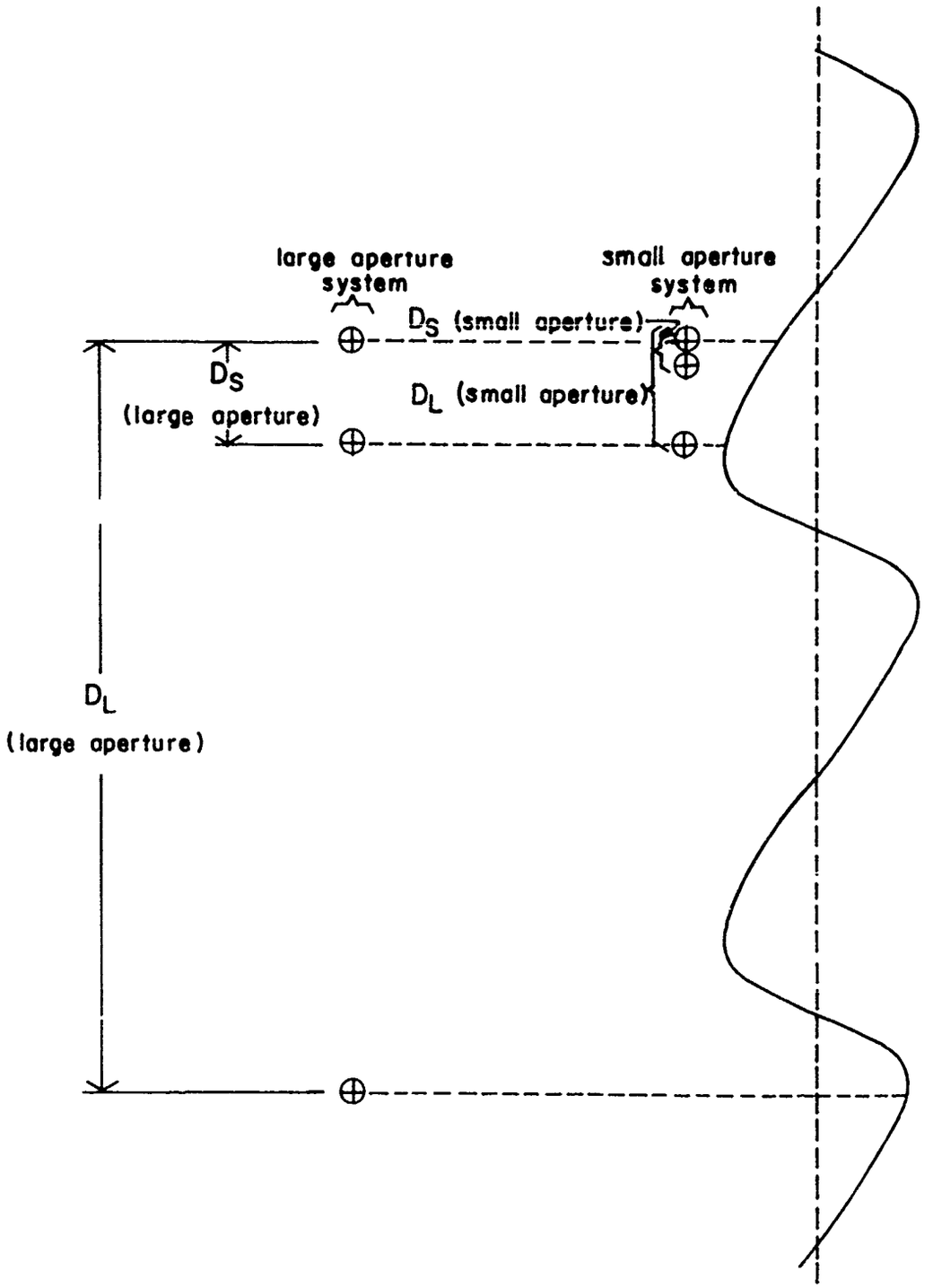

Figure 17. Comparison of Phase Proportionality in Small Aperture and Large Aperture Small/Large Baseline Arrays (Case 1)

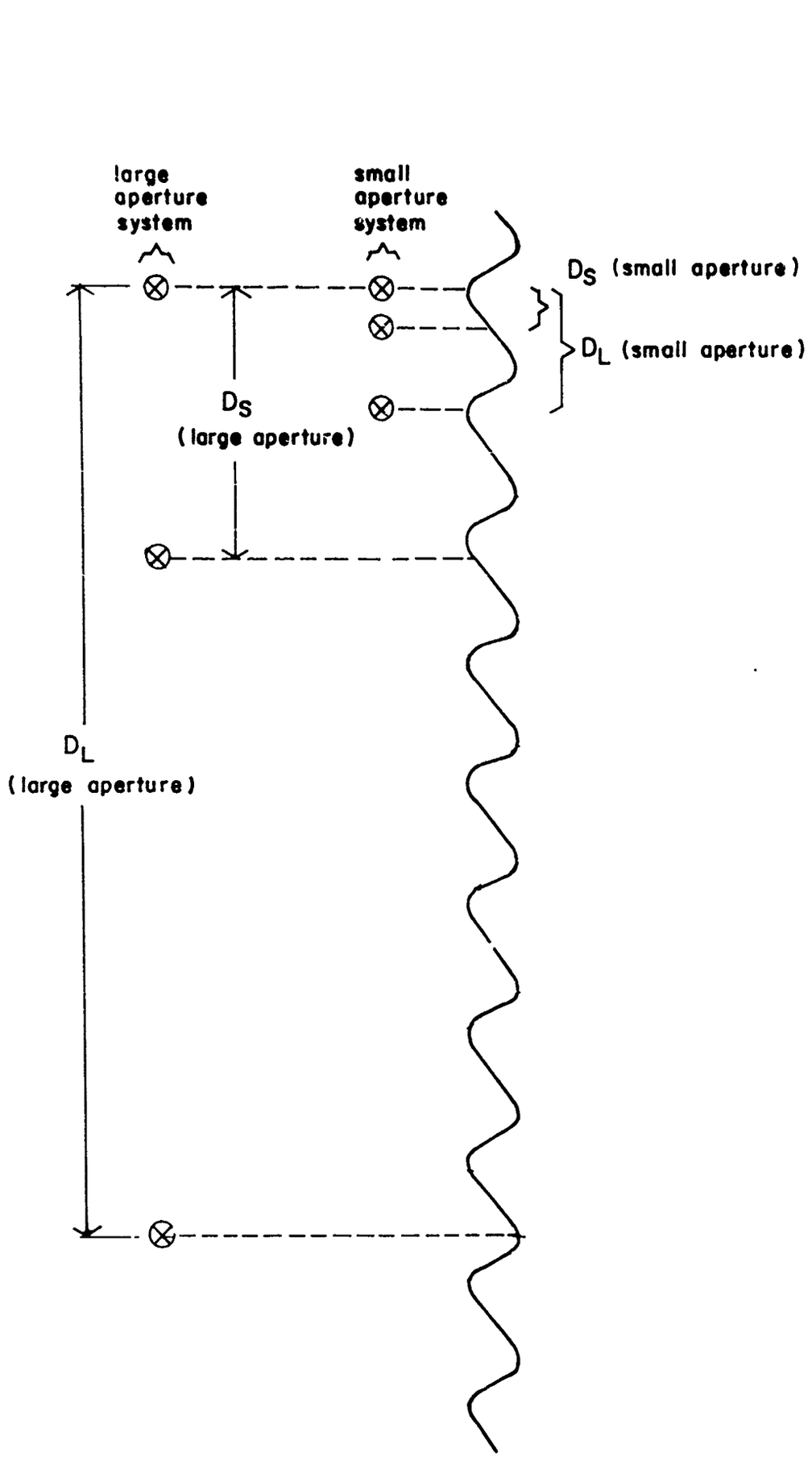

Figure 18. Comparison of Phase Proportionality in Small Aperture and Large Aperture Arrays (Case 2)

waves is constant, such as in a situation in which a siting error exists, time averaging of the interferometer phases will not remove the wave interference error. This results in degradation of ambiguity resolution capability as well as system accuracy. Of course, increasing the large array baseline will still result in a reduction of the effects of wave interference. However, the array baseline cannot be made too large, lest the task of ambiguity resolution become impossible.

In an azimuth-only (two-dimensional) RDF system, attempts have been made to correct the siting error by making many azimuth measurements of signals emanating from known DOA's. A calibration curve of the indicated DOA versus the siting error-corrected DOA may then be constructed. However it seems somewhat doubtful that this method is very reliable. It has been shown that the extent of the wave interference effects (and hence siting error) depends upon the angle between the interfering waves. It is likely that the RDF system has been "calibrated" using signals with a 90° incidence angle, as the calibration source is probably a transmitter placed at the ground level. For signals arriving from smaller incidence angles, it is likely that the nature of the siting error will differ, as the relative angles between the interfering waves have changed. Hence, such an RDF system which has had the siting error "calibrated out" of it in this manner will be accurate only for waves with an incidence angle near 90°. Nevertheless, it seems theoretically sound that the siting errors could be successfully "calibrated out" of a three-dimensional RDF system in this manner. But this would be practically impossible, as measurements of many known azimuth and incidence angles would be necessary.

FOOTNOTES

1. M. I. Glick, "Studies in Time Averaging and Wave Interference in Radio Direction Finding," Master's Thesis, University of Illinois, Urbana, Illinois, June 1966, Chapter 2. (RRL Publication No. 312.)

2. J. B. Church, "A Digital Bearing Computer for an Interferometer RDF System," Master's Thesis, University of Illinois, Urbana, Illinois, January 1967, Chapters 2 and 3.

3. Glick, op. cit., pp. 12-15.

4. H. L. Grush, "An Investigation of a Di .tal Bearing Computer for a Small Aperture Radio Direction Finding System," Ph.D. Thesis, University of Illinois, Urbana, Illinois June 1965, p. 27. (RRL Publication No. 280.)

5. C. R. Talbott, "Aperture Size Effects in a HF Interferometer RDF System," Master's Thesis, University of Illinois, Urbana, Illinois, August 1970. (RRL Publication No. 375.)

6. L. C. Allen, "Improved Digital Bearing Computer Techniques," Master's Thesis, University of Illinois, Urbana, Illinois, June 1966, p. 9. (RRL Publication No. 314.)

7. Grush, op. cit., pp. 19-23.

8. Allen, op. cit., p. 9.

VIII. REDUCTION OF THE EXTENT OF PHASE MEASUREMENT ERROR

This chapter describes techniques which have been used to improve system performance by increasing the accuracy of the interferometer phase measurements. One of the major problems in the interferometer phase measurement process lies not in the phase meter itself, but in keeping the separate signal paths in the multichannel receiver of the same effective electrical length. (This was discussed in Chapter VI.) The solution to this problem seems somewhat obvious in retrospect. At regular intervals a common calibration signal is applied to the input of each receiver channel. As the receiver phase delay characteristics vary with time, it is likely that the receiver channels will not remain at exactly the same effective length. Consequently the phase difference readings taken at the outputs of the multichannel receiver may differ greatly from the expected value of zero degrees. The phase differences measured in this manner are known as "calibration phases." Any subsequent interferometer phase measurements may then be corrected for this type of systematic error by merely subtracting the appropriate calibration phase from them. New calibration phases must be obtained at a rate proportional to the rate at which the receiver phase delay characteristics are changing.[1]

Another type of error in the phase measurement process is caused by noise transients, as discussed in Chapter VI. It appears that phase averaging is the solution to this problem. Furthermore, it has been shown in Chapter VI that a three-channel receiver may have distinct advantages over a two-channel receiver in a transient noise environment.

Even after the above phase measurement error reduction techniques have been applied, some error remains. If the phase measurements were

error-free, their sum (after successful phase ambiguity resolution) would equal zero, as demonstrated in Chapter I. (See equation I-3.) A look at some real interferometer phase data (see Appendix J) reveals that the sum of the interferometer phases is rarely zero. In this case each ambiguity resolved, measured phase may be written as $\phi_{ij} = \phi_{ij}^{\text{actual}} + \Delta_{ij}$, where Δ_{ij} denotes the error incurred in the measuring process. Therefore, in practice, equation I-3 must be written as:

$$\phi_{21} + \phi_{13} + \phi_{32} = \phi_{21}^{\text{actual}} + \phi_{13}^{\text{actual}} + \phi_{32}^{\text{actual}}$$

$$+ \Delta_{21} + \Delta_{13} + \Delta_{32} = (\Delta_{21} + \Delta_{13} + \Delta_{32}) = \Delta. \qquad \text{(VIII-1)}$$

One might be tempted to assume that the closer Δ is to zero, the more accurate the phase measurements are. Because the individual Δ_{ij}'s may be either positive or negative, this assumption is questionable. The individual phase measurement errors, Δ_{ij}, may be large, and yet Δ could be very close to zero. This will be the case if two or all of the Δ_{ij}'s are large and of opposite sign such that their sum is relatively small. If $|\Delta|$ is large, it is certain that at least one of the phase measurements is inaccurate. On the other hand, a small value of $|\Delta|$ is a necessary but not a sufficient indication of low phase measurement error.

For non-zero values of Δ, the DOA equations (equations I-2) are no longer equivalent. It is impossible to determine in which phase (or phases) the phase measurement error has been made. Consequently, one has no way of knowing which two of the three interferometer phases (and

correspondingly, which equation in equations I-2) should be used to obtain the most accurate DOA. It is apparent that the smaller Δ is, the more equivalent equations I-2 become; hence, the choice of which two phases should be used to calculate the DOA is not as important. However, as noted in the preceding paragraph, this does not necessarily imply that the phase measurements have been made accurately.

As can be seen from the real data samples of Appendix I, the sum of the averaged phases is always relatively close to 0, as contrasted with the sums of the individual unaveraged phases. This is an indication that phase averaging does indeed reduce the extent of phase measurement error. If sufficient phase measurements have been averaged such that Δ is within a few degrees of zero, it will essentially not matter which of the three phases are used in the DOA calculations. Of course, this can be done only if the signal is present for a sufficiently long time.

If $|\Delta|$ remains appreciably large after phase averaging, the interferometer phases may be taken two at a time and used to calculate three distinct directions of arrival. Figure 19 illustrates this process, and shows the three DOA's plotted on a section of a hemispherical projection. Because it is not known which of these DOA's is more accurate, it seems that the most logical choice of the indicated DOA is at the centroid of the triangle formed by the three calculated DOA's. This DOA is determined by vector averaging the three calculated DOA's. If the three indicated azimuths are given by α_{21-32}, α_{21-13}, and α_{32-13}, as in equations I-2, the vector average of the indicated azimuths is given as:

$$\alpha_{avg} = \tan^{-1}\left\{\frac{\sin \alpha_{21-32} + \sin \alpha_{21-13} + \sin \alpha_{32-13}}{\cos \alpha_{21-32} + \cos \alpha_{21-13} + \cos \alpha_{32-13}}\right\}. \quad \text{(VIII-2)}$$

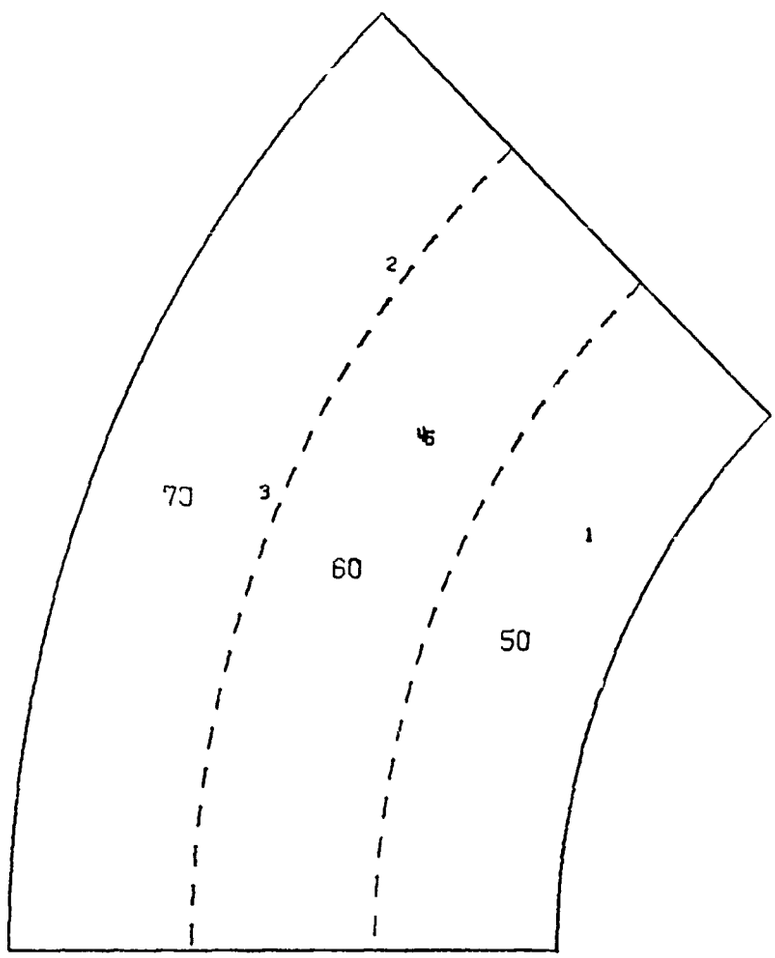

$D/\lambda = 8$ $\gamma = 60°$

$\phi_{21} = 1000°$ $\phi_{13} = 1000°$ $\phi_{32} = -2500°$

$\Delta = \phi_{21} + \phi_{13} + \phi_{32} = -500°$

1 DOA indicated by ϕ_{21} and ϕ_{32}

2 DOA indicated by ϕ_{21} and ϕ_{13}

3 DOA indicated by ϕ_{32} and ϕ_{13}

4 Estimated DOA (Angle avging. method)

5 Estimated DOA (Delta method)

Figure 19. Graphical Comparison of Two Methods of Processing Erroneous Interferometer Phase Data

It should be noted that this method of azimuthal averaging requires substantial computation. The three individual azimuths must first be computed, then their average taken. It turns out that the expression for the average incidence angle simplifies in such a way that it may be computed directly from the interferometer phases. Vector averaging the expressions of equation I-2 for θ_{21-32}, θ_{21-13}, and θ_{32-13} (as in equation VIII-2) yields:

$$\theta_{avg} = \sin^{-1} \left\{ \frac{\sqrt{\phi_{21}^2 + \phi_{32}^2 + \phi_{13}^2}}{\left(\frac{2\pi D}{\lambda}\right)\sqrt{3/2}} \right\} . \qquad \text{(VIII-3)}$$

A less tedious method of azimuth computation would be useful from the standpoint of system speed. Such a method has been suggested by E. K. Walton.[2] Assume that the sum of the interferometer phase measurements is Δ, as in equation VIII-1. Subtracting $\Delta/3$ from each of the phase measurements such that:

$$\phi_{ij}' = (\phi_{ij} + \Delta_{ij}) - \Delta/3 \qquad \text{(VIII-4)}$$

will re-establish the condition of equation I-3, that is:

$$\phi_{13}' + \phi_{32}' + \phi_{21}' = 0. \qquad \text{(VIII-5)}$$

Using any two of these "corrected" phase values ϕ_{ij}', the appropriate formula from equations I-2 may be used to compute the azimuth. Because equations I-2 are again equivalent, angle averaging is no longer necessary. The required azimuth computation is greatly reduced.

The results of these two methods are plotted in figure 19. Both methods appear to give answers which are equally acceptable. It is the object of the work that will follow to examine the equivalence of these two methods. It is shown in Appendix K that if:

$$\tan \alpha_{21-32} = y_1/x_1, \tan \alpha_{21-13} = y_2/x_2, \tan \alpha_{32-13} = y_3/x_3, \quad \text{(VIII-6)}$$

then the first method described (called the angle averaging method) implies that:

$$\alpha_{avg} = \tan^{-1} \frac{y_1/r_1 + y_2/r_2 + y_3/r_3}{x_1/r_1 + x_2/r_2 + x_3/r_3}, \quad \text{(VIII-7)}$$

where $r_i = \sqrt{x_i^2 + y_i^2}$.

On the other hand, the second, faster method (called the delta method) implies that:

$$\alpha_\Delta = \tan^{-1} \frac{y_1 + y_2 + y_3}{x_1 + x_2 + x_3}. \quad \text{(VIII-8)}$$

Making use of figure K-1 (in Appendix K) and equations VIII-1 and VIII-7, it may be shown that:

$$r_1 = 2\sqrt{\phi_{13}^2 + \phi_{21}\phi_{13} + \phi_{21}^2}$$

$$r_2 = 2\sqrt{\phi_{13}^2 + \phi_{21}\phi_{13} + \phi_{21}^2 + [\Delta^2 - 2\Delta\phi_{13} - \Delta\phi_{21}]} \quad \text{(VIII-9)}$$

$$r_3 = 2\sqrt{\phi_{13}^2 + \phi_{21}\phi_{13} + \phi_{21}^2 + [\Delta^2 - \Delta\phi_{13} - 2\Delta\phi_{21}]}.$$

Hence, for small $|\Delta|$, $r_1 \simeq r_2 \simeq r_3$, and equations VIII-7 and VIII-8 imply that:

$$\alpha_{avg} \simeq \alpha_\Delta. \quad \text{(VIII-10)}$$

To get a feeling for just how large $|\Delta|$ might be before the two methods are no longer comparable, a more inductive type of investigation was carried out, utilizing the G-20 digital computer. Both methods were "programmed," and erroneous phase measurement data were processed using both methods. Most of the erroneous data was simulated in order to maintain control of the error distribution over the three interferometer phases. (See Appendix L.) However, some of the data was real, taken at the triple interferometer RDF station at the University of Illinois' Monticello Road Field Station. (See Appendix J.) From the computer simulation results, it is apparent that even for rather large values of $|\Delta|$, equation VIII-9 holds.

FOOTNOTES

1. J. J. Henderson, "Mismatch Correction Techniques for Twin-Channel Receivers," August 1965. (RRL Publication No. 282.)

2. E. K. Walton, from a private communication at this laboratory.

IX. CONCLUSION

The basic principles of operation of the triple radio interferometer RDF system have been discussed. Particular attention has been paid to the ambiguity resolution portion of the system. It has been shown that phase ambiguity resolution offers advantages over direction ambiguity resolution. The factors that influence system accuracy have been examined and suggestions have been made on how to minimize the effects of these factors. Some of these suggestions are commonly used in modern interferometer systems. Some have not yet been tried. It seems that further work in this area should involve experimental work in which some of the theoretical points raised in this study are further checked for validity.

APPENDIX A

This appendix contains sample output from the computer program flow-charted in figure 6. This program is capable of tabulating all possible ambiguities indicated by a simple interferometer system for any given direction of arrival and baseline/wavelength value. The samples included in this appendix were particularly chosen to demonstrate how the number of ambiguities varies with D/λ and with the direction of arrival, as discussed in Chapter IV.

Table A-1. List of Direction Ambiguities (D/λ = 1)

BASELINE = 100.0 WAVELENGTH = 100.0 PHI21 = -58.74 PHI13 = 47.89 PHI32 = 10.86

ACTUAL DIRECTION OF ARRIVAL..... AZIMUTH = 200.00 INCIDENCE = 10.00 GAMMA = 60.00

AMBIGUITY NO. 1 PHI21+2 PI* 0 PHI32+2 PI* 0 ALPHA = 200.00 THETA = 10.00
AMBIGUITY NO. 2 PHI21+2 PI* 1 PHI32+2 PI* 0 ALPHA = 31.76 THETA = 79.79
**** BLOCK ADDRESS: 052

Table A-2. List of Direction Ambiguities (D/λ = 2)

BASELINE = 200.0 WAVELENGTH = 100.0 PHI21 = -117.49 PHI13 = 95.78 PHI32 = 21.71

ACTUAL DIRECTION OF ARRIVAL..... AZIMUTH = 200.00 INCIDENCE = 10.00 GAMMA = 60.00

AMBIGUITY NO.	1	PHI21+2 PI*	-1	PHI32+2 PI*	0	ALPHA =	207.69	THETA =	48.50
AMBIGUITY NO.	2	PHI21+2 PI*	-1	PHI32+2 PI*	1	ALPHA =	160.93	THETA =	44.56
AMBIGUITY NO.	3	PHI21+2 PI*	0	PHI32+2 PI*	-1	ALPHA =	255.63	THETA =	41.10
AMBIGUITY NO.	4	PHI21+2 PI*	0	PHI32+2 PI*	0	ALPHA =	200.00	THETA =	10.00
AMBIGUITY NO.	5	PHI21+2 PI*	0	PHI32+2 PI*	1	ALPHA =	107.49	THETA =	32.89
AMBIGUITY NO.	6	PHI21+2 PI*	1	PHI32+2 PI*	-2	ALPHA =	290.00	THETA =	80.00
AMBIGUITY NO.	7	PHI21+2 PI*	1	PHI32+2 PI*	-1	ALPHA =	314.06	THETA =	28.97
AMBIGUITY NO.	8	PHI21+2 PI*	1	PHI32+2 PI*	0	ALPHA =	34.24	THETA =	24.05
AMBIGUITY NO.	9	PHI21+2 PI*	1	PHI32+2 PI*	1	ALPHA =	67.34	THETA =	60.94
AMBIGUITY NO.	10	PHI21+2 PI*	2	PHI32+2 PI*	-1	ALPHA =	355.94	THETA =	57.03
AMBIGUITY NO.	11	PHI21+2 PI*	2	PHI32+2 PI*	0	ALPHA =	31.76	THETA =	79.79

Table A-3. List of Direction Ambiguities (D/λ = 3)

BASELINE = 300.0 WAVELENGTH = 100.0 PHI21 = -176.23 PHI13 = 143.66 PHI32 = 32.57

ACTUAL DIRECTION OF ARRIVAL..... AZIMUTH = 200.00 INCIDENCE = 10.00 GAMMA = 60.00

AMBIGUITY NO.	1	PHI21+2 PI*	-2	PHI32+2 PI*	0	ALPHA =	208.16	THETA =	70.27
AMBIGUITY NO.	2	PHI21+2 PI*	-2	PHI32+2 PI*	1	ALPHA =	184.09	THETA =	56.30
AMBIGUITY NO.	3	PHI21+2 PI*	-2	PHI32+2 PI*	2	ALPHA =	158.58	THETA =	63.05
AMBIGUITY NO.	4	PHI21+2 PI*	-1	PHI32+2 PI*	-1	ALPHA =	232.05	THETA =	53.85
AMBIGUITY NO.	5	PHI21+2 PI*	-1	PHI32+2 PI*	0	ALPHA =	206.90	THETA =	33.83
AMBIGUITY NO.	6	PHI21+2 PI*	-1	PHI32+2 PI*	1	ALPHA =	165.00	THETA =	30.93
AMBIGUITY NO.	7	PHI21+2 PI*	-1	PHI32+2 PI*	2	ALPHA =	133.79	THETA =	45.85
AMBIGUITY NO.	8	PHI21+2 PI*	0	PHI32+2 PI*	-2	ALPHA =	258.87	THETA =	57.68
AMBIGUITY NO.	9	PHI21+2 PI*	0	PHI32+2 PI*	-1	ALPHA =	249.83	THETA =	28.25
AMBIGUITY NO.	10	PHI21+2 PI*	0	PHI32+2 PI*	0	ALPHA =	200.00	THETA =	10.00
AMBIGUITY NO.	11	PHI21+2 PI*	0	PHI32+2 PI*	1	ALPHA =	116.62	THETA =	21.35
AMBIGUITY NO.	12	PHI21+2 PI*	0	PHI32+2 PI*	2	ALPHA =	102.94	THETA =	46.79
AMBIGUITY NO.	13	PHI21+2 PI*	1	PHI32+2 PI*	-2	ALPHA =	284.96	THETA =	41.23
AMBIGUITY NO.	14	PHI21+2 PI*	1	PHI32+2 PI*	-1	ALPHA =	304.04	THETA =	17.69
AMBIGUITY NO.	15	PHI21+2 PI*	1	PHI32+2 PI*	0	ALPHA =	38.02	THETA =	12.47
AMBIGUITY NO.	16	PHI21+2 PI*	1	PHI32+2 PI*	1	ALPHA =	71.81	THETA =	33.04
AMBIGUITY NO.	17	PHI21+2 PI*	1	PHI32+2 PI*	2	ALPHA =	79.33	THETA =	66.74
AMBIGUITY NO.	18	PHI21+2 PI*	2	PHI32+2 PI*	-3	ALPHA =	301.27	THETA =	75.95
AMBIGUITY NO.	19	PHI21+2 PI*	2	PHI32+2 PI*	-2	ALPHA =	318.57	THETA =	42.18
AMBIGUITY NO.	20	PHI21+2 PI*	2	PHI32+2 PI*	-1	ALPHA =	353.27	THETA =	30.46
AMBIGUITY NO.	21	PHI21+2 PI*	2	PHI32+2 PI*	0	ALPHA =	32.88	THETA =	36.84
AMBIGUITY NO.	22	PHI21+2 PI*	2	PHI32+2 PI*	1	ALPHA =	54.67	THETA =	60.54
AMBIGUITY NO.	23	PHI21+2 PI*	3	PHI32+2 PI*	-2	ALPHA =	343.25	THETA =	60.91
AMBIGUITY NO.	24	PHI21+2 PI*	3	PHI32+2 PI*	-1	ALPHA =	9.03	THETA =	57.92
AMBIGUITY NO.	25	PHI21+2 PI*	3	PHI32+2 PI*	0	ALPHA =	31.76	THETA =	79.79

Table A-4. List of Direction Ambiguities (D/λ = 4)

BASELINE = 400.0 WAVELENGTH = 100.0 PHI21 = 125.03 PHI13 = -168.45 PHI32 = 43.42

ACTUAL DIRECTION OF ARRIVAL..... AZIMUTH = 200.00 INCIDENCE = 10.00 GAMMA = 60.00

AMBIGUITY NO.	1	PHI21+2 PI*	-4	PHI32+2 PI*	1	ALPHA =	192.58	THETA =	69.33
AMBIGUITY NO.	2	PHI21+2 PI*	-4	PHI32+2 PI*	2	ALPHA =	174.69	THETA =	66.51
AMBIGUITY NO.	3	PHI21+2 PI*	-4	PHI32+2 PI*	3	ALPHA =	157.75	THETA =	80.63
AMBIGUITY NO.	4	PHI21+2 PI*	-3	PHI32+2 PI*	-1	ALPHA =	223.83	THETA =	66.83
AMBIGUITY NO.	5	PHI21+2 PI*	-3	PHI32+2 PI*	0	ALPHA =	207.69	THETA =	48.50
AMBIGUITY NO.	6	PHI21+2 PI*	-3	PHI32+2 PI*	1	ALPHA =	185.12	THETA =	41.75
AMBIGUITY NO.	7	PHI21+2 PI*	-3	PHI32+2 PI*	2	ALPHA =	160.93	THETA =	44.56
AMBIGUITY NO.	8	PHI21+2 PI*	-3	PHI32+2 PI*	3	ALPHA =	142.01	THETA =	57.30
AMBIGUITY NO.	9	PHI21+2 PI*	-2	PHI32+2 PI*	-2	ALPHA =	242.12	THETA =	62.08
AMBIGUITY NO.	10	PHI21+2 PI*	-2	PHI32+2 PI*	-1	ALPHA =	230.00	THETA =	40.00
AMBIGUITY NO.	11	PHI21+2 PI*	-2	PHI32+2 PI*	0	ALPHA =	206.25	THETA =	27.43
AMBIGUITY NO.	12	PHI21+2 PI*	-2	PHI32+2 PI*	1	ALPHA =	168.38	THETA =	24.95
AMBIGUITY NO.	13	PHI21+2 PI*	-2	PHI32+2 PI*	2	ALPHA =	137.88	THETA =	33.85
AMBIGUITY NO.	14	PHI21+2 PI*	-2	PHI32+2 PI*	3	ALPHA =	121.96	THETA =	51.32
AMBIGUITY NO.	15	PHI21+2 PI*	-1	PHI32+2 PI*	-3	ALPHA =	260.00	THETA =	70.00
AMBIGUITY NO.	16	PHI21+2 PI*	-1	PHI32+2 PI*	-2	ALPHA =	255.63	THETA =	41.10
AMBIGUITY NO.	17	PHI21+2 PI*	-1	PHI32+2 PI*	-1	ALPHA =	244.88	THETA =	22.61
AMBIGUITY NO.	18	PHI21+2 PI*	-1	PHI32+2 PI*	0	ALPHA =	200.00	THETA =	10.00
AMBIGUITY NO.	19	PHI21+2 PI*	-1	PHI32+2 PI*	1	ALPHA =	125.44	THETA =	16.34
AMBIGUITY NO.	20	PHI21+2 PI*	-1	PHI32+2 PI*	2	ALPHA =	107.49	THETA =	32.89
AMBIGUITY NO.	21	PHI21+2 PI*	-1	PHI32+2 PI*	3	ALPHA =	101.44	THETA =	55.38
AMBIGUITY NO.	22	PHI21+2 PI*	0	PHI32+2 PI*	-3	ALPHA =	276.34	THETA =	51.80
AMBIGUITY NO.	23	PHI21+2 PI*	0	PHI32+2 PI*	-2	ALPHA =	280.00	THETA =	30.00
AMBIGUITY NO.	24	PHI21+2 PI*	0	PHI32+2 PI*	-1	ALPHA =	293.08	THETA =	12.79
AMBIGUITY NO.	25	PHI21+2 PI*	0	PHI32+2 PI*	0	ALPHA =	44.37	THETA =	6.98
AMBIGUITY NO.	26	PHI21+2 PI*	0	PHI32+2 PI*	1	ALPHA =	76.92	THETA =	22.56
AMBIGUITY NO.	27	PHI21+2 PI*	0	PHI32+2 PI*	2	ALPHA =	82.53	THETA =	41.91
AMBIGUITY NO.	28	PHI21+2 PI*	0	PHI32+2 PI*	3	ALPHA =	84.78	THETA =	72.73
AMBIGUITY NO.	29	PHI21+2 PI*	1	PHI32+2 PI*	-4	ALPHA =	290.00	THETA =	80.00
AMBIGUITY NO.	30	PHI21+2 PI*	1	PHI32+2 PI*	-3	ALPHA =	297.88	THETA =	46.08
AMBIGUITY NO.	31	PHI21+2 PI*	1	PHI32+2 PI*	-2	ALPHA =	314.06	THETA =	28.97
AMBIGUITY NO.	32	PHI21+2 PI*	1	PHI32+2 PI*	-1	ALPHA =	350.00	THETA =	20.00
AMBIGUITY NO.	33	PHI21+2 PI*	1	PHI32+2 PI*	0	ALPHA =	34.24	THETA =	24.05
AMBIGUITY NO.	34	PHI21+2 PI*	1	PHI32+2 PI*	1	ALPHA =	56.96	THETA =	38.16
AMBIGUITY NO.	35	PHI21+2 PI*	1	PHI32+2 PI*	2	ALPHA =	67.34	THETA =	60.94
AMBIGUITY NO.	36	PHI21+2 PI*	2	PHI32+2 PI*	-4	ALPHA =	306.92	THETA =	77.68
AMBIGUITY NO.	37	PHI21+2 PI*	2	PHI32+2 PI*	-3	ALPHA =	320.00	THETA =	50.00
AMBIGUITY NO.	38	PHI21+2 PI*	2	PHI32+2 PI*	-2	ALPHA =	340.85	THETA =	38.40
AMBIGUITY NO.	39	PHI21+2 PI*	2	PHI32+2 PI*	-1	ALPHA =	8.24	THETA =	36.37
AMBIGUITY NO.	40	PHI21+2 PI*	2	PHI32+2 PI*	0	ALPHA =	32.48	THETA =	44.08
AMBIGUITY NO.	41	PHI21+2 PI*	2	PHI32+2 PI*	1	ALPHA =	48.46	THETA =	62.24
AMBIGUITY NO.	42	PHI21+2 PI*	3	PHI32+2 PI*	-3	ALPHA =	337.42	THETA =	65.00
AMBIGUITY NO.	43	PHI21+2 PI*	3	PHI32+2 PI*	-2	ALPHA =	355.94	THETA =	57.03
AMBIGUITY NO.	44	PHI21+2 PI*	3	PHI32+2 PI*	-1	ALPHA =	15.32	THETA =	60.19
AMBIGUITY NO.	45	PHI21+2 PI*	3	PHI32+2 PI*	0	ALPHA =	31.76	THETA =	79.79

Table A-5. List of Direction Ambiguities ($\alpha = 0^{\circ}$, $\theta = 0^{\circ}$)

BASELINE = 300.0 WAVELENGTH = 100.0 PHI21 = 0.00 PHI13 = 0.00 PHI32 = 0.00

ACTUAL DIRECTION OF ARRIVAL..... AZIMUTH = 0.00 INCIDENCE = 0.00 GAMMA = 60.00

AMBIGUITY NO.	1	PHI21+2 PI*	-2	PHI32+2 PI*	0	ALPHA =	210.00	THETA =	50.34
AMBIGUITY NO.	2	PHI21+2 PI*	-2	PHI32+2 PI*	1	ALPHA =	180.00	THETA =	41.81
AMBIGUITY NO.	3	PHI21+2 PI*	-2	PHI32+2 PI*	2	ALPHA =	150.00	THETA =	50.34
AMBIGUITY NO.	4	PHI21+2 PI*	-1	PHI32+2 PI*	-1	ALPHA =	240.00	THETA =	41.81
AMBIGUITY NO.	5	PHI21+2 PI*	-1	PHI32+2 PI*	0	ALPHA =	210.00	THETA =	22.64
AMBIGUITY NO.	6	PHI21+2 PI*	-1	PHI32+2 PI*	1	ALPHA =	150.00	THETA =	22.64
AMBIGUITY NO.	7	PHI21+2 PI*	-1	PHI32+2 PI*	2	ALPHA =	120.00	THETA =	41.81
AMBIGUITY NO.	8	PHI21+2 PI*	0	PHI32+2 PI*	-2	ALPHA =	270.00	THETA =	50.34
AMBIGUITY NO.	9	PHI21+2 PI*	0	PHI32+2 PI*	-1	ALPHA =	270.00	THETA =	22.64
AMBIGUITY NO.	10	PHI21+2 PI*	0	PHI32+2 PI*	0	ALPHA =	0.00	THETA =	0.00
AMBIGUITY NO.	11	PHI21+2 PI*	0	PHI32+2 PI*	1	ALPHA =	90.00	THETA =	22.64
AMBIGUITY NO.	12	PHI21+2 PI*	0	PHI32+2 PI*	2	ALPHA =	90.00	THETA =	50.34
AMBIGUITY NO.	13	PHI21+2 PI*	1	PHI32+2 PI*	-2	ALPHA =	300.00	THETA =	41.81
AMBIGUITY NO.	14	PHI21+2 PI*	1	PHI32+2 PI*	-1	ALPHA =	330.00	THETA =	22.64
AMBIGUITY NO.	15	PHI21+2 PI*	1	PHI32+2 PI*	0	ALPHA =	30.00	THETA =	22.64
AMBIGUITY NO.	16	PHI21+2 PI*	1	PHI32+2 PI*	1	ALPHA =	60.00	THETA =	41.81
AMBIGUITY NO.	17	PHI21+2 PI*	2	PHI32+2 PI*	-2	ALPHA =	330.00	THETA =	50.34
AMBIGUITY NO.	18	PHI21+2 PI*	2	PHI32+2 PI*	-1	ALPHA =	0.00	THETA =	41.81
AMBIGUITY NO.	19	PHI21+2 PI*	2	PHI32+2 PI*	0	ALPHA =	30.00	THETA =	50.34

Table A-6. List of Direction Ambiguities ($\alpha = 0^{\circ}$, $\theta = 30^{\circ}$)

BASELINE = 300.0 WAVELENGTH = 100.0 PHI21 = -180.00 PHI13 = 90.00 PHI32 = 90.00

ACTUAL DIRECTION OF ARRIVAL..... AZIMUTH = 0.00 INCIDENCE = 30.00 GAMMA = 60.00

AMBIGUITY NO.	1	PHI21+2 PI*	-2	PHI32+2 PI*	0	ALPHA =	204.79	THETA =	67.63
AMBIGUITY NO.	2	PHI21+2 PI*	-2	PHI32+2 PI*	1	ALPHA =	180.00	THETA =	56.44
AMBIGUITY NO.	3	PHI21+2 PI*	-2	PHI32+2 PI*	2	ALPHA =	155.21	THETA =	66.62
AMBIGUITY NO.	4	PHI21+2 PI*	-1	PHI32+2 PI*	-1	ALPHA =	229.11	THETA =	49.80
AMBIGUITY NO.	5	PHI21+2 PI*	-1	PHI32+2 PI*	0	ALPHA =	201.05	THETA =	32.40
AMBIGUITY NO.	6	PHI21+2 PI*	-1	PHI32+2 PI*	1	ALPHA =	158.95	THETA =	32.40
AMBIGUITY NO.	7	PHI21+2 PI*	-1	PHI32+2 PI*	2	ALPHA =	130.89	THETA =	49.80
AMBIGUITY NO.	8	PHI21+2 PI*	0	PHI32+2 PI*	-2	ALPHA =	257.78	THETA =	51.96
AMBIGUITY NO.	9	PHI21+2 PI*	0	PHI32+2 PI*	-1	ALPHA =	246.59	THETA =	24.80
AMBIGUITY NO.	10	PHI21+2 PI*	0	PHI32+2 PI*	0	ALPHA =	180.00	THETA =	9.59
AMBIGUITY NO.	11	PHI21+2 PI*	0	PHI32+2 PI*	1	ALPHA =	113.41	THETA =	24.80
AMBIGUITY NO.	12	PHI21+2 PI*	0	PHI32+2 PI*	2	ALPHA =	102.22	THETA =	51.96
AMBIGUITY NO.	13	PHI21+2 PI*	1	PHI32+2 PI*	-3	ALPHA =	279.83	THETA =	77.57
AMBIGUITY NO.	14	PHI21+2 PI*	1	PHI32+2 PI*	-2	ALPHA =	286.10	THETA =	36.94
AMBIGUITY NO.	15	PHI21+2 PI*	1	PHI32+2 PI*	-1	ALPHA =	310.89	THETA =	14.75
AMBIGUITY NO.	16	PHI21+2 PI*	1	PHI32+2 PI*	0	ALPHA =	49.11	THETA =	14.75
AMBIGUITY NO.	17	PHI21+2 PI*	1	PHI32+2 PI*	1	ALPHA =	73.90	THETA =	36.94
AMBIGUITY NO.	18	PHI21+2 PI*	1	PHI32+2 PI*	2	ALPHA =	80.17	THETA =	77.57
AMBIGUITY NO.	19	PHI21+2 PI*	2	PHI32+2 PI*	-3	ALPHA =	303.00	THETA =	66.62
AMBIGUITY NO.	20	PHI21+2 PI*	2	PHI32+2 PI*	-2	ALPHA =	322.41	THETA =	39.12
AMBIGUITY NO.	21	PHI21+2 PI*	2	PHI32+2 PI*	-1	ALPHA =	0.00	THETA =	30.00
AMBIGUITY NO.	22	PHI21+2 PI*	2	PHI32+2 PI*	0	ALPHA =	37.59	THETA =	39.12
AMBIGUITY NO.	23	PHI21+2 PI*	2	PHI32+2 PI*	1	ALPHA =	57.00	THETA =	66.63
AMBIGUITY NO.	24	PHI21+2 PI*	3	PHI32+2 PI*	-2	ALPHA =	347.00	THETA =	58.79
AMBIGUITY NO.	25	PHI21+2 PI*	3	PHI32+2 PI*	-1	ALPHA =	13.00	THETA =	58.79

Table A-7. List of Direction Ambiguities ($\alpha = 45^{\circ}$, $\theta = 45^{\circ}$)

BASELINE = 300.0 WAVELENGTH = 100.0 PHI21 = -180.00 PHI13 = -17.65 PHI32 = -162.35

ACTUAL DIRECTION OF ARRIVAL..... AZIMUTH = 45.00 INCIDENCE = 45.00 GAMMA = 60.00

AMBIGUITY NO.	1	PHI21+2 PI*	-2	PHI32+2 PI*	1	ALPHA =	197.94	THETA =	61.15
AMBIGUITY NO.	2	PHI21+2 PI*	-2	PHI32+2 PI*	2	ALPHA =	172.14	THETA =	57.27
AMBIGUITY NO.	3	PHI21+2 PI*	-2	PHI32+2 PI*	3	ALPHA =	145.04	THETA =	76.37
AMBIGUITY NO.	4	PHI21+2 PI*	-1	PHI32+2 PI*	-1	ALPHA =	239.45	THETA =	79.64
AMBIGUITY NO.	5	PHI21+2 PI*	-1	PHI32+2 PI*	0	ALPHA =	222.75	THETA =	42.92
AMBIGUITY NO.	6	PHI21+2 PI*	-1	PHI32+2 PI*	1	ALPHA =	188.79	THETA =	30.39
AMBIGUITY NO.	7	PHI21+2 PI*	-1	PHI32+2 PI*	2	ALPHA =	148.40	THETA =	35.95
AMBIGUITY NO.	8	PHI21+2 PI*	-1	PHI32+2 PI*	3	ALPHA =	125.83	THETA =	58.66
AMBIGUITY NO.	9	PHI21+2 PI*	0	PHI32+2 PI*	-1	ALPHA =	255.72	THETA =	42.50
AMBIGUITY NO.	10	PHI21+2 PI*	0	PHI32+2 PI*	0	ALPHA =	238.29	THETA =	18.49
AMBIGUITY NO.	11	PHI21+2 PI*	0	PHI32+2 PI*	1	ALPHA =	145.37	THETA =	11.69
AMBIGUITY NO.	12	PHI21+2 PI*	0	PHI32+2 PI*	2	ALPHA =	108.43	THETA =	31.81
AMBIGUITY NO.	13	PHI21+2 PI*	0	PHI32+2 PI*	3	ALPHA =	100.67	THETA =	64.22
AMBIGUITY NO.	14	PHI21+2 PI*	1	PHI32+2 PI*	-2	ALPHA =	281.13	THETA =	59.70
AMBIGUITY NO.	15	PHI21+2 PI*	1	PHI32+2 PI*	-1	ALPHA =	289.83	THETA =	29.43
AMBIGUITY NO.	16	PHI21+2 PI*	1	PHI32+2 PI*	0	ALPHA =	335.10	THETA =	10.59
AMBIGUITY NO.	17	PHI21+2 PI*	1	PHI32+2 PI*	1	ALPHA =	61.55	THETA =	20.48
AMBIGUITY NO.	18	PHI21+2 PI*	1	PHI32+2 PI*	2	ALPHA =	76.47	THETA =	45.42
AMBIGUITY NO.	19	PHI21+2 PI*	2	PHI32+2 PI*	-2	ALPHA =	307.37	THETA =	55.47
AMBIGUITY NO.	20	PHI21+2 PI*	2	PHI32+2 PI*	-1	ALPHA =	331.65	THETA =	34.82
AMBIGUITY NO.	21	PHI21+2 PI*	2	PHI32+2 PI*	0	ALPHA =	12.96	THETA =	30.87
AMBIGUITY NO.	22	PHI21+2 PI*	2	PHI32+2 PI*	1	ALPHA =	45.00	THETA =	45.00
AMBIGUITY NO.	23	PHI21+2 PI*	3	PHI32+2 PI*	-2	ALPHA =	330.98	THETA =	72.35
AMBIGUITY NO.	24	PHI21+2 PI*	3	PHI32+2 PI*	-1	ALPHA =	354.70	THETA =	56.82
AMBIGUITY NO.	25	PHI21+2 PI*	3	PHI32+2 PI*	0	ALPHA =	20.26	THETA =	62.66

Table A-8. List of Direction Ambiguities ($\alpha = 45^{\circ}$, $\theta = 80^{\circ}$)

BASELINE = 300.0 WAVELENGTH = 100.0 PHI21 = 32.07 PHI13 = 52.65 PHI32 = -84.72

ACTUAL DIRECTION OF ARRIVAL..... AZIMUTH = 45.00 INCIDENCE = 80.00 GAMMA = 60.00

AMBIGUITY NO.	1	PHI21+2 PI*	-3	PHI32+2 PI*	2	ALPHA =	173.01	THETA =	77.84
AMBIGUITY NO.	2	PHI21+2 PI*	-2	PHI32+2 PI*	0	ALPHA =	215.74	THETA =	51.70
AMBIGUITY NO.	3	PHI21+2 PI*	-2	PHI32+2 PI*	1	ALPHA =	186.58	THETA =	39.88
AMBIGUITY NO.	4	PHI21+2 PI*	-2	PHI32+2 PI*	2	ALPHA =	153.94	THETA =	45.16
AMBIGUITY NO.	5	PHI21+2 PI*	-2	PHI32+2 PI*	3	ALPHA =	132.45	THETA =	70.69
AMBIGUITY NO.	6	PHI21+2 PI*	-1	PHI32+2 PI*	-1	ALPHA =	244.99	THETA =	45.90
AMBIGUITY NO.	7	PHI21+2 PI*	-1	PHI32+2 PI*	0	ALPHA =	221.21	THETA =	23.80
AMBIGUITY NO.	8	PHI21+2 PI*	-1	PHI32+2 PI*	1	ALPHA =	158.60	THETA =	19.03
AMBIGUITY NO.	9	PHI21+2 PI*	-1	PHI32+2 PI*	2	ALPHA =	121.07	THETA =	36.04
AMBIGUITY NO.	10	PHI21+2 PI*	-1	PHI32+2 PI*	3	ALPHA =	108.86	THETA =	69.93
AMBIGUITY NO.	11	PHI21+2 PI*	0	PHI32+2 PI*	-2	ALPHA =	272.02	THETA =	57.54
AMBIGUITY NO.	12	PHI21+2 PI*	0	PHI32+2 PI*	-1	ALPHA =	273.71	THETA =	27.34
AMBIGUITY NO.	13	PHI21+2 PI*	0	PHI32+2 PI*	0	ALPHA =	292.02	THETA =	4.54
AMBIGUITY NO.	14	PHI21+2 PI*	0	PHI32+2 PI*	1	ALPHA =	84.55	THETA =	18.23
AMBIGUITY NO.	15	PHI21+2 PI*	0	PHI32+2 PI*	2	ALPHA =	87.56	THETA =	44.19
AMBIGUITY NO.	16	PHI21+2 PI*	1	PHI32+2 PI*	-2	ALPHA =	299.15	THETA =	48.18
AMBIGUITY NO.	17	PHI21+2 PI*	1	PHI32+2 PI*	-1	ALPHA =	323.78	THETA =	26.74
AMBIGUITY NO.	18	PHI21+2 PI*	1	PHI32+2 PI*	0	ALPHA =	18.15	THETA =	22.46
AMBIGUITY NO.	19	PHI21+2 PI*	1	PHI32+2 PI*	1	ALPHA =	54.23	THETA =	38.39
AMBIGUITY NO.	20	PHI21+2 PI*	1	PHI32+2 PI*	2	ALPHA =	67.78	THETA =	73.76
AMBIGUITY NO.	21	PHI21+2 PI*	2	PHI32+2 PI*	-2	ALPHA =	326.65	THETA =	56.48
AMBIGUITY NO.	22	PHI21+2 PI*	2	PHI32+2 PI*	-1	ALPHA =	353.98	THETA =	44.45
AMBIGUITY NO.	23	PHI21+2 PI*	2	PHI32+2 PI*	0	ALPHA =	24.10	THETA =	49.72
AMBIGUITY NO.	24	PHI21+2 PI*	2	PHI32+2 PI*	1	ALPHA =	45.00	THETA =	80.00

APPENDIX B

This appendix contains unit hemisphere projection plots which precisely correspond to the ambiguity data found in Appendix A. Note the symmetry of these plots. Note also how the plots vary with D/λ, as discussed in Chapter IV.

UNIT HEMISPHERE AMBIGUITY PLOT

D/LAMBDA = 1.00 AZIMUTH = 200.00 INCIDENCE 10.00

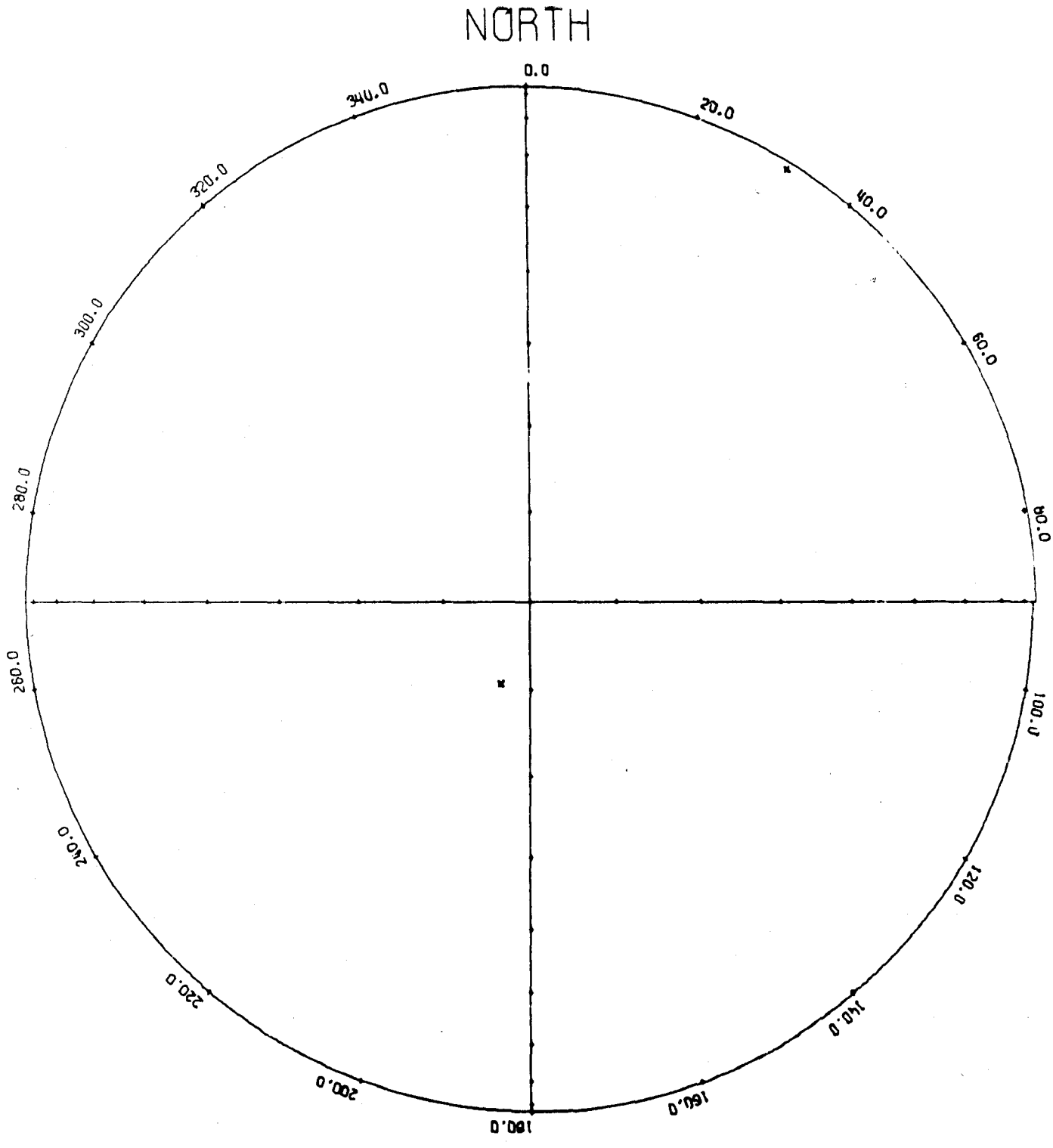

ARRAY ANGLE = 60.00

Figure B-1. Hemispherical Projection Plot (D/λ = 1)

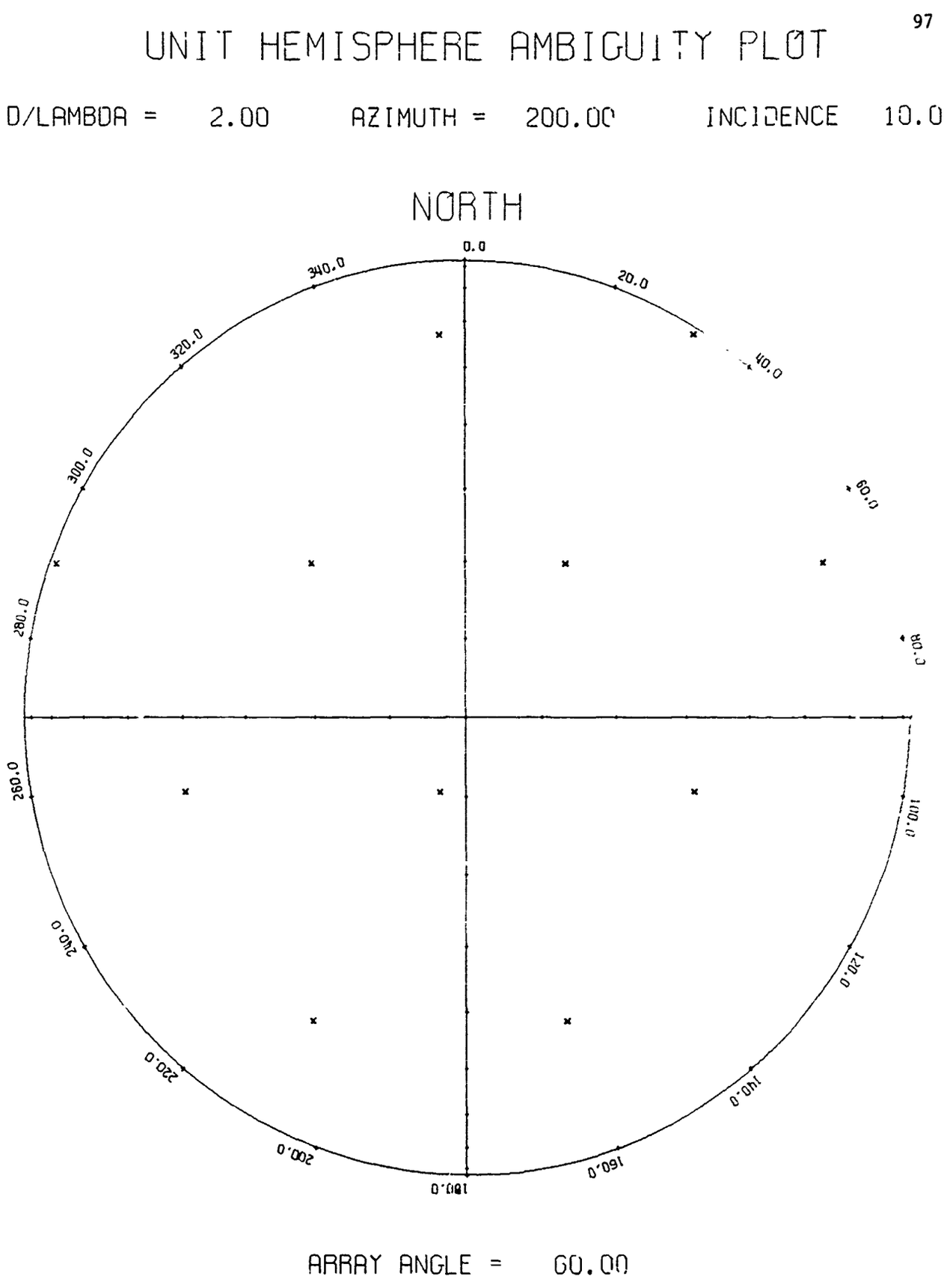

Figure B-2. Hemispherical Projection Plot ($d/\lambda = 2$)

UNIT HEMISPHERE AMBIGUITY PLOT

D/LAMBDA = 3.00 AZIMUTH = 200.00 INCIDENCE 10.00

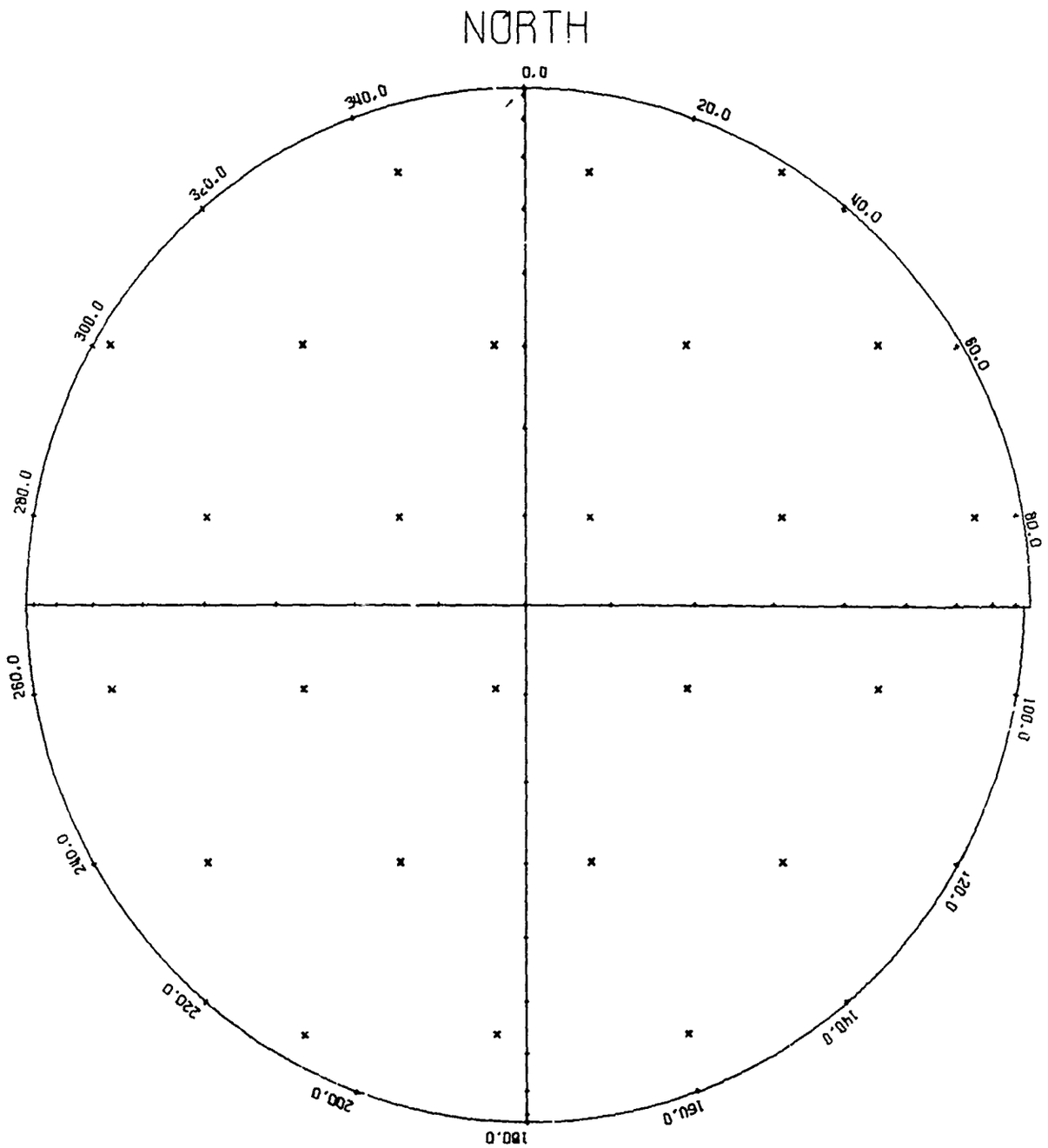

ARRAY ANGLE = 60.00

Figure B-3. Hemispherical Projection Plot (D/λ = 3)

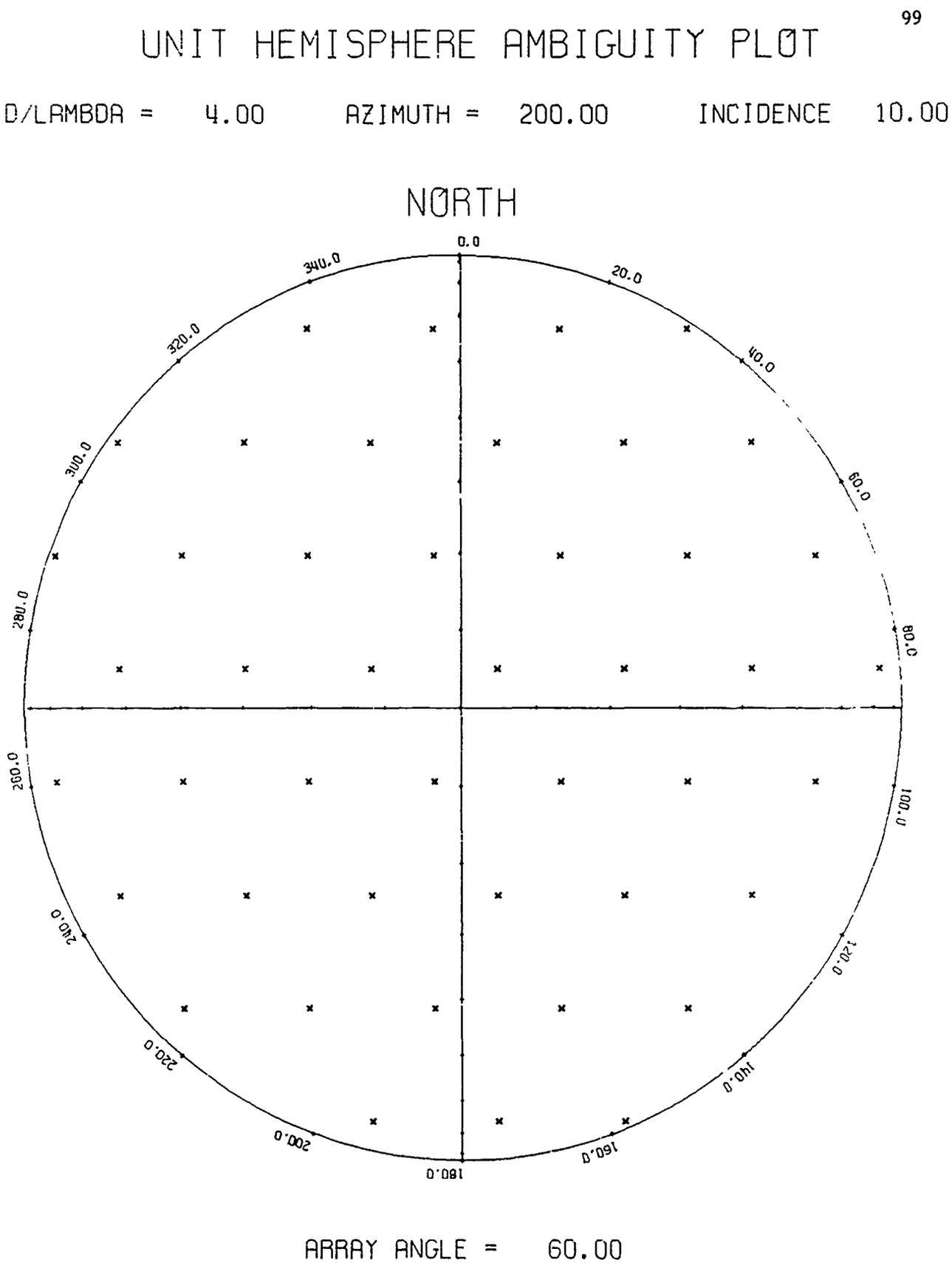

Figure B-4. Hemispherical Projection Plot (D/λ = 4)

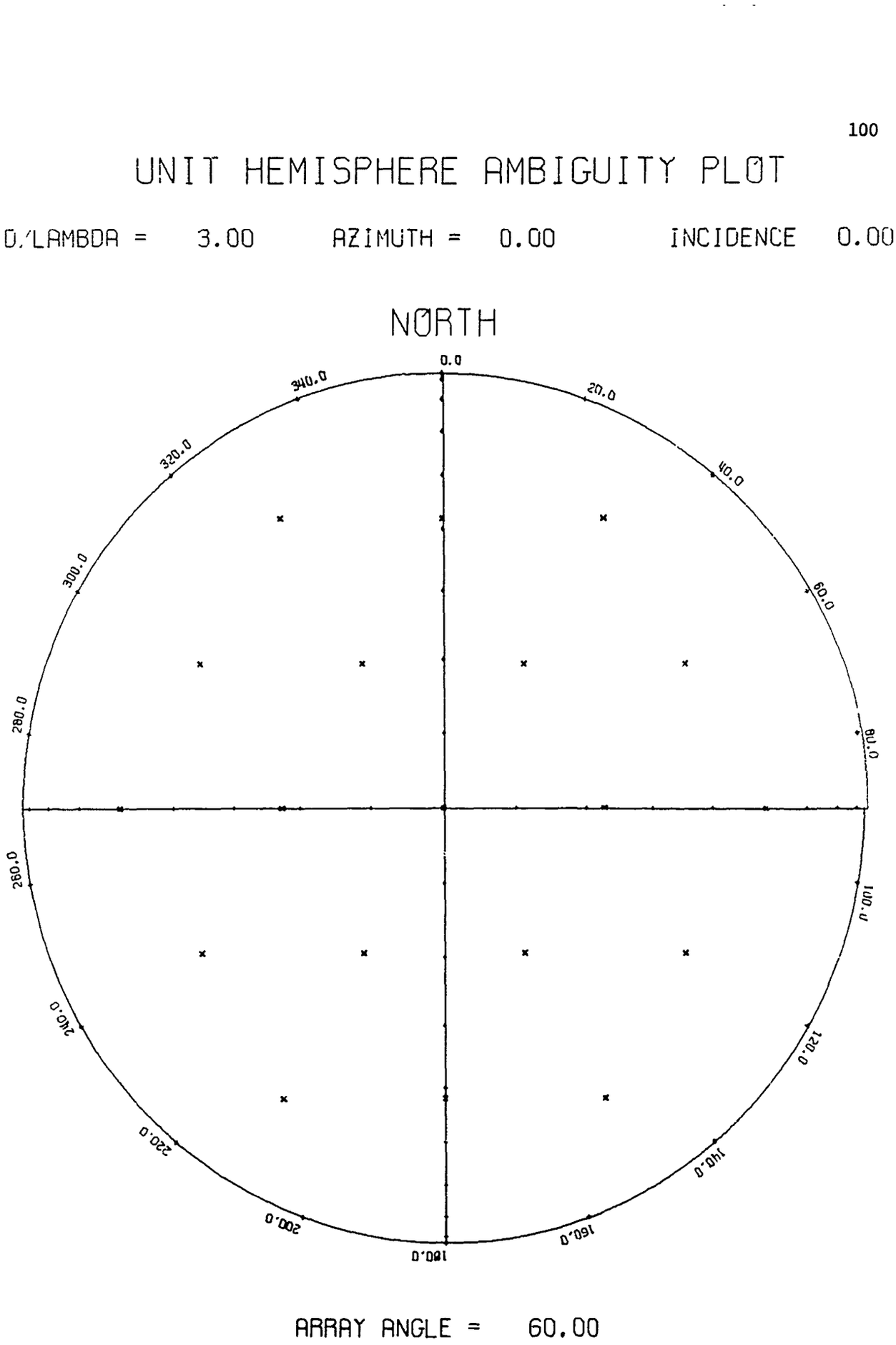

Figure B-5. Hemispherical Projection Plot ($\gamma = 0^{o}$, $\theta = 0^{o}$)

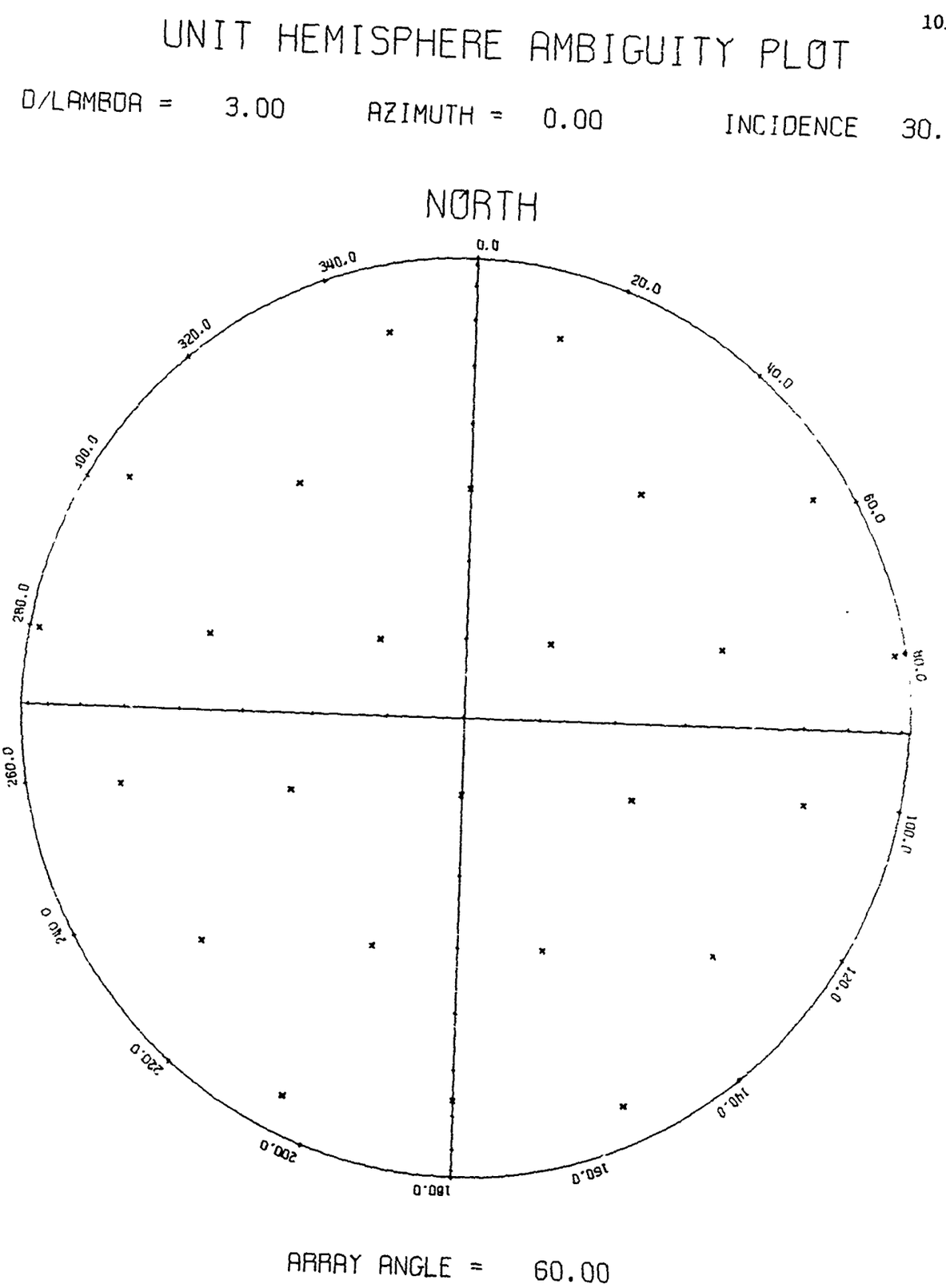

Figure B-6. Hemispherical Projection Plot (γ 0°, θ = 30°)

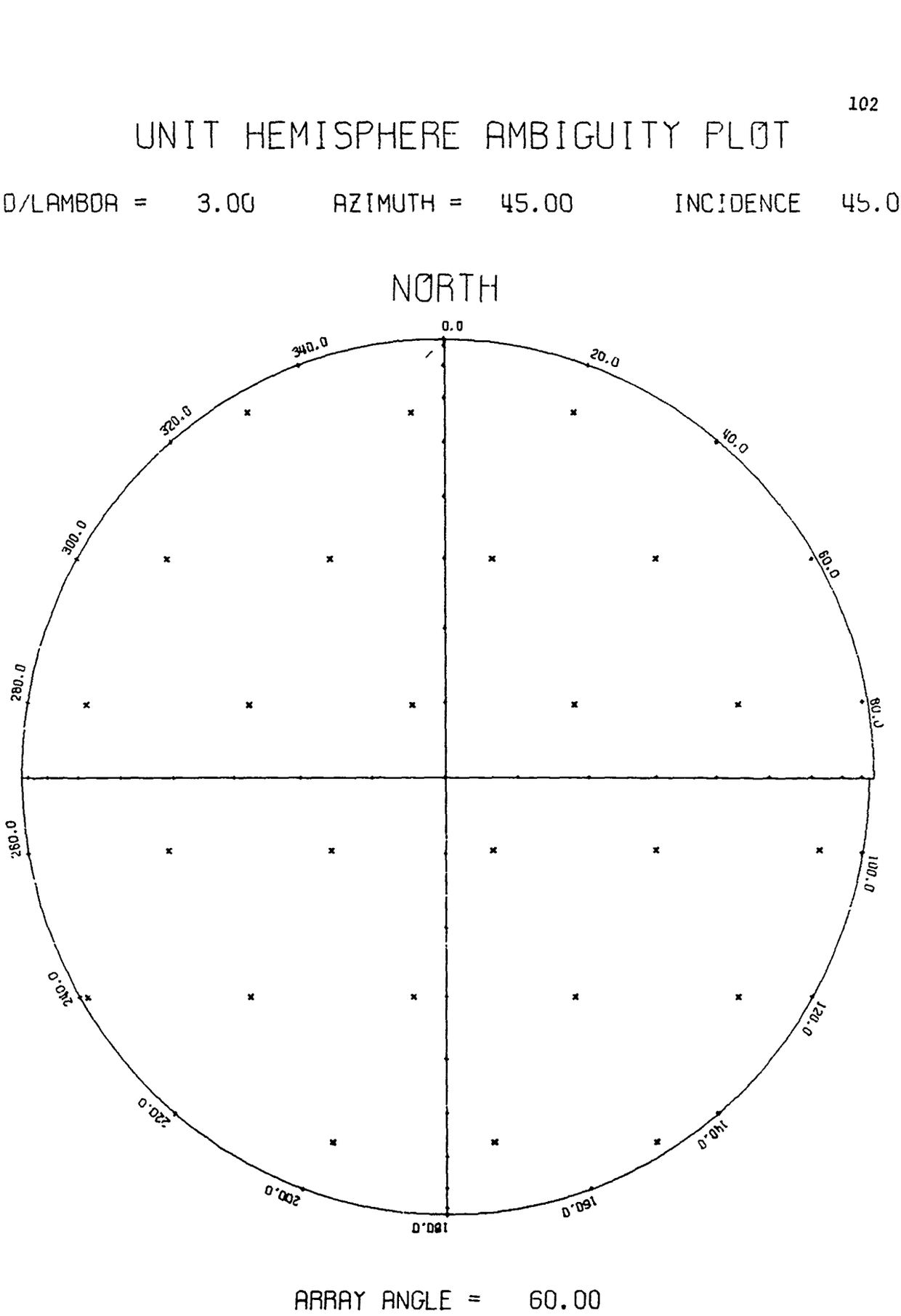

Figure B-7. Hemispherical Projection Plot ($\gamma = 45^{o}$, $\theta = 45^{o}$)

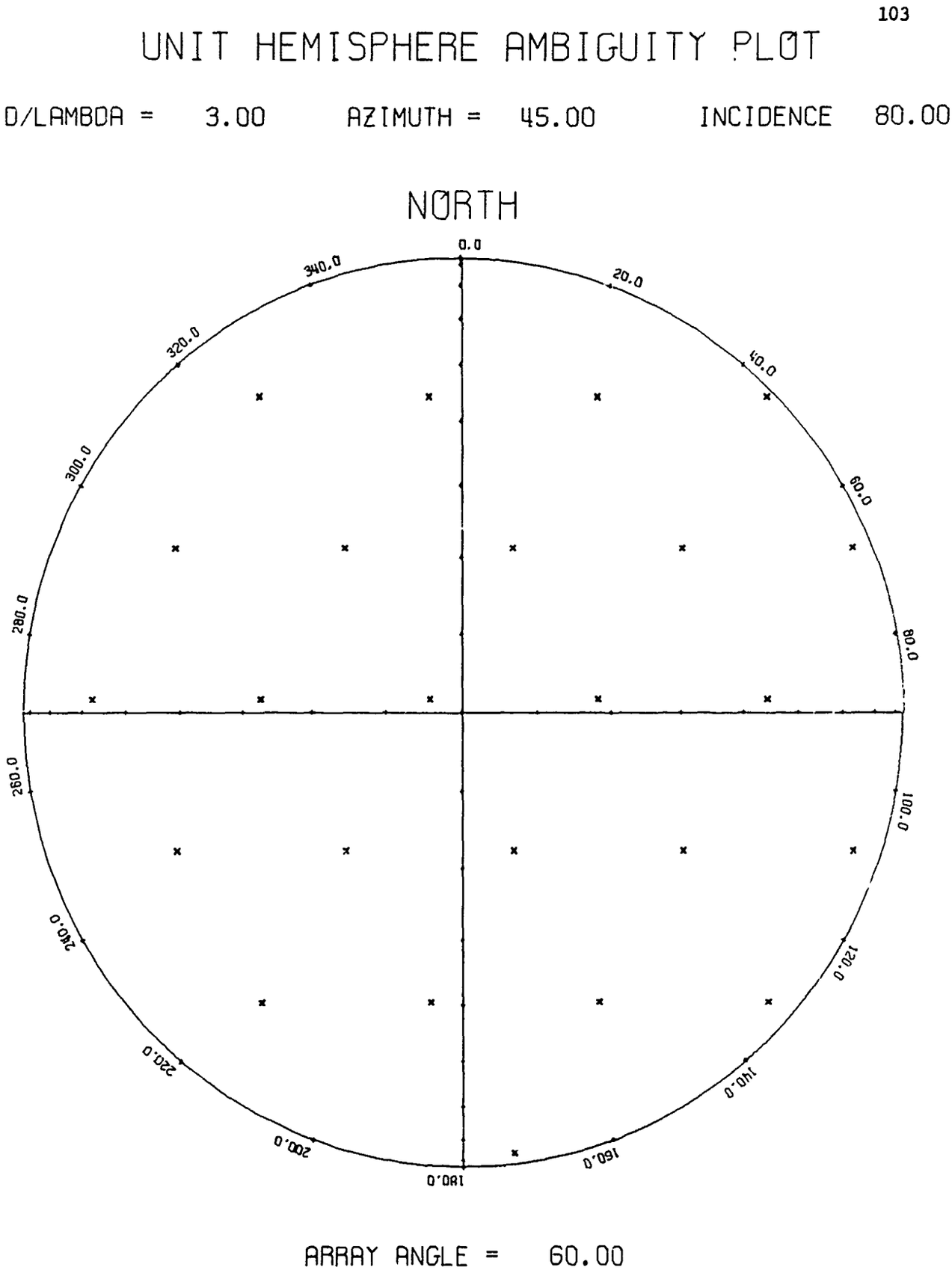

Figure B-8. Hemispherical Projection Plot ($\gamma = 45^{o}$, $\theta = 80^{o}$)

APPENDIX C

A listing of the general ambiguity locating program (GNAMLC) as well as four sample hemispherical projection plots is included in this appendix. Program GNAMLC is structured according to the flow chart of figure 6, except that it uses the more general isosceles array interferometer equations. (See equations IV-1.)

Due to the symmetry of these plots, it has been found that such hemispherical projection plots may be constructed in a much simpler manner (without the use of a computer!), using equations IV-10 through IV-13. This is discussed at the end of Chapter IV.

The four sample plots have been specifically chosen to illustrate how the number of direction ambiguities and the ambiguity distribution pattern varies with the isosceles array angle, gamma.

The user-written subroutine "REDUCE," called by program GNAMLC, is documented and listed in Appendix M. All other subroutines called are part of the G-20 digital computer system library. Information on these library subroutines or on the G-20 Fortran-M language (in which all programs listed in this thesis are coded) may be obtained from the G-20 computing facility of this laboratory.

```
$     INPUT SOURCE CARDS
$     EXECUTE
$     FORTRAN
H      NAME GNAMLC;
H      EQUIP=PRINTE,CARDRE,CARDPU;
H      SINGLEALL;
C*****
C*****THIS IS A GENERAL ISOSCELES INTERFEROMETER ARRAY AMBIGUITY LOCATING
C*****PROGRAM.  INPUT DATA CONSISTS OF THE SPECIFIED AZIMUTH AND INCIDENCE
C*****ANGLES (IN DEGREES), THE ARRAY BASELINE, AND OPERATING WAVELENGTH (IN
C*****METERS),AND THE ISOSCELES ARRAY ANGLE (IN DEGREES).   (5F10.5 FORMAT.)
C*****THIS PROGRAM LISTS ALL POSSIBLE AMBIGUITIES AS SEEN BY THE INTERFEROMETER
C*****ARRAY.   IT THEN PLOTS THEM ON A UNIT HEMISPERICAL PROJECTION.
C*****
      DIMENSION IWRK(1000),X(500),Y(500)
      PI=3.1415926535898
      TUPI=2.*PI
      DEG=180./PI
      DO 999 IREQ=1,3
      READ 10, XALPHA,XTHETA,D,XLAMB,DGAMMA
      GAMMA=DGAMMA/DEG
      TPDL=TUPI*D/XLAMB
      RXALPH=XALPHA/DEG
      RXTHET=XTHETA/DEG
      SNTH=SIN(RXTHET)
C*****USE ALPHA TO DETERMINE UNAMBIGUOUS INTERFEROMETER PHASES
      PHI21=TPDL*COS(RXALPH)*SNTH
      PHI13=-TPDL*COS(RXALPH-GAMMA)*SNTH
      PHI32=TPDL*(COS(RXALPH-GAMMA)-COS(RXALPH))*SNTH
C*****REDUCE PHI'S BY MULTIPLES OF 2 PI UNTIL BETWEEN - PI AND + PI
      CALL REDUCE(PHI21)
      CALL REDUCE(PHI13)
      CALL REDUCE(PHI32)
      DL=D/XLAMB
      DPHI13=DEG*PHI13
      DPHI21=DEG*PHI21
      DPHI32=DEG*PHI32
10    FORMAT(5F10.5)
      PRINT 20,D,XLAMB,DPHI21,DPHI13,DPHI32
20    FORMAT(12H1BASELINE = ,F5.1,5X,14H WAVELENGTH = ,F5.1,5X,9H PHI21
     $= ,F7.2,5X,9H PHI13 = ,F7.2,5X,9H PHI32 = ,F7.2)
      PRINT 21,XALPHA,XTHETA,DGAMMA
21    FORMAT(//34H ACTUAL DIRECTION OF ARRIVAL.....,8X,10HAZIMUTH =  ,
     $F7.2,8X,12HINCIDENCE = ,F7.2,4X,8HGAMMA = ,F7.2,///)
      TPDL=TUPI*D/XLAMB
      N=D/XLAMB+1
      M=2*N+1
      JCOUNT=0
C*****BEGIN VARYING PHI21 AND PHI31 BY + OR - 2 PI
      DO 40 M21=1,M
      N21=M21-N-1
      TPHI21=PHI21+TUPI*N21
      DO 40M32=1,M
      N32=M32-N-1
      TPHI32=PHI32+TUPI*N32
      SMSQ=TPHI21**2+TPHI32**2+TPHI21*TPHI32
C*****REJECT PHASE AMBIGUITY COMINATIONS THAT YIELD IMAGINARY INCIDENCE ANGLES
      XNUM1=TPHI21+TPHI32-TPHI21*COS(GAMMA)
      XDEN1=TPHI21*SIN(GAMMA)
```

```
      XTN=ATAN2(XNUM1,XDEN1)
      REJECT=COS(XTN)*COS(XTN-GAMMA)
      CONDX=COS(XTN)**2+COS(XTN-GAMMA)**2
      SQRT1=SQRT(SMSQ/(CONDX-REJECT))
      IF(SQRT1-TPDL) 30,40,40
C*****IF TPHI21 AND TPHI32 PASS THIS TEST, COMPUTE ALPHA AND THETA
30    ALPHA=XTN
      DALPHA=DEG*ALPHA
      THETA=ASIN(SQRT1/TPDL)
      DTHETA=THETA*DEG
      STH=SIN(THETA)
      JCOUNT=JCOUNT+1
      Y(JCOUNT)=COS(ALPHA)*STH*3.5
      X(JCOUNT)=SIN(ALPHA)*STH*3.5
      PRINT 31,JCOUNT,N21,N32,DALPHA,DTHETA
31    FORMAT(15H AMBIGUITY NO. ,I4,3X,11HPHI21+2 PI*,I3,3X,
     $11HPHI32+2 PI*,I3,3X,9H ALPHA = ,F7.2,3X,8HTHETA = ,F7.2)
40    CONTINUE
      CALL PLOTS(IWRK,1000,150.,11.)
C*****SHIFT ORIGIN (ASSUMING PEN STARTED IN LOWER RIGHT) TO CENTER OF PAGE
      CALL PLOT(4.,5.,-3)
C*****DRAW X,Y AXES
      CALL PLOT(0.,-3.5,3)
      CALL PLOT(0.,3.5,2)
      CALL PLOT(-3.5,0.,3)
      CALL PLOT(3.5,0.,2)
C*****DRAW UNIT CIRCLE (PROJECTION OF ERICS UNIT HEMISPHERE)
      CALL PLOT(3.5,0.,3)
      W=0.
      DO 200 J=1,151
      A=COS(W)*3.5
      B=SIN(W)*3.5
      CALL PLOT(A,B,2)
200   W=W+TWOPI/150.
      TENRAD=10./DEG
      EITRD=-80./DEG
      DGAZ=0.
      RADAZ=0.
C*****CALIBRATE UNIT CIRCLE IN DEGREES AS ON A COMPASS (DRAW AZIMUTHAL SCALE).
      DO 201 INC=1,18
      DGAZM=-DGAZ
      C=COS(RADAZ)*3.5
      D=SIN(RADAZ)*3.5
      CALL SYMBOL(D,C,.07,4,DGAZM,-1)
      C=1.02*C
      D=1.02*D
      CALL NUMBER(D,C,.07,DGAZ,DGAZM,1)
      DGAZ=DGAZ+20.
201   RADAZ=RADAZ+TWOPI/18.
      THETA=EITRD
C*****DRAW SINUSOIDALLY SPACED TICK MARKS ON X,Y AXES, INDICATING INCIDENCE
C*****ANGLES (10. DEGREE INTERVALS)
      DO 203 ICT=1,17
      STH=SIN(THETA)*3.5
      CALL SYMBOL(STH,0.,.07,4,0.,-1)
203   THETA=THETA+TENRAD
      THETA=EITRD
      DO 204 ICT=1,17
      STH=SIN(THETA)*3.5
      CALL SYMBOL(0.,STH,.07,4,90.,-1)
```

```
204    THETA=THETA+TENRAD
C*****PLOT AMBIGUITIES
       DO 202 LOOP=1,JCOUNT
202    CALL SYMBOL(X(LOOP),Y(LOOP),.08,5,0.,-1)
C*****DRAW IN SYSTEM PARAMETERS ON PLOT
       CALL SYMBOL(-1.25,-4.25,.14,14HARRAY ANGLE = ,0.,14)
       CALL NUMBER(.7,-4.25,.14,DGAMMA,0.,2)
       CALL SYMBOL(-.4,3.8,.21,5HNORTH,0.,5)
       CALL SYMBOL(-2.5,5.,.21,30HUNIT HEMISPHERE AMBIGUITY PLOT,0.,30)
       CALLSYMBOL(-3.6,4.5,.14,11HD/LAMBDA = ,0.,11)
       CALLNUMBER(-2.,4.5,.14,DL,0.,2)
       CALLSYMBOL(-.88,4.5,.14,10HAZIMUTH = ,0.,10)
       CALL NUMBER( .5,4.5,.14,XALPHA,0.,2)
       CALL SYMBOL( 1.9,4.5,.14,12HINCIDENCE = ,0.,10)
       CALL NUMBER( 3.3,4.5,.14,XTHETA,0.,2)
C*****MOVE PEN TO NEW STARTING POSITION FOR NEW PLOT TO BE INITIATED
       CALL PLOT(5.,-5.,-3)
999    CONTINUE
       CALL EXIT
       END
```

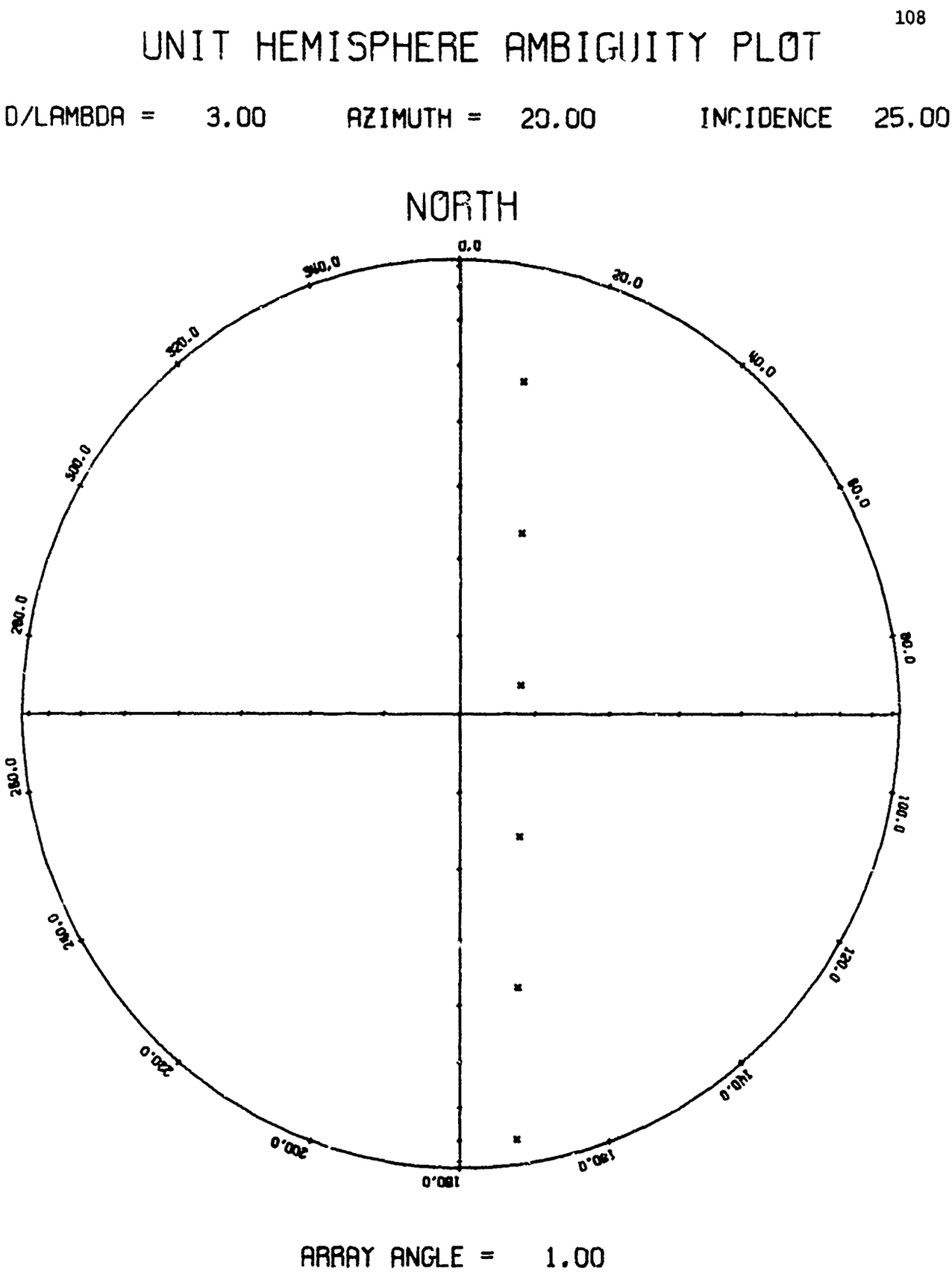

Figure C-1. Hemispherical Projection Plot ($\gamma = 1^{o}$)

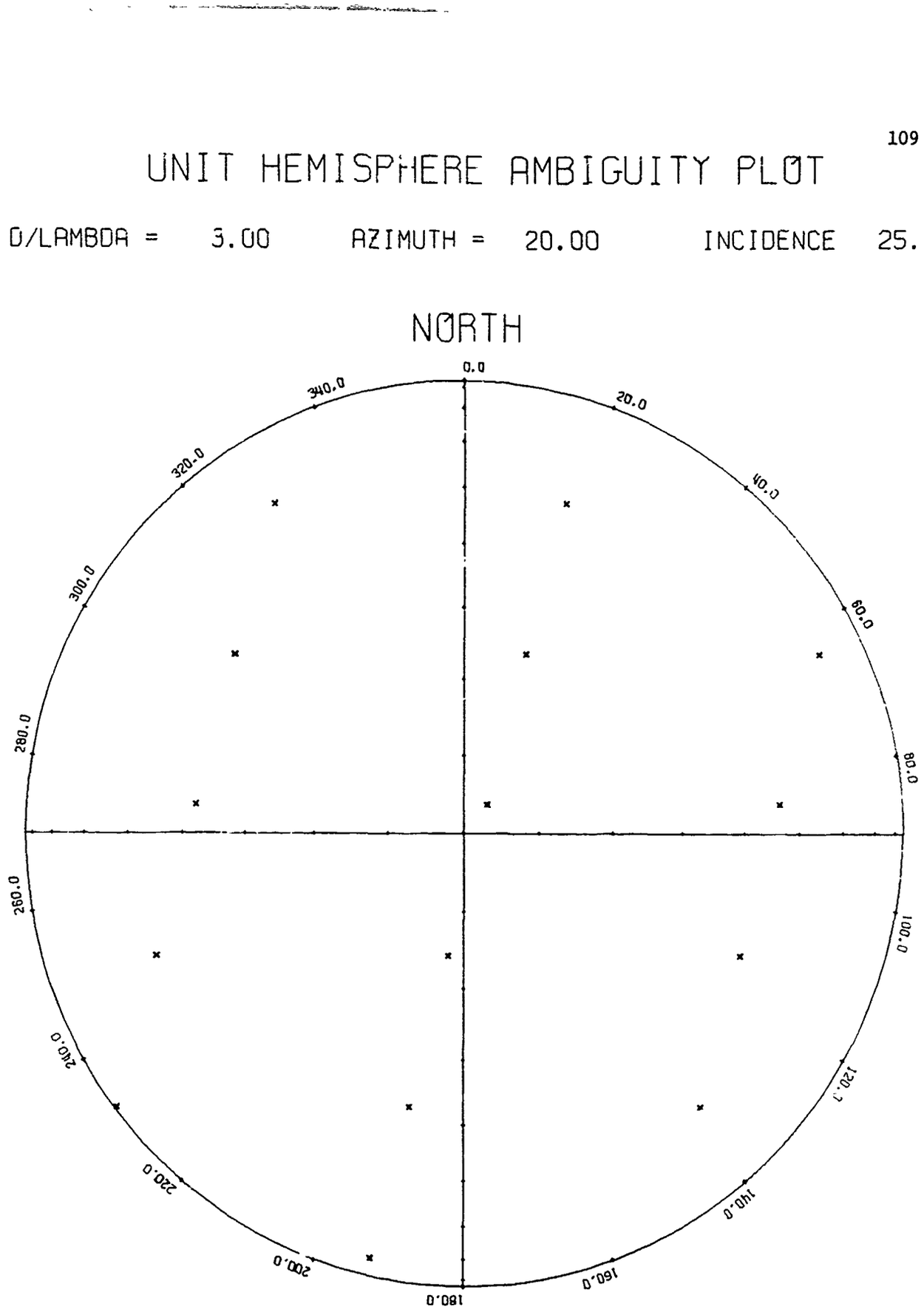

Figure C-2. Hemispherical Projection Plot ($\gamma = 30^{o}$)

UNIT HEMISPHERE AMBIGUITY PLOT

D/LAMBDA = 3.00 AZIMUTH = 20.00 INCIDENCE 25.00

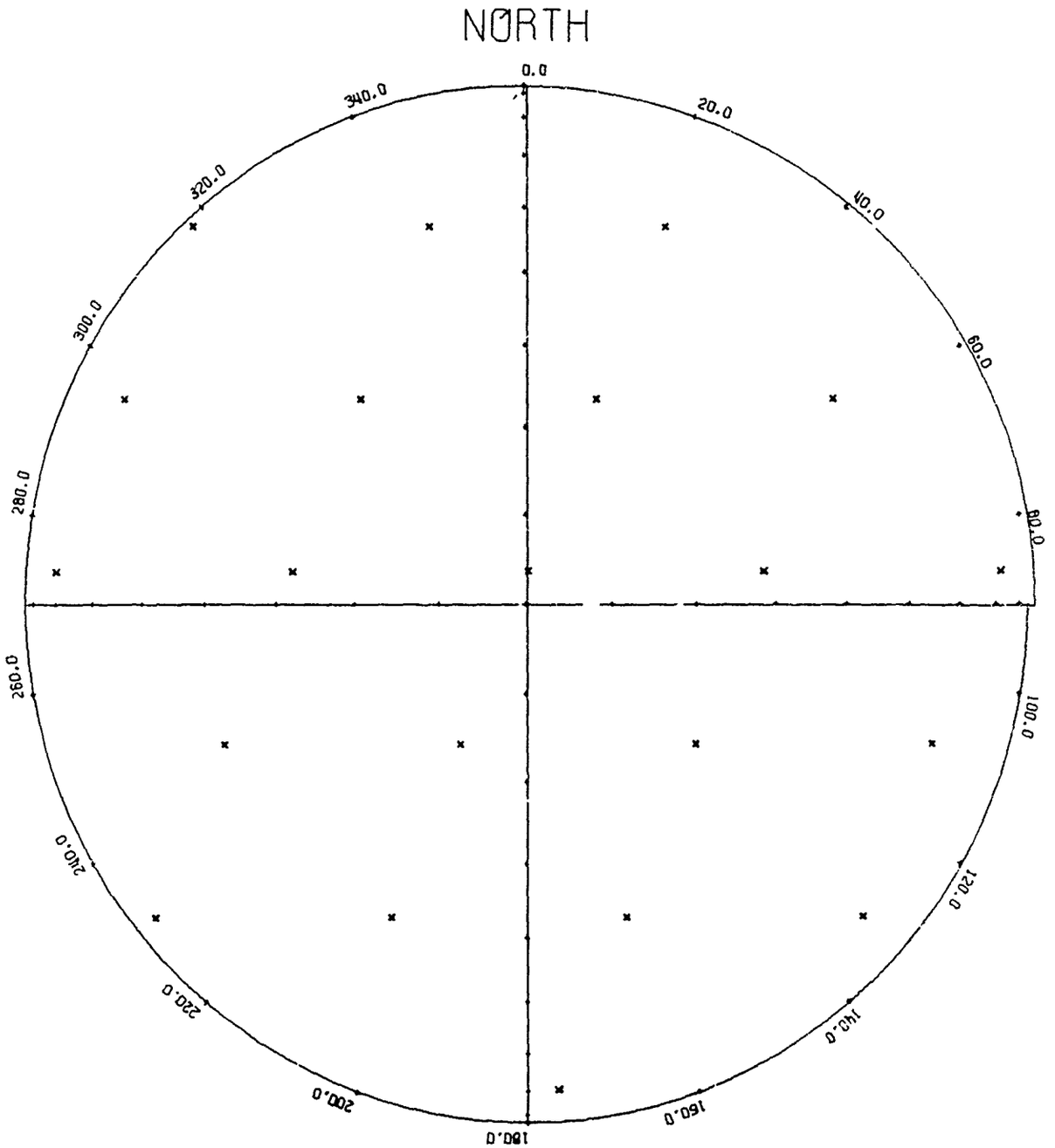

ARRAY ANGLE = 45.00

Figure C-3. Hemispherical Projection Plot ($\gamma = 45^{o}$)

UNIT HEMISPHERE AMBIGUITY PLOT

D/LAMBDA = 3.00 AZIMUTH = 20.00 INCIDENCE 25.00

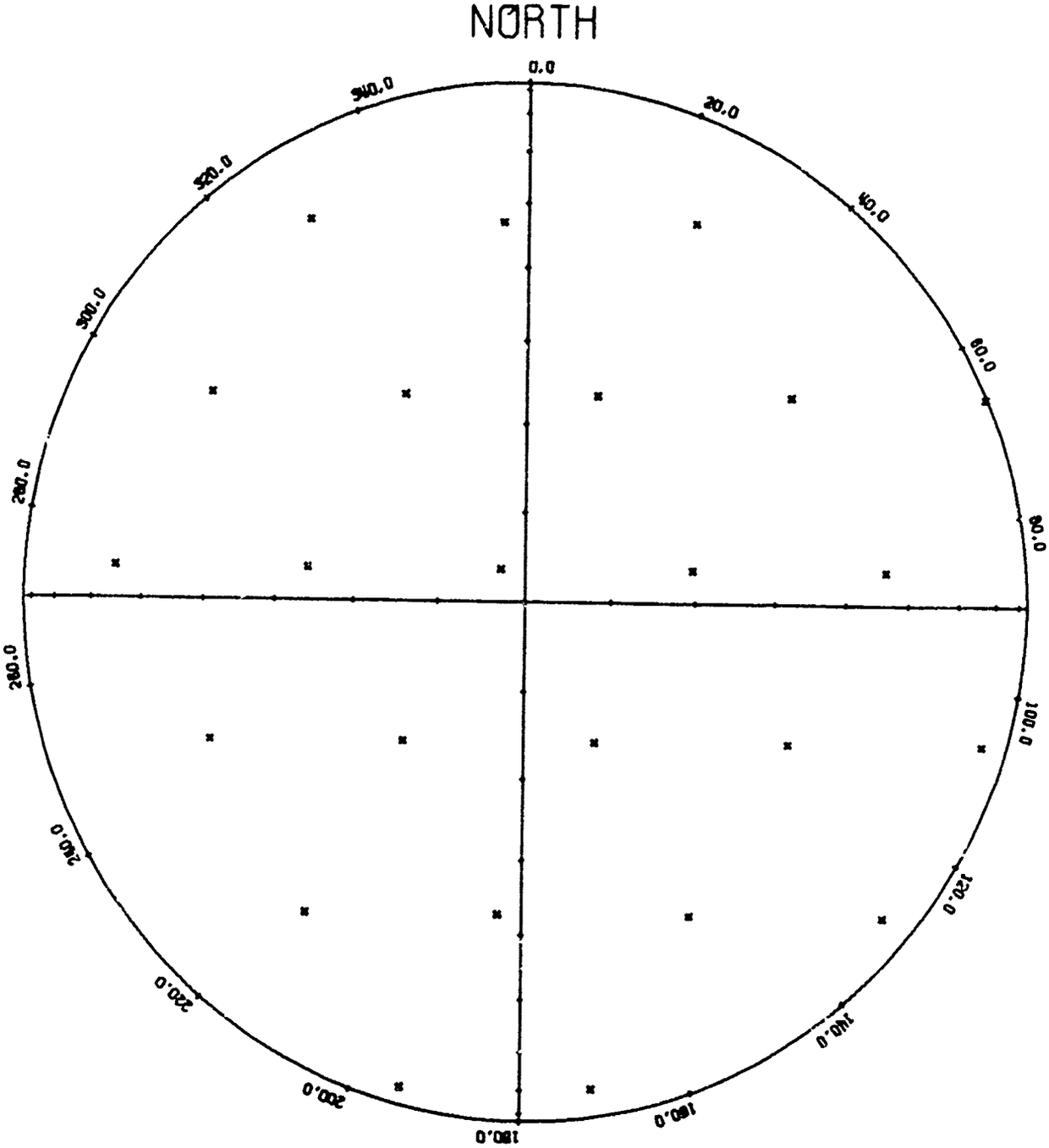

ARRAY ANGLE = 60.00

Figure C-4. Hemispherical Projection Plot ($\gamma = 60^{o}$)

UNIT HEMISPHERE AMBIGUITY PLOT

D/LAMBDA = 3.00 AZIMUTH = 20.00 INCIDENCE 25.00

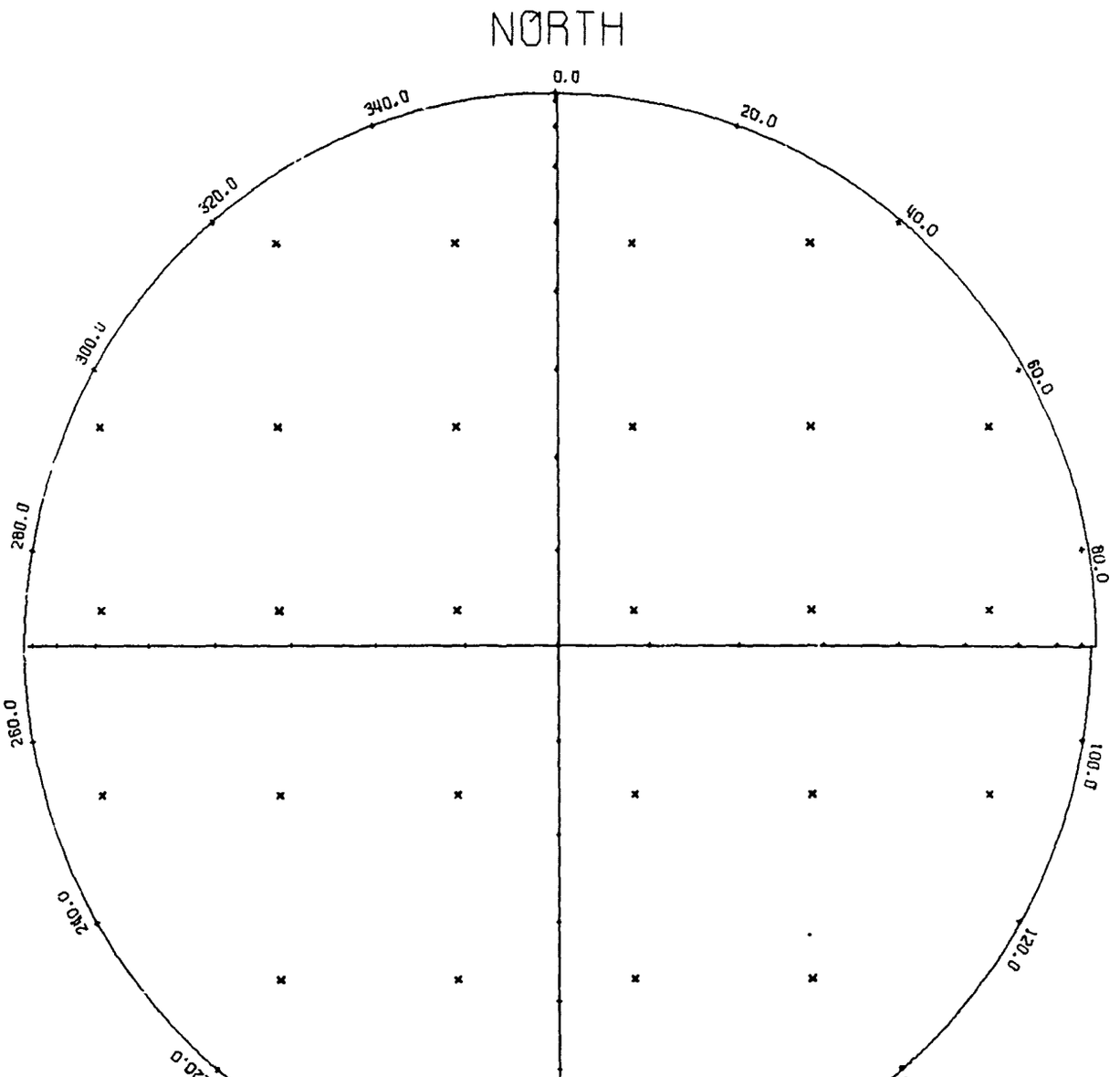

ARRAY ANGLE = 90.00

Figure C-5. Hemisp'erical Projection Plot ($\gamma = 90^{o}$)

APPENDIX D

The limitations of an approximate azimuth direction ambiguity resolution system are studied in this appendix. The significance of the results contained herein is explained in Chapter V.

The program listing is included. All user-written subroutines called are listed in Appendix M.

```
$     INPUT SOURCE CARDS
$     EXECUTE
$     FORTRAN
H      NAME AMBPLT;
H      EQUIP=CARDRE,PRINTE,CARDPU;
H      SINGLEALL;
C*****
C*****THIS IS AN AMBIGUITY CHOOSING PROGRAM.  FROM ALL POSSIBLE AMBIGUITIES
C*****IT CHOOSES AND COUNTS ALL AMBIGUITIES WITHIN A SPECIFIED AZIMUTHAL SECTOR
C*****OF ARRIVAL.  IT THEN PLOTS THE NUMBER OF AMBIGUITIES FOUND WITHIN THIS
C*****CERTAIN TOLERANCE VS D/LAMBDA.  ALL PROGRAM PARAMETERS ARE VARIED
C*****INTERNALLY. HENCE THERE IS NO INPUT DATA REQUIRED OTHER THAN SOME
C*****ALPHANUMERIC LABELLING INFORMATION.
C*****
      DIMENSION LABEL1(11),LABEL2(11)
      DIMENSION MAP(15,20),DTHETA(500),DALPHA(500)
      NTEST=0
      PI=3.1415926535898
      TUPI=2.*PI
      DEG=180./PI
      SQRH=SQRT(1.5)
      READ 1,LABEL1,LABEL2
1     FORMAT(11A1)
      XTHETA=15.
      XALPHA=0.
      DO 101 ITHETA=2,6
      DO 100 IALPHA=1,16
C*****COMPUTE AMBIGUOUS INTERF PHASES FROM XALPHA, XTHETA
      RXALPH=XALPHA/DEG
      RXTHET=XTHETA/DEG
      SNTH=SIN(RXTHET)
C*****SET UP LOOP TO VARY D/LAMBDA FROM 1 TO 6 IN INCREMENTS OF 1/3
      DL=.66666666667
13    DO 60 NDL=1,16
14    DL=DL+.33333333333333
      TPDL=TUPI*DL
C*****USE ALPHA TO DETERMINE INTERFEROMETER PHASES (UNAMBIGUOUS)
      PHI21=TPDL*COS(RXALPH)*SNTH
      PHI13=TPDL*COS(RXALPH-2.*TUPI/3.)*SNTH
      PHI32=TPDL*COS(RXALPH-TUPI/3.)*SNTH
C*****REDUCE PHIIJS BY MULTIPLES OF 2 PI UNTIL BETWEEN - PI AND + PI
      CALL REDUCE(PHI21)
      CALL REDUCE(PHI13)
      CALL REDUCE(PHI32)
      DPHI21=PHI21*DEG
      DPHI13=PHI13*DEG
      DPHI32=PHI32*DEG
21     TPDLH=(TPDL**2)*.75
      N=DL+1
      M=2*N+1
      JCOUNT=0
C*****BEGIN VARYING PHI21 AND PHI32 BY + OR - 2 PI
      DO 40 M21=1,M
      N21=M21-N-1
      TPHI21=PHI21+TUPI*N21
      DO 40 M32=1,M
      N32=M32-N-1
      TPHI32=PHI32+TUPI*N32
      SMSQ=TPHI21**2+TPHI32**2+TPHI21*TPHI32
```

```
C*****THROW OUT IF THE PROPOSED COMBINATION OF PHI21 AND PHI32
C*****       DOES NOT YIELD SIN THETA = OR LESS THAN 1
      IF(TPDLH-SMSQ)40,30,30
C*****IF(PHI21 AND PHI32 PASS THIS TEST COMPUTE ALPHA AND THETA
30    ARG1=2.*TPHI32+TPHI21
      ARG2=1.732051*TPHI21
      ALPHA=ATAN2(ARG1,ARG2)
      STH=SQRT(2.*SMSQ)/(TPDL*SQRH)
      JCOUNT=JCOUNT+1
      DALPHA(JCOUNT)=DEG*ALPHA
      DTHETA(JCOUNT)=DEG*ASIN(STH)
40    CONTINUE
C*****SET UP LOOP WHICH VARIES ERRTOL FROM 0 TO + OR - 10 DEGREES OF XALPHA
C*****ERRTOL IS NOT SET PRECISELY EQUAL TO ZERO DUE TO PROBLEMS WITH
C*****COMPUTER ROUNDOFF ERROR.  HOWEVER IT IS ESSENTIALLY ZERO
41    ERRTOL=.0049
      DO 60 LOOP=1,11
C*****COUNT NUMBER OF AMBIGUITIES THAT LIE WITHIN + OR - ERRTOL OF THE TRUE AZ
      NUMAM = 0
      DO 49 NL=1,JCOUNT
      IF(DALPHA(NL)-XALPHA-ERRTOL)42,42,46
42    IF(DALPHA(NL)-XALPHA+ERRTOL)44,43,43
43    NUMAM=NUMAM+1
      GO TO 49
44    IF(XALPHA+ERRTOL-360.)49,45,45
45    IF(XALPHA-360.+ERRTOL-DALPHA(NL))49,43,43
46    IF(XALPHA-ERRTOL)47,47,49
47    IF(XALPHA+360.-ERRTOL-DALPHA(NL))43,43,49
49    CONTINUE
C*****SAVE NUMAM IN PROPER LOCATION OF MAP ARRAY
      LP=12-LOOP
      MAP(LP,NDL)=NUMAM
60    ERRTOL=ERRTOL+1.
C*****MAP NOW CONTAINS OUTPUT INFORMATION
72    IF(NTEST)75,74,75
74    PRINT 73
73    FORMAT(1H1)
      NTEST=1
      GO TO 76
75    NTEST=0
76    CONTINUE
69    PRINT 61,XALPHA,XTHETA
61    FORMAT(1H ./////,108H CHART OF THE NUMBER OF AMBIGUITIES THAT FALL
     $WITHIN A CERTAIN PROXIMITY (+ OR - ERROR) OF A GIVEN AZIMUTH  ,
     $///,41X,10HAZIMUTH = ,F7.2,8H DEGREES,/,40X,12HINCIDENCE = ,F7.2,
     $8H DEGREES.//)
      DO 62 I=1,11
      KOUNT=11-I
62    PRINT 63,LABEL1(I),LABEL2(I),KOUNT,(MAP(I,J),J=1,16)
63    FORMAT(1H .A1,2X,A1,4X,I2,3X,16I6)
      PRINT 64
64    FORMAT(// .17X,96H 1.00  1.33  1.67  2.00  2.33  2.67  3.00  3.33
     $ 3.67  4.00  4.33  4.67  5.00  5.33  5.67  6.00      ,//45X,19HBASE
     $LINE/WAVELENGTH  )
      XALPHA=XALPHA+22.
100   CONTINUE
      XTHETA=XTHETA+15.
      XALPHA=0.
101   CONTINUE
      CALL EXIT

      END
```

+ , - ERROR
IN DEGREES

Table D-1. Typical Ambiguity Proximity Chart

CHART OF THE NUMBER OF AMBIGUITIES THAT FALL WITHIN A CERTAIN PROXIMITY (+ OR - ERROR) OF A GIVEN AZIMUTH

AZIMUTH = 176.00 DEGREES
INCIDENCE = 75.00 DEGREES

+ ERROR		1.00	1.33	1.67	2.00	2.33	2.67	3.00	3.33	3.67	4.00	4.33	4.67	5.00	5.33	5.67	6.00
	10	1	1	1	1	1	1	2	2	2	2	3	3	4	5	5	6
	9	1	1	1	1	1	1	2	2	2	2	2	3	3	4	5	6
	8	1	1	1	1	1	1	1	2	2	2	2	2	3	3	3	5
	7	1	1	1	1	1	1	1	2	2	2	2	2	2	2	3	3
- ERROR	6	1	1	1	1	1	1	1	1	2	2	2	2	2	2	2	2
	5	1	1	1	1	1	1	1	1	1	2	2	2	2	2	2	2
	4	1	1	1	1	1	1	1	1	1	1	2	2	2	2	2	2
	3	1	1	1	1	1	1	1	1	1	1	1	1	2	2	2	2
	2	1	1	1	1	1	1	1	1	1	1	1	1	1	1	1	1
	1	1	1	1	1	1	1	1	1	1	1	1	1	1	1	1	1
	0	1	1	1	1	1	1	1	1	1	1	1	1	1	1	1	1

BASELINE/WAVELENGTH

CHART OF THE NUMBER OF AMBIGUITIES THAT FALL WITHIN A CERTAIN PROXIMITY (+ OR - ERROR) OF A GIVEN AZIMUTH

AZIMUTH = 198.00 DEGREES
INCIDENCE = 75.00 DEGREES

+ ERROR		1.00	1.33	1.67	2.00	2.33	2.67	3.00	3.33	3.67	4.00	4.33	4.67	5.00	5.33	5.67	6.00
	10	1	1	1	1	1	2	2	2	2	2	2	2	2	4	6	7
	9	1	1	1	1	1	1	2	2	2	2	2	2	2	3	5	5
	8	1	1	1	1	1	1	2	2	2	2	2	2	2	3	3	5
	7	1	1	1	1	1	1	1	2	2	2	2	2	2	2	3	3
- ERROR	6	1	1	1	1	1	1	1	1	2	2	2	2	2	2	3	3
	5	1	1	1	1	1	1	1	1	1	1	2	2	2	2	2	3
	4	1	1	1	1	1	1	1	1	1	1	1	1	2	2	2	2
	3	1	1	1	1	1	1	1	1	1	1	1	1	1	1	1	2
	2	1	1	1	1	1	1	1	1	1	1	1	1	1	1	1	1
	1	1	1	1	1	1	1	1	1	1	1	1	1	1	1	1	1
	0	1	1	1	1	1	1	1	1	1	1	1	1	1	1	1	1

BASELINE/WAVELENGTH

Table D-2. "Best Case" Ambiguity Proximity Chart

CHA T OF THE NUMBER OF AMBIGUITIES THAT FALL WITHIN A CERTAIN PROXIMITY (+ OR - ERROR) OF A GIVEN AZIMUTH

AZIMUTH = 44.00 DEGREES
INCIDENCE = 45.00 DEGREES

+ ERROR	1.00	1.33	1.67	2.00	2.33	2.67	3.00	3.33	3.67	4.00	4.33	4.67	5.00	5.33	5.67	6.00
10	1	1	1	1	1	1	1	1	1	3	3	3	3	3	4	5
9	1	1	1	1	1	1	1	1	1	2	3	3	3	3	3	4
8	1	1	1	1	1	1	1	1	1	2	2	3	3	3	3	4
7	1	1	1	1	1	1	1	1	1	2	2	2	3	3	3	4
6	1	1	1	1	1	1	1	1	1	2	2	2	2	2	3	4
5	1	1	1	1	1	1	1	1	1	2	2	2	2	2	2	2
4	1	1	1	1	1	1	1	1	1	1	2	2	2	2	2	2
3	1	1	1	1	1	1	1	1	1	1	1	1	1	1	1	2
2	1	1	1	1	1	1	1	1	1	1	1	1	1	1	1	1
1	1	1	1	1	1	1	1	1	1	1	1	1	1	1	1	1
0	1	1	1	1	1	1	1	1	1	1	1	1	1	1	1	1

BASELINE/WAVELENGTH

CHA-T OF THE NUMRER OF AMBIGUITIES THAT FALL WITHIN A CERTAIN PROXIMITY (+ OR - ERROR) OF A GIVEN AZIMUTH

AZIMUTH = 66.00 DEGREES
INCIDENCE = 45.00 DEGREES

+ ERROR	1.00	1.33	1.67	2.00	2.33	2.67	3.00	3.33	3.67	4.00	4.33	4.67	5.00	5.33	5.67	6.00
10	1	1	1	1	1	1	1	1	1	2	3	4	4	5	5	5
9	1	1	1	1	1	1	1	1	1	2	2	2	4	4	4	5
8	1	1	1	1	1	1	1	1	1	2	2	2	3	3	4	4
7	1	1	1	1	1	1	1	1	1	2	2	2	2	3	3	3
6	1	1	1	1	1	1	1	1	1	1	1	1	2	2	3	3
5	1	1	1	1	1	1	1	1	1	1	1	1	1	1	1	1
4	1	1	1	1	1	1	1	1	1	1	1	1	1	1	1	1
3	1	1	1	1	1	1	1	1	1	1	1	1	1	1	1	1
2	1	1	1	1	1	1	1	1	1	1	1	1	1	1	1	1
1	1	1	1	1	1	1	1	1	1	1	1	1	1	1	1	1
0	1	1	1	1	1	1	1	1	1	1	1	1	1	1	1	1

BASELINE/WAVELENGTH

Table D-3. "Worst Case" Ambiguity Proximity Chart

CHART OF THE NUMBER OF AMBIGUITIES THAT FALL WITHIN A CERTAIN PROXIMITY (+ OR - ERROR) OF A GIVEN AZIMUTH

AZIMUTH = 308.00 DEGREES
INCIDENCE = 75.00 DEGREES

+ ERROR	1.00	1.33	1.67	2.00	2.33	2.67	3.00	3.33	3.67	4.00	4.33	4.67	5.00	5.33	5.67	6.00
10	1	1	1	1	1	1	1	1	2	3	4	4	4	5	5	6
9	1	1	1	1	1	1	1	1	1	3	4	4	4	4	5	5
8	1	1	1	1	1	1	1	1	1	1	4	4	4	4	4	4
7	1	1	1	1	1	1	1	1	1	1	1	3	4	4	4	4
6	1	1	1	1	1	1	1	1	1	1	1	1	3	3	4	4
5	1	1	1	1	1	1	1	1	1	1	1	1	2	2	3	3
4	1	1	1	1	1	1	1	1	1	1	1	1	1	1	2	2
3	1	1	1	1	1	1	1	1	1	1	1	1	1	1	1	1
2	1	1	1	1	1	1	1	1	1	1	1	1	1	1	1	1
1	1	1	1	1	1	1	1	1	1	1	1	1	1	1	1	1
0	1	1	1	1	1	1	1	1	1	1	1	1	1	1	1	1

BASELINE/WAVELENGTH

CHART OF THE NUMBER OF AMBIGUITIES THAT FALL WITHIN A CERTAIN PROXIMITY (+ OR - ERROR) OF A GIVEN AZIMUTH

AZIMUTH = 330.00 DEGREES
INCIDENCE = 75.00 DEGREES

+ ERROR	1.00	1.33	1.67	2.00	2.33	2.67	3.00	3.33	3.67	4.00	4.33	4.67	5.00	5.33	5.67	6.00
10	1	2	2	2	2	3	3	3	4	4	4	4	5	5	5	6
9	1	2	2	2	2	3	3	3	4	4	4	4	5	5	5	6
8	1	2	2	2	2	3	3	3	4	4	4	4	5	5	5	6
7	1	2	2	2	2	3	3	3	4	4	4	4	5	5	5	6
6	1	2	2	2	2	3	3	3	4	4	4	4	5	5	5	6
5	1	2	2	2	2	3	3	3	4	4	4	4	5	5	5	6
4	1	2	2	2	2	3	3	3	4	4	4	4	5	5	5	6
3	1	2	2	2	2	3	3	3	4	4	4	4	5	5	5	6
2	1	2	2	2	2	3	3	3	4	4	4	4	5	5	5	6
1	1	2	2	2	2	3	3	3	4	4	4	4	5	5	5	6
0	1	2	2	2	2	3	3	3	3	4	4	4	5	5	5	5

BASELINE/WAVELENGTH

```
$     EXECUTE
$      INPUT PROGRAM TAPE,CDDUP
$     INPUT SOURCE CARDS
$     EXECUTE
$     FORTRAN
H      NAME AMBPLT;  (MODIFIED VERSION)
H      EQUIP=CARDRE,PRINTE,CARDPU;
H      SINGLEALL;
C*****************************************************************************
C*****THIS PROGRAM HAS BEEN MODIFIED TO TEST AN AMBIGUITY REJECTION
C*****CRITERION BASED ON A KNOWLEDGE OF THE APPROXIMATE AZIMUTH (TEN DEGREE
C*****TOLERANCE).....................
C*****************************************************************************
C*****
C*****THIS IS AN AMBIGUITY CHOOSING PROGRAM.  FROM ALL POSSIBLE AMBIGUITIES
C*****IT CHOOSES AND COUNTS ALL AMBIGUITIES WITHIN A SPECIFIED AZIMUTHAL SECTOR
C*****OF ARRIVAL.  IT THEN PLOTS THE NUMBER OF AMBIGUITIES FOUND WITHIN THIS
C*****CERTAIN TOLERANCE VS D/LAMBDA.  ALL PROGRAM PARAMETERS ARE VARIED
C*****INTERNALLY. EXCEPT SOME ALPHANUMERIC LABELLING INFORMATION AND THE ACTUAL
C*****DOA (IN 2F10.5 FORMAT)
C*****
      DIMENSION LABEL1(11),LABEL2(11),CALPHA(200,16)
      DIMENSION MAP(15,20),DTHETA(500),DALPHA(500)
      PI=3.1415926535898
      TUPI=2.*PI
      DEG=180./PI
      SQRH=SQRT(1.5)
      READ 1,LABEL1,LABEL2
1     FORMAT(11A1)
      READ 10,XALPHA,XTHETA
10    FORMAT(2F10.5)
C*****************************************************************************
C*****SET UP REJECTION CRITERIA FOR AMBIGUITIES BY ESTABLISHING MAX AND MIN
C*****LIMITS ON PHIIJS, BASED ON APPROX AZIMUTH INFO.  (ACTUALLY APPROX AZIMUTH
C*****OFF FROM TRUE AZIMUTH BY 9 DEGREES)  THE LIMITS ARE CHOSEN BY RANGE ROUTIN
C*****ASSUMING APPROX AZ IS OFF BY + OR - 10 DEGREES
      AZ=XALPHA+9.9
      CALL RANGE(AZ,0.,FIMX21,FIMN21)
      CALL RANGE(AZ,120.,FIMX32,FIMN32)
      CALL RANGE(AZ,240.,FIMX13,FIMN13)
C*****COMPUTE AMBIGUOUS INTERF PHASES FROM XALPHA, XTHETA
      RXALPH=XALPHA/DEG
      RXTHET=XTHETA/DEG
      SNTH=SIN(RXTHET)
      IQUIT=0
C*****INITIALIZE MAP BY SETTING MAP(I,J)=0
      DO 11 INIT=1,11
      DO 11 JNIT=1,16
      MAP(INIT,JNIT)=0
11    CONTINUE
C*****SET UP LOOP TO VARY D/LAMBDA FROM 1 TO 6 IN INCREMENTS OF 1/3
      DL=.6666666666667
13    DO 60 NDL=1,16
      IF(IQUIT)48,14,48
14    DL=DL+.33333333333333
      TPDL=TUPI*DL
C*****USE ALPHA TO DETERMINE INTERFEROMETER PHASES (UNAMBIGUOUS)
      PHI21=TPDL*COS(RXALPH)*SNTH
      PHI13=TPDL*COS(RXALPH-2.*TUPI/3.)*SNTH
```

```
      PHI32=TPDL*COS(RXALPH-TUPI/3.)*SNTH
C*****REDUCE PHIIJS BY MULTIPLES OF 2 PI UNTIL BETWEEN - PI AND + PI
      CALL REDUCE(PHI21)
      CALL REDUCE(PHI13)
      CALL REDUCE(PHI32)
      FI21MX=TPDL*FIMX21
      FI21MN=TPDL*FIMN21
      FI32MX=TPDL*FIMX32
      FI32MN=TPDL*FIMN32
      FI13MX=TPDL*FIMX13
      FI13MN=TPDL*FIMN13
      DPHI21=PHI21*DEG
      DPHI13=PHI13*DEG
      DPHI32=PHI32*DEG
      IF(TPDL-5.5)21,21,99
99    PRINT 12
12    FORMAT(/////)
19    PRINT 20 ,DL,XALPHA,XTHETA,DPHI21,DPHI13,DPHI32
20    FORMAT(12H D/LAMBDA = ,F7.3,5X,10HAZIMUTH = ,F7.2,5X,8HTHETA = ,F7.2,/,37H
     $.2,/,37H AMBIGUOUS INTERFEROMETER PHASES ARE.,5X,9H PHI21 = ,F7.2,
     $5X,9H PHI13 = ,F7.2,5X,9H PHI32 = ,F7.2,///)
21     TPDLH=(TPDL**2)*.75
      N=DL+1
      M=2*N+1
      JCOUNT=0
C*****BEGIN VARYING PHI21 AND PHI32 BY + OR - 2 PI
      DO 40 M21=1,M
      N21=M21-N-1
      TPHI21=PHI21+TUPI*N21
      DO 40 M32=1,M
      N32=M32-N-1
      TPHI32=PHI32+TUPI*N32
      SMSQ=TPHI21**2+TPHI32**2+TPHI21*TPHI32
C*****THROW OUT IF THE PROPOSED COMBINATION OF PHI21 AND PHI32
C*****       DOES NOT YIELD SIN THETA = OR LESS THAN 1
      IF(TPDLH-SMSQ)40,30,30
C*****IF(PHI21 AND PHI32 PASS THIS TEST COMPUTE ALPHA AND THETA
30    ARG1=2.*TPHI32+TPHI21
      ARG2=1.732051*TPHI21
      ALPHA=ATAN2(ARG1,ARG2)
      STH=SQRT(2.*SMSQ)/(TPDL*SQRH)
      JCOUNT=JCOUNT+1
      DALPHA(JCOUNT)=DEG*ALPHA
      DTHETA(JCOUNT)=DEG*ASIN(STH)
      TPHI13=-TPHI21-TPHI32
      IF(FI21MX-TPHI21)997,980,980
980   IF(TPHI21-FI21MN)997,981,981
981   IF(FI32MX-TPHI32)997,982,982
982   IF(TPHI32-FI32MN)997,983,983
983   IF(FI13MX-TPHI13)997,984,984
984   IF(TPHI13-FI13MN)997,985,985
985   XMARK=4H
      CALPHA(JCOUNT,NDL)=DALPHA(JCOUNT)
      GO TO 999
997   CALPHA(JCOUNT,NDL)=180.+XALPHA
      XMARK=4H****
      IF(TPDL-5.5)40,40,999
999   PRINT 31,JCOUNT,N21,N32,DALPHA(JCOUNT),DTHETA(JCOUNT),XMARK
31    FORMAT(15H AMBIGUITY NO. ,I4,3X,11HPHI21+2 PI*,I3,3X,
     $ 11HPHI32+2 PI*,I3,3X,9H ALPHA = ,F7.2,3X,8HTHETA = ,F7.2,A4)
```

```
40    CONTINUE
C*****SET UP LOOP WHICH VARIES ERRTOL FROM 0 TO + OR - 10 DEGREES OF XALPHA
      GO TO 41
48    DO 480 ICT=1,JCOUNT
480   DALPHA(ICT)=CALPHA(ICT,NDL)
41    ERRTOL=.0049
      DO 60 LOOP=1,11
C*****COUNT NUMBER OF AMBIGUITIES THAT LIE WITHIN + OR - ERRTOL OF THE TRUE AZ
      NUMAM = 0
      DO 49 NL=1,JCOUNT
      IF(DALPHA(NL)-XALPHA+ERRTOL)42,42,46
42    IF(DALPHA(NL)-XALPHA+ERRTOL)44,43,43
43    NUMAM=NUMAM+1
      GO TO 49
44    IF(XALPHA+ERRTOL-360.)49,45,45
45    IF(XALPHA-360.+ERRTOL-DALPHA(NL))49,43,43
46    IF(XALPHA-ERRTOL)47,47,49
47    IF(XALPHA+360.-ERRTOL-DALPHA(NL))43,43,49
49    CONTINUE
C*****SAVE NUMAM IN PROPER LOCATION OF MAP ARRAY
      LP=12-LOOP
      MAP(LP,NDL)=NUMAM
60    ERRTOL=ERRTOL+1.
C*****MAP NOW CONTAINS OUTPUT INFORMATION
      IF(IQUIT)69,68,69
68    PRINT 59
59    FORMAT(1H1,/////,104H (ALL POSSIBLE AMBIGUITIES FOR THE GIVEN REDU
     $CED SET OF INTERFEROMETER PHASE ANGLES BETWEEN -PI AND PI)  ,///)
69    PRINT 61,XALPHA,XTHETA
61    FORMAT(1H ,////,108H CHART OF THE NUMBER OF AMBIGUITIES THAT FALL
     $WITHIN A CERTAIN PROXIMITY (+ OR - ERROR) OF A GIVEN AZIMUTH  ,
     $///,41X,10HAZIMUTH = ,F7.2,8H DEGREES,/,40X,12HINCIDENCE = ,F7.2,
     $8H DEGREES,//)
      DO 62 I=1,11
      KOUNT=11-I
62    PRINT 63,LABEL1(I),LABEL2(I),KOUNT,(MAP(I,J),J=1,16)
63    FORMAT(1H ,A1,2X,A1,4X,I2,3X,16I6)
      PRINT 64
64    FORMAT(// ,17X,96H 1.00  1.33  1.67  2.00  2.33  2.67  3.00  3.33
     $ 3.67  4.00  4.33  4.67  5.00  5.33  5.67  6.00     ,//45X,19HBASE
     $LINE/WAVELENGTH  )
      IF(IQUIT)66,67,66
67    PRINT 65
65    FORMAT(1H1,//,4X,100H (ALL AMBIGUITIES THAT REMAIN AFTER CONSIDERI
     $NG RESTRICTIONS THE APPROX AZIMUTH PUTS ON THE PHIJS)     ,/,34X,
     $41H (REJECTED VALUES ARE STARRED ON LISTING)        ,///)
      IQUIT=2
      GO TO 13
66    CONTINUE
      CALL EXIT
      END



+ , - ERROR
 IN DEGREES
330.      75.
```

Table D-4. Ambiguities Rejected on the Basis of Approximate Azimuth Information

D/LAMBDA = 1.000 AZIMUTH = 330.00 THETA = 75.00
AMBIGUOUS INTERFEROMETER PHASES ARE. PHI21 = -58.85 PHI13 = -0.00 PHI32 = 58.85

AMBIGUITY NO.	1	PHI21+2 PI*	0	PHI32+2 PI*	0	ALPHA =	150.00	THETA = 10.88****
AMBIGUITY NO.	2	PHI21+2 PI*	1	PHI32+2 PI*	-1	ALPHA =	330.00	THETA = 75.00

D/LAMBDA = 1.333 AZIMUTH = 330.00 THETA = 75.00
AMBIGUOUS INTERFEROMETER PHASES ARE. PHI21 = 41.53 PHI13 = -0.00 PHI32 = -41.53

AMBIGUITY NO.	1	PHI21+2 PI*	-1	PHI32+2 PI*	0	ALPHA =	216.05	THETA = 55.15****
AMBIGUITY NO.	2	PHI21+2 PI*	-1	PHI32+2 PI*	1	ALPHA =	150.00	THETA = 50.01****
AMBIGUITY NO.	3	PHI21+2 PI*	0	PHI32+2 PI*	-1	ALPHA =	275.40	THETA = 66.93****
AMBIGUITY NO.	4	PHI21+2 PI*	0	PHI32+2 PI*	0	ALPHA =	330.00	THETA = 5.73
AMBIGUITY NO.	5	PHI21+2 PI*	0	PHI32+2 PI*	1	ALPHA =	83.95	THETA = 55.15****
AMBIGUITY NO.	6	PHI21+2 PI*	1	PHI32+2 PI*	-1	ALPHA =	330.00	THETA = 75.00
AMBIGUITY NO.	7	PHI21+2 PI*	1	PHI32+2 PI*	0	ALPHA =	24.60	THETA = 66.93****

D/LAMBDA = 1.667 AZIMUTH = 330.00 THETA = 75.00
AMBIGUOUS INTERFEROMETER PHASES ARE. PHI21 = 141.91 PHI13 = -0.00 PHI32 = -141.91

AMBIGUITY NO.	1	PHI21+2 PI*	-2	PHI32+2 PI*	1	ALPHA =	188.07	THETA = 76.68****
AMBIGUITY NO.	2	PHI21+2 PI*	-1	PHI32+2 PI*	0	ALPHA =	233.03	THETA = 37.19****
AMBIGUITY NO.	3	PHI21+2 PI*	-1	PHI32+2 PI*	1	ALPHA =	150.00	THETA = 24.82****
AMBIGUITY NO.	4	PHI21+2 PI*	-1	PHI32+2 PI*	2	ALPHA =	111.93	THETA = 76.69****
AMBIGUITY NO.	5	PHI21+2 PI*	0	PHI32+2 PI*	-1	ALPHA =	285.92	THETA = 59.59****
AMBIGUITY NO.	6	PHI21+2 PI*	0	PHI32+2 PI*	0	ALPHA =	330.00	THETA = 15.85
AMBIGUITY NO.	7	PHI21+2 PI*	0	PHI32+2 PI*	1	ALPHA =	66.97	THETA = 37.19****
AMBIGUITY NO.	8	PHI21+2 PI*	1	PHI32+2 PI*	-1	ALPHA =	330.00	THETA = 75.00
AMBIGUITY NO.	9	PHI21+2 PI*	1	PHI32+2 PI*	0	ALPHA =	14.08	THETA = 59.59****

D/LAMBDA = 2.000 AZIMUTH = 330.00 THETA = 75.00
AMBIGUOUS INTERFEROMETER PHASES ARE. PHI21 = -117.71 PHI13 = -0.00 PHI32 = 117.71

```
AMBIGUITY NO.     1   PHI21+2 PI* -1   PHI32+2 PI*  0    ALPHA =  196.32   THETA =  43.74****
AMBIGUITY NO.     2   PHI21+2 PI* -1   PHI32+2 PI*  1    ALPHA =  150.00   THETA =  50.01****
AMBIGUITY NO.     3   PHI21+2 PI*  0   PHI32+2 PI* -1    ALPHA =  251.30   THETA =  30.66****
AMBIGUITY NO.     4   PHI21+2 PI*  0   PHI32+2 PI*  0    ALPHA =  150.00   THETA =  10.88****
AMBIGUITY NO.     5   PHI21+2 PI*  0   PHI32+2 PI*  1    ALPHA =  103.68   THETA =  43.74****
AMBIGUITY NO.     6   PHI21+2 PI*  1   PHI32+2 PI* -2    ALPHA =  293.56   THETA =  57.33****
AMBIGUITY NO.     7   PHI21+2 PI*  1   PHI32+2 PI* -1    ALPHA =  330.00   THETA =  22.67
AMBIGUITY NO.     8   PHI21+2 PI*  1   PHI32+2 PI*  0    ALPHA =   48.70   THETA =  30.66****
AMBIGUITY NO.     9   PHI21+2 PI*  2   PHI32+2 PI* -2    ALPHA =  330.00   THETA =  75.00
AMBIGUITY NO.    10   PHI21+2 PI*  2   PHI32+2 PI* -1    ALPHA =    6.44   THETA =  57.33****


D/LAMBDA =   2.333     AZIMUTH =  330.00     THETA =   75.00
AMBIGUOUS INTERFEROMETER PHASES ARE.      PHI21 =  -17.33      PHI13 =   -0.00      PHI32 =   17.33


AMBIGUITY NO.     1   PHI21+2 PI* -2   PHI32+2 PI*  1    ALPHA =  179.22   THETA =  61.38****
AMBIGUITY NO.     2   PHI21+2 PI* -1   PHI32+2 PI* -1    ALPHA =  238.41   THETA =  59.03****
AMBIGUITY NO.     3   PHI21+2 PI* -1   PHI32+2 PI*  0    ALPHA =  207.67   THETA =  30.48****
AMBIGUITY NO.     4   PHI21+2 PI* -1   PHI32+2 PI*  1    ALPHA =  150.00   THETA =  31.24****
AMBIGUITY NO.     5   PHI21+2 PI* -1   PHI32+2 PI*  2    ALPHA =  120.78   THETA =  61.38****
AMBIGUITY NO.     6   PHI21+2 PI*  0   PHI32+2 PI* -2    ALPHA =  268.79   THETA =  77.97****
AMBIGUITY NO.     7   PHI21+2 PI*  0   PHI32+2 PI* -1    ALPHA =  267.55   THETA =  28.91****
AMBIGUITY NO.     8   PHI21+2 PI*  0   PHI32+2 PI*  0    ALPHA =  149.99   THETA =   1.36
AMBIGUITY NO.     9   PHI21+2 PI*  0   PHI32+2 PI*  1    ALPHA =   92.33   THETA =  30.48****
AMBIGUITY NO.    10   PHI21+2 PI*  1   PHI32+2 PI* -2    ALPHA =  299.18   THETA =  56.78****
AMBIGUITY NO.    11   PHI21+2 PI*  1   PHI32+2 PI* -1    ALPHA =  330.00   THETA =  28.10
AMBIGUITY NO.    12   PHI21+2 PI*  1   PHI32+2 PI*  0    ALPHA =   32.45   THETA =  28.91
AMBIGUITY NO.    13   PHI21+2 PI*  1   PHI32+2 PI*  1    ALPHA =   61.59   THETA =  59.03****
AMBIGUITY NO.    14   PHI21+2 PI*  2   PHI32+2 PI* -2    ALPHA =  330.00   THETA =  75.00
AMBIGUITY NO     15   PHI21+2 PI*  2   PHI32+2 PI* -1    ALPHA =    0.82   THETA =  56.78
AMBIGUITY NO.    16   PHI21+2 PI*  2   PHI32+2 PI*  0    ALPHA =   31.21   THETA =  77.97****


D/LAMBDA =   2.667     AZIMUTH =  330.00     THETA =   75.00
AMBIGUOUS INTERFEROMETER PHASES ARE.      PHI21 =   83.05      PHI13 =   -0.00      PHI32 =  -83.05


AMBIGUITY NO.     1   PHI21+2 PI* -2   PHI32+2 PI*  0    ALPHA =  216.05   THETA =  55.15****
AMBIGUITY NO.     2   PHI21+2 PI* -2   PHI32+2 PI*  1    ALPHA =  184.31   THETA =  41.71****
AMBIGUITY NO.     3   PHI21+2 PI* -2   PHI32+2 PI*  2    ALPHA =  150.00   THETA =  50.01****
AMBIGUITY NO.     4   PHI21+2 PI* -1   PHI32+2 PI* -1    ALPHA =  247.59   THETA =  49.17****
AMBIGUITY NO.     5   PHI21+2 PI* -1   PHI32+2 PI*  0    ALPHA =  222.73   THETA =  23.12****
AMBIGUITY NO.     6   PHI21+2 PI* -1   PHI32+2 PI*  1    ALPHA =  150.00   THETA =  19.46****
AMBIGUITY NO.     7   PHI21+2 PI* -1   PHI32+2 PI*  2    ALPHA =  115.69   THETA =  41.71****
AMBIGUITY NO.     8   PHI21+2 PI*  0   PHI32+2 PI* -2    ALPHA =  275.40   THETA =  66.93****
AMBIGUITY NO.     9   PHI21+2 PI*  0   PHI32+2 PI* -1    ALPHA =  280.16   THETA =  29.38****
AMBIGUITY NO.    10   PHI21+2 PI*  0   PHI32+2 PI*  0    ALPHA =  330.00   THETA =   5.73
```

```
AMBIGUITY NO.   11   PHI21+2 PI*  0   PHI32+2 PI*  1    ALPHA =   77.27   THETA =   23.12****
AMBIGUITY NO.   12   PHI21+2 PI*  0   PHI32+2 PI*  2    ALPHA =   83.95   THETA =   55.15****
AMBIGUITY NO.   13   PHI21+2 PI*  1   PHI32+2 PI* -2    ALPHA =  303.42   THETA =   56.93****
AMBIGUITY NO.   14   PHI21+2 PI*  1   PHI32+2 PI* -1    ALPHA =  330.00   THETA =   32.20
AMBIGUITY NO.   15   PHI21+2 PI*  1   PHI32+2 PI*  0    ALPHA =   19.84   THETA =   29.38
AMBIGUITY NO.   16   PHI21+2 PI*  1   PHI32+2 PI*  1    ALPHA =   52.41   THETA =   49.17****
AMBIGUITY NO.   17   PHI21+2 PI*  2   PHI32+2 PI* -2    ALPHA =  330.00   THETA =   75.00
AMBIGUITY NO.   18   PHI21+2 PI*  2   PHI32+2 PI* -1    ALPHA =  356.58   THETA =   56.93
AMBIGUITY NO.   19   PHI21+2 PI*  2   PHI32+2 PI*  0    ALPHA =   24.60   THETA =   66.93****


D/LAMBDA =   3.000     AZIMUTH =  330.00     THETA =   75.00
AMBIGUOUS INTERFEROMETER PHASES ARE.      PHI21 = -176.56      PHI13 =   -0.00      PHI32 =  176.57


AMBIGUITY NO.    1   PHI21+2 PI* -2   PHI32+2 PI*  0    ALPHA =  199.29   THETA =   61.58****
AMBIGUITY NO.    2   PHI21+2 PI* -2   PHI32+2 PI*  1    ALPHA =  173.51   THETA =   56.67****
AMBIGUITY NO.    3   PHI21+2 PI* -2   PHI32+2 PI*  2    ALPHA =  150.00   THETA =   73.45****
AMBIGUITY NO.    4   PHI21+2 PI* -1   PHI32+2 PI* -1    ALPHA =  224.19   THETA =   43.86****
AMBIGUITY NO.    5   PHI21+2 PI* -1   PHI32+2 PI*  0    ALPHA =  191.17   THETA =   30.42****
AMBIGUITY NO.    6   PHI21+2 PI* -1   PHI32+2 PI*  1    ALPHA =  150.00   THETA =   35.01****
AMBIGUITY NO.    7   PHI21+2 PI* -1   PHI32+2 PI*  2    ALPHA =  126.49   THETA =   56.67****
AMBIGUITY NO.    8   PHI21+2 PI*  0   PHI32+2 PI* -2    ALPHA =  256.39   THETA =   44.02****
AMBIGUITY NO.    9   PHI21+2 PI*  0   PHI32+2 PI* -1    ALPHA =  240.63   THETA =   19.47****
AMBIGUITY NO.   10   PHI21+2 PI*  0   PHI32+2 PI*  0    ALPHA =  150.00   THETA =   10.88****
AMBIGUITY NO.   11   PHI21+2 PI*  0   PHI32+2 PI*  1    ALPHA =  108.83   THETA =   30.42****
AMBIGUITY NO.   12   PHI21+2 PI*  0   PHI32+2 PI*  2    ALPHA =  100.71   THETA =   61.58****
AMBIGUITY NO.   13   PHI21+2 PI*  1   PHI32+2 PI* -2    ALPHA =  281.07   THETA =   62.17****
AMBIGUITY NO.   14   PHI21+2 PI*  1   PHI32+2 PI* -1    ALPHA =  289.38   THETA =   30.79****
AMBIGUITY NO.   15   PHI21+2 PI*  1   PHI32+2 PI*  0    ALPHA =  330.00   THETA =   11.31
AMBIGUITY NO.   16   PHI21+2 PI*  1   PHI32+2 PI*  1    ALPHA =   59.37   THETA =   19.47****
AMBIGUITY NO.   17   PHI21+2 PI*  1   PHI32+2 PI*  2    ALPHA =   75.81   THETA =   43.86****
AMBIGUITY NO.   18   PHI21+2 PI*  2   PHI32+2 PI* -2    ALPHA =  306.69   THETA =   57.38****
AMBIGUITY NO.   19   PHI21+2 PI*  2   PHI32+2 PI* -1    ALPHA =  330.00   THETA =   35.52
AMBIGUITY NO.   20   PHI21+2 PI*  2   PHI32+2 PI*  0    ALPHA =   10.62   THETA =   30.79
AMBIGUITY NO.   21   PHI21+2 PI*  2   PHI32+2 PI*  1    ALPHA =   43.61   THETA =   44.02****
AMBIGUITY NO.   22   PHI21+2 PI*  3   PHI32+2 PI* -2    ALPHA =  330.00   THETA =   75.00
AMBIGUITY NO.   23   PHI21+2 PI*  3   PHI32+2 PI* -1    ALPHA =  353.31   THETA =   57.38
AMBIGUITY NO.   24   PHI21+2 PI*  3   PHI32+2 PI*  0    ALPHA =   18.93   THETA =   62.17****


D/LAMBDA =   3.333     AZIMUTH =  330.00     THETA =   75.00
AMBIGUOUS INTERFEROMETER PHASES ARE.      PHI21 =  -76.18      PHI13 =   -0.00      PHI32 =   76.18


AMBIGUITY NO.    1   PHI21+2 PI* -3   PHI32+2 PI*  1    ALPHA =  188.07   THETA =   76.68****
AMBIGUITY NO.    2   PHI21+2 PI* -3   PHI32+2 PI*  2    ALPHA =  167.71   THETA =   80.43****
AMBIGUITY NO.    3   PHI21+2 PI* -2   PHI32+2 PI* -1    ALPHA =  224.68   THETA =   68.93****
AMBIGUITY NO.    4   PHI21+2 PI* -2   PHI32+2 PI*  0    ALPHA =  205.03   THETA =   47.07****
AMBIGUITY NO.    5   PHI21+2 PI* -2   PHI32+2 PI*  1    ALPHA =  176.84   THETA =   41.64****
```

AMBIGUITY NO.	6	PHI21+2 PI* -2	PHI32+2 PI* 2	ALPHA =	150.00	THETA =	50.01****
AMBIGUITY NO.	7	PHI21+2 PI* -2	PHI32+2 PI* 3	ALPHA =	132.29	THETA =	80.43****
AMBIGUITY NO.	8	PHI21+2 PI* -1	PHI32+2 PI* -2	ALPHA =	246.33	THETA =	64.89****
AMBIGUITY NO.	9	PHI21+2 PI* -1	PHI32+2 PI* -1	ALPHA =	233.03	THETA =	37.19****
AMBIGUITY NO.	10	PHI21+2 PI* -1	PHI32+2 PI* 0	ALPHA =	200.59	THETA =	22.85****
AMBIGUITY NO.	11	PHI21+2 PI* -1	PHI32+2 PI* 1	ALPHA =	150.00	THETA =	24.82****
AMBIGUITY NO.	12	PHI21+2 PI* -1	PHI32+2 PI* 2	ALPHA =	123.16	THETA =	41.64****
AMBIGUITY NO.	13	PHI21+2 PI* -1	PHI32+2 PI* 3	ALPHA =	111.93	THETA =	76.68****
AMBIGUITY NO.	14	PHI21+2 PI* 0	PHI32+2 PI* -2	ALPHA =	264.47	THETA =	41.24****
AMBIGUITY NO.	15	PHI21+2 PI* 0	PHI32+2 PI* -1	ALPHA =	258.42	THETA =	18.43****
AMBIGUITY NO.	16	PHI21+2 PI* 0	PHI32+2 PI* 0	ALPHA =	150.00	THETA =	4.20
AMBIGUITY NO.	17	PHI21+2 PI* 0	PHI32+2 PI* 1	ALPHA =	99.41	THETA =	22.85****
AMBIGUITY NO.	18	PHI21+2 PI* 0	PHI32+2 PI* 2	ALPHA =	94.97	THETA =	47.07****
AMBIGUITY NO.	19	PHI21+2 PI* 1	PHI32+2 PI* -3	ALPHA =	285.92	THETA =	59.59****
AMBIGUITY NO.	20	PHI21+2 PI* 1	PHI32+2 PI* -2	ALPHA =	296.09	THETA =	32.53****
AMBIGUITY NO.	21	PHI21+2 PI* 1	PHI32+2 PI* -1	ALPHA =	330.00	THETA =	15.85
AMBIGUITY NO.	22	PHI21+2 PI* 1	PHI32+2 PI* 0	ALPHA =	41.58	THETA =	18.43
AMBIGUITY NO.	23	PHI21+2 PI* 1	PHI32+2 PI* 1	ALPHA =	66.97	THETA =	37.19****
AMBIGUITY NO.	24	PHI21+2 PI* 1	PHI32+2 PI* 2	ALPHA =	75.32	THETA =	68.93****
AMBIGUITY NO.	25	PHI21+2 PI* 2	PHI32+2 PI* -3	ALPHA =	309.27	THETA =	57.95****
AMBIGUITY NO.	26	PHI21+2 PI* 2	PHI32+2 PI* -2	ALPHA =	330.00	THETA =	38.28
AMBIGUITY NO.	27	PHI21+2 PI* 2	PHI32+2 PI* -1	ALPHA =	3.91	THETA =	32.53
AMBIGUITY NO.	28	PHI21+2 PI* 2	PHI32+2 PI* 0	ALPHA =	35.53	THETA =	41.24****
AMBIGUITY NO.	29	PHI21+2 PI* 2	PHI32+2 PI* 1	ALPHA =	53.67	THETA =	64.90****
AMBIGUITY NO.	30	PHI21+2 PI* 3	PHI32+2 PI* -3	ALPHA =	330.00	THETA =	75.00
AMBIGUITY NO.	31	PHI21+2 PI* 3	PHI32+2 PI* -2	ALPHA =	350.73	THETA =	57.95
AMBIGUITY NO.	32	PHI21+2 PI* 3	PHI32+2 PI* -1	ALPHA =	14.08	THETA =	59.59****

D/LAMBDA = 3.667 AZIMUTH = 330.00 THETA = 75.00
AMBIGUOUS INTERFEROMETER PHASES ARE. PHI21 = 24.20 PHI13 = -0.00 PHI32 = -24.20

AMBIGUITY NO.	1	PHI21+2 PI* -3	PHI32+2 PI* 0	ALPHA =	211.12	THETA =	69.12****
AMBIGUITY NO.	2	PHI21+2 PI* -3	PHI32+2 PI* 1	ALPHA =	191.86	THETA =	54.82****
AMBIGUITY NO.	3	PHI21+2 PI* -3	PHI32+2 PI* 2	ALPHA =	169.59	THETA =	54.41****
AMBIGUITY NO.	4	PHI21+2 PI* -3	PHI32+2 PI* 3	ALPHA =	150.00	THETA =	67.46****
AMBIGUITY NO.	5	PHI21+2 PI* -2	PHI32+2 PI* -1	ALPHA =	230.54	THETA =	56.04****
AMBIGUITY NO.	6	PHI21+2 PI* -2	PHI32+2 PI* 0	ALPHA =	211.70	THETA =	38.28****
AMBIGUITY NO.	7	PHI21+2 PI* -2	PHI32+2 PI* 1	ALPHA =	181.15	THETA =	31.82****
AMBIGUITY NO.	8	PHI21+2 PI* -2	PHI32+2 PI* 2	ALPHA =	150.00	THETA =	37.49****
AMBIGUITY NO.	9	PHI21+2 PI* -2	PHI32+2 PI* 3	ALPHA =	130.40	THETA =	54.41****
AMBIGUITY NO.	10	PHI21+2 PI* -1	PHI32+2 PI* -2	ALPHA =	252.32	THETA =	56.87****
AMBIGUITY NO.	11	PHI21+2 PI* -1	PHI32+2 PI* -1	ALPHA =	242.22	THETA =	33.08****
AMBIGUITY NO.	12	PHI21+2 PI* -1	PHI32+2 PI* 0	ALPHA =	213.45	THETA =	17.75****
AMBIGUITY NO.	13	PHI21+2 PI* -1	PHI32+2 PI* 1	ALPHA =	150.00	THETA =	17.08****
AMBIGUITY NO.	14	PHI21+2 PI* -1	PHI32+2 PI* 2	ALPHA =	118.85	THETA =	31.82****
AMBIGUITY NO.	15	PHI21+2 PI* -1	PHI32+2 PI* 3	ALPHA =	108.13	THETA =	54.82****
AMBIGUITY NO.	16	PHI21+2 PI* 0	PHI32+2 PI* -3	ALPHA =	271.10	THETA =	72.85****
AMBIGUITY NO.	17	PHI21+2 PI* 0	PHI32+2 PI* -2	ALPHA =	271.64	THETA =	39.84****
AMBIGUITY NO.	18	PHI21+2 PI* 0	PHI32+2 PI* -1	ALPHA =	273.22	THETA =	19.03****
AMBIGUITY NO.	19	PHI21+2 PI* 0	PHI32+2 PI* 0	ALPHA =	330.01	THETA =	1.21
AMBIGUITY NO.	20	PHI21+2 PI* 0	PHI32+2 PI* 1	ALPHA =	86.55	THETA =	17.75****
AMBIGUITY NO.	21	PHI21+2 PI* 0	PHI32+2 PI* 2	ALPHA =	88.30	THETA =	38.28****
AMBIGUITY NO.	22	PHI21+2 PI* 0	PHI32+2 PI* 3	ALPHA =	88.88	THETA =	69.12****

```
AMBIGUITY NO.   23   PHI21+2 PI*  1   PHI32+2 PI* -3    ALPHA =  290.04   THETA =  58.14****
AMBIGUITY NO.   24   PHI21+2 PI*  1   PHI32+2 PI* -2    ALPHA =  301.08   THETA =  34.32****
AMBIGUITY NO.   25   PHI21+2 PI*  1   PHI32+2 PI* -1    ALPHA =  330.00   THETA =  19.64
AMBIGUITY NO.   26   PHI21+2 PI*  1   PHI32+2 PI*  0    ALPHA =   26.78   THETA =  19.03
AMBIGUITY NO.   27   PHI21+2 PI*  1   PHI32+2 PI*  1    ALPHA =   57.78   THETA =  33.08****
AMBIGUITY NO.   28   PHI21+2 PI*  1   PHI32+2 PI*  2    ALPHA =   69.46   THETA =  56.04****
AMBIGUITY NO.   29   PHI21+2 PI*  2   PHI32+2 PI* -3    ALPHA =  311.36   THETA =  58.56****
AMBIGUITY NO.   30   PHI21+2 PI*  2   PHI32+2 PI* -2    ALPHA =  330.00   THETA =  40.62
AMBIGUITY NO.   31   PHI21+2 PI*  2   PHI32+2 PI* -1    ALPHA =  358.92   THETA =  34.33
AMBIGUITY NO.   32   PHI21+2 PI*  2   PHI32+2 PI*  0    ALPHA =   28.36   THETA =  39.84****
AMBIGUITY NO.   33   PHI21+2 PI*  2   PHI32+2 PI*  1    ALPHA =   47.68   THETA =  56.87****
AMBIGUITY NO.   34   PHI21+2 PI*  3   PHI32+2 PI* -3    ALPHA =  330.00   THETA =  75.00
AMBIGUITY NO.   35   PHI21+2 PI*  3   PHI32+2 PI* -2    ALPHA =  348.64   THETA =  58.56
AMBIGUITY NO.   36   PHI21+2 PI*  3   PHI32+2 PI* -1    ALPHA =    9.96   THETA =  58.14****
AMBIGUITY NO.   37   PHI21+2 PI*  3   PHI32+2 PI*  0    ALPHA =   28.90   THETA =  72.85****


D/LAMBDA =   4.000     AZIMUTH =  330.00     THETA =   75.00
AMBIGUOUS INTERFEROMETER PHASES ARE.      PHI21 =  124.58      PHI13 =   -0.00      PHI32 = -124.58


AMBIGUITY NO.    1   PHI21+2 PI* -4   PHI32+2 PI*  1    ALPHA =  200.34   THETA =  76.96****
AMBIGUITY NO.    2   PHI21+2 PI* -4   PHI32+2 PI*  2    ALPHA =  183.13   THETA =  66.18****
AMBIGUITY NO.    3   PHI21+2 PI* -4   PHI32+2 PI*  3    ALPHA =  165.35   THETA =  70.76****
AMBIGUITY NO.    4   PHI21+2 PI* -3   PHI32+2 PI*  0    ALPHA =  216.05   THETA =  55.15****
AMBIGUITY NO.    5   PHI21+2 PI* -3   PHI32+2 PI*  1    ALPHA =  196.32   THETA =  43.74****
AMBIGUITY NO.    6   PHI21+2 PI* -3   PHI32+2 PI*  2    ALPHA =  171.90   THETA =  42.08****
AMBIGUITY NO.    7   PHI21+2 PI* -3   PHI32+2 PI*  3    ALPHA =  150.00   THETA =  50.01****
AMBIGUITY NO.    8   PHI21+2 PI* -3   PHI32+2 PI*  4    ALPHA =  134.65   THETA =  70.76****
AMBIGUITY NO.    9   PHI21+2 PI* -2   PHI32+2 PI* -1    ALPHA =  236.61   THETA =  48.70****
AMBIGUITY NO.   10   PHI21+2 PI* -2   PHI32+2 PI*  0    ALPHA =  219.32   THETA =  32.31****
AMBIGUITY NO.   11   PHI21+2 PI* -2   PHI32+2 PI*  1    ALPHA =  186.89   THETA =  24.61****
AMBIGUITY NO.   12   PHI21+2 PI* -2   PHI32+2 PI*  2    ALPHA =  150.00   THETA =  28.52****
AMBIGUITY NO.   13   PHI21+2 PI* -2   PHI32+2 PI*  3    ALPHA =  128.10   THETA =  42.08****
AMBIGUITY NO.   14   PHI21+2 PI* -2   PHI32+2 PI*  4    ALPHA =  116.87   THETA =  66.18****
AMBIGUITY NO.   15   PHI21+2 PI* -1   PHI32+2 PI* -2    ALPHA =  258.04   THETA =  52.07****
AMBIGUITY NO.   16   PHI21+2 PI* -1   PHI32+2 PI* -1    ALPHA =  251.30   THETA =  30.66****
AMBIGUITY NO.   17   PHI21+2 PI* -1   PHI32+2 PI*  0    ALPHA =  229.92   THETA =  14.71****
AMBIGUITY NO.   18   PHI21+2 PI* -1   PHI32+2 PI*  1    ALPHA =  150.00   THETA =  10.88****
AMBIGUITY NO.   19   PHI21+2 PI* -1   PHI32+2 PI*  2    ALPHA =  113.11   THETA =  24.61****
AMBIGUITY NO.   20   PHI21+2 PI* -1   PHI32+2 PI*  3    ALPHA =  103.68   THETA =  43.74****
AMBIGUITY NO.   21   PHI21+2 PI* -1   PHI32+2 PI*  4    ALPHA =   99.66   THETA =  76.97****
AMBIGUITY NO.   22   PHI21+2 PI*  0   PHI32+2 PI* -3    ALPHA =  275.40   THETA =  66.93****
AMBIGUITY NO.   23   PHI21+2 PI*  0   PHI32+2 PI* -2    ALPHA =  277.85   THETA =  39.29****
AMBIGUITY NO.   24   PHI21+2 PI*  0   PHI32+2 PI* -1    ALPHA =  284.33   THETA =  20.46****
AMBIGUITY NO.   25   PHI21+2 PI*  0   PHI32+2 PI*  0    ALPHA =  330.00   THETA =   5.73
AMBIGUITY NO.   26   PHI21+2 PI*  0   PHI32+2 PI*  1    ALPHA =   70.08   THETA =  14.71****
AMBIGUITY NO.   27   PHI21+2 PI*  0   PHI32+2 PI*  2    ALPHA =   80.68   THETA =  32.31****
AMBIGUITY NO.   28   PHI21+2 PI*  0   PHI32+2 PI*  3    ALPHA =   83.95   THETA =  55.15****
AMBIGUITY NO.   29   PHI21+2 PI*  1   PHI32+2 PI* -3    ALPHA =  293.56   THETA =  57.33****
AMBIGUITY NO.   30   PHI21+2 PI*  1   PHI32+2 PI* -2    ALPHA =  304.87   THETA =  36.06****
AMBIGUITY NO.   31   PHI21+2 PI*  1   PHI32+2 PI* -1    ALPHA =  330.00   THETA =  22.87
AMBIGUITY NO.   32   PHI21+2 PI*  1   PHI32+2 PI*  0    ALPHA =   15.67   THETA =  20.46
AMBIGUITY NO.   33   PHI21+2 PI*  1   PHI32+2 PI*  1    ALPHA =   48.70   THETA =  30.66****
AMBIGUITY NO.   34   PHI21+2 PI*  1   PHI32+2 PI*  2    ALPHA =   63.39   THETA =  48.70****
```

AMBIGUITY NO.	35	PHI21+2 PI*	2	PHI32+2 PI*	-3	ALPHA =	313.08	THETA =	59.18****
AMBIGUITY NO.	36	PHI21+2 PI*	2	PHI32+2 PI*	-2	ALPHA =	330.00	THETA =	42.63
AMBIGUITY NO.	37	PHI21+2 PI*	2	PHI32+2 PI*	-1	ALPHA =	355.13	THETA =	36.06
AMBIGUITY NO.	38	PHI21+2 PI*	2	PHI32+2 PI*	0	ALPHA =	22.15	THETA =	39.29****
AMBIGUITY NO.	39	PHI21+2 PI*	2	PHI32+2 PI*	1	ALPHA =	41.96	THETA =	52.07****
AMBIGUITY NO.	40	PHI21+2 PI*	3	PHI32+2 PI*	-3	ALPHA =	330.00	THETA =	75.00
AMBIGUITY NO.	41	PHI21+2 PI*	3	PHI32+2 PI*	-2	ALPHA =	346.92	THETA =	59.18
AMBIGUITY NO.	42	PHI21+2 PI*	3	PHI32+2 PI*	-1	ALPHA =	6.44	THETA =	37.33****
AMBIGUITY NO.	43	PHI21+2 PI*	3	PHI32+2 PI*	0	ALPHA =	24.60	THETA =	66.93****

D/LAMBDA = 4.333 AZIMUTH = 330.00 THETA = 75.00
AMBIGUOUS INTERFEROMETER PHASES ARE. PHI21 = -135.04 PHI13 = -0.00 PHI32 = 135.04

AMBIGUITY NO.	1	PHI21+2 PI*	-3	PHI32+2 PI*	+1	ALPHA =	218.35	THETA =	83.29****
AMBIGUITY NO.	2	PHI21+2 PI*	-3	PHI32+2 PI*	0	ALPHA =	204.18	THETA =	58.63****
AMBIGUITY NO.	3	PHI21+2 PI*	-3	PHI32+2 PI*	1	ALPHA =	186.10	THETA =	51.56****
AMBIGUITY NO.	4	PHI21+2 PI*	-3	PHI32+2 PI*	2	ALPHA =	166.76	THETA =	53.14****
AMBIGUITY NO.	5	PHI21+2 PI*	-3	PHI32+2 PI*	3	ALPHA =	150.00	THETA =	64.07****
AMBIGUITY NO.	6	PHI21+2 PI*	-2	PHI32+2 PI*	+2	ALPHA =	233.82	THETA =	68.20****
AMBIGUITY NO.	7	PHI21+2 PI*	-2	PHI32+2 PI*	+1	ALPHA =	221.39	THETA =	46.93****
AMBIGUITY NO.	8	PHI21+2 PI*	-2	PHI32+2 PI*	0	ALPHA =	201.55	THETA =	36.11****
AMBIGUITY NO.	9	PHI21+2 PI*	-2	PHI32+2 PI*	1	ALPHA =	174.79	THETA =	33.39****
AMBIGUITY NO.	10	PHI21+2 PI*	-2	PHI32+2 PI*	2	ALPHA =	150.00	THETA =	39.26****
AMBIGUITY NO.	11	PHI21+2 PI*	-2	PHI32+2 PI*	3	ALPHA =	133.24	THETA =	53.14****
AMBIGUITY NO.	12	PHI21+2 PI*	-1	PHI32+2 PI*	-3	ALPHA =	250.23	THETA =	69.71****
AMBIGUITY NO.	13	PHI21+2 PI*	-1	PHI32+2 PI*	-2	ALPHA =	242.75	THETA =	43.88****
AMBIGUITY NO.	14	PHI21+2 PI*	-1	PHI32+2 PI*	+1	ALPHA =	227.78	THETA =	28.18****
AMBIGUITY NO.	15	PHI21+2 PI*	-1	PHI32+2 PI*	0	ALPHA =	194.70	THETA =	19.15****
AMBIGUITY NO.	16	PHI21+2 PI*	-1	PHI32+2 PI*	1	ALPHA =	150.00	THETA =	21.50****
AMBIGUITY NO.	17	PHI21+2 PI*	-1	PHI32+2 PI*	2	ALPHA =	125.21	THETA =	33.39****
AMBIGUITY NO.	18	PHI21+2 PI*	-1	PHI32+2 PI*	3	ALPHA =	110.90	THETA =	51.56****
AMBIGUITY NO.	19	PHI21+2 PI*	0	PHI32+2 PI*	+3	ALPHA =	263.41	THETA =	48.97****
AMBIGUITY NO.	20	PHI21+2 PI*	0	PHI32+2 PI*	+2	ALPHA =	259.84	THETA =	29.38****
AMBIGUITY NO.	21	PHI21+2 PI*	0	PHI32+2 PI*	+1	ALPHA =	248.21	THETA =	13.48****
AMBIGUITY NO.	22	PHI21+2 PI*	0	PHI32+2 PI*	0	ALPHA =	150.00	THETA =	5.74
AMBIGUITY NO.	23	PHI21+2 PI*	0	PHI32+2 PI*	1	ALPHA =	105.30	THETA =	19.15****
AMBIGUITY NO.	24	PHI21+2 PI*	0	PHI32+2 PI*	2	ALPHA =	98.45	THETA =	36.11****
AMBIGUITY NO.	25	PHI21+2 PI*	0	PHI32+2 PI*	3	ALPHA =	95.82	THETA =	58.63****
AMBIGUITY NO.	26	PHI21+2 PI*	1	PHI32+2 PI*	-4	ALPHA =	279.28	THETA =	63.43****
AMBIGUITY NO.	27	PHI21+2 PI*	1	PHI32+2 PI*	-3	ALPHA =	283.17	THETA =	39.26****
AMBIGUITY NO.	28	PHI21+2 PI*	1	PHI32+2 PI*	-2	ALPHA =	292.41	THETA =	22.23****
AMBIGUITY NO.	29	PHI21+2 PI*	1	PHI32+2 PI*	+1	ALPHA =	330.00	THETA =	9.59
AMBIGUITY NO.	30	PHI21+2 PI*	1	PHI32+2 PI*	0	ALPHA =	51.79	THETA =	13.48
AMBIGUITY NO.	31	PHI21+2 PI*	1	PHI32+2 PI*	1	ALPHA =	72.22	THETA =	28.18****
AMBIGUITY NO.	32	PHI21+2 PI*	1	PHI32+2 PI*	2	ALPHA =	78.61	THETA =	46.93****
AMBIGUITY NO.	33	PHI21+2 PI*	1	PHI32+2 PI*	3	ALPHA =	81.65	THETA =	83.29****
AMBIGUITY NO.	34	PHI21+2 PI*	2	PHI32+2 PI*	+4	ALPHA =	296.58	THETA =	56.93****
AMBIGUITY NO.	35	PHI21+2 PI*	2	PHI32+2 PI*	-3	ALPHA =	307.83	THETA =	37.69****
AMBIGUITY NO.	36	PHI21+2 PI*	2	PHI32+2 PI*	+2	ALPHA =	330.00	THETA =	25.66
AMBIGUITY NO.	37	PHI21+2 PI*	2	PHI32+2 PI*	+1	ALPHA =	7.59	THETA =	22.23
AMBIGUITY NO.	38	PHI21+2 PI*	2	PHI32+2 PI*	0	ALPHA =	40.16	THETA =	29.38****
AMBIGUITY NO.	39	PHI21+2 PI*	2	PHI32+2 PI*	1	ALPHA =	57.25	THETA =	43.88****
AMBIGUITY NO.	40	PHI21+2 PI*	2	PHI32+2 PI*	2	ALPHA =	66.18	THETA =	68.20****

AMBIGUITY NO.	41	PHI21+2 PI*	3	PHI32+2 PI*	4	ALPHA =	314.51	THETA =	59.78****
AMBIGUITY NO.	42	PHI21+2 PI*	3	PHI32+2 PI*	-3	ALPHA =	330.00	THETA =	44.38
AMBIGUITY NO.	43	PHI21+2 PI*	3	PHI32+2 PI*	-2	ALPHA =	352.17	THETA =	37.69
AMBIGUITY NO.	44	PHI21+2 PI*	3	PHI32+2 PI*	-1	ALPHA =	16.83	THETA =	39.26****
AMBIGUITY NO.	45	PHI21+2 PI*	3	PHI32+2 PI*	0	ALPHA =	36.59	THETA =	48.97****
AMBIGUITY NO.	46	PHI21+2 PI*	3	PHI32+2 PI*	1	ALPHA =	49.77	THETA =	69.71****
AMBIGUITY NO.	47	PHI21+2 PI*	4	PHI32+2 PI*	-4	ALPHA =	330.00	THETA =	75.00
AMBIGUITY NO.	48	PHI21+2 PI*	4	PHI32+2 PI*	-3	ALPHA =	345.49	THETA =	59.78
AMBIGUITY NO.	49	PHI21+2 PI*	4	PHI32+2 PI*	-2	ALPHA =	3.42	THETA =	56.93****
AMBIGUITY NO.	50	PHI21+2 PI*	4	PHI32+2 PI*	-1	ALPHA =	20.72	THETA =	63.43****

Table D-5. Typical Ambiguity Proximity Chart Before Rejection

(ALL POSSIBLE AMBIGUITIES FOR THE GIVEN REDUCED SET OF INTERFEROMETER PHASE ANGLES BETWEEN -PI AND PI)

CHART OF THE NUMBER OF AMBIGUITIES THAT FALL WITHIN A CERTAIN PROXIMITY (+ OR - ERROR) OF A GIVEN AZIMUTH

AZIMUTH = 330.00 DEGREES
INCIDENCE = 75.00 DEGREES

+		10	1	2	2	2	2	3	3	3	4	4	4	4	5	5	5	6
	I	9	1	2	2	2	2	3	3	3	4	4	4	4	5	5	5	6
,	N	8	1	2	2	2	2	3	3	3	4	4	4	4	5	5	5	6
		7	1	2	2	2	2	3	3	3	4	4	4	4	5	5	5	6
-	D	6	1	2	2	2	2	3	3	3	4	4	4	4	5	5	5	6
	E	5	1	2	2	2	2	3	3	3	4	4	4	4	5	5	5	6
E	G	4	1	2	2	2	2	3	3	3	4	4	4	4	5	5	5	6
R	R	3	1	2	2	2	2	3	3	3	4	4	4	4	5	5	5	6
R	E	2	1	2	2	2	2	3	3	3	4	4	4	4	5	5	5	6
O	E	1	1	2	2	2	2	3	3	3	4	4	4	4	5	5	5	6
R	S	0	1	2	2	2	2	3	3	3	3	4	4	4	5	5	5	5
			1.00	1.33	1.67	2.00	2.33	2.67	3.00	3.33	3.67	4.00	4.33	4.67	5.00	5.33	5.67	6.00

BASELINE/WAVELENGTH

Table D-6. Typical Ambiguity Proximity Chart After Rejection

(ALL AMBIGUITIES THAT REMAIN AFTER CONSIDERING RESTRICTIONS THE APPROX AZIMUTH PUTS ON THE PHIIJS)
(REJECTED VALUES ARE STARRED ON LISTING)

CHART OF THE NUMBER OF AMBIGUITIES THAT FALL WITHIN A CERTAIN PROXIMITY (+ OR - ERROR) OF A GIVEN AZIMUTH

AZIMUTH = 330.00 DEGREES
INCIDENCE = 75.00 DEGREES

+		10	1	2	2	2	2	3	3	3	4	4	4	4	5	5	5	6
	I	9	1	2	2	2	2	3	3	3	4	4	4	4	5	5	5	6
,	N	8	1	2	2	2	2	3	3	3	4	4	4	4	5	5	5	6
		7	1	2	2	2	2	3	3	3	4	4	4	4	5	5	5	6
-	D	6	1	2	2	2	2	3	3	3	4	4	4	4	5	5	5	6
	E	5	1	2	2	2	2	3	3	3	4	4	4	4	5	5	5	6
E	G	4	1	2	2	2	2	3	3	3	4	4	4	4	5	5	5	6
R	R	3	1	2	2	2	2	3	3	3	4	4	4	4	5	5	5	6
R	E	2	1	2	2	2	2	3	3	3	4	4	4	4	5	5	5	6
O	E	1	1	2	2	2	2	3	3	3	4	4	4	4	5	5	5	6
R	S	0	1	2	2	2	2	3	3	3	3	4	4	4	5	5	5	5
			1.00	1.33	1.67	2.00	2.33	2.67	3.00	3.33	3.67	4.00	4.33	4.67	5.00	5.33	5.67	6.00

BASELINE/WAVELENGTH

APPENDIX E

This appendix demonstrates the apparent equivalence of phase ambiguity resolution and direction ambiguity resolution in a small/large baseline interferometer system, as outlined in Chapter V. The case of a signal arriving from directly overhead and an array with a D/λ value of 2 was chosen. (See plot E-1.) Various approximate directions of arrival were chosen. They were defined in terms of their Cartesian coordinates on plot E-1. (The approximate DOA's are labelled as (X_{approx}, Y_{approx}) on the computer output that follows.) Next, the interferometer phases that corresponded to these approximate DOA's were computed. These "approximate" phases were used to perform a phase ambiguity resolution. The phase ambiguity resolved phases were then used to compute the indicated (phase ambiguity resolved) DOA. This DOA is denoted by the point (X_{phase}, Y_{phase}) as would be plotted on the unit hemispherical projection. (See plot E-1.) Similarly, a direction ambiguity resolution was performed using the approximate DOA information as outlined in Chapter V. The results of this process are indicated by the point (X_{dir}, Y_{dir}) as would be plotted on the unit hemispherical projection.

It can be seen from the computer output that both methods generally obtain identical results depending on the location that is "chosen" as the approximate DOA. If it is assumed that the point (0, 0) is the actual DOA, it is evident that the approximate DOA must be chosen fairly close to this point for the two processes to succeed. At times one method fails while the other one succeeds. This discrepancy is attributed to roundoff error in the digital computer.

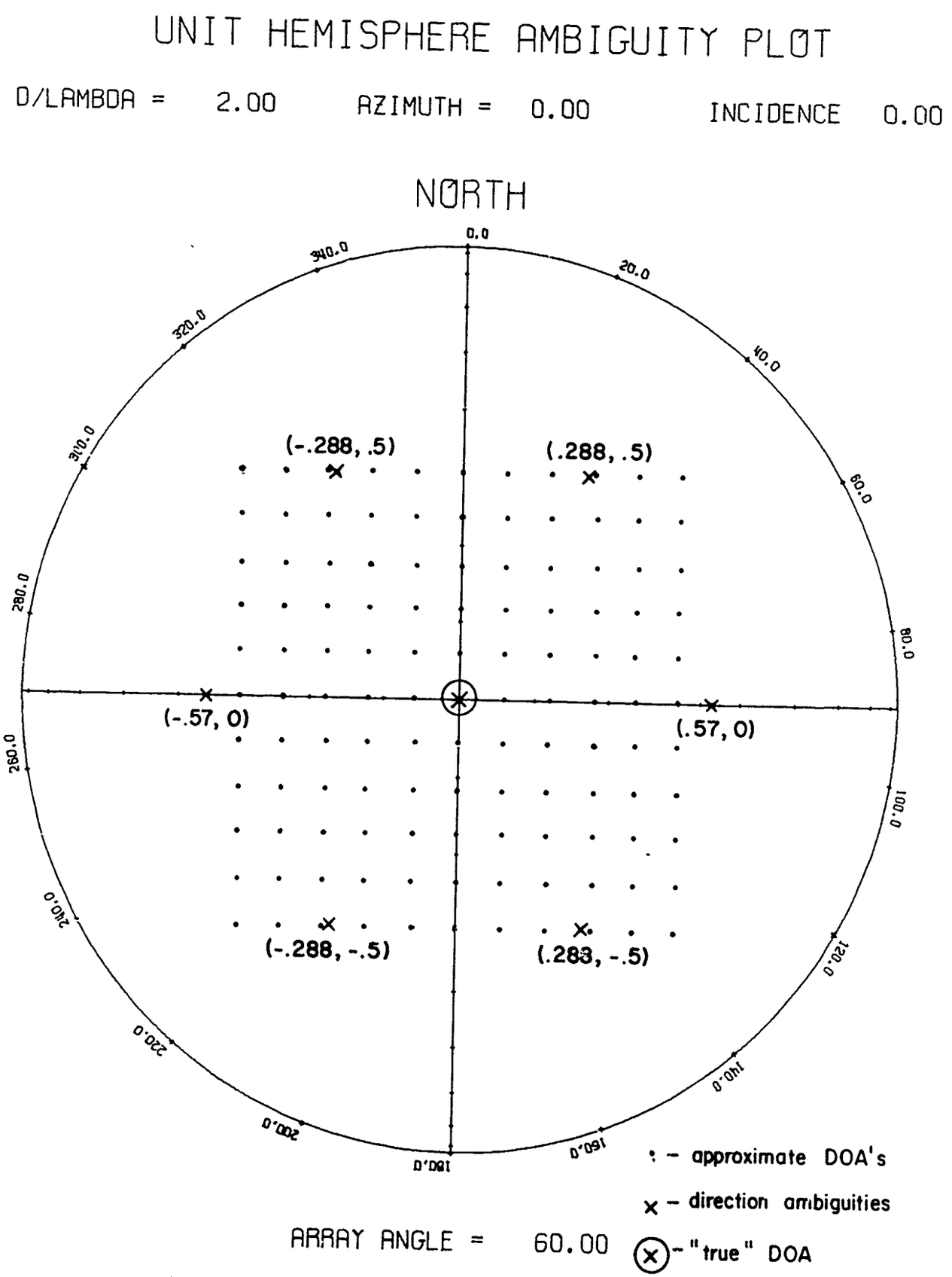

Figure E-1. Location of the Approximate DOA's Specified in the Comparison Study of Appendix E

```
$     INPUT SOURCE CARDS
$     EXECUTE
$     FORTRAN
H      NAME RESCMP)
H      EQUIP=CARDRE,PRINTE,CARDPU)
C*****
C*****THIS PROGRAM SIMULATES BOTH PHASE AND DIRECTION AMBIGUITY RESOLUTION IN A
C*****SMALL/LARGE BASELINE (SYMMETRIC ARRAY) INTERFEROMETER SYSTEM.  IT USES
C*****DOUBLE PRECISION VERSIONS OF THE REDUCE (CALLED REDUCD) AND CHOS (CALLED
C*****CHOD) SUBROUTINES OF APPENDIX M.  THE FIRST PORTION OF THE PGM DETERMINES
C*****THE LOCATION OF THE AMBIGUITIES FROM THE SPECIFIED INPUT PARAMETERS
C*****(AZIMUTH, INCIDENCE, ARRAY BASELINE, AND WAVELENGTH, IN 4F10.5 FORMAT.)
C*****ON THE BASIS OF A GIVEN APPROXIMATE DOA, WHICH IS AUTOMATICALLY VARIED BY
C*****THE PROGRAM.
C*****THE SECOND PORTION PERFORMS THE PHASE AND DIRECTION AMBIGUITY RESOLUTION
C*****
      DIMENSION X(500),Y(500)
      PI=3.1415926535898
      TUPI=2 *PI
      DEG=180./PI
      SQRH=SQRT(1.5)
      SQRT3=SQRT(3.)
      READ 10, XALPHA,XTHETA,D,XLAMB
      TPDL=TUPI*D/XLAMB
      RXALPH=XALPHA/DEG
      RXTHET=XTHETA/DEG
      SNTH=SIN(RXTHET)
C*****USE ALPHA TO DETERMINE UNAMBIGUOUS INTERFEROMETER PHASES
      PHI21=TPDL*COS(RXALPH)*SNTH
      PHI13=TPDL*COS(RXALPH-2.*TUPI/3.)*SNTH
      PHI32=TPDL*COS(RXALPH-TUPI/3.)*SNTH
C*****REDUCE PHIIJS BY MULTIPLES OF 2 PI UNTIL BETWEEN - PI AND + PI
      CALL REDUCD(PHI21)
      CALL REDUCD(PHI13)
      CALL REDUCD(PHI32)
      DL=D/XLAMB
      DPHI13=DEG*PHI13
      DPHI21=DEG*PHI21
      DPHI32=DEG*PHI32
10    FORMAT(4F10.5)
      PRINT 20,D,XLAMB,DPHI21,DPHI13,DPHI32
20    FORMAT(12H BASELINE = ,F5.1,5X,14H WAVELENGTH = ,F5.1,5X,9H PHI21
     $= ,F7.2,5X,9H PHI13 = ,F7.2,5X,9H PHI32 = ,F7.2)
      PRINT 21,XALPHA,XTHETA
21    FORMAT(//34H ACTUAL DIRECTION OF ARRIVAL.....,8X,10HAZIMUTH =  ,
     $F7.2,8X,12HINCIDENCE = ,F7.2,///)
      TPDL=TUPI*D/XLAMB
      TPDLH=(TPDL**2)*.75
      N=D/XLAMB+1
      M=2*N+1
      JCOUNT=0
C*****BEGIN VARYING PHI21 AND PHI31 BY + OR - 2 PI
      DO 40 M21=1,M
      N21=M21-N-1
      TPHI21=PHI21+TUPI*N21
      DO 40M32=1,M
      N32=M32-N-1
      TPHI32=PHI32+TUPI*N32
      SMSQ=TPHI21**2+TPHI32**2+TPHI21*TPHI32
```

```
C*****THROW OUT IF THE PROPOSED COMBINATION OF PHI21 AND PHI32
C*****DO NOT YIELD SIN(THETA) = OR LESS THAN 1
      IF(TPDLH-SMSQ)40,30,30
C*****IF(PHI21 AND PHI32 PASS THIS TEST    COMPUTE ALPHA AND THETA
30    ARG1=2.*TPHI32+TPHI21
      ARG2=SQRT3*TPHI21
      ALPHA=ATAN2(ARG1,ARG2)
      DALPHA=DEG*ALPHA
      STH=SQRT(2.*SMSQ)/(TPDL*SQRH)
      DTHETA=DEG*ASIN(STH)
      JCOUNT=JCOUNT+1
      Y(JCOUNT)=COS(ALPHA)*STH*3.5
      X(JCOUNT)=SIN(ALPHA)*STH*3.5
      PRINT 31,JCOUNT,N21,N32,DALPHA,DTHETA
31    FORMAT(15H AMBIGUITY NO. ,I4,3X,11HPHI21+2 PI*,I3,3X,
     $11HPHI32+2 PI*,I3,3X,9H ALPHA = ,F7.2,3X,8HTHETA = ,F7.2)
40    CONTINUE
      DO 210 J=1,JCOUNT
C*****BEGIN LOOKING AT THE THREE DIMENSIONAL DISTANCE FROM APPROX DOA
C*****(XAPROX, YAPROX) TO EACH AMBIGUOUS DOA.
      X(J)=X(J)/3.5
210   Y(J)=Y(J)/3.5
C*****DE-SCALE ABOVE PLOT DATA -- REDUCE TO UNIT HEMISPHERE PLOT
      XAPROX=-.6
      PRINT 300
300   FORMAT(//1H1,9X,5HXAPRX,10X,5HYAPRX,10X,3HXPH,12X,3HYPH,12X,
     $4HXDIR,11X,4HYDIR/)
      DO 500 ICNT=1,11
      XAPROX=XAPROX+.1
      YAPROX=.6
      DO 500 JCNT=1,11
      YAPROX=YAPROX-.1
C*****COMPUTE PHASES FROM SIMPLIFIED HEMISPHERE PROJECTION EQUATIONS
C*****(SOLVED SIMULTANEOUSLY FOR PHI32,PHI21.)
      P32APX=TUPI*(SQRT3*XAPROX-YAPROX)
      P21APX=2.*TUPI*YAPROX
C*****PERFORM PHASE AMBIGUITY RESOLUTION
      CALL CHOD(PHI32,P32APX,UNAM32)
      CALL CHOD(PHI21,P21APX,UNAM21)
C*****XPH AND YPH ARE THE PHASE AMBIGUITY RESOLVED COORDS OF THE DOA, AS PLOTTED
C*****ON THE HEMISPHERICAL PROJECTION PLOT.
      XPH=(2.*UNAM32+UNAM21)/(2.*SQRT3*TUPI)
      YPH = UNAM21/(2.*TUPI)
      DMIN=100.
C*****COMPUTE Z ORDINATE OF APPROX DOA ON UNIT HEM. FR  THE PROJECTION COORDS X,
C*****Y
      ZAPROX=SQRT(1.-XAPROX**2-YAPROX**2)
      DO 420 J=1,JCOUNT
      ARG=1.-X(J)**2-Y(J)**2
      IF(ARG)405,405,406
406   ZZ=SQRT(ARG)
      GO TO 407
405   ZZ=0.
407   CONTINUE
      DIST=(X(J)-XAPROX)**2+(Y(J)-YAPROX)**2+(ZZ-ZAPROX)**2
C*****COMPUTE SQUARED DIST OF (XAPROX,YAPROX) TO EACH AMBIGUITY, AND
C*****HENCE FIND WHICH AMBIGUITY IS CLOSEST TO IT.
      IF(DIST-DMIN)410,410,420
410   DMIN=DIST
      JCATCH=J
```

```
420    CONTINUE
C******JCATCH IS THE NUMBER OF THE CLOSEST AMBIGUITY TO (XAPROX,YAPROX) AND
C******IS THUS CHOSEN AS THE TRUE DOA.
       XDIR=X(JCATCH)
       YDIR=Y(JCATCH)
       PRINT 430,XAPROX,YAPROX,XPH,YPH,XDIR,YDIR
430    FORMAT(1H ,6F15.5)
500    CONTINUE
C*******
       CALL EXIT
       END
```

XAPRX	YAPRX	XPH	YPH	XDIR	YDIR
-0.50000	0.50000	-0.28868	0.50000	-0.28868	0.50000
-0.50000	0.40000	-0.28868	0.50000	-0.28868	0.50000
-0.50000	0.30000	-0.28868	0.50000	-0.28868	0.50000
-0.50000	0.20000	-0.57735	0.00000	-0.57735	0.00000
-0.50000	0.10000	-0.57735	0.00000	-0.57735	0.00000
-0.50000	0.00000	-0.57735	0.00000	-0.57735	0.00000
-0.50000	-0.10000	-0.57735	0.00000	-0.57735	0.00000
-0.50000	-0.20000	-0.57735	0.00000	-0.57735	0.00000
-0.50000	-0.30000	-0.86603	-0.50000	-0.28868	-0.50000
-0.50000	-0.40000	-0.28868	-0.50000	-0.28868	-0.50000
-0.50000	-0.50000	-0.28868	-0.50000	-0.28868	-0.50000
-0.40000	0.50000	-0.28868	0.50000	-0.28868	0.50000
-0.40000	0.40000	-0.28868	0.50000	-0.28868	0.50000
-0.40000	0.30000	-0.28868	0.50000	-0.28868	0.50000
-0.40000	0.20000	-0.57735	0.00000	-0.57735	0.00000
-0.40000	0.10000	-0.57735	0.00000	-0.57735	0.00000
-0.40000	0.00000	-0.57735	0.00000	-0.57735	0.00000
-0.40000	-0.10000	-0.57735	0.00000	-0.57735	0.00000
-0.40000	-0.20000	0.00000	0.00000	-0.57735	0.00000
-0.40000	-0.30000	-0.28868	-0.50000	-0.28868	-0.50000
-0.40000	-0.40000	-0.28868	-0.50000	-0.28868	-0.50000
-0.40000	-0.50000	-0.28868	-0.50000	-0.28868	-0.50000
-0.30000	0.50000	-0.28868	0.50000	-0.28868	0.50000
-0.30000	0.40000	-0.28868	0.50000	-0.28868	0.50000
-0.30000	0.30000	-0.28868	0.50000	-0.28868	0.50000
-0.30000	0.20000	-0.57735	0.00000	-0.28868	0.50000
-0.30000	0.10000	-0.57735	0.00000	-0.28868	0.50000
-0.30000	0.00000	-0.57735	0.00000	0.00000	0.00000
-0.30000	-0.10000	0.00000	0.00000	0.00000	0.00000
-0.30000	-0.20000	0.00000	0.00000	0.00000	0.00000
-0.30000	-0.30000	-0.28868	-0.50000	-0.28868	-0.50000
-0.30000	-0.40000	-0.28868	-0.50000	-0.28868	-0.50000
-0.30000	-0.50000	-0.28868	-0.50000	-0.28868	-0.50000
-0.20000	0.50000	-0.28868	0.50000	-0.28868	0.50000
-0.20000	0.40000	-0.28868	0.50000	-0.28868	0.50000
-0.20000	0.30000	-0.28868	0.50000	-0.28868	0.50000
-0.20000	0.20000	-0.57735	0.00000	-0.28868	0.50000
-0.20000	0.10000	-0.57735	0.00000	-0.28868	0.50000
-0.20000	0.00000	-0.57735	0.00000	0.00000	0.00000
-0.20000	-0.10000	0.00000	0.00000	0.00000	0.00000
-0.20000	-0.20000	0.00000	0.00000	0.00000	0.00000
-0.20000	-0.30000	0.00000	0.00000	0.00000	0.00000
-0.20000	-0.40000	0.00000	0.00000	0.00000	0.00000
-0.20000	-0.50000	-0.28868	-0.50000	-0.28868	-0.50000
-0.10000	0.50000	-0.28868	-0.50000	-0.28868	-0.50000
-0.10000	0.40000	-0.28868	-0.50000	-0.28868	-0.50000
-0.10000	0.30000	-0.28868	0.50000	-0.28868	0.50000
-0.10000	0.20000	-0.28868	0.50000	-0.28868	0.50000
-0.10000	0.10000	0.28868	0.50000	-0.28868	0.50000
-0.10000	0.00000	0.00000	0.00000	0.00000	0.00000
-0.10000	-0.10000	0.00000	0.00000	0.00000	0.00000
-0.10000	-0.20000	0.00000	0.00000	0.00000	0.00000
-0.10000	-0.30000	0.00000	0.00000	0.00000	0.00000
-0.10000	-0.40000	0.00000	0.00000	0.00000	0.00000
-0.10000	-0.50000	-0.28868	-0.50000	-0.28868	-0.50000
-0.00000	0.50000	-0.28868	-0.50000	-0.28868	-0.50000
-0.00000	0.40000	-0.28868	-0.50000	-0.28868	-0.50000
-0.00000	0.30000	-0.28868	0.50000	-0.28868	0.50000
		0.28868	0.50000	-0.28868	0.50000
		0.28868	0.50000	0.00000	0.00000

-0.00000	0.20000	0.00000	0.00000	0.00000	0.00000
-0.00000	0.10000	0.00000	0.00000	0.00000	0.00000
-0.00000	0.00000	0.00000	0.00000	0.00000	0.00000
-0.00000	-0.10000	0.00000	0.00000	0.00000	0.00000
-0.00000	-0.20000	0.00000	0.00000	0.00000	0.00000
-0.00000	-0.30000	-0.28868	-0.50000	0.00000	0.00000
-0.00000	-0.40000	-0.28868	-0.50000	0.28868	-0.50000
-0.00000	-0.50000	-0.28868	-0.50000	-0.28868	-0.50000
0.10000	0.50000	0.28868	0.50000	0.28868	0.50000
0.10000	0.40000	0.28868	0.50000	0.28868	0.50000
0.10000	0.30000	0.28868	0.50000	0.28868	0.50000
0.10000	0.20000	0.00000	0.00000	0.00000	0.00000
0.10000	0.10000	0.00000	0.00000	0.00000	0.00000
0.10000	0.00000	0.00000	0.00000	0.00000	0.00000
0.10000	-0.10000	0.00000	0.00000	0.00000	0.00000
0.10000	-0.20000	0.00000	0.00000	0.00000	0.00000
0.10000	-0.30000	-0.28868	-0.50000	0.28868	-0.50000
0.10000	-0.40000	0.28868	-0.50000	0.28868	-0.50000
0.10000	-0.50000	0.28868	-0.50000	0.28868	-0.50000
0.20000	0.50000	0.28868	0.50000	0.28868	0.50000
0.20000	0.40000	0.28868	0.50000	0.28868	0.50000
0.20000	0.30000	0.28868	0.50000	0.28868	0.50000
0.20000	0.20000	0.00000	0.00000	0.00000	0.00000
0.20000	0.10000	0.00000	0.00000	0.00000	0.00000
0.20000	0.00000	0.00000	0.00000	0.00000	0.00000
0.20000	-0.10000	0.00000	0.00000	0.00000	0.00000
0.20000	-0.20000	0.57735	0.00000	0.00000	0.00000
0.20000	-0.30000	0.28868	-0.50000	0.28868	-0.50000
0.20000	-0.40000	0.28868	-0.50000	0.28868	-0.50000
0.20000	-0.50000	0.28868	-0.50000	0.28868	-0.50000
0.30000	0.50000	0.28868	0.50000	0.28868	0.50000
0.30000	0.40000	0.28868	0.50000	0.28868	0.50000
0.30000	0.30000	0.28868	0.50000	0.28868	0.50000
0.30000	0.20000	0.00000	0.00000	0.28868	0.50000
0.30000	0.10000	0.00000	0.00000	0.00000	0.00000
0.30000	0.00000	0.57735	0.00000	0.00000	0.00000
0.30000	-0.10000	0.57735	0.00000	0.00000	0.00000
0.30000	-0.20000	0.57735	0.00000	0.28868	-0.50000
0.30000	-0.30000	0.28868	-0.50000	0.28868	-0.50000
0.30000	-0.40000	0.28868	-0.50000	0.28868	-0.50000
0.30000	-0.50000	0.28868	-0.50000	0.28868	-0.50000
0.40000	0.50000	0.28868	0.50000	0.28868	0.50000
0.40000	0.40000	0.28868	0.50000	0.28868	0.50000
0.40000	0.30000	0.28868	0.50000	0.28868	0.50000
0.40000	0.20000	0.00000	0.00000	0.57735	0.00000
0.40000	0.10000	0.57735	0.00000	0.57735	0.00000
0.40000	0.00000	0.57735	0.00000	0.57735	0.00000
0.40000	-0.10000	0.57735	0.00000	0.57735	0.00000
0.40000	-0.20000	0.57735	0.00000	0.57735	0.00000
0.40000	-0.30000	0.28868	-0.50000	0.28868	-0.50000
0.40000	-0.40000	0.28868	-0.50000	0.28868	-0.50000
0.40000	-0.50000	0.28868	-0.50000	0.28868	-0.50000
0.50000	0.50000	0.28868	0.50000	0.28868	0.50000
0.50000	0.40000	0.28868	0.50000	0.28868	0.50000
0.50000	0.30000	0.86603	0.50000	0.28868	0.50000
0.50000	0.20000	0.57735	0.00000	0.57735	0.00000
0.50000	0.10000	0.57735	0.00000	0.57735	0.00000
0.50000	0.00000	0.57735	0.00000	0.57735	0.00000
0.50000	-0.10000	0.57735	0.00000	0.57735	0.00000
0.50000	-0.20000	0.57735	0.00000	0.57735	0.00000
0.50000	-0.30000	0.28868	-0.50000	0.28868	-0.50000
0.50000	-0.40000	0.28868	-0.50000	0.28868	-0.50000
0.50000	-0.50000	0.28868	-0.50000	0.28868	-0.50000

APPENDIX F

This appendix ,caled plots of interferometer phase variation under wave interference conditions. The phases are plotted as a function of ϕ_d. The plots are centered about their average values (taken over one period of phase variation). The interferometer phases that correspond to the primary wave DOA are also displayed as PHI21P, PHI13P, and PHI32P. The similarity of the primary wave phases and the averaged interferometer phases should be noted.

The program listing is included. All user written subroutines called in this program may be found listed in Appendix M.

```
$     INPUT SOURCE CARDS
$      EXECUTE
$      FORTRAN
H      NAME INTPLT;
H      EQUIP=CARDRE,PRINTE,CARDPU;
H      SINGLEALL;
C*****
C*****THIS PGM PLOTS ALL THREE ISOSCELES INTERFEROMETER ARRAY PHASES
C*****UNDER WAVE INTERFERENCE CONDX AS A FUNCTION OF THE RELATIVE PHASE DIF-
C*****FERENCE BETWEEN THE INTERFERING WAVES (PHID).  ONE PERIOD OF PHASE
C*****VARIATION IS PLOTTED.  THE PGM IS SELF-SCALING.  ANY SET OF PRIMARY,
C*****SECONDARY, AND H VALUES CAN BE PLOTTED.  INPUT REQUIRED CONSISTS OF THE
C*****PRIMARY AND SECONDARY AZIMUTH AND INCIDENCE ANGLES, (IN DEGREES), THE
C*****ARRAY ANGLE (IN DEGREES), AND THE BASELINE/WAVELE  T  RATIO.  (IN 6F10.5
C*****FORMAT.)
C*****
      DIMENSION PH21(150),PH13(150),PH32(150),IBUF(7500),PHID(150)
      PI=3.1415926535898
      TUPI=2.*PI
      DEG=180./PI
      DO 200 LCNT=1,5
C*****ANGLES OF ARRIVAL READ IN DEGREES, H MUST BE BETWEEN 0 AND 1
      READ 10,ALPHP,THETP,ALPHS,THETS,H,DGAMMA,DL
10    FORMAT(7F10.3)
      GAMMA=DGAMMA/DEG
      PRINT 20,LCNT,ALPHP,ALPHS,THETP,THETS,H
20    FORMAT(9H1RUN NO. ,I2,//,24H PRIMARY MODE AZIMUTH = ,F6.2,15X,26H SE
     $SECONDARY MODE AZIMUTH = ,F6.2,/,26H PRIMARY MODE INCIDENCE = ,F6.2,13X,28
     $2,13X,28H SECONDARY MODE INCIDENCE = ,F6.2,//,31H AMPLITUDE OF SEC
     $ONDARY WAVE = ,F4.3,40H TIMES THE AMPLITUDE OF THE PRIMARY WAVE)
      PRINT 21, DGAMMA
21    FORMAT(//25H ISOSCELES ARRAY ANGLE = ,F6.2)
      RALPHP=ALPHP/DEG
      RALPHS=ALPHS/DEG
      RTHETP=THETP/DEG
      RTHETS=THETS/DEG
      PRINT 30,DL
30    FORMAT(///,23H BASELINE/WAVELENGTH = ,F4.2,/)
      CALL PRTPHI(RALPHP,RTHETP,DL,PHIP21,PHIP13,PHIP32, GAMMA)
      CALL PRTPHI(RALPHS,RTHETS,DL,PHIS21,PHIS13,PHIS32, GAMMA)
      DP21=DEG*PHIP21
      DP13=DEG*PHIP13
      DP32=DEG*PHIP32
      PHIDIF=-.05
      SMFI21=0.
      SMFI13=0.
      SMFI32=0.
      DO 50 JCNT=1,126
      PHIDIF=PHIDIF+.05
      PHID(JCNT)=PHIDIF*5./TUPI
      X1=ATAN2(H*SIN(PHIDIF),1.+H*COS(PHIDIF))
      PHI21=ATAN2(SIN(PHIP21)+H*SIN( PHIDIF+PHIS21),COS(PHIP21)+H*COS(PH
     $IDIF+PHIS21))-X1
      CALL REDUCE(PHI21)
      CALL CHOS (PHI21,PHIP21,FI21)
      PHI21=FI21
      PHIP31=-PHIP13
      PHIS31=-PHIS13
      PHI31= ATAN2(SIN(PHIP31)+H*SIN(PHIDIF+PHIS31),COS(PHIP31)+H*COS(PH
```

```
     $IDIF+PHIS31))-X1
      CALL REDUCE(PHI31)
      CALL CHOS (PHI31,PHIP31,FI31)
      PHI31=FI31
      PHI32=PHI31-PHI21
      PHI13=-PHI31
C*****SUM UP ALL INTERF PHASES TO CALCULATE AVG INTERF PHASES.
      SMFI21=SMFI21+PHI21
      SMFI13=SMFI13+PHI13
      SMFI32=SMFI32+PHI32
      DPHIDF=DEG*PHIDIF
      PH21(JCNT)=PHI21
      PH13(JCNT)=PHI13
      PH32(JCNT)=PHI32
50    CONTINUE
      AVFI21=SMFI21/126.
      AVFI13=SMFI13/126.
      AVFI32=SMFI32/126.
C*****FIND MIN VALUE OF PHASES
      FI21MN=PH21(1)
      FI32MN=PH32(1)
      FI13MN=PH13(1)
      DO 85 L=2,126
      IF(PH21(L)-FI21MN)60,60,65
60    FI21MN=PH21(L)
65    IF(PH32(L)-FI32MN)70,70,75
70    FI32MN=PH32(L)
75    IF(PH13(L)-FI13MN)80,80,85
80    FI13MN=PH13(L)
85    CONTINUE
C*****USE THE MAXIMUM, MINIMUM, AND AVG PHASE VALUES TO PROPERLY SCALE AXES OF
C*****THE PLOT.
      FI21MX=PH21(1)
      FI32MX=PH32(1)
      FI13MX=PH13(1)
      DO 115 L=2,126
      IF(FI21MX-PH21(L))90,90,95
90    FI21MX=PH21(L)
95    IF(FI32MX-PH32(L))100,100,105
100   FI32MX=PH32(L)
105   IF(FI13MX-PH13(L))110,110,115
110   FI13MX=PH13(L)
115   CONTINUE
      CALL PLOTS(IBUF,7500,100.,11.)
C*****DRAW PH21 AXES
      CALL PLOT(2.,6.8,-3)
      IPNT=1
      GO TO 300
116   CONTINUE
C*****COMPUTE PHI21 SCALE FACTOR ON BASIS OF MAX, AVG, AND MIN PHASE VALUES
      DF21MX=FI21MX-AVFI21
      DF21MN=AVFI21-FI21MN
      IF(DF21MX-DF21MN)117,117,118
117   DIF21=DF21MN
      GO TO 119
118   DIF21=DF21MX
119   CONTINUE
      SCA21=1.14/DIF21
C*****SCALE AND PLOT PH21 VALUES
      N=3
```

```
      DO 120 ICNT=1,126
      XPH21=(PH21(ICNT)-AVFI21)*SCA21
      CALL PLOT(PHID(ICNT),XPH21,N)
120   N=2
      CALL SYMBOL(-.8,1.32,.14,5HPHI21,0.,5)
      XF21MX=DEG*FI21MX
      XF13MX=DEG*FI13MX
      XF32MX=DEG*FI32MX
      XF21MN=DEG*FI21MN
      XF13MN=DEG*FI13MN
      XF32MN=DEG*FI32MN
      DF21AV=DEG*AVFI21
      DF13AV=DEG*AVFI13
      DF32AV=DEG*AVFI32
      SF21AV=AVFI21*SCA21
      SF21MX=FI21MX*SCA21-SF21AV
      SF21MN=FI21MN*SCA21-SF21AV
      CALL NUMBER(-.5,SF21MX,.10,XF21MX,0.,1)
      CALL SYMBOL(0.,SF21MX,.10,5,0.,-1)
      CALL SYMBOL(-.8,.15,.1,9HAVG PHI21,0.,9)
      CALL NUMBER(-.5,0.,.10,DF21AV,0.,1)
      CALL NUMBER(-.5,SF21MN,.10,XF21MN,0.,1)
      CALL SYMBOL(0.,SF21MN,.10,5,0.,-1)
C*****DRAW PHI13 AXES
      CALL PLOT(0.,-2.67,-3)
      IPNT=2
      GO TO 300
125   CONTINUE
C*****COMPUTE PHI13 SCALE FACTOR BASED ON MAX, AVG, AND MIN PHASE VALUES.
      DF13MX=FI13MX-AVFI13
      DF13MN=AVFI13-FI13MN
      IF(DF13MX-DF13MN)127,127,128
127   DIF13=DF13MN
      GO TO 129
128   DIF13=DF13MX
129   CONTINUE
      SCA13=1.14/DIF13
C*****SCALE AND PLOT PHI13 VALUES
      N=3
      DO 130 ICNT=1,126
      XPH13=(PH13(ICNT)-AVFI13)*SCA13
      CALL PLOT(PHID(ICNT),XPH13,N)
130   N=2
      CALL SYMBOL(-.8,1.32,.14,5HPHI13,0.,5)
      SF13AV=AVFI13*SCA13
      SF13MX=FI13MX*SCA13-SF13AV
      SF13MN=FI13MN*SCA13-SF13AV
      CALL NUMBER(-.5,SF13MX,.10,XF13MX,0.,1)
      CALL SYMBOL(0.,SF13MX,.10,5,0.,-1)
      CALL SYMBOL(-.8,.15,.1,9HAVG PHI13,0.,9)
      CALL NUMBER(-.5,0.,.10,DF13AV,0.,1)
      CALL NUMBER(-.5,SF13MN,.10,XF13MN,0.,1)
      CALL SYMBOL(0.,SF13MN,.10,5,0.,-1)
C*****DRAW PHI32 AXES
      CALL PLOT(0.,-2.67,-3)
      IPNT=3
      GO TO 300
135   CONTINUE
C*****COMPUTE PHI32 SCALE FACTOR BASED ON MAX, AVG, AND MIN PHASE VALUES.
      DF32MX=FI32MX-AVFI32
```

```
      DF32MX=AVFI32-FI32MN
      IF(DF32MX-DF32MN)137,137,138
137   DIF32=DF32MN
      GO TO 139
138   DIF32=DF32MX
139   CONTINUE
      SCA32=1.14/DIF32
C*****SCALE AND PLOT PH32 VALUES
      N=3
      DO 140 ICNT=1,126
      XPH32=(PH32(ICNT)-AVFI32)*SCA32
      CALL PLOT(PHID(ICNT),XPH32,N)
140   N=2
      CALL SYMBOL(-.8,1.30,.14,5HPHI32,0.,5)
      SF32AV=AVFI32*SCA32
      SF32MX=FI32MX*SCA32-SF32AV
      SF32MN=FI32MN*SCA32-SF32AV
      CALL NUMBER(-.5,SF32MX,.10,XF32MX,0.,1)
      CALL SYMBOL(0.,SF32MX,.10,5,0.,-1)
      CALL SYMBOL(-.8,.15,.1,9HAVG PHI32,0.,9)
      CALL NUMBER(-.5,0.,.10,DF32AV,0.,1)
      CALL NUMBER(-.5,SF32MN,.10,XF32MN,0.,1)
      CALL SYMBOL(0.,SF32MN,.10,5,0.,-1)
      CALL PLOT(-1.1,6.6,-3)
C*****PRINT SYSTEM PARAMETER AND WAVE INTERFERENCE INFORMATION
      CALL SYMBOL(.94,2.00,.14,35HINTERF PHASES UNDER WAVE INT CONDX ,
     $0.,35)
      CALL SYMBOL(999.,999.,.14,11H(VS PHIDIF),0.,11)
      CALL SYMBOL(0.92,1.7,.14,38HPRI AZ =                    PRI INC =
     $,0.,38)
      CALL NUMBER(2.57,1.7,.14,ALPHP,0.,2)
      CALL NUMBER(5.89,1.7,.14,THETP,0.,2)
      CALL SYMBOL(.92,1.4,.14,38HSEC AZ =                    SEC INC = ,
     $0.,38)
      CALL NUMBER(2.57,1.4,.14,ALPHS,0.,2)
      CALL NUMBER(5.89,1.4,.14,THETS,0.,2)
      CALL SYMBOL(.92,1.1,.14,10HSEC/PRI = ,0.,10)
      CALL NUMBER(2.57,1.1,.14,H,0.,2)
      CALL SYMBOL(4.25,1.1,.14,14HARRAY ANGLE = ,0.,14)
      CALL NUMBER(5.87,1.1,.14,DGAMMA,0.,1)
      CALL SYMBOL(.84,.8,.14,35HINTERF PHASES CORRESPONDING TO THE ,
     $0.,35)
      CALL SYMBOL(999.,999.,.14,14HPRI WAVE ALONE,0.,14)
      CALL SYMBOL(.84,.5,.14,35HPHI21P =          PHI13P =          P,0.,3
     $5)
      CALL SYMBOL(999.,999.,.14,8HHI32P = ,0.,8)
      CALL NUMBER(1.87,.5,.14,DP21,0.,2)
      CALL NUMBER(3.92,.5,.14,DP13,0.,2)
      CALL NUMBER(5.92,.5,.14,DP32,0.,2)
      CALL SYMBOL(2.9,.2,.14,10HD/LAMBDA =,0.,10)
      CALL NUMBER(4.2,.2,.14,DL,0.,2)
      CALL PLOT(9.0,-8.05,-3)
200   CONTINUE
      CALL EXIT
C*****PHID AXIS LABELLING ROUTINE BEGINS HERE
300   CALL PLOT(0.,-1.14,3)
      CALL PLOT(0.,1.14,2)
      CALL PLOT(5.,0.,3)
      CALL PLOT(0.,0.,2)
      CALL SYMBOL(.15,-.2,.10,2H0.,0.,2)

      CALL SYMBOL(1.15,-.2,.10,3H90.,0.,3)
      CALL SYMBOL(1.25,0.,.10,5,0.,-1)
      CALL SYMBOL(2.35,-.2,.10,4H180.,0.,4)
      CALL SYMBOL(2.5,0.,.10,5,0.,-1)
      CALL SYMBOL(3.6,-.2,.10,4H270.,0.,4)
      CALL SYMBOL(3.75,0.,.10,5,0.,-1)
      CALL SYMBOL(4.85,-.2,.10,4H360.,0.,4)
      CALL SYMBOL(5.,0.,.10,5.07,-1)
      CALL SYMBOL(5.2,-.07,.14,6HPHIDIF,0.,6)
      GO TO (116,125,135),IPNT
      END
```

INTERF PHASES UNDER WAVE INT CONDX (VS PHIDIF)

PRI AZ =	310.00	PRI INC =	20.00
SEC AZ =	315.00	SEC INC =	45.00
SEC/PRI =	0.25	ARRAY ANGLE =	90.0

INTERF PHASES CORRESPONDING TO THE PRI WAVE ALONE

PHI21P = 79.14 PHI13P = 94.32 PHI32P = -173.46

D/LAMBDA = 1.00

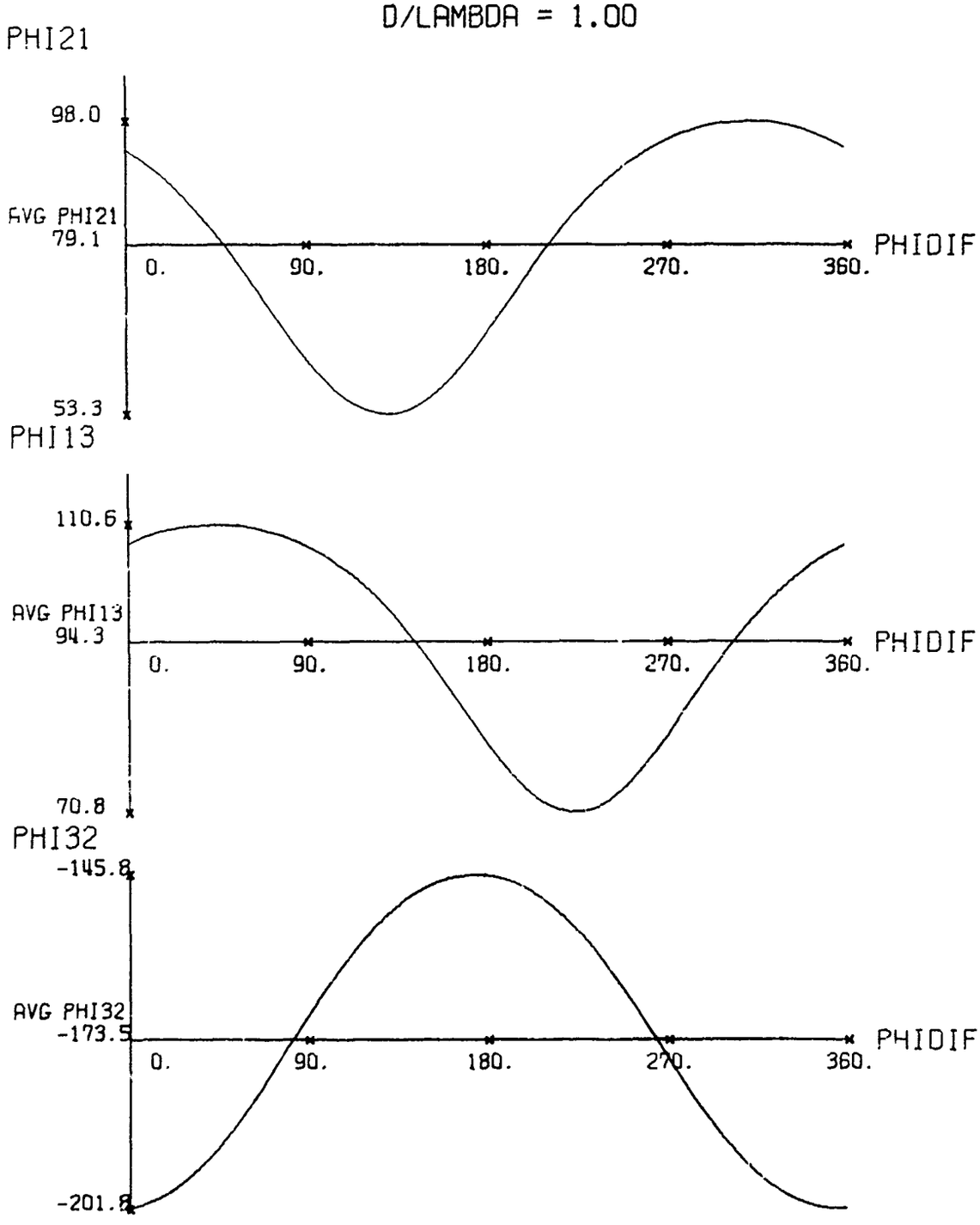

Figure F-1. Plots of the ϕ_d-Variation of the Interferometer Phases (h = .25)

INTERF PHASES UNDER WAVE INT CONDX (VS PHIDIF)

PRI AZ =	310.00	PRI INC =	20.00
SEC AZ =	315.00	SEC INC =	45.00
SEC/PRI =	0.50	ARRAY ANGLE =	90.0

INTERF PHASES CORRESPONDING TO THE PRI WAVE ALONE

PHI21P = 79.14 PHI13P = 94.32 PHI32P = -173.46

D/LAMBDA = 1.00

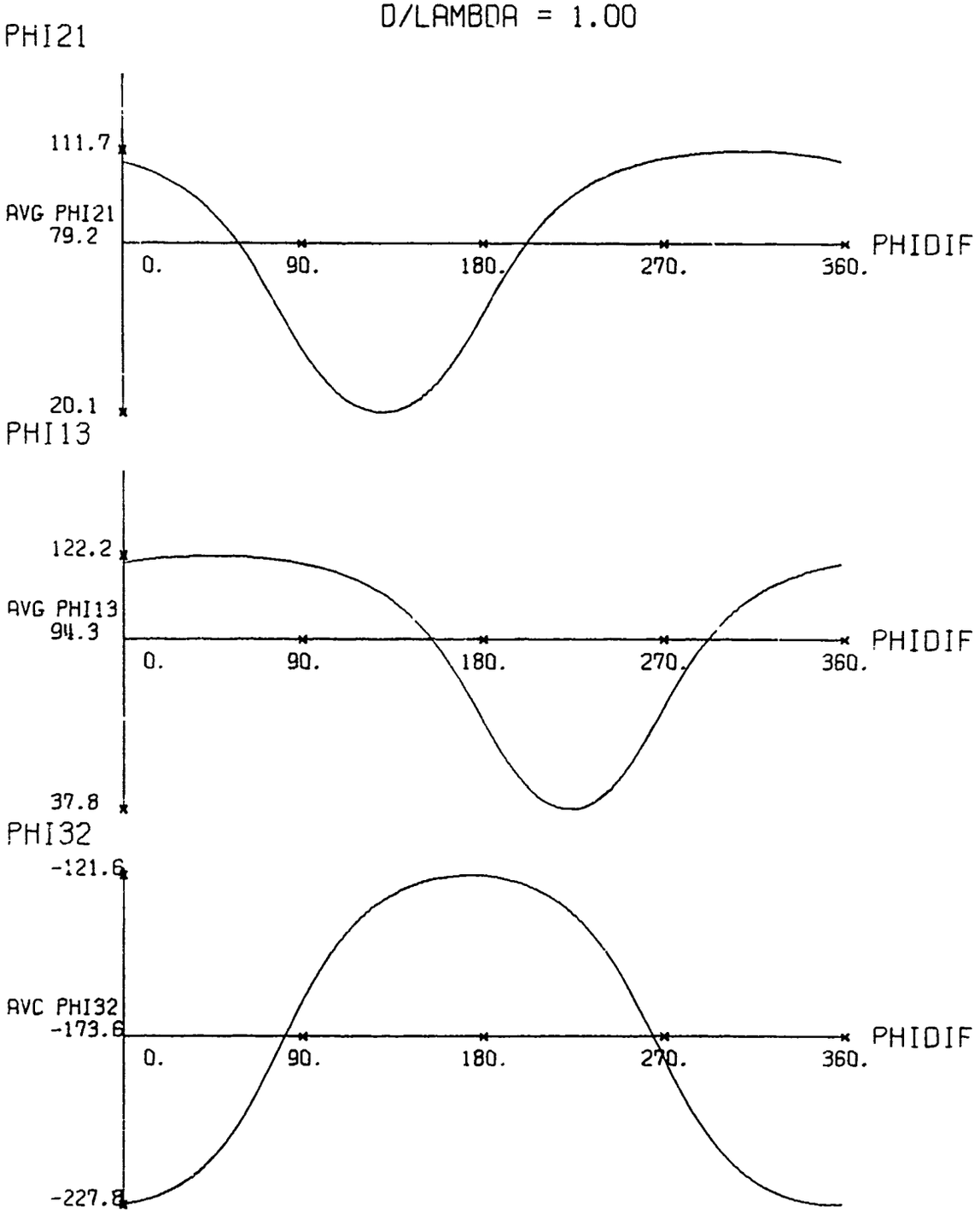

Figure F-2. Plots of the ϕ_d-Variation of the Interferometer Phases (H = .5)

INTERF PHASES UNDER WAVE INT CONDX (VS PHIDIF)

PRI AZ = 310.00 PRI INC = 20.00

SEC AZ = 315.00 SEC INC = 45.00

SEC/PRI = 0.75 ARRAY ANGLE = 90.0

INTERF PHASES CORRESPONDING TO THE PRI WAVE ALONE

PHI21P = 79.14 PHI13P = 94.32 PHI32P = -173.46

D/LAMBDA = 1.00

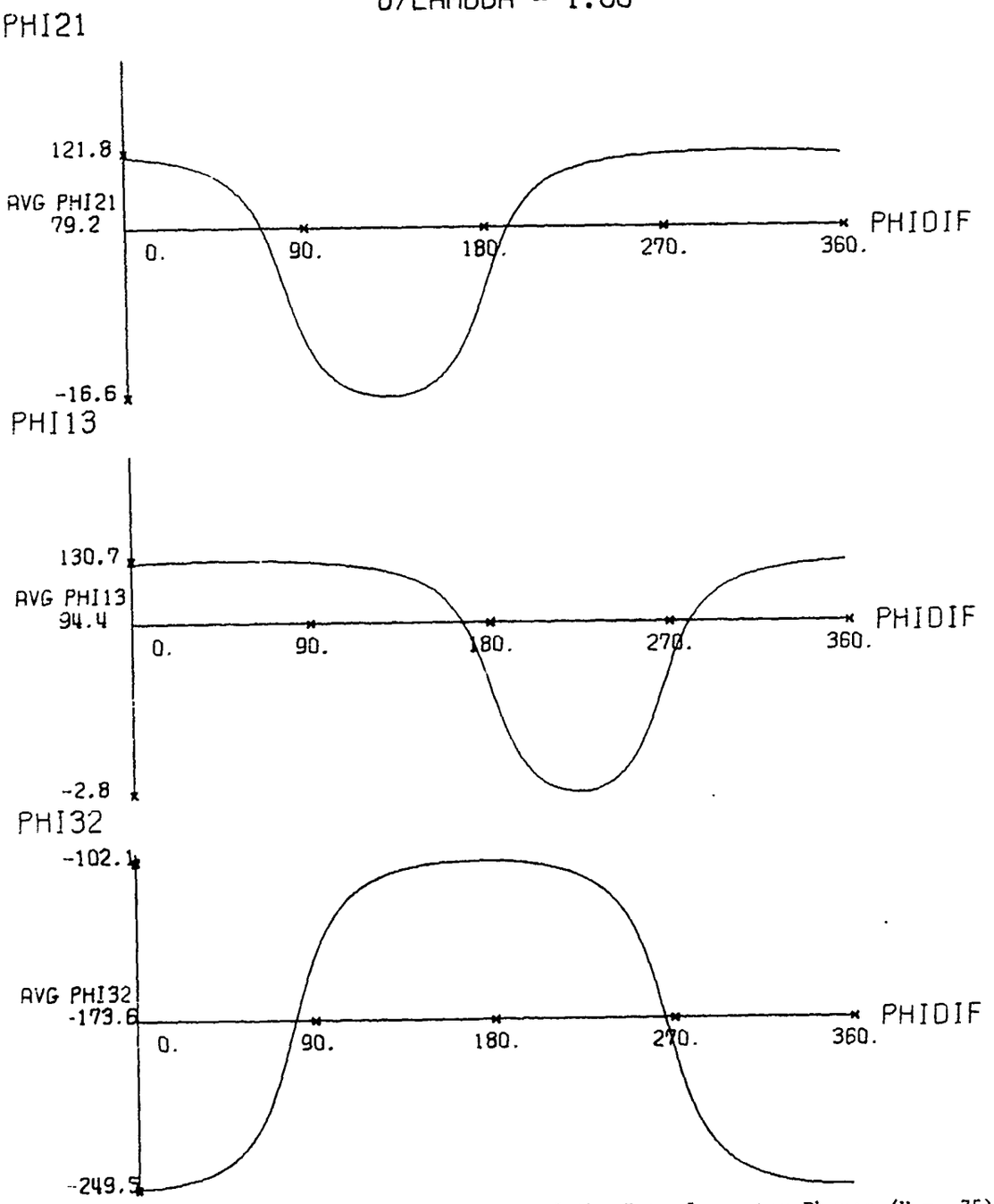

Figure F-3. Plots of the ϕ -Variation of the Interferometer Phases (H = .75)

INTERF PHASES UNDER WAVE INT CONDX (VS PHIDIF)

PRI AZ = 310.00 PRI INC = 20.00

SEC AZ = 315.00 SEC INC = 30.00

SEC/PRI = 0.50 ARRAY ANGLE = 90.0

INTERF PHASES CORRESPONDING TO THE PRI WAVE ALONE

PHI21P = 79.14 PHI13P = 94.32 PHI32P = -173.46

D/LAMBDA = 1.00

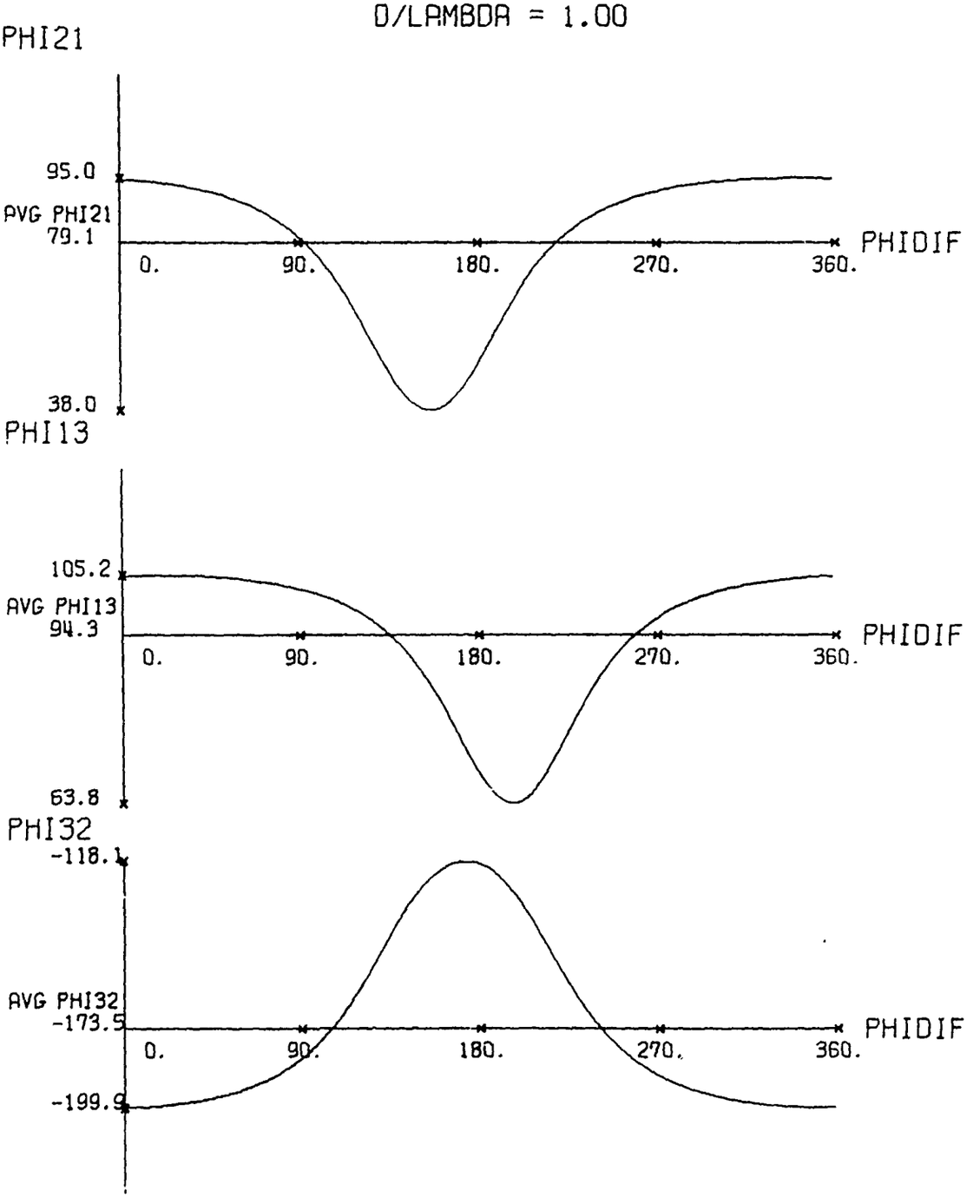

Figure F-4. Plots of the ϕ_d-Variation of the Interferometer Phases (θ_s = 30°)

INTERF PHASES UNDER WAVE INT CONDX (VS PHIDIF)

PRI AZ = 310.00 PRI INC = 20.00

SEC AZ = 315.00 SEC INC = 60.00

SEC/PRI = 0.50 ARRAY ANGLE = 90.0

INTERF PHASES CORRESPONDING TO THE PRI WAVE ALONE

PHI21P = 79.14 PHI13P = 94.32 PHI32P = -173.46

D/LAMBDA = 1.00

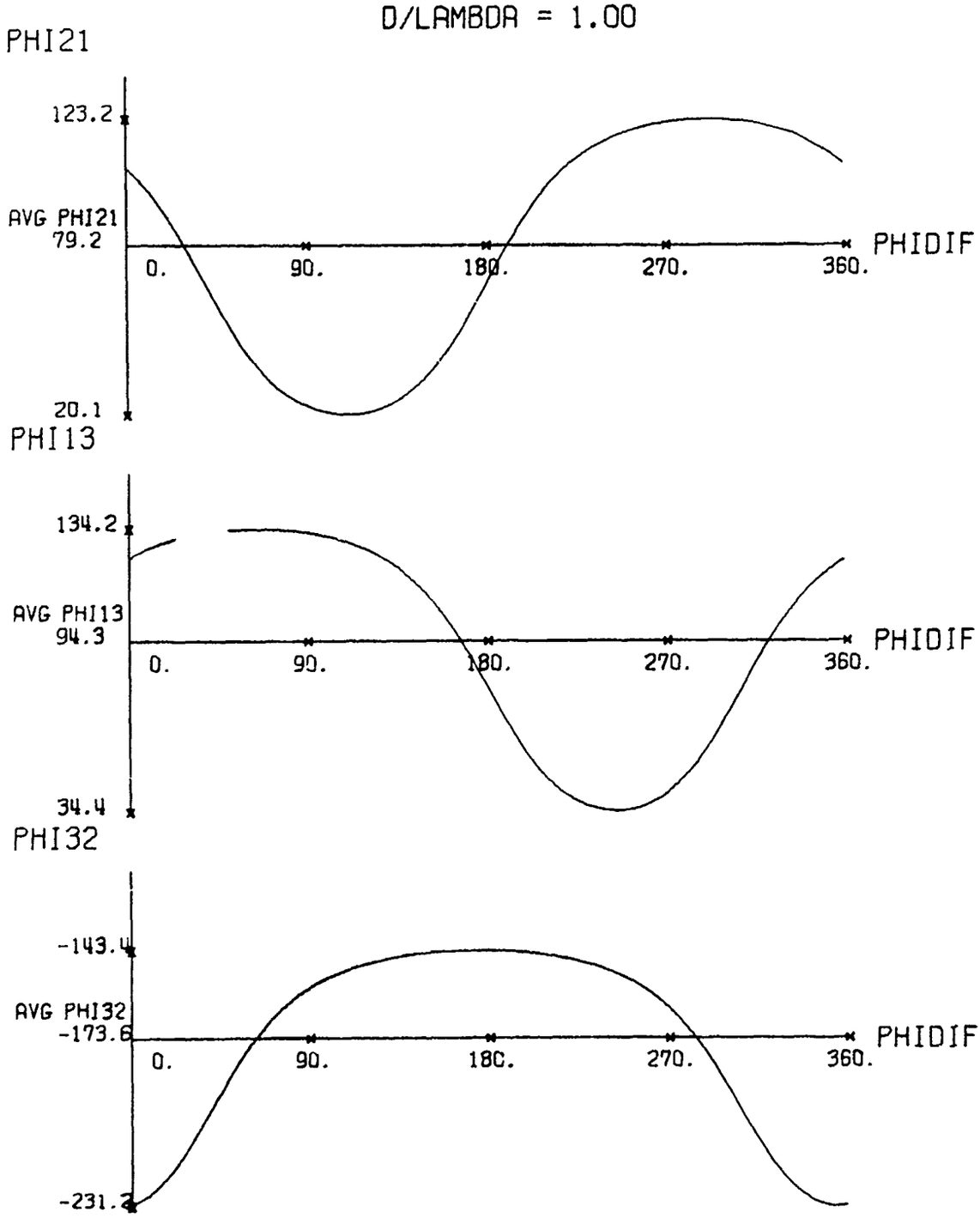

Figure F-5. Plots of the ϕ_d-Variation of the Interferometer Phases (θ_s = 60°)

APPENDIX G

This appendix contains plots that demonstrate the fluctuation of indicated DOA by an interferometer under ϕ_d-variant wave interference conditions. The plots are discussed in Chapter VII.

A listing of the plotting program follows. All user-written subroutines are listed in Appendix G except MUG2DR, which is a general purpose, self scaling polar plotting subroutine written by Bill Little.[1]

```
$     INPUT SOURCE CARDS
$     EXECUTE
$      FORTRAN
H      NAME WINTER;
H      EQUIP=CARDRE,PRINTE,CARDPU;
H      SINGLEALL;
C*****
C*****THIS IS A GENERAL ISOSCELES INTERFEROMETER ARRAY WAVE INTERFERENCE
C*****SIMULATION PROGRAM.  IT PLOTS THE DOA TRAJECTORY VS. PHID, THE RELATIVE
C*****PHASE DIFFERENCE BETWEEN TWO INTERFERING WAVES, AS IT IS VARIED IN 32
C*****INCREMENTS FROM 0 TO 360 DEGREES.  INPUT DATA CONSISTS OF THE PRIMARY AND
C*****SECONDARY AZIMUTH AND INCIDENCE ANGLES (IN DEGREES), THE RELATIVE AMP.
C*****H, AND THE ARRAY ANGLE (IN DEGREES).  (6F10.5 FORMAT.)
C*****
      DIMENSION ICON(20),PRAM(20),AZANG(200),THETA(200),IBUF(7500)
      CALL PLOTS(IBUF,7500,100.,11.5)
C*****INITIALIZE PARAMETER MATRIX USED BY SUBROUTINE MUG2DR
      DO 1 I=1,20
      ICON(I)=0
1     PRAM(I)=0
      PI=3.1415926535898
      TUPI=2.*PI
      PRAM(18)=1
      PRAM(19)=0
      DEG=180./PI
      ICON(18)=1
      ICON(19)=0
      DO 70 ICNT=1,2
C*****ANGLES OF ARRIVAL READ IN DEGREES, H MUST BE BETWEEN 0 AND 1
      READ 10,ALPHP,THETP,ALPHS,THETS,H,DGAMMA
10    FORMAT(6F10.3)
      GAMMA=DGAMMA/DEG
      PRINT 20,ICNT,ALPHP,ALPHS,THETP,THETS,H
20    FORMAT(9H1RUN NO. ,I2,//,24H PRIMARY MODE AZIMUTH = ,F6.2,15X,26H SE
     $CONDARY MODE AZIMUTH = ,F6.2,/,26H PRIMARY MODE INCIDENCE = ,F6.2,13X,28
     $2,13X,28H SECONDARY MODE INCIDENCE = ,F6.2,//,31H AMPLITUDE OF SEC
     $ONDARY WAVE = ,F4.3,40H TIMES THE AMPLITUDE OF THE PRIMARY WAVE)
      PRINT 21, DGAMMA
21    FORMAT(//25H ISOSCELES ARRAY ANGLE = ,F6.2)
      RALPHP=ALPHP/DEG
      RALPHS=ALPHS/DEG
      RTHETP=THETP/DEG
      RTHETS=THETS/DEG
      DL=0.
      NCNT=-32
      DO 51 ICNT=1,2
      NCNT=NCNT+32
C*****FIRST RUN THRU WAVE INT SIMULATION PGM DL=.5, SECOND RUN THRU, DL= 1.
      DL=DL+.5
      PRINT 30,DL
30    FORMAT(///,23H BASELINE/WAVELENGTH = ,F4.2,/)
C*****COMPUTE PRI AND SEC WAVE INTERFEROMETER PHASE CONTRIBUTIONS
      CALL PRTPHI(RALPHP,RTHETP,DL,PHIP21,PHIP13,PHIP32, GAMMA)
      CALL PRTPHI(RALPHS,RTHETS,DL,PHIS21,PHIS13,PHIS32, GAMMA)
      PHIDIF=-.2
      TSUM=0.
      ASUM=0.
      SMFI21=0.
      SMFI13=0.
```

```
      SMFI32=0.
      DO 50 JCNT=1,32
      PHIDIF=PHIDIF+.2
C*****COMPUTE RESULTANT INTERFEROMETER PHASE PHI21 AS DISCUSSED IN CHAPTER VII.
      X1=ATAN2(H*SIN(PHIDIF),1.+H*COS(PHIDIF))
      PHI21=ATAN2(SIN(PHIP21)+H*SIN( PHIDIF+PHIS21),COS(PHIP21)+H*COS(PH
     $IDIF+PHIS21))-X1
C*****PUT PHI21 WITHIN BRANCH CUT OF -180 TO 180 DEGREES
      CALL REDUCE(PHI21)
C*****NOW FIND ACTUAL, UNAMBIGUOUS VALUE OF PHI21, KNOWING IT MUST LIE
C*****WITHIN 180 DEGREES OF PHI21P. (SEE CHAPTER VII.)
      CALL CHOS (PHI21,PHIP21,FI21)
      PHI21=FI21
      PHIP31=-PHIP13
      PHIS31=-PHIS13
C*****REPEAT ABOVE PROCESS FOR PHI13.
      PHI31= ATAN2(SIN(PHIP31)+H*SIN(PHIDIF+PHIS31),COS(PHIP31)+H*COS(PH
     $IDIF+PHIS31))-X1
      CALL REDUCE(PHI31)
      CALL CHOS (PHI31,PHIP31,FI31)
      PHI31=FI31
      PHI32=PHI31-PHI21
      PHI13=-PHI31
C*****SUM UP ALL INTERF PHASES TO CALCULATE AVG INTERF PHASES.
      SMFI21=SMFI21+PHI21
      SMFI13=SMFI13+PHI13
      SMFI32=SMFI32+PHI32
      DPHIDF=DEG*PHIDIF
      CALL DIR(PHI21,PHI32,DL,GAMMA,AZ,VINC)
C*****AZ AVGING ASSUMES NO WRAP AROUND FROM 360. TO 0. DEGREES
C*****THAT IS, BRANCH CUT CHOSEN IS 0 TO 360 DEGREES.
      ASUM=AZ+ASUM
      TSUM=VINC+TSUM
      PRINT 40,DPHIDF,AZ,VINC
40    FORMAT(17H REL PHASE DIF = ,F6.2,5X,20H INFERRED AZIMUTH = ,F6.2,5X,22
     $X,22H INFERRED INCIDENCE = ,F6.2)
      MCNT=MCNT+JCNT
      AZANG(MCNT)=AZ
      THETA(MCNT)=VINC
50    CONTINUE
C*****COMPUTE AVG DOA
      THAVG=TSUM/32.
      AZAVG=ASUM/32.
      PRINT 500,AZAVG,THAVG
500   FORMAT(//15H AVG AZIMUTH = ,F5.2,30X,17H AVG INCIDENCE = ,F5.2/)
      AVFI21=SMFI21/32.
      AVFI13=SMFI13/32.
      AVFI32=SMFI32/32.
C*****CALCULATE DOA FROM AVGD PHASE READINGS
      CALL DIR(AVFI21,AVFI32,DL,GAMMA,AVZ,AVI)
      PRINT 501,AVZ,AVI
501   FORMAT(/35H AZIMUTH FROM AVGD INTERF PHASES = ,F5.2,10X,37H INCIDE
     $NCE FROM AVGD INTERF PHASES = ,F5.2/)
      THETA(MCNT-31)=-THETA(MCNT-31)
51    CONTINUE
      AZANG(65)=ALPHP
      THETA(65)=-THETP
      AZANG(66)=ALPHP
      THETA(66)=THETP
      N=66
```

```
C*****INITIALIZE PLOT PARAMETERS USED BY BILL LITTLE S POLAR PLOT ROUTINE     150
      ICON(1)=1
      ICON(10)=1
      ICON(11)=1
      ICON(20)=2
      ICON(1)=3
C*****MUG2DR CALLS MUG2 BOTH POLAR PLOT ROUTINES WERE WRITTEN BY BILL LITTLE
C*****(SEE REFERENCE NO. 27)
      CALL MUG2DR(AZANG,THETA,N,PRAM,ICON)
60    CONTINUE
      CALL PLOT(-7.75,.75,-3)
C*****PRINT SYSTEM PARAMETERS AND WAVE INTERFERENCE INFORMATION.
      CALL SYMBOL(1.,2.,.14,35HDCA FOR WAVE INT CONDX WITH VARYING,0.,35
     $)
      CALL SYMBOL(999.,999.,.14,10H REL PHASE,0.,10)
      CALL SYMBOL(0.92,1.5,.14,38HPRI AZ =                    PRI INC =
     $,0.,38)
      CALL NUMBER(2.57,1.5,.14,ALPHP,0.,2)
      CALL NUMBER(5.89,1.5,.14,THETP,0.,2)
      CALL SYMBOL(0.92,1.,.14,38HSEC AZ =                    SEC INC = ,
     $0.,38)
      CALL NUMBER(2.57,1.0,.14,ALPHS,0.,2)
      CALL NUMBER(5.89,1.0,.14,THETS,0.,2)
      CALL SYMBOL(2.73,.5,.14,10HSEC/PRI = ,0.,10)
      CALL NUMBER(4.,.5,.14,H,0.,2)
      CALL SYMBOL(2.5,0.,.14,14HARRAY ANGLE = ,0.,14)
      CALL NUMBER(4.25,0.,.14,DGAMMA,0.,1)
      CALL PLOT(7.75,-.75,-3)
70    CONTINUE
      CALL EXIT
      END
```

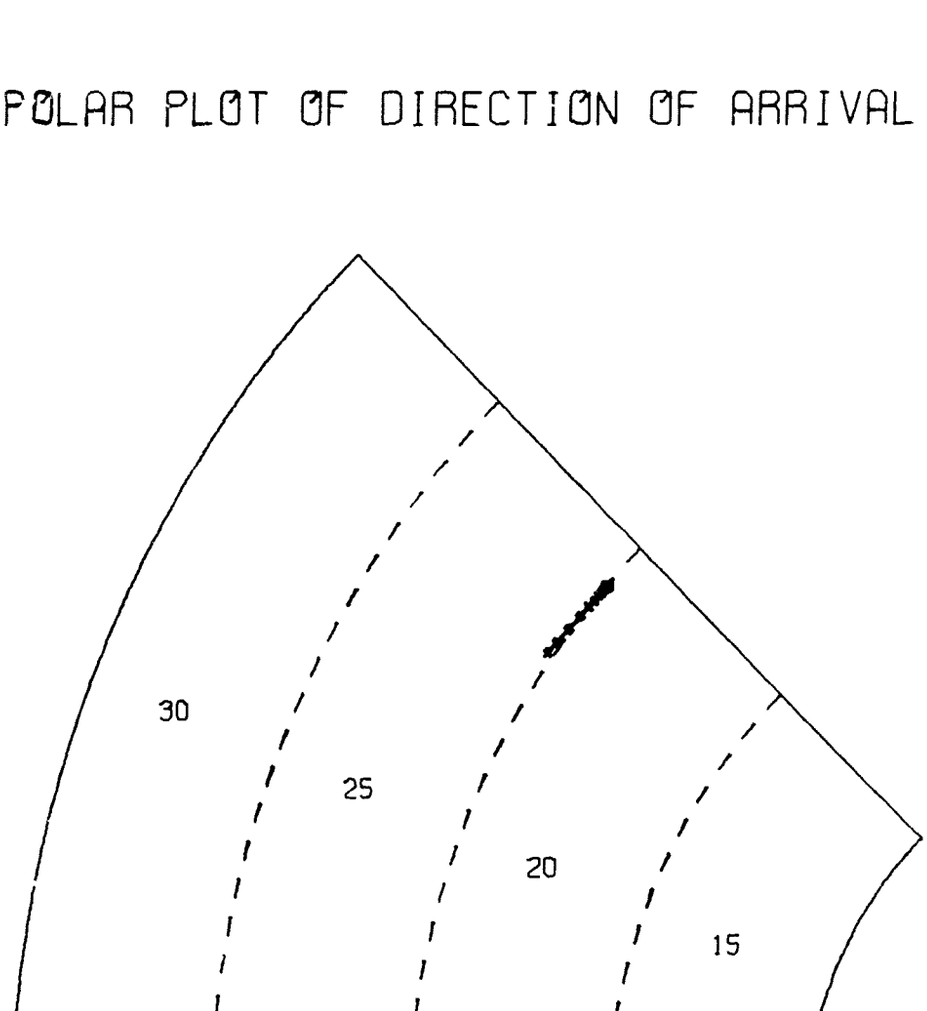

Figure G-1. Plots of the ϕ_d-Variation of the Indicated DOA (θ_s = 20°)

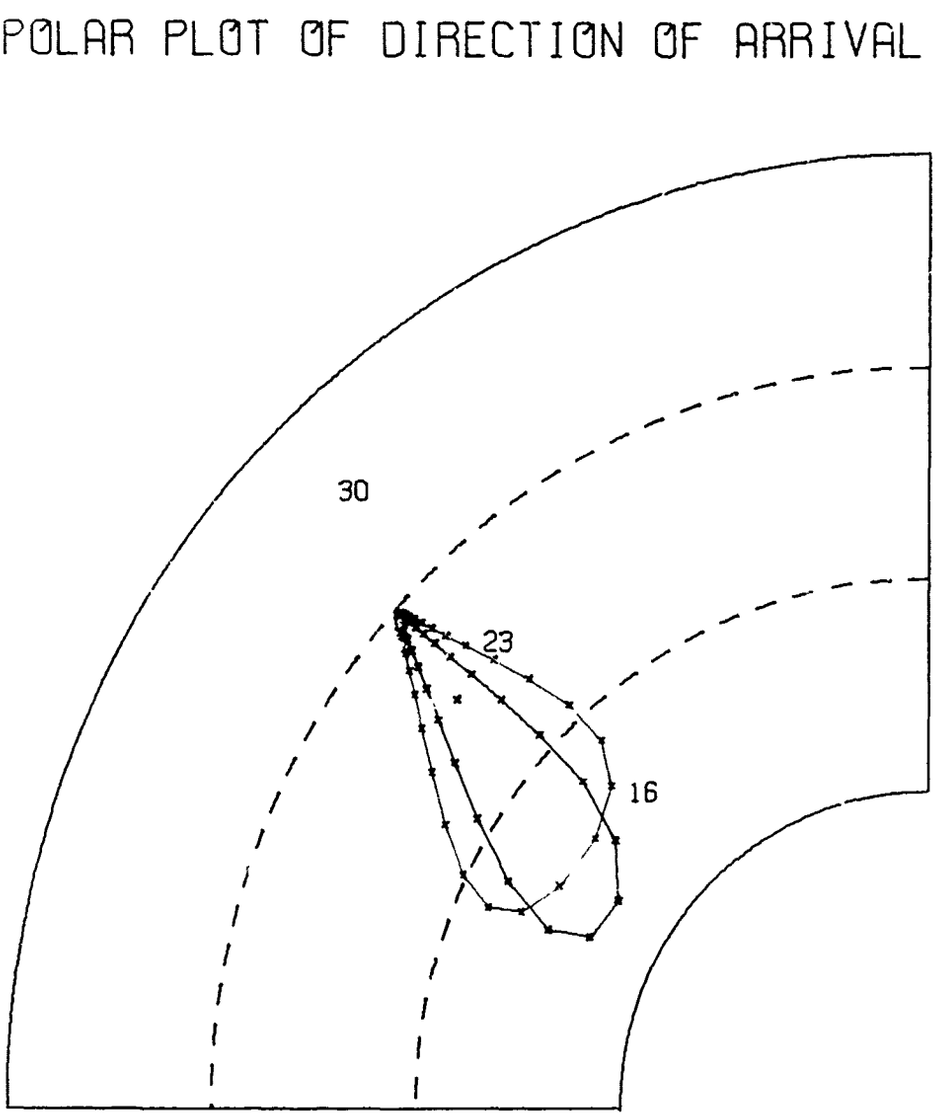

Figure G-2. Plots of the ϕ_d-Variation of the Indicated DOA (θ_s = 30°)

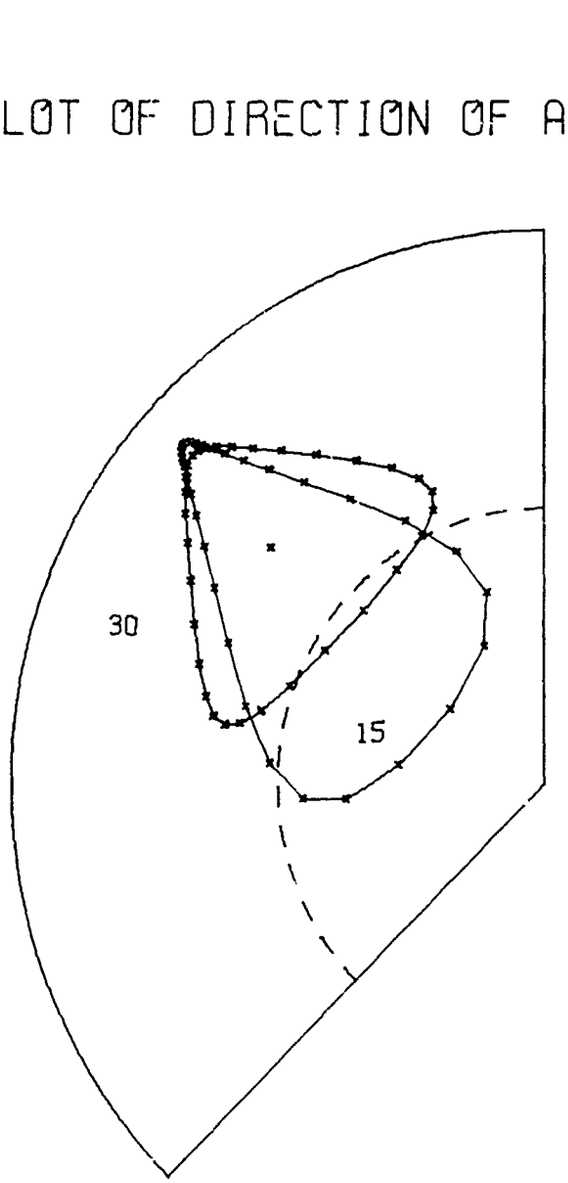

Figure G-3. Plots of the ϕ_d-Variation of the Indicated DOA ($\theta_s = 45°$)

POLAR PLOT OF DIRECTION OF ARRIVAL

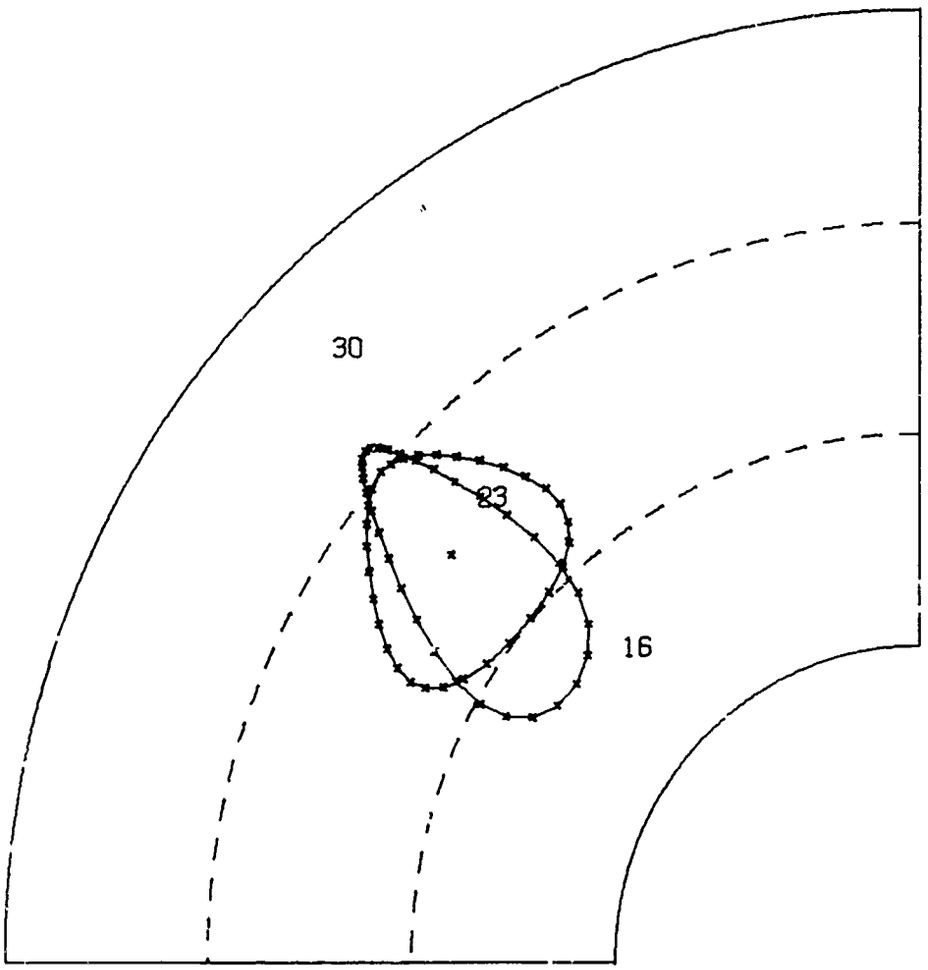

DOA FOR WAVE INT CONDX WITH VARYING REL PHASE

PRI AZ = 310.00 PRI INC = 20.00

SEC AZ = 315.00 SEC INC = 45.00

SEC/PRI = 0.25

ARRAY ANGLE = 90.0

Figure C-4. Plots of the ϕ_d-Variation of the Indicated DOA (H = .25)

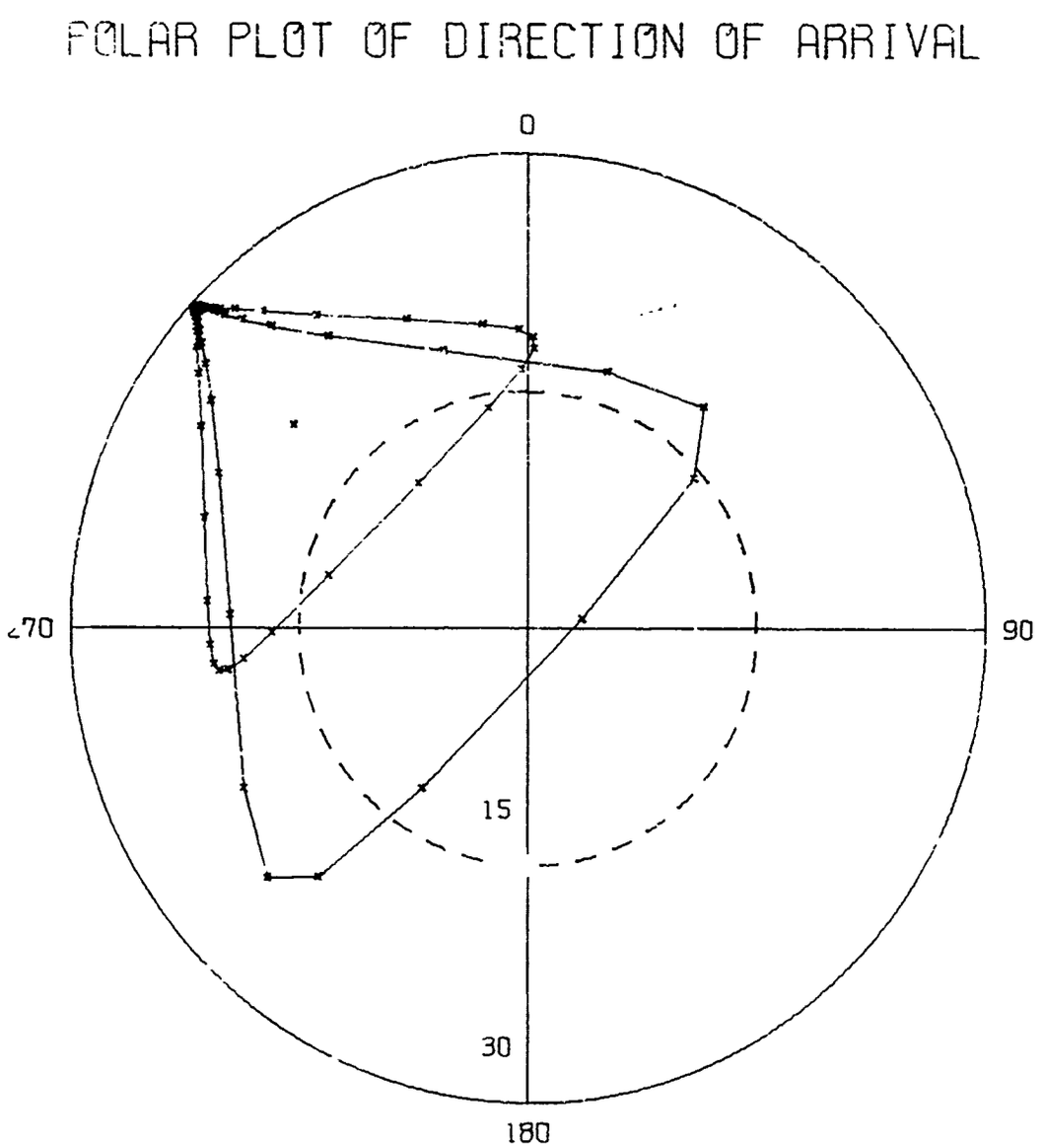

Figure G-5. Plots of the ϕ_d-Variation of the Indicated DOA (H = .75)

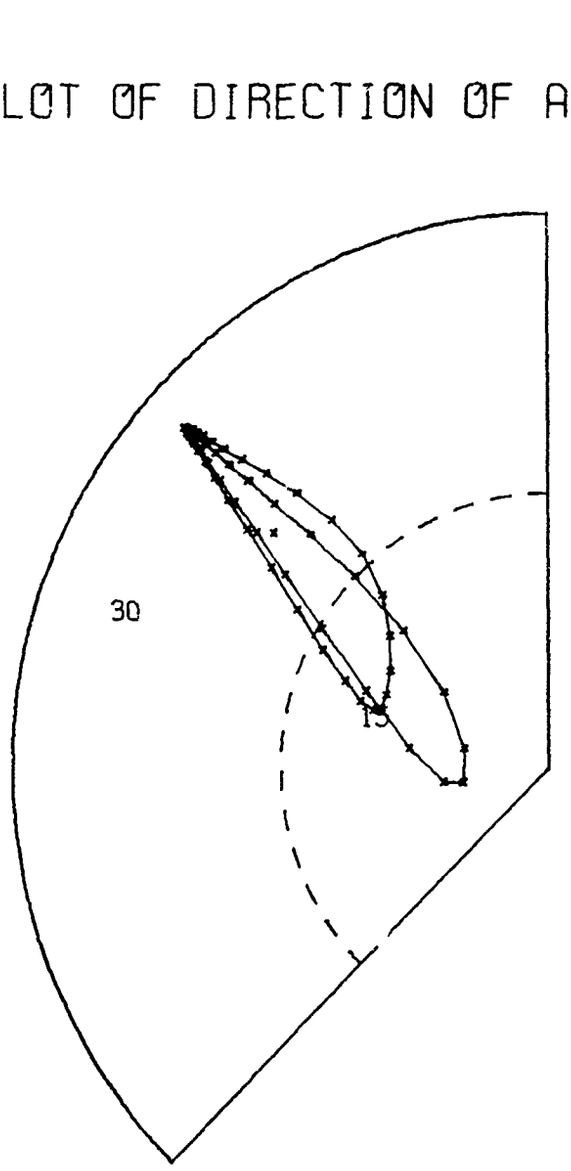

Figure G-6. Plots of the ϕ_d-Variation of the Indicated DOA (H = .50)

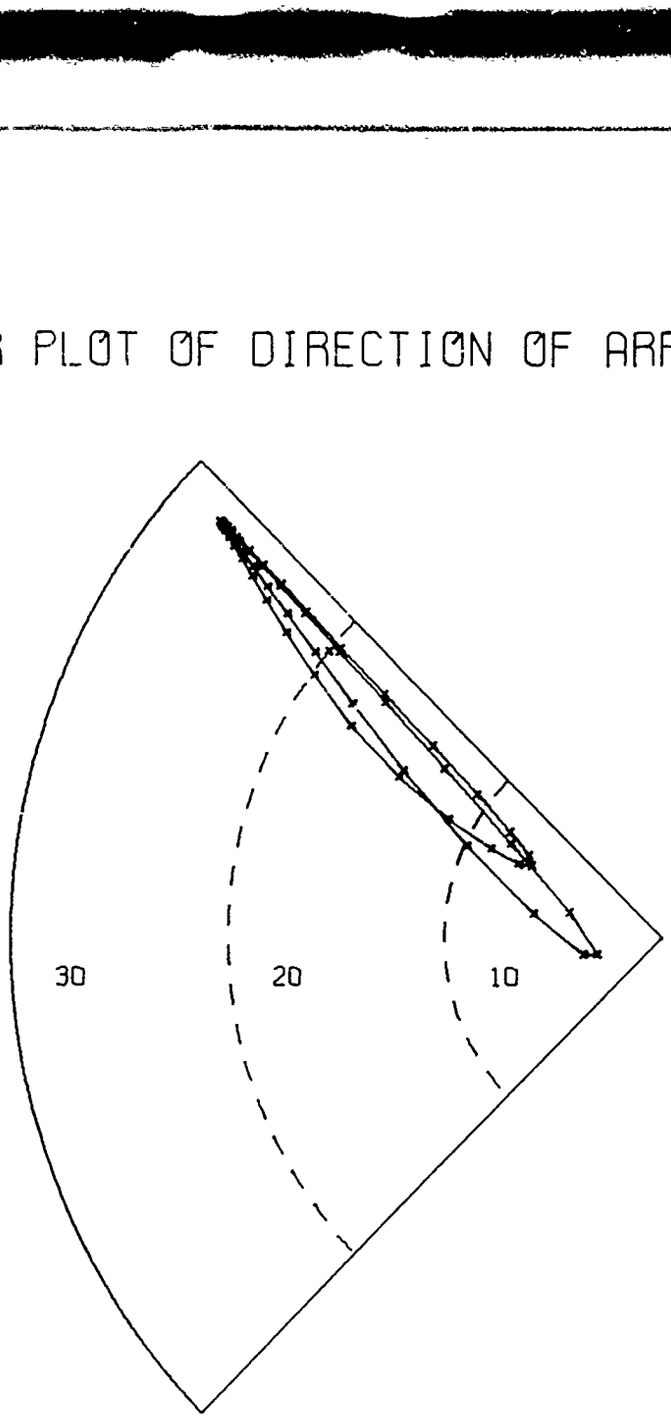

Figure G-7. Plots of the ϕ_d-Variation of the Indicated DOA ($\gamma = 45°$)

POLAR PLOT OF DIRECTION OF ARRIVAL

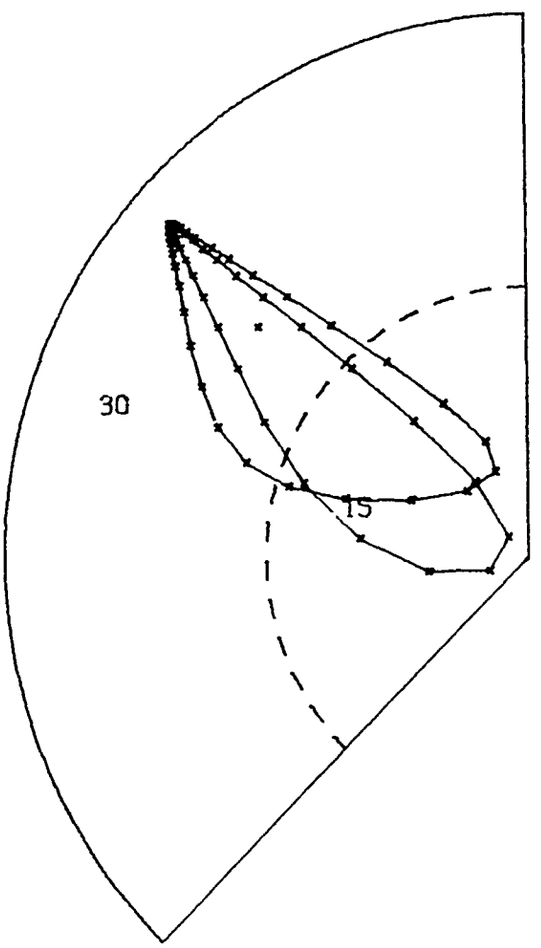

DOA FOR WAVE INT CONDX WITH VARYING REL PHASE

PRI AZ = 310.00 PRI INC = 20.00

SEC AZ = 315.00 SEC INC = 45.00

SEC/PRI = 0.50

ARRAY ANGLE = 25.0

Figure G-8. Plots of the ϕ_d-Variation of the Indicated DOA ($\gamma = 25°$)

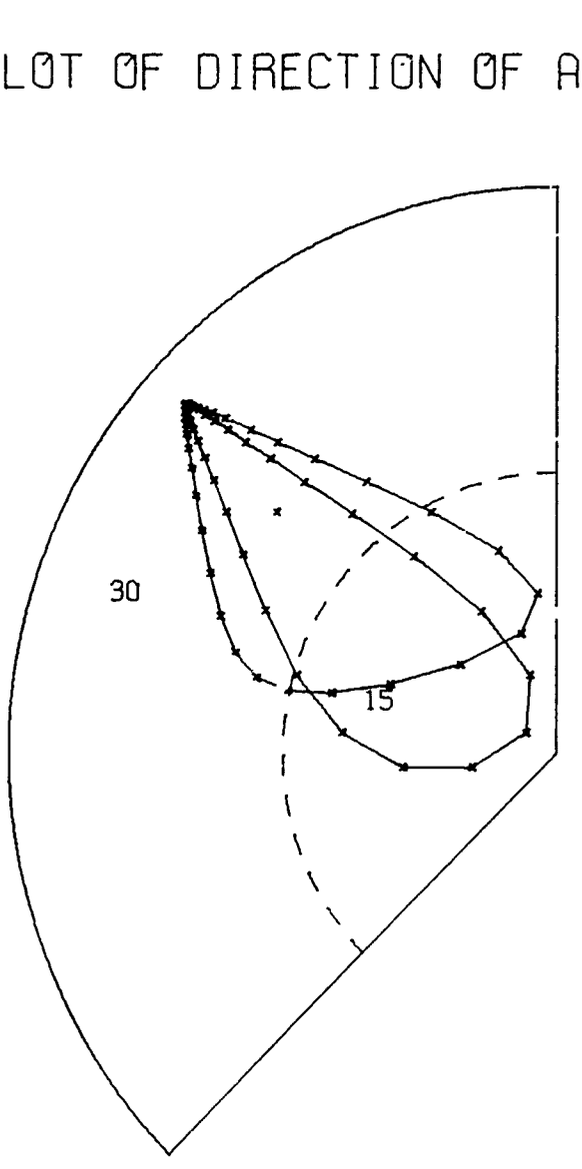

Figure G-9. Plots of the ϕ_d-Variation of the Indicated DOA ($\gamma = 5°$)

APPENDIX H

This appendix contains a comparison of two different approaches to phase ambiguity resolution in a large/small baseline interferometer system under wave interference conditions. (See Chapter VII.)

The program listing follows. All user-written subroutines called are listed in Appendix M.

```
$     INPUT SOURCE CARDS
$     EXECUTE
$      FORTRAN
H      NAME MTHCHK;
H      EQUIP=CARDRE,PRINTE,CARDPU;
H      SINGLEALL;
C*****
C*****THIS PROGRAM COMPARES THE INSTANTANEOUS PHASE AMBIGUITY RESOLUTION METHOD
C*****AND THE AVG PHASE RESOLUTION IN A SMALL/LARGE BASELINE INTERFEROMETER
C*****SYSTEM.  (SEE CHAPTER VII.)  ALL ANGLES ARE IN DEGREES.  THE INPUT DATA
C*****REQUIRED ARE THE PRIMARY AND SECONDARY AZIMUTH AND INCIDENCE ANGLES
C*****(IN DEGREES), H, THE ARRAY ANGLE (IN DEGREES), AND THE SMALL AND LARGE
C*****BASELINE LENGTHS,RESPECTIVELY,(IN METERS).  (8F10.3 FORMAT.)
C*****
      DIMENSION PHISM(40,2),PHILG(40,2),RES(40,2),DPHI(40)
      PI=3.1415926535898
      TWPI=2.*PI
      XINC=TWPI/36.
      DEG=180./PI
      DO 85 ICNT=1,2
C*****ANGLES OF ARRIVAL READ IN DEGREES, H MUST BE BETWEEN 0 AND 1
      READ 10,ALPHP,THETP,ALPHS,THETS,H,DGAMMA,DLS,DLL
10    FORMAT(8F10.3)
      GAMMA=DGAMMA/DEG
      PRINT 15,ICNT,DGAMMA
15    FORMAT(9H1RUN NO. ,I2,16X,25H ISOSCELES ARRAY ANGLE = ,F6.2)
      PRINT 20,ALPHP,ALPHS,THETP,THETS,H
20    FORMAT(                    /,24H PRIMARY MODE AZIMUTH = ,F6.2,15X,26H
     $SECONDARY MODE AZIMUTH = ,F6.2,/,26H PRIMARY MODE INCIDENCE = ,F6.
     $2,13X,28H SECONDARY MODE INCIDENCE = ,F6.2,//,31H AMPLITUDE OF SEC
     $ONDARY WAVE = ,F4.3,40H TIMES THE AMPLITUDE OF THE PRIMARY WAVE)
      RALPHP=ALPHP/DEG
      RALPHS=ALPHS/DEG
      RTHETP=THETP/DEG
      RTHETS=THETS/DEG
      DL=DLS
C*****THIS SECTION OF PROGRAM IS IDENTICAL TO THE WAVE INTERFERENCE SIMULATION
C*****PROGRAM OF APPENDIX G.  THIS PGM IS RUN THROUGH TWICE, ONCE FOR THE
C*****SMALL BASELINE ARRAY AND ONCE FOR THE LARGE BASELINE ARRAY.
      DO 54 ICNT=1,2
      CALL PRTPHI(RALPHP,RTHETP,DL,PHIP21,PHIP13,PHIP32, GAMMA)
      CALL PRTPHI(RALPHS,RTHETS,DL,PHIS21,PHIS13,PHIS32, GAMMA)
      PHIDIF=-XINC
      SMFI21=0.
      SMFI13=0.
      SMFI32=0.
      DO 50 JCNT=1,36
      PHIDIF=PHIDIF+XINC
      X1=ATAN2(H*SIN(PHIDIF),1.+H*COS(PHIDIF))
      PHI21=ATAN2(SIN(PHIP21)+H*SIN( PHIDIF+PHIS21),COS(PHIP21)+H*COS(PH
     $IDIF+PHIS21))-X1
      CALL REDUCE(PHI21)
      CALL CHOS (PHI21,PHIP21,FI21)
      PHI21=FI21
      PHIP31=-PHIP13
      PHIS31=-PHIS13
      PHI31= ATAN2(SIN(PHIP31)+H*SIN(PHIDIF+PHIS31),COS(PHIP31)+H*COS(PH
     $IDIF+PHIS31))-X1
      CALL REDUCE(PHI31)
```

```
      CALL CHOS (PHI31,PHIP31,FI31)
      PHI31=FI31
      PHI32=PHI31-PHI21
      PHI13=-PHI31
C*****SUM UP ALL INTERF PHASES TO CALCULATE AVG INTERF PHASES.
      SMFI21=SMFI21+PHI21
      SMFI13=SMFI13+PHI13
      SMFI32=SMFI32+PHI32
      DPHI(JCNT)=DEG*PHIDIF
      IF(ICNT-1,5)45,45,46
45    PHISM(JCNT,1)=PHI21
      PHISM(JCNT,2)=PHI32
      GO TO 50
46    PHILG(JCNT,1)=PHI21
      PHILG(JCNT,2)=PHI32
50    CONTINUE
      AVFI21=SMFI21/36.
      AVFI32=SMFI32/36.
      IF(ICNT-1,5)52,52,53
52    AVSM21=AVFI21
      AVSM32=AVFI32
      DL=DLL
      GO TO 54
53    AVLG21 =AVFI21
      AVLG32=AVFI32
54    CONTINUE
C*****PERFORM INST PHASE AMBIGUITY RESOLUTION
      SMRES1=0.
      SMRES2=0.
      DRAT=DLL/DLS
      DO 60 ICT=1,36
C*****REDUCE TE ACTUAL INTERF PHASES TO LIE WITHIN THE PRINCIPLE BRANCH OF
C*****-180. TO 180. DEGREES, AS WOULD BE MEASURED
      CALL REDUCE(PHILG(ICT,1))
      CALL REDUCE(PHILG(ICT,2))
C*****COMPUTE APPROX. LARGE ARRAY PHASES FRM SMALL ARRAY PHASES.
      X1=PHISM(ICT,1)*DRAT
      X2=PHISM(ICT,2)*DRAT
C*****ADD + OR - 360. DEGREES TO THE REDUCED INSTANTANEOUS PHASES
C*****UNTIL THEY LIE WITHIN 180 DEGREES OF THE APPROX. PHASES INDICATED
C*****BY THE SMALL ARRAY. THUS AFFECTING INSTANTANEOUS AMBIGUITY RESOLUTION.
      CALL CHOS(PHILG(ICT,1),X1,RES(ICT,1))
      CALL CHOS(PHILG(ICT,2),X2,RES(ICT,2))
      SMRES1=SMRES1+RES(ICT,1)
      SMRES2=SMRES2+RES(ICT,2)
60    CONTINUE
      AVRES1=SMRES1/36.
      AVRES2=SMRES2/36.
      PRINT 69
69    FORMAT(1H1)
      PRINT 70
70    FORMAT( /,80(1H*)/,22X,37HINSTANTANEOUS PHASE RESOLUTION METHOD,/,
     $80(1H*))
      PRINT 71,DLS,DLL
71    FORMAT( /,5X,69HPHASE DIF     SMALL ARRAY PHASES     LARGE ARRAY PHA
     $SES          RESULTS /64X,10HINST PHASE,/,22X,5H D/L=,F5.2,11X,
     $5H D/L=,F5.2,11X,9HAMBIGUITY   /,64X,10HRESOLUTION)
      PRINT 72
72    FORMAT(  21X,12HPHI21  PHI32,9X,12HPHI21  PHI32,8X,12HPHI21  PHI32
     $)
```

```
      DO 720 J=1,36
      PS1=PHISM(J,1)*DEG
      PS2=PHISM(J,2)*DEG
      PL1=PHILG(J,1)*DEG
      PL2=PHILG(J,2)*DEG
      R1=RES(J,1)*DEG
      R2=RES(J,2)*DEG
720   PRINT 73,DPHI(J),PS1,PS2,PL1,PL2,R1,R2
73    FORMAT(7X,F5.2,9X,F5.2,2X,F5.2,9X,F5.2,2X,F5.2,8X,F5.2,2X,F5.2)
      DAVS1=DEG*AVSM21
      DAVS2=DEG*AVSM32
      DAVL1=DEG*AVLG21
      DAVL2=DEG*AVLG32
      DAVR1=DEG*AVRES1
      DAVR2=DEG*AVRES2
      PRINT 730
730   FORMAT(80(1H-))
      PRINT 74,DAVS1,DAVS2,DAVL1,DAVL2,DAVR1,DAVR2
74    FORMAT(13H AVGED PHASES,8X,F5.2,2X,F5.2,9X,F5.2,2X,F5.2,8X,F5.2,
     $2X,F5.2)
C*****COMPUTE INDICATED DOA FOR INST METHOD
      CALL DIR(AVRES1,AVRES2,DL,GAMMA,AZINST,XINST)
      PRINT 75,AZINST,XINST
75    FORMAT(/,50H DOA OBTAINED FRM AVGED INST PHASES.....AZIMUTH = ,
     $F5.2,11H.....INC = ,F5.2)
C*****PERFORM AVERAGE PHASE AMBIGUITY RESOLUTION
C*****REDUCE THE ACTUAL AVG INTERF PHASES TO LIE WITHIN THE PRINCIPLE BRANCH OF
C*****-,80 TO 180 DEGREES, AS THEY WOULD BE MEASURED (AFTER A SIMILAR
C*****SATISFACTORY BRANCH CUT WERE MADE).
      CALL REDUCE(AVLG21)
      CALL REDUCE(AVLG32)
C*****COMPUTE APPROX LARGE INTERF PHASES FROM SMALL INTERF PHASES
      X3=AVSM21*DRAT
      X4=AVSM32*DRAT
C*****PERFORM AVG PHASE RESOLUTION BY ADDING + OR - 360. DEGREES TO THE
C*****LARGE ARRAY PHASES UNTIL THEY ARE WITHIN  180 DEGREES OF THE ALPROX PHASES
      CALL CHOS(AVLG21,X3,FI21)
      CALL CHOS(AVLG32,X4,FI32)
C*****COMPUTE DOA INDICATED BY THE AVG RESOLUTION METHOD
      CALL DIR(FI21,FI32,DL,GAMMA,AZAVG,AVGINC)
      PRINT 77
77    FORMAT(    80(1H*),25X,/,22X,28H AVG PHASE RESOLUTION METHOD/80(1H
     $*))
      DFI21=DEG*FI21
      DFI32=DEG*FI32
      PRINT 80,DFI21,DFI32
80    FORMAT( / 74H PHASE AMBIGUITY RESOLVED PHASES (USING AVGD LARGE AN
     $D SMALL ARRAY PHASES)    ,/,15X,8HPHI21 = ,F7.2,6X,8HPHI32 = ,F7.2)
      PRINT 82,AZAVG,AVGINC
82    FORMAT(,,50H DOA OBTAINED FRM THESE PHASES.........AZIMUTH = ,
     $F5.2,11H.....INC = ,F5.2)
85    CONTINUE

      CALL EXIT
      END
```

Table H-1. A Case in Which Both the Instantaneous and Average Phase Resolution Methods Field Correct Results

RUN NO. 1 ISOSCELES ARRAY ANGLE = 90.00

PRIMARY MODE AZIMUTH = 310.00 SECONDARY MODE AZIMUTH = 315.00
PRIMARY MODE INCIDENCE = 20.00 SECONDARY MODE INCIDENCE = 45.00

AMPLITUDE OF SECONDARY WAVE = 0.25 TIMES THE AMPLITUDE OF THE PRIMARY WAVE

****

INSTANTANEOUS PHASE RESOLUTION METHOD

****

PHASE DIF	SMALL ARRAY PHASES D/L= 0.10		LARGE ARRAY PHASES D/L= 1.00		RESULTS INST PHASE AMBIGUITY RESOLUTION	
	PHI21	PHI32	PHI21	PHI32	PHI21	PHI32
0.00	9.93	-21.0	93.59	158.3	93.59	-201.
10.00	9.90	-21.0	91.53	159.3	91.53	-200.
20.00	9.84	-20.9	89.01	161.0	89.01	-198.
30.00	9.74	-20.8	86.02	163.5	86.02	-196.
40.00	9.62	-20.6	82.54	166.8	82.54	-193.
50.00	9.45	-20.3	78.63	170.7	78.63	-189.
60.00	9.24	-19.9	74.38	175.3	74.38	-184.
70.00	8.99	-19.5	69.95	-179.	69.95	-179.
80.00	8.68	-19.0	65.58	-174.	65.58	-174.
90.00	8.31	-18.3	61.54	-169.	61.54	-169.
100.0	7.89	-17.6	58.09	-163.	58.09	-163.
110.0	7.40	-16.7	55.47	-159.	55.47	-159.
120.0	6.86	-15.8	53.84	-155.	53.84	-155.
130.0	6.29	-14.7	53.33	-152.	53.33	-152.
140.0	5.72	-13.7	53.94	-149.	53.94	-149.
150.0	5.20	-12.7	55.65	-147.	55.65	-147.
160.0	4.81	-11.9	58.35	-146.	58.35	-146.
170.0	4.59	-11.3	61.86	-145.	61.86	-145.
180.0	4.59	-11.1	65.95	-146.	65.95	-146.
190.0	4.81	-11.4	70.33	-146.	70.33	-146.
200.0	5.21	-12.0	74.75	-148	74.75	-148.
210.0	5.72	-12.8	78.98	-15	78.98	-150.
220.0	6.29	-13.8	82.86	-153.	82.86	-153.
230.0	6.86	-14.9	86.29	-157.	86.29	-157.
240.0	7.40	-15.9	89.25	-161.	89.25	-161.
250.0	7.89	-16.9	91.73	-166.	91.73	-166.
260.0	8.32	-17.7	93.75	-171.	93.75	-171.
270.0	8.68	-18.4	95.35	-177.	95.35	-177.
280.0	8.99	-19.0	96.55	177.7	96.55	-182.
290.0	9.24	-19.6	97.38	172.9	97.38	-187.
300.0	9.45	-20.0	97.87	168.6	97.87	-191.
310.0	9.62	-20.3	98.02	165.0	98.02	-194.
320.0	9.74	-20.6	97.84	162.1	97.84	-197.
330.0	9.84	-20.8	97.32	160.0	97.32	-199.
340.0	9.90	-20.9	96.46	158.7	96.46	-201.
350.0	9.93	-21.0	95.23	158.1	95.23	-201.
AVGED PHASES	7.91	-17.3	79.15	-173.	79.15	-173.

DOA OBTAINED FRM AVGED INST PHASES.....AZIMUTH = 310.0.....INC = 20.00

****

AVG PHASE RESOLUTION METHOD

****

PHASE AMBIGUITY RESOLVED PHASES (USING AVGD LARGE AND SMALL ARRAY PHASES)
PHI21 = 79.15 PHI32 = -173.47

DOA OBTAINED FRM THESE PHASES.....AZIMUTH = 310.0.....INC = 20.00

Table H-2. A Case in Which the Instantaneous Phase Resolution Method Fails

RUN NO. 2 ISOSCELES ARRAY ANGLE = 90.00

PRIMARY MODE AZIMUTH = 310.00 SECONDARY MODE AZIMUTH = 315.00
PRIMARY MODE INCIDENCE = 20.00 SECONDARY MODE INCIDENCE = 45.00

AMPLITUDE OF SECONDARY WAVE = 0.75 TIMES THE AMPLITUDE OF THE PRIMARY WAVE

****

INSTANTANEOUS PHASE RESOLUTION METHOD

****

PHASE DIF	SMALL ARRAY PHASES D/L= 0.10		LARGE ARRAY PHASES D/L= 1.00		RESULTS INST PHASE AMBIGUITY RESOLUTION	
	PH121	PH132	PH121	PH132	PH121	PH132
0.00	12.24	-25.3	119.7	110.6	119.7	-249.
10.00	12.22	-25.3	118.5	111.3	118.5	-248.
20.00	12.20	-25.2	116.8	112.6	116.8	-247.
30.00	12.17	-25.2	114.4	114.9	114.4	-245.
40.00	12.12	-25.1	110.6	118.6	110.6	-241.
50.00	12.05	-25.0	104.5	124.6	104.5	-235.
60.00	11.95	-24.8	94.02	135.4	94.02	-224.
70.00	11.82	-24.6	74.52	155.1	74.52	-204.
80.00	11.65	-24.4	43.42	-173.	43.42	-173.
90.00	11.41	-24.0	14.07	-143.	14.07	-143.
100.0	11.07	-23.4	-2.95	-125.	-2.95	-125.
110.0	10.57	-22.6	-11.5	-115	-11.5	-115.
120.0	9.79	-21.4	-15.5	-110.	-15.5	-110.
130.0	8.51	-19.4	-16.6	-106.	-16.6	-106.
140.0	6.25	-16.1	-15.3	-104.	-15.3	-104.
150.0	1.88	-9.75	-11.0	-103.	-11.0	-103.
160.0	-6.77	2.77	-1.89	-102.	-1.89	-102.
170.0	-18.8	22.48	16.10	-102.	-343.	257.8
180.0	-18.7	32.76	46.31	-102.	-313.	257.7
190.0	-6.67	19.43	76.68	-102.	76.68	257.2
200.0	1.94	0.31	95.19	-103.	95.19	-103.
210.0	6.28	-11.0	105.2	-105.	105.2	-105.
220.0	8.53	-16.7	111.0	-108.	111.0	-108.
230.0	9.80	-19.8	114.6	-112.	114.6	-112.
240.0	10.57	-21.6	117.0	-120.	117.0	-120.
250.0	11.07	-22.8	118.7	-133.	118.7	-133.
260.0	11.41	-23.5	119.8	-157.	119.8	-157.
270.0	11.65	-24.0	120.6	169.2	120.6	-190.
280.0	11.82	-24.4	121.2	143.4	121.2	-216.
290.0	11.95	-24.7	121.6	129.0	121.6	-230.
300.0	12.05	-24.9	121.8	121.1	121.8	-238.
310.0	12.12	-25.0	121.8	116.4	121.8	-243.
320.0	12.17	-25.1	121.8	113.6	121.8	-246.
330.0	12.20	-25.2	121.5	111.8	121.5	-248.
340.0	12.22	-25.3	121.1	110.8	121.1	-249.
350.0	12.24	-25.3	120.6	110.4	120.6	-249.
AVGED PHASES	7.91	-17.3	79.15	-173.	59.15	-143.

DOA OBTAINED FROM AVGED INST PHASES.....AZIMUTH = 305.0.....INC = 16.62

****

AVG PHASE RESOLUTION METHOD

****

PHASE AMBIGUITY RESOLVED PHASES (USING AVGD LARGE AND SMALL ARRAY PHASES)
PH121 = 79.15 PH132 = -173.47

DOA OBTAINED FROM THESE PHASES.....AZIMUTH = 310.0.....INC = 20.00

APPENDIX I

This appendix contains a tabulation of the results of numerous executions of the comparison program of Appendix H. It shows how the instantaneous phase resolution method fails as various parameters are varied. (See Chapter VII.)

A listing of the modified program follows. All user-written subroutines may be found listed in Appendix M.

```
$     INPUT SOURCE CARDS
$      EXECUTE
$      FORTRAN
H      NAME TABCHK;
H      EQUIP=CARDRE,PRINTE,CARDPU;
H      SINGLEALL;
C*****
C*****THIS PGM WORKS IN EXACTLY THE SAME MANNER AS PGM METHCHK, OF APPENDIX
C*****VII.  DETAILED DOCUMENTATION MAY BE FOUND THERE.
C*****
       DIMENSION PHISM(40,2),PHILG(40,2),RES(40,2),DPHI(40)
       PI=3.1415926535898
       TUPI=2.*PI
       XINC=TUPI/36.
       DEG=180./PI
       DO 85 LCNT=1,5
       GO TO (200,300,400,500,600),LCNT
200    PRINT 210
210    FORMAT(1H1,///59H COMPARISON OF AMBIGUITY RESOLUTION METHODS VARYI
      $NG PRI DOA  //)
       PRINT 215
215    FORMAT(71H NOTE.....SEC AZ = PRI AZ + DELAZ    ALSO    SEC INC = P
      $RI INC + DELINC //)
       PRINT 220
220    FORMAT(3X,108HPRI WAVE      SEC WAVE      REL AMP      SM D/L
      $G D/L    GAMMA      INST RESOLUTION      AVG RESOLUTION ,/,2X,
      $36HAZ    INC    DELAZ  DELINC   SEC/PRI,25X,45HARR ANG       AZ
      $  INC           AZ     INC //)
C*****INITIALIZE PARAMETERS
       ALPHP=-15.
       DELAZ=5.
       DELINC=10.
       M=.8
       DGAMMA=90.
       DLS=.15
       DLI=1.5
C*****BEGIN VARYING PRI DOA
       DO185 J1=1,8
       ALPHP=ALPHP+15.
       THETP=0.
       DO185 J2=1,5
       THETP=THETP+15.
       GO TO 700
184    CONTINUE
185    CONTINUE
       GO TO 85
300    PRINT 310
310    FORMAT(1H1,///59H COMPARISON OF AMBIGUITY RESOLUTION METHODS VARYING
      $NG SEC DOA  //)
       PRINT 215
       PRINT 220
C*****INITIALIZE PARAMETERS
       ALPHP=310.
       THETP=20.
       DELAZ=-20.
C*****BEGIN VARYING DEVIATION OF SEC DOA FROM PRI DOA
       DO285 J3=1,7
       DELAZ=DELAZ+15.
       DELINC=-15.
```

```
      DO285 J4=1,5
      DELINC=DELINC+5
      GO TO 700
284   CONTINUE
285   CONTINUE
      GO TO 85
400   PRINT 410
410   FORMAT(1H1.///87H COMPARISON OF AMBIGUITY RESOLUTION METHODS VARYI
     $NG REL AMPLITUDE (H) BETWEEN THE WAVES  //)
      PRINT 215
      PRINT 220
C*****INITIALIZE PARAMETERS
      DELAZ=-180.
      DELINC=30.
      H=-.05
      DO385 J5=1,20
      H=H+.05
      GO TO 700
384   CONTINUE
385   CONTINUE
      GO TO 85
500   PRINT 510
510   FORMAT(1H1.///100H COMPARISON OF AMBIGUITY RESOLUTION METHODS VARY
     $ING SMALL AND LARGE ARRAY BASELINE/WAVELENGTH RATIOS  //)
      PRINT 215
      PRINT 220
C*****INITIALIZE PARAMETERS
      H=.35
      DLS=0.
      DO485 J6=1,5
      DLS=DLS+.1
      DLL=0
      DO485 J7=1,6
      DLL=DLL+1.
      GO TO 700
484   CONTINUE
485   CONTINUE
      GO TO 85
600   PRINT 610
610   FORMAT(1H1.///71H COMPARISON OF AMBIGUITY RESOLUTION METHODS VARYI
     $NG ARRAY ANGLE, GAMMA  //)
      PRINT 215
      PRINT 220
C*****INITIALIZE PARAMETERS
      DLS=.5
      DLL=2.
      DGAMMA=0.
      DO585 J8=1,9
      DGAMMA=DGAMMA+10.
      PRINT 583
583   FORMAT(/)
      GO TO 700
584   CONTINUE
585   CONTINUE
      GO TO 85
700   ALPHS=ALPHP+DELAZ
      THETS=THETP+DELINC
      GAMMA=DGAMMA/DEG
      RALPHP=ALPHP/DEG
      RALPHS=ALPHS/DEG
```

```
      RTHETP=THETP/DEG
      RTHETS=THETS/DEG
      DL=DLS
      DO 54 ICNT=1,2
      CALL PRTPHI(RALPHP,RTHETP,DL,PHIP21,PHIP13,PHIP32, GAMMA)
      CALL PRTPHI(RALPHS,RTHETS,DL,PHIS21,PHIS13,PHIS32, GAMMA)
      PHIDIF=-XINC
      SMFI21=0.
      SMFI13=0.
      SMFI32=0.
      DO 50 JCNT=1,36
      PHIDIF=PHIDIF+XINC
      X1=ATAN2(H*SIN(PHIDIF),1.+H*COS(PHIDIF))
      PHI21=ATAN2(SIN(PHIP21)+H*SIN( PHIDIF+PHIS21),COS(PHIP21)+H*COS(PH
     $IDIF+PHIS21))-X1
      CALL REDUCE(PHI21)
      CALL CHOS (PHI21,PHIP21,FI21)
      PHI21=FI21
      PHIP31=-PHIP13
      PHIS31=-PHIS13
      PHI31= ATAN2(SIN(PHIP31)+H*SIN(PHIDIF+PHIS31),COS(PHIP31)+H*COS(PH
     $IDIF+PHIS31))-X1
      CALL REDUCE(PHI31)
      CALL CHOS (PHI31,PHIP31,FI31)
      PHI31=FI31
      PHI32=PHI31-PHI21
      PHI13=-PHI31
C*****SUM UP ALL INTERF PHASES TO CALCULATE AVG INTERF PHASES.
      SMFI21=SMFI21+PHI21
      SMFI13=SMFI13+PHI13
      SMFI32=SMFI32+PHI32
      DPHI(JCNT)=DEG*PHIDIF
      IF(ICNT-1.5)45,45,46
45    PHISM(JCNT,1)=PHI21
      PHISM(JCNT,2)=PHI32
      GO TO 50
46    PHILG(JCNT,1)=PHI21
      PHILG(JCNT,2)=PHI32
50    CONTINUE
      AVFI21=SMFI21/36.
      AVFI32=SMFI32/36.
      IF(ICNT-1.5)52,52,53
52    AVSM21=AVFI21
      AVSM32=AVFI32
      DL=DLL
      GO TO 54
53    AVLG21 =AVFI21
      AVLG32=AVFI32
54    CONTINUE
C*****PERFORM INST PHASE AMBIGUITY RESOLUTION
      SMRES1=0.
      SMRES2=0.
      DRAT=DLL/DLS
      DO 60 ICT=1,36
      CALL REDUCE(PHILG(ICT,1))
      CALL REDUCE(PHILG(ICT,2))
      X1=PHISM(ICT,1)*DRAT
      X2=PHISM(ICT,2)*DRAT
      CALL CHOS(PHILG(ICT,1),X1,RES(ICT,1))
      CALL CHOS(PHILG(ICT,2),X2,RES(ICT,2))
```

```
      SMRES1=SMRES1+RES(ICT,1)                                          170
      SMRES2=SMRES2+RES(ICT,2)
60    CONTINUE
      AVRES1=SMRES1/36.
      AVRES2=SMRES2/36.
C*****COMPUTE INDICATED DOA FOR INST METHOD
      CALL DIR(AVRES1,AVRES2,DL,GAMMA,AZINST,XINST)
C*****PERFORM AVERAGE PHASE AMBIGUITY RESOLUTION
      CALL REDUCE(AVLG21)
      CALL REDUCE(AVLG32)
      X3=AVSM21*DRAT
      X4=AVSM32*DRAT
      CALL CHOS(AVLG21,X3,FI21)
      CALL CHOS(AVLG32,X4,FI32)
      CALL DIR(FI21,FI32,DL,GAMMA,AZAVG,AVGINC)
      PRINT 80,ALPHP,THETP,DELAZ,DELINC,H,DLS,DLL,DGAMMA,AZINST,XINST,
     $AZAVG,AVGINC
80    FORMAT(1X,F5.2,1X,F5.2,3X,2(F5.2,2X),3X,F5.2,7X,3(F5.2,5X),2(2X,F5.2),5X,2
     Z.2),5X,2(3X,F5.2))
      GO TO (184,284,384,484,584),LCNT
85    CONTINUE
      CALL EXIT
      END
```

Table I-1. Comparison of the Two Resolution Methods Varying the Primary DOA

COMPARISON OF AMBIGUITY RESOLUTION METHODS VARYING PRI DOA

NOTE.....SEC AZ = PRI AZ + DELAZ ALSO SEC INC = PRI INC + DELINC

PRI WAVE AZ	PRI WAVE INC	SEC WAVE DELAZ	SEC WAVE DELINC	REL AMP SEC/PRI	SM D/L	LG D/L	GAMMA ARR ANG	INST RESOLUTION AZ	INST RESOLUTION INC	AVG RESOLUTION AZ	AVG RESOLUTION INC
0.00	15.00	5.00	10.00	0.80	0.15	1.50	90.00	360.0	12.81	360.0	15.00
0.00	30.00	5.00	10.00	0.80	0.15	1.50	90.00	357.8	28.81	360.0	30.00
0.00	45.00	5.00	10.00	0.80	0.15	1.50	90.00	360.0	45.00	360.0	45.00
0.00	60.00	5.00	10.00	0.80	0.15	1.50	90.00	0.00	60.00	0.00	60.00
0.00	75.00	5.00	10.00	0.80	0.15	1.50	90.00	360.0	75.00	360.0	75.00
15.00	15.00	5.00	10.00	0.80	0.15	1.50	90.00	11.83	13.68	15.00	15.00
15.00	30.00	5.00	10.00	0.80	0.15	1.50	90.00	13.43	28.52	15.00	30.00
15.00	45.00	5.00	10.00	0.80	0.15	1.50	90.00	15.00	45.00	15.00	45.00
15.00	60.00	5.00	10.00	0.80	0.15	1.50	90.00	15.00	60.00	15.00	60.00
15.00	75.00	5.00	10.00	0.80	0.15	1.50	90.00	15.00	75.00	15.00	75.00
30.00	15.00	5.00	10.00	0.80	0.15	1.50	90.00	28.34	13.51	30.00	15.00
30.00	30.00	5.00	10.00	0.80	0.15	1.50	90.00	30.00	30.00	30.00	30.00
30.00	45.00	5.00	10.00	0.80	0.15	1.50	90.00	30.00	45.00	30.00	45.00
30.00	60.00	5.00	10.00	0.80	0.15	1.50	90.00	30.00	60.00	30.00	60.00
30.00	75.00	5.00	10.00	0.80	0.15	1.50	90.00	30.00	75.00	30.00	75.00
45.00	15.00	5.00	10.00	0.80	0.15	1.50	90.00	45.00	15.00	45.00	15.00
45.00	30.00	5.00	10.00	0.80	0.15	1.50	90.00	45.00	30.00	45.00	30.00
45.00	45.00	5.00	10.00	0.80	0.15	1.50	90.00	43.92	43.96	45.00	45.00
45.00	60.00	5.00	10.00	0.80	0.15	1.50	90.00	45.00	60.00	45.00	60.00
45.00	75.00	5.00	10.00	0.80	0.15	1.50	90.00	45.00	75.00	45.00	75.00
60.00	15.00	5.00	10.00	0.80	0.15	1.50	90.00	55.33	13.15	60.00	15.00
60.00	30.00	5.00	10.00	0.80	0.15	1.50	90.00	57.73	27.92	60.00	30.00
60.00	45.00	5.00	10.00	0.80	0.15	1.50	90.00	59.23	43.72	60.00	45.00
60.00	60.00	5.00	10.00	0.80	0.15	1.50	90.00	59.38	58.22	60.00	60.00
60.00	75.00	5.00	10.00	0.80	0.15	1.50	90.00	60.01	75.00	60.00	75.00
75.00	15.00	5.00	10.00	0.80	0.15	1.50	90.00	72.54	12.90	75.00	15.00
75.00	30.00	5.00	10.00	0.80	0.15	1.50	90.00	73.82	27.67	75.00	30.00
75.00	45.00	5.00	10.00	0.80	0.15	1.50	90.00	74.60	43.57	75.00	45.00
75.00	60.00	5.00	10.00	0.80	0.15	1.50	90.00	74.68	58.01	75.00	60.00
75.00	75.00	5.00	10.00	0.80	0.15	1.50	90.00	75.00	75.00	75.00	75.00

Table I-2. Comparison of the Two Resolution Methods Varying the Secondary DOA

COMPARISON OF AMBIGUITY RESOLUTION METHODS VARYING SEC DOA

NOTE.....SEC AZ = PRI AZ + DELAZ ALSO SEC INC = PRI INC + DELINC

PRI WAVE AZ	PRI WAVE INC	SEC WAVE DELAZ	SEC WAVE DELINC	PRI AMB SEC/PRI	SM D/L	LG D/L	GAMMA ARR ANG	INST RESOLUTION AZ	INST RESOLUTION INC	AVG RESOLUTION AZ	AVG RESOLUTION INC
310.0	20.00	-15.0	-10.0	0.80	0.15	1.50	90.00	308.5	22.48	310.0	20.00
310.0	20.00	-15.0	-5.00	0.80	0.15	1.50	90.00	308.0	20.88	310.0	20.00
310.0	20.00	-15.0	0.00	0.80	0.15	1.50	90.00	310.0	20.00	310.0	20.00
310.0	20.00	-15.0	5.00	0.80	0.15	1.50	90.00	310.0	20.00	310.0	20.00
310.0	20.00	-15.0	10.00	0.80	0.15	1.50	90.00	314.3	18.33	310.0	20.00
310.0	20.00	-10.0	-10.0	0.80	0.15	1.50	90.00	308.5	22.48	310.0	20.00
310.0	20.00	-10.0	-5.00	0.80	0.15	1.50	90.00	310.0	20.00	310.0	20.00
310.0	20.00	-10.0	0.00	0.80	0.15	1.50	90.00	310.0	20.00	310.0	20.00
310.0	20.00	-10.0	5.00	0.80	0.15	1.50	90.00	310.0	20.00	310.0	20.00
310.0	20.00	-10.0	10.00	0.80	0.15	1.50	90.00	314.3	18.33	310.0	20.00
310.0	20.00	-5.00	-10.0	0.80	0.15	1.50	90.00	308.5	22.48	310.0	20.00
310.0	20.00	-5.00	-5.00	0.80	0.15	1.50	90.00	310.0	20.00	310.0	20.00
310.0	20.00	-5.00	0.00	0.80	0.15	1.50	90.00	310.0	20.00	310.0	20.00
310.0	20.00	-5.00	5.00	0.80	0.15	1.50	90.00	310.0	20.00	310.0	20.00
310.0	20.00	-5.00	10.00	0.80	0.15	1.50	90.00	314.3	18.33	310.0	20.00
310.0	20.00	0.00	-10.0	0.80	0.15	1.50	90.00	304.6	22.72	310.0	20.00
310.0	20.00	0.00	-5.00	0.80	0.15	1.50	90.00	310.0	20.00	310.0	20.00
310.0	20.00	0.00	0.00	0.80	0.15	1.50	90.00	310.0	20.00	310.0	20.00
310.0	20.00	0.00	5.00	0.80	0.15	1.50	90.00	310.0	20.00	310.0	20.00
310.0	20.00	0.00	10.00	0.80	0.15	1.50	90.00	314.3	18.33	310.0	20.00
310.0	20.00	5.00	-10.0	0.80	0.15	1.50	90.00	306.3	21.79	310.0	20.00
310.0	20.00	5.00	-5.00	0.80	0.15	1.50	90.00	310.0	20.00	310.0	20.00
310.0	20.00	5.00	0.00	0.80	0.15	1.50	90.00	310.0	20.00	310.0	20.00
310.0	20.00	5.00	5.00	0.80	0.15	1.50	90.00	310.0	20.00	310.0	20.00
310.0	20.00	5.00	10.00	0.80	0.15	1.50	90.00	309.5	18.42	310.0	20.00
310.0	20.00	10.00	-10.0	0.80	0.15	1.50	90.00	306.3	21.79	310.0	20.00
310.0	20.00	10.00	-5.00	0.80	0.15	1.50	90.00	310.0	20.00	310.0	20.00
310.0	20.00	10.00	0.00	0.80	0.15	1.50	90.00	310.0	20.00	310.0	20.00
310.0	20.00	10.00	5.00	0.80	0.15	1.50	90.00	310.0	20.00	310.0	20.00
310.0	20.00	10.00	10.00	0.80	0.15	1.50	90.00	304.9	18.63	310.0	20.00
310.0	20.00	15.00	-10.0	0.80	0.15	1.50	90.00	306.3	21.79	310.0	20.00
310.0	20.00	15.00	-5.00	0.80	0.15	1.50	90.00	310.0	20.00	310.0	20.00
310.0	20.00	15.00	0.00	0.80	0.15	1.50	90.00	310.0	20.00	310.0	20.00
310.0	20.00	15.00	5.00	0.80	0.15	1.50	90.00	307.5	19.29	310.0	20.00
310.0	20.00	15.00	10.00	0.80	0.15	1.50	90.00	304.9	18.63	310.0	20.00

Table I-3. Comparison of the Two Resolution Methods Varying the Relative Amplitude (H)

COMPARISON OF AMBIGUITY RESOLUTION METHODS VARYING REL AMPLITUDE (H) BETWEEN THE WAVES

NOTE... SEC AZ = PRI AZ + DELAZ AND SEC INC = PRI INC + DELINC

PRI WAVE AZ	PRI WAVE INC	SEC WAVE DELAZ	SEC WAVE DELINC	REL AMP SEC/PRI	SM D/L	LG D/L	GAMMA ARR ANG	INST RESOLUTION AZ	INST RESOLUTION INC	AVG RESOLUTION AZ	AVG RESOLUTION INC
310.0	20.00	0.00	30.00	-0.00	0.15	1.50	90.00	310.0	20.00	310.0	20.00
310.0	20.00	0.00	30.00	0.05	0.15	1.50	90.00	310.0	20.00	310.0	20.00
310.0	20.00	0.00	30.00	0.10	0.15	1.50	90.00	310.0	20.00	310.0	20.00
310.0	20.00	0.00	30.00	0.15	0.15	1.50	90.00	310.0	20.00	310.0	20.00
310.0	20.00	0.00	30.00	0.20	0.15	1.50	90.00	310.0	20.00	310.0	20.00
310.0	20.00	0.00	30.00	0.25	0.15	1.50	90.00	310.0	20.00	310.0	20.00
310.0	20.00	0.00	30.00	0.30	0.15	1.50	90.00	310.0	20.00	310.0	20.00
310.0	20.00	0.00	30.00	0.35	0.15	1.50	90.00	310.0	20.00	310.0	20.00
310.0	20.00	0.00	30.00	0.40	0.15	1.50	90.00	316.8	17.55	310.0	20.00
310.0	20.00	0.00	30.00	0.45	0.15	1.50	90.00	319.4	16.81	310.0	20.00
310.0	20.00	0.00	30.00	0.50	0.15	1.50	90.00	322.3	16.11	310.0	20.00
310.0	20.00	0.00	30.00	0.55	0.15	1.50	90.00	322.3	16.11	310.0	20.00
310.0	20.00	0.00	30.00	0.60	0.15	1.50	90.00	311.5	16.01	310.0	20.00
310.0	20.00	0.00	30.00	0.65	0.15	1.50	90.00	311.5	16.01	310.0	20.00
310.0	20.00	0.00	30.00	0.70	0.15	1.50	90.00	308.5	15.30	310.0	20.00
310.0	20.00	0.00	30.00	0.75	0.15	1.50	90.00	307.8	13.76	310.0	20.00
310.0	20.00	0.00	30.00	0.80	0.15	1.50	90.00	307.8	13.76	310.0	20.00
310.0	20.00	0.00	30.00	0.85	0.15	1.50	90.00	306.9	12.23	310.0	20.00
310.0	20.00	0.00	30.00	0.90	0.15	1.50	90.00	317.7	11.36	310.0	20.00
310.0	20.00	0.00	30.00	0.95	0.15	1.50	90.00	313.9	10.60	310.0	20.02

Table I-4. Comparison of the Two Resolution Methods Varying the Array D/λ Ratios

COMPARISON OF AMBIGUITY RESOLUTION METHODS VARYING SMALL AND LARGE ARRAY BASELINE/WAVELENGTH RATIOS

NOTE.....SEC AZ = PRI AZ + DELAZ AND SEC INC = PRI INC + DELINC

PRI WAVE AZ	PRI WAVE INC	SEC WAVE DELAZ	SEC WAVE DELINC	REL AMP SEC/PRI	SM D/L	LG D/L	GAMMA ARR ANG	INST RESOLUTION AZ	INST RESOLUTION INC	AVG RESOLUTION AZ	AVG RESOLUTION INC
310.0	20.00	0.00	30.00	0.45	0.10	1.00	90.00	310.0	20.00	310.0	20.00
310.0	20.00	0.00	30.00	0.45	0.10	2.00	90.00	323.1	15.95	310.0	20.00
310.0	20.00	0.00	30.00	0.45	0.10	3.00	90.00	297.3	22.22	310.0	20.00
310.0	20.00	0.00	30.00	0.45	0.10	4.00	90.00	298.7	21.73	310.0	20.00
310.0	20.00	0.00	30.00	0.45	0.10	5.00	90.00	299.2	21.74	310.0	20.00
310.0	20.00	0.00	30.00	0.45	0.10	6.00	90.00	312.7	19.74	310.0	20.00
310.0	20.00	0.00	30.00	0.45	0.20	1.00	90.00	310.0	20.00	310.0	20.00
310.0	20.00	0.00	30.00	0.45	0.20	2.00	90.00	323.1	15.95	310.0	20.00
310.0	20.00	0.00	30.00	0.45	0.20	3.00	90.00	296.6	22.74	310.0	20.00
310.0	20.00	0.00	30.00	0.45	0.20	4.00	90.00	300.2	21.57	310.0	20.00
310.0	20.00	0.00	30.00	0.45	0.20	5.00	90.00	301.3	21.02	310.0	20.00
310.0	20.00	0.00	30.00	0.45	0.20	6.00	90.00	310.5	20.18	310.0	20.00
310.0	20.00	0.00	30.00	0.45	0.30	1.00	90.00	310.0	20.00	310.0	20.00
310.0	20.00	0.00	30.00	0.45	0.30	2.00	90.00	323.1	15.95	310.0	20.00
310.0	20.00	0.00	30.00	0.45	0.30	3.00	90.00	297.3	22.22	310.0	20.00
310.0	20.00	0.00	30.00	0.45	0.30	4.00	90.00	297.7	22.48	310.0	20.00
310.0	20.00	0.00	30.00	0.45	0.30	5.00	90.00	300.1	21.14	310.0	20.00
310.0	20.00	0.00	30.00	0.45	0.30	6.00	90.00	310.5	20.18	310.0	20.00
310.0	20.00	0.00	30.00	0.45	0.40	1.00	90.00	310.0	20.00	310.0	20.00
310.0	20.00	0.00	30.00	0.45	0.40	2.00	90.00	323.1	15.95	310.0	20.00
310.0	20.00	0.00	30.00	0.45	0.40	3.00	90.00	300.6	21.00	310.0	20.00
310.0	20.00	0.00	30.00	0.45	0.40	4.00	90.00	299.7	21.94	310.0	20.00
310.0	20.00	0.00	30.00	0.45	0.40	5.00	90.00	301.3	21.02	310.0	20.00
310.0	20.00	0.00	30.00	0.45	0.40	6.00	90.00	310.5	19.78	310.0	20.00
310.0	20.00	0.00	30.00	0.45	0.50	1.00	90.00	310.0	20.00	310.0	20.00
310.0	20.00	0.00	30.00	0.45	0.50	2.00	90.00	320.9	16.46	310.0	20.00
310.0	20.00	0.00	30.00	0.45	0.50	3.00	90.00	299.3	20.72	310.0	20.00
310.0	20.00	0.00	30.00	0.45	0.50	4.00	90.00	299.3	21.35	310.0	20.00
310.0	20.00	0.00	30.00	0.45	0.50	5.00	90.00	299.2	21.74	310.0	20.00
310.0	20.00	0.00	30.00	0.45	0.50	6.00	90.00	309.4	19.82	310.0	20.00

Table I-5. Comparison of the Two Resolution Methods Varying the Array Angle

COMPARISON OF AMBIGUITY RESOLUTION METHODS VARYING ARRAY ANGLE, GAMMA

NOTE.....SEC AZ = PRI AZ + DELAZ ALSO SEC INC = PRI INC + DELINC

PRI WAVE AZ	INC	SEC WAVE DELAZ	DELINC	REL AMP SEC/PRI	SM D/L	LG D/L	GAMMA ARR ANG	INST RESOLUTION AZ	INC	AVG RESOLUTION AZ	INC
310.0	20.00	0.00	30.00	0.45	0.50	2.00	10.00	310.0	20.00	310.0	20.00
310.0	20.00	0.00	30.00	0.45	0.50	2.00	20.00	310.0	20.00	310.0	20.00
310.0	20.00	0.00	30.00	0.45	0.50	2.00	30.00	310.0	20.00	310.0	20.00
310.0	20.00	0.00	30.00	0.45	0.50	2.00	40.00	310.0	20.00	310.0	20.00
310.0	20.00	0.00	30.00	0.45	0.50	2.00	50.00	310.0	20.00	310.0	20.00
310.0	20.00	0.00	30.00	0.45	0.50	2.00	60.00	310.0	20.00	310.0	20.00
310.0	20.00	0.00	30.00	0.45	0.50	2.00	70.00	317.3	17.41	310.0	20.00
310.0	20.00	0.00	30.00	0.45	0.50	2.00	80.00	318.9	16.95	310.0	20.00
310.0	20.00	0.00	30.00	0.45	0.50	2.00	90.00	320.9	16.46	310.0	20.00

Table I-6. Comparison of the Two Resolution Methods Varying the Array D/λ Ratios

COMPARIS N OF AMBIGUITY RESOLUTION METHODS VARYING SMALL AND LARGE ARRAY BASELINE/WAVELENGTH RATIOS

NOTE.....SEC AZ = PRI AZ + DELAZ ALSO SEC INC = PRI INC + DELINC

PRI WAVE AZ	INC	SEC WAVE DELAZ	DELINC	REL AMP SEC/PRI	SM D/L	LG D/L	GAMMA ARR ANG	INST RESOLUTION AZ	INC	AVG RESOLUTION AZ	INC
310.0	20.00	-10.0	30.00	0.35	0.10	1.00	90.00	294.4	32.13	310.0	20.00
310.0	20.00	-10.0	30.00	0.35	0.10	2.00	90.00	332.4	19.04	310.0	20.00
310.0	20.00	-10.0	30.00	0.35	0.10	3.00	90.00	316.5	19.93	310.0	20.00
310.0	20.00	-10.0	30.00	0.35	0.10	4.00	90.00	303.5	20.34	310.0	20.00
310.0	20.00	-10.0	30.00	0.35	0.10	5.00	90.00	311.8	19.23	310.0	20.00
310.0	20.00	-10.0	30.00	0.35	0.10	6.00	90.00	307.9	20.48	310.0	20.00
310.0	20.00	-10.0	30.00	0.35	0.20	1.00	90.00	295.7	30.44	310.0	20.00
310.0	20.00	-10.0	30.00	0.35	0.20	2.00	90.00	332.4	19.04	310.0	20.00
310.0	20.00	-10.0	30.00	0.35	0.20	3.00	90.00	317.6	20.34	310.0	20.00
310.0	20.00	-10.0	30.00	0.35	0.20	4.00	90.00	302.3	21.06	310.0	20.00
310.0	20.00	-10.0	30.00	0.35	0.20	5.00	90.00	307.3	20.11	310.0	20.00
310.0	20.00	-10.0	30.00	0.35	0.20	6.00	90.00	310.0	20.00	310.0	20.00
310.0	20.00	-10.0	30.00	0.35	0.30	1.00	90.00	310.0	20.00	310.0	20.00
310.0	20.00	-10.0	30.00	0.35	0.30	2.00	90.00	316.5	19.93	310.0	20.00
310.0	20.00	-10.0	30.00	0.35	0.30	3.00	90.00	320.9	20.03	310.0	20.00
310.0	20.00	-10.0	30.00	0.35	0.30	4.00	90.00	304.1	19.99	310.0	20.00
310.0	20.00	-10.0	30.00	0.35	0.30	5.00	90.00	303.5	20.34	310.0	20.00
310.0	20.00	-10.0	30.00	0.35	0.30	6.00	90.00	310.5	19.78	310.0	20.00
310.0	20.00	-10.0	30.00	0.35	0.40	1.00	90.00	310.0	20.00	310.0	20.00
310.0	20.00	-10.0	30.00	0.35	0.40	2.00	90.00	320.9	16.46	310.0	20.00
310.0	20.00	-10.0	30.00	0.35	0.40	3.00	90.00	328.7	20.12	310.0	20.00
310.0	20.00	-10.0	30.00	0.35	0.40	4.00	90.00	306.9	20.73	310.0	20.00
310.0	20.00	-10.0	30.00	0.35	0.40	5.00	90.00	305.0	20.73	310.0	20.00
310.0	20.00	-10.0	30.00	0.35	0.40	6.00	90.00	306.5	19.74	310.0	20.00
310.0	20.00	-10.0	30.00	0.35	0.50	1.00	90.00	310.0	20.00	310.0	20.00
310.0	20.00	-10.0	30.00	0.35	0.50	2.00	90.00	310.0	20.00	310.0	20.00
310.0	20.00	-10.0	30.00	0.35	0.50	3.00	90.00	29.2	19.35	310.0	20.00
310.0	20.00	-10.0	30.00	0.35	0.50	4.00	90.00	-14.0	17.84	310.0	20.00
310.0	20.00	-10.0	30.00	0.35	0.50	5.00	90.00	308.5	19.57	310.0	20.00
310.0	20.00	-10.0	30.00	0.35	0.50	6.00	90.00	307.3	20.31	310.0	20.00

Table I-7. Comparison of the Two Resolution Methods Varying the Array Angle (¥)

COMPARISON OF AMBIGUITY RESOLUTION METHODS VARYING ARRAY ANGLE, GAMMA

NOTE.....SEC AZ = PRI AZ + DELAZ ALSO SEC INC = PRI INC + DELINC

PRI WAVE AZ	INC	SEC WAVE DELAZ	DELINC	REL AMP SEC/PRI	SM D/L	LG D/L	GAMMA ARR ANG	INST RESOLUTION AZ	INC	AVG RESOLUTION AZ	INC
310.0	20.00	-180.	30.00	0.45	0.50	2.00	10.00	310.0	20.00	310.0	20.00
310.0	20.00	-180.	30.00	0.45	0.50	2.00	20.00	310.0	20.00	310.0	20.00
310.0	20.00	-180.	30.00	0.45	0.50	2.00	30.00	298.7	27.21	310.0	20.00
310.0	20.00	-180.	30.00	0.45	0.50	2.00	40.00	310.0	20.00	310.0	20.00
310.0	20.00	-180.	30.00	0.45	0.50	2.00	50.00	304.7	22.66	310.0	20.00
310.0	20.00	-180.	30.00	0.45	0.50	2.00	60.00	311.7	19.26	310.0	20.00
310.0	20.00	-180.	30.00	0.45	0.50	2.00	70.00	310.0	20.00	310.0	20.00
310.0	20.00	-180.	30.00	0.45	0.50	2.00	80.00	310.0	20.00	310.0	20.00
310.0	20.00	-180.	30.00	0.45	0.50	2.00	90.00	316.3	17.55	310.0	20.00

APPENDIX J

This appendix illustrates the equivalence of the two methods of handling erroneous phase measurement data described in Chapter VIII. The data presented here are "live." They were collected at this laboratory's Monticello Road Field Station, on April 11, 1972, as part of a three-transmitter ionospheric "tilt" experiment.[2] The presence of ionospheric tilt is probably the reason why the indicated azimuths do not agree precisely with the actual compass bearings of the transmitter locations from the RDF site, as indicated in the following tables. Each data point represents a group average of ten sets of interferometer phase measurements. The time between each successive phase measurement was two seconds. The experiment was set up such that every minute ten phase measurements from each transmitter would be recorded at the RDF site. (This was done by properly timing the transmitters such that each transmitter would be on and the other two off for 1/3 of a minute.)

These data were taken over a period beginning at 22:39:01 and ending at 22:57:00, GMT.[3]

A listing of the processing program follows. The user-written subroutines are listed in Appendix M.

```
$     INPUT SOURCE CARDS
$      SCRATCH TAPE,3,4,3
$      EXECUTE
$     FORTRAN
H      NAME RIDTA;
H      EQUIP=CARDRE,PRINTE,CARDPU;
H      SINGLEALL;
C******THIS PGM COMPARES 2 METHODS OF DOA CALCULATION USING LIVE DATA
C      THE FOLLOWING DATA CARDS ARE REQUIRED.......
C         1. DATE AND PLACE OF DATA COLLECTION (23A1 FORMAT)
C         2. BEARING AND LOCATION OF TARGET TRANSMITTER (23A1 FORMAT)
C         3. BASELINE + FREQUENCY IN MHZ (2F10.5 FORMAT)
C         4. NUMBER OF DATA CARDS TO BE PROCESSED (I3 FORMAT, RIGHT JUSTIFIED)
C         5. DATA CARDS.....PHI21, PHI13, PHI32 UNAMB. AND IN DEGREES (3F10.5)
C          .
C          .
C          .
       DIMENSION ALPHA1(15), ALPHA2(15)
       PI=3.1415926535898
       DEG=180./PI
       DO 999 LLL=1,3
       READ 10,(ALPHA1(I),I=1,15)
10     FORMAT(15A2)
       READ 10, (ALPHA2(I),I=1,15)
       READ 20,D,FREQ
20     FORMAT(2F10.5)
       DL=D*FREQ/300.
       PRINT 30,ALPHA1,ALPHA2,DL
30     FORMAT(1H1,15X,69HCOMPARISON OF 2 DOA CALC TECHNIQUES USING LIVE P
      $HASE MEASUREMENT DATA//19X,34HDATE+PLACE OF DATA COLLECTION-----,1
      $5A2//19X,34HBEARING AND LOCATION OF SOURCE----,15A2//35X,6HD/L = ,
      $F5.3,2X,18HGAMMA = 60 DEGREES////)
       PRINT 40
40     FORMAT(14X,74HUNAMBIGUOUS        SUM OF        DELTA METHOD
      $ANGLE AVERAGING METHOD/ 13X,73HINTERF PHASES      PHASES    AZIMUT
      $H    INCIDENCE      AZIMUTH   INCIDENCE/13X,14HAVG AMPLITUDE /10X,
      $19HPHI21  PHI13  PHI32/)
       READ 50, NDATA
50     FORMAT(I3)
       DLASM=0.
       DLISM=0.
       AVASM=0.
       AVISM=0.
       AMPSM=0.
       P21SM=0.
       P13SM=0.
       P32SM=0.
       ICHECK=0
       DO 80 LCNT=1,NDATA
       READ 60, PHI21,PHI13,PHI32,AVAMP
60     FORMAT(6F10.5)
65     PHASUM=PHI13+PHI21+PHI32
       RPHI21=PHI21/DEG
       RPHI13=PHI13/DEG
       RPHI32=PHI32/DEG
       CALL AVDIR(RPHI21,RPHI13,RPHI32,DL,AVAZ,AVINC)
       THRDEL=PHASUM/3.
       CPHI21=(PHI21-THRDEL)/DEG
       CPHI13=(PHI13-THRDEL)/DEG
```

```
      CPHI32=(PHI32-THRDEL)/DEG                                          180
      CALL AVDIR(CPHI21,CPHI13,CPHI32,DL,DELAZ,DELINC)
C*****PERFORM BRANCH CUT.  FOR THE FOLLOWING DATA A CUT EXTENDING FROM -PI TO PI
C*****IS APPROPRIATE
      IF(DELAZ-180.)651,651,650
650   DELAZ=DELAZ-360.
651   CONTINUE
      IF(AVAZ-180.) 653,653,652
652   AVAZ=AVAZ-360.
653   CONTINUE
      DLASM=DLASM+DELAZ
      DLISM=DLISM+DELINC
      AVASM=AVASM+AVAZ
      AVISM=AVISM+AVINC
      P21SM=P21SM+PHI21
      P13SM=P13SM+PHI13
      P32SM=P32SM+PHI32
      AMPSM=AMPSM+AVAMP
      PRINT 70,PHI21,PHI13,PHI32,PHASUM,DELAZ,DELINC,AVAZ,AVINC
     $,AVAMP
70    FORMAT(1H ,8X,F6.1,1X,F6.1,2X,F5.1,3X,F6.3,5X,F5.2,6X,F5.2,9X,F5.2
     $,6X,F5.2)
      IF(ICHECK)100,80,100
80    CONTINUE
C*****NOTE THIS AVGING PROCESS IGNORES THE 0 TO 360 DEGREE WRAPAROUND PROBLEM
C*****AND IS THEREFORE NOT VALID UNDER SOME CONDITIONS
      DLA=DLASM/NDATA
      DLI=DLISM/NDATA
      AVA=AVASM/NDATA
      AVI=AVISM/NDATA
C*****CONVERT -180 TO 180 CUT BACK TO THE ORIGINAL 0 TO 360, CUT
      IF(DLA)654.654,655
654   DLA=DLA+360.
655   IF(AVA)656.656,657
656   AVA=AVA+360.
657   CONTINUE
      PRINT 90 ,DLA,DLI,AVA,AVI
90    FORMAT(10X,76(1H*)//10X,12HAVERAGED DOA,21X,F5.2,6X,F5.2,9X,F5.2,6
     $X,F5.2)
      PHI21=P21SM/NDATA
      PHI13=P13SM/NDATA
      PHI32=P32SM/NDATA
      AVAMP=AMPSM/NDATA
      ICHECK=1
      PRINT 95
95    FORMAT(/,9X,78H AVGED PHASES AND AMPLITUDES---AND THE DOA CALCULAT
     $ED FROM THESE AVGED PHASES    )
      GO TO 65
100   CONTINUE
999   CONTINUE
      CALL EXIT
      END
```

COMPARISON OF 2 DOA CALC TECHNIQUES USING LIVE PHASE MEASUREMENT DATA

DATE+PLACE OF DATA COLLECTION-----APRIL 11, 1972 MRFS

BEARING AND LOCATION OF SOURCE----GILMAN, ILL (AZ APRX 18.5)

D/L = 1.542 GAMMA = 60 DEGREES

UNAMBIGUCUS INTERF PHASES AVG AMPLITUDE			SUM OF PHASES	DELTA METHOD		ANGLE AVERAGING METHOD	
PHI21	PHI13	PHI32		AZIMUTH	INCIDENCE	AZIMUTH	INCIDENCE
85.5	-53.3	-34.7	-2.500	7.09	9.02	7.09	9.02
4.8							
87.3	-47.1	-38.7	1.500	3.20	9.01	3.20	9.01
4.2							
90.3	-41.8	-46.3	2.200	-1.66	9.29	-1.66	9.29
4.0							
90.5	-49.1	-43.8	-2.400	1.92	9.47	1.92	9.47
4.2							
96.8	-52.6	-53.1	-8.900	-0.17	10.36	-0.17	10.37
4.3							
101.8	-56.3	-50.9	-5.400	1.72	10.76	1.72	10.77
4.8							
102.5	-54.8	-51.1	-3.400	1.18	10.76	1.18	10.77
4.8							
87.9	-39.3	-50.4	-1.800	-4.14	9.20	-4.14	9.20
4.8							
86.5	-37.1	-48.0	1.400	-4.18	8.94	-4.18	8.94
4.8							
86.9	-42.9	-49.5	-5.500	-2.46	9.21	-2.46	9.21
4.8							
97.9	-60.3	-37.5	0.100	7.66	10.25	7.66	10.25
4.6							
96.8	-74.2	-24.3	-1.700	16.48	10.54	16.48	10.54
4.5							
99.0	-70.2	-19.8	9.000	16.86	10.41	16.87	10.42
4.2							
93.6	-83.2	-13.3	-2.900	23.11	10.68	23.11	10.68
4.0							
90.0	-79.5	-14.5	-4.000	22.34	10.25	22.34	10.25
4.8							
78.9	-60.0	-17.8	1.100	17.24	8.52	17.24	8.52
4.8							
80.8	-54.1	-24.3	2.400	12.14	8.48	12.14	8.48
4.6							
86.6	-53.0	-26.3	7.300	10.38	8.87	10.38	8.88
3.9							
**********							
AVERAGED DOA				7.15	9.67	7.15	9.67
AVGED PHASES AND AMPLITUDES---AND THE DOA CALCULATED FROM THESE AVGED PHASES							
91.1	-56.0	-35.6	-0.750	7.29	9.55	7.29	9.55
4.5							

COMPARISON OF 2 DOA CALC TECHNIQUES USING LIVE PHASE MEASUREMENT DATA

DATE+PLACE OF DATA COLLECTION-----APRIL 11, 1972 MRFS

BEARING AND LOCATION OF SOURCE----LODA, ILL (AZ APRX 21.5)

D/L = 1.542 GAMMA = 60 DEGREES

UNAMBIGUOUS INTERF PHASES AVG AMPLITUDE			SUM OF PHASES	DELTA METHOD		ANGLE AVERAGING METHOD	
PHI21	PHI13	PHI32		AZIMUTH	INCIDENCE	AZIMUTH	INCIDENCE
68.1	-35.2	-32.9	0.000	1.12	7.05	1.12	7.05
2.9							
75.3	-39.9	-34.0	2.300	2.22	7.72	2.22	7.72
1.3							
68.9	-20.5	-38.4	10.000	-8.96	6.87	-8.97	6.89
1.6							
74.7	-49.4	-29.4	-4.100	8.63	7.97	8.63	7.97
2.3							
51.5	-29.5	-31.4	-9.600	-1.27	5.66	-1.27	5.68
3.8							
53.9	-27.7	-32.2	-6.000	-2.66	5.79	-2.66	5.79
3.1							
57.9	-11.8	-44.3	1.800	-18.1	6.24	-18.1	6.24
2.7							
52.4	-10.1	-31.6	10.700	-14.2	5.21	-14.3	5.23
2.3							
68.9	-22.6	-42.4	3.900	-9.60	7.10	-9.60	7.10
2.0							
52.7	-29.9	-39.5	-16.70	-5.43	6.05	-5.39	6.11
2.6							
58.8	-43.2	-22.4	-6.800	11.13	6.44	11.12	6.45
2.9							
56.4	-52.8	-14.4	-10.80	20.28	6.62	20.25	6.64
3.1							
75.7	-65.2	-3.2	7.300	26.04	8.45	26.04	8.46
2.6							
54.6	-59.1	-7.6	-12.10	26.89	6.80	26.85	6.83
2.7							
55.4	-37.8	-4.3	13.300	20.78	5.64	20.86	5.67
2.2							
48.0	-24.0	-13.4	10.600	7.84	4.64	7.87	4.67
1.7							
67.9	-69.1	-26.4	-27.60	17.73	8.39	17.53	8.49
1.5							
71.8	-50.2	-35.3	-13.70	6.43	7.96	6.42	7.99
1.4							
**********							
AVERAGED DOA				4.93	6.70	4.92	6.72
AVGED PHASES AND AMPLITUDES---AND THE DOA CALCULATED FROM THESE AVGED PHASES							
61.8	-37.6	-26.8	-2.639	5.66	6.52	5.66	6.52
2.3							

COMPARISON OF 2 DOA CALC TECHNIQUES USING LIVE PHASE MEASUREMENT DATA

DATE+PLACE OF DATA COLLECTION-----APRIL 11, 1972 MRFS

BEARING AND LOCATION OF SOURCE----TISBORO, ILL (AZ APRX 21.5)

D/L = 1.542 GAMMA = 60 DEGREES

UNAMBIGUCUS INTERF PHASES AVG AMPLITUDE			SUM OF PHASES	DELTA METHOD		ANGLE AVERAGING METHOD	
PHI21	PHI13	PHI32		AZIMUTH	INCIDENCE	AZIMUTH	INCIDENCE
40.1 4.8	-18.7	-24.1	-2.700	-4.35	4.25	-4.35	4.25
41.2 4.3	-19.6	-20.8	0.800	-0.97	4.23	-0.97	4.23
43.4 4.5	-24.4	-17.0	2.000	5.71	4.44	5.71	4.44
33.9 4.5	-9.1	-17.4	7.400	-8.67	3.28	-8.70	3.30
27.9 4.8	-9.3	-25.8	-7.200	-17.4	3.28	-17.3	3.30
34.0 4.8	-0.2	-27.5	6.300	-26.2	3.68	-26.3	3.69
39.4 4.4	-1.1	-34.8	3.500	-26.9	4.43	-26.9	4.44
37.3 4.7	-6.0	-32.5	-1.200	-22.0	4.20	-22.0	4.20
32.6 4.8	-16.7	-18.1	-2.200	-1.39	3.44	-1.39	3.45
25.0 4.8	-2.5	-12.6	9.900	-15.0	2.32	-15.4	2.37
23.4 4.8	-25.1	-9.1	-10.80	18.89	2.95	18.60	2.99
23.7 4.8	-16.3	-10.1	-2.700	8.28	2.57	8.28	2.57
16.2 4.6	-14.6	-14.0	-10.40	0.92	2.24	0.88	2.29
34.9 4.1	-17.6	-11.3	6.000	6.31	3.42	6.32	3.43
34.5 3.5	-18.4	-19.6	-3.500	-1.11	3.69	-1.11	3.69
46.3 3.5	-20.1	-16.9	9.300	2.45	4.47	2.46	4.49
49.1 3.1	-30.4	-21.1	-2.400	6.14	5.19	6.14	5.19
52.7 4.2	-30.1	-22.2	0.400	4.96	5.46	4.96	5.46
**********							
AVERAGED DOA				356.0	3.75	356.0	3.77
AVGED PHASES AND AMPLITUDES---AND THE DOA CALCULATED FROM THESE AVGED PHASES							
35.4 4.4	-15.6	-19.7	0.139	-3.87	3.66	-3.87	3.66

APPENDIX K

This appendix contains derivations of equations VIII-7 and VIII-8. From elementary trigonometry, it may be inferred from equation VIII-6 that:

$$\sin \alpha_{21-32} = y_1/r_1 \qquad \cos \alpha_{21-32} = x_1/r_1$$

$$\sin \alpha_{21-13} = y_2/r_2 \qquad \cos \alpha_{21-13} = x_2/r_2 \qquad \text{(K-1)}$$

$$\sin \alpha_{32-13} = y_3/r_3 \qquad \cos \alpha_{32-13} = x_3/r_3,$$

where $r_i = \sqrt{x_i^2 + y_i^2}$, $i = 1, 2, 3$.

Substituting equations K-1 into equation VIII-2 yields:

$$\alpha_{avg} = \tan^{-1} \frac{y_1/r_1 + y_2/r_2 + y_3/r_3}{x_1/r_1 + x_2/r_2 + x_3/r_3} . \qquad \text{(K-2)}$$

Equation K-2 is identical to equation VIII-7.

Next, equations VIII-4 (expressions for the "delta method" - corrected phases) are substituted into equations I-4. (For simplicity of notation, the symmetric array equations will be used.) Because the sum of the "corrected" phases is zero, equations I-4 will yield identical results; hence only equation I-4(e) will be used. This results in:

$$\alpha_\Delta = \tan^{-1} \frac{2(\phi_{32} - \Delta/3) + (\phi_{21} - \Delta/3)}{\sqrt{3}\ (\phi_{21} - \Delta/3)} . \qquad \text{(K-3)}$$

But, equation VIII-3 states that:

$$\Delta = \phi_{21} + \phi_{13} + \phi_{32}. \qquad \text{(K-4)}$$

Substitution of K-4 into K-3 results in:

$$\alpha_\Delta = \tan^{-1} \frac{\sqrt{3}\ (\phi_{32} - \phi_{13})}{2\phi_{21} - \phi_{32} - \phi_{13}} . \qquad \text{(K-5)}$$

It will now be shown that expression K-5 is equivalent to the expression: [4]

$$\alpha_\Delta = \tan^{-1} \frac{y_1 + y_2 + y_3}{x_1 + x_2 + x_3}. \qquad \text{(K-6)}$$

This is the expression we wish to verify (equation VIII-8). Perhaps this equivalence can best be demonstrated by working backwards from equation K-6.

From equations I-4(d), (e), and (f), x_1, x_2, x_3, y_1, y_2, and y_3 may be computed, as in figure K-1. Substituting these values of x_i and y_i ($i = 1$, 2, or 3) into equation K-5 yields:

$$\alpha_\Delta = \tan^{-1} \frac{-(2\phi_{13} + \phi_{21}) + 2\phi_{32} + \phi_{21} + \phi_{32} - \phi_{13}}{\sqrt{3}\ (\phi_{21} + \phi_{21} - \phi_{32} - \phi_{13})}$$

or, after simplification,

$$\alpha_\Delta = \tan^{-1} \frac{\sqrt{3}\ (-\phi_{13} + \phi_{32})}{(2\phi_{21} - \phi_{32} - \phi_{13})}. \qquad \text{(K-7)}$$

But this expression is equivalent to expression K-6. Hence equations K-5 and K-6 are indeed equivalent.

Eqn 1-4d:

$$\tan \alpha_{21-13} = \frac{-2\phi_{13} - \phi_{21}}{\sqrt{3}\ \phi_{21}}$$

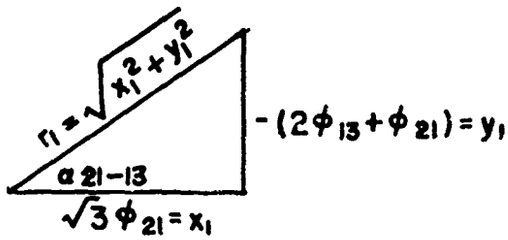

Eqn 1-4e:

$$\tan \alpha_{21-32} = \frac{2\phi_{32} + \phi_{21}}{\sqrt{3}\ \phi_{21}}$$

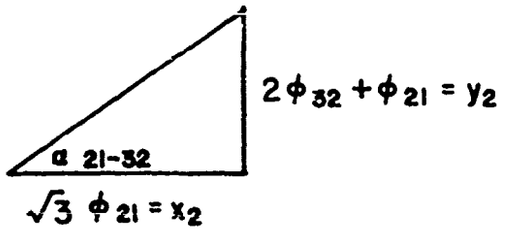

Eqn 1-5f:

$$\tan \alpha_{32-13} = \frac{\phi_{32} - \phi_{13}}{-\sqrt{3}\,(\phi_{32} + \phi_{13})}$$

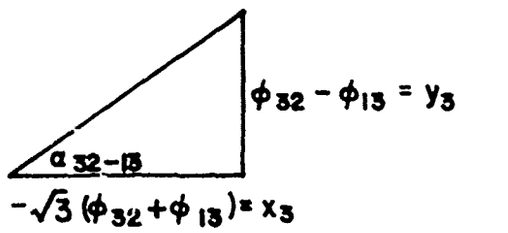

Figure K-1. Simple Trigonometric Relationships Used in the Work of Appendix K.

APPENDIX L

This appendix contains typical results of a comparison study of the equivalence of the two methods of processing erroneous phase measurement data. This study uses computer-generated erroneous phases as contrasted with the real phase data processed in Appendix J. Even for very large values of Δ, it is obvious that the two methods are essentially equivalent.

A listing of the program follows. Any user-written subroutines called may be found listed in Appendix M.

```
$     INPUT SOURCE CARDS
$     EXECUTE
$     FORTRAN
H      NAME COMPAR;
H      EQUIP=CARDRE,PRINTE,CARDPU;
H      SINGLEALL;
C*****
C*****THIS PROGRAM COMPARES TWO DOA CALCULATION SCHEMES USING ERRONEOUS
C*****PHASE DATA.  ONE METHOD INVOLVES AZIMUTH ANGLE AVERAGING (ANGLE AVERAGING
C*****METHOD), THE OTHER INVOLVES SUBTRACTING 1/3 THE SUM OF THE INTERFEROMETER
C*****PHASES FROM EACH INDIVIDUAL PHASE (DELTA METHOD).
C*****REQUIRED INPUT DATA ARE THE ACTUAL AZIMUTH AND INCIDENCE (IN DEGREES),
C*****AND THE BASELINE/WAVELENGTH RATIO. (3F10.5 FORMAT)
C*****
      PI=3.1415926535
      DEG=180./PI
      DO 30 ICNT=1,5
      READ 10,AZ,THET,DL
10    FORMAT(3F10.5)
      RAZ=AZ/DEG
      RTHET=THET/DEG
C*****COMPUTE NON-ERRONEOUS INTERFEROMETER PHASES FROM SPECIFIED DOA AND D/L
C*****VALUES
      CALL ERTPH1(RAZ,RTHET,DL,PHI21,PHI13,PHI32)
      DPHI21=PHI21*DEG
      DPHI13=PHI13*DEG
      DPHI32=PHI32*DEG
      DO 30 JCONT=1,3
      DEL=-1.1
      PRINT 20,AZ,THET,DL
20    FORMAT(1H1, 71HCOMPARISON OF 2 DOA CALC. TECHNIQUES USING ERRONEOU
     $S PHASE MEASUREMENTS    ,//16H TRUE AZIMUTH = ,F5.2,10X,17HTRUE IN
     $CIDENCE = ,F5.2,10X,22HBASELINE/WAVELENGTH = ,F5.2,/)
      PRINT 18,DPHI21,DPHI13,DPHI32
18    FORMAT(14H TRUE PHI21 = ,F7.2,10X,14H TRUE PHI13 = ,F7.2,10X,14H T
     $RUE PHI32 = ,F7.2,/)
      GO TO (21,22,23),JCONT
21    PRINT 27
27    FORMAT(///42H ERROR SUM CONCENTRATED IN PHI13 PHASE..../// )
      GO TO 24
22    PRINT 28
28    FORMAT(///49H ERROR SUM DIVIDED EQUALLY AMONG PHI13, PHI32..../// )
      GO TO 24
23    PRINT 29
29    FORMAT(///56H ERROR SUM DIVIDED EQUALLY AMONG PHI13, PHI21, PHI32.
     $..   //)
24    CONTINUE
      PRINT 240
240   FORMAT(74H (ALSO ASSUMING PHI13, PHI32 HAVE CANCELLING ERRORS OF +
     $,-(SUM OF PHASES))///)
      PRINT 25
25    FORMAT(11X,91HSUM OF PHASES          AZIMUTH              AZIMUTH
     $          INCIDENCE          INCIDENCE    ,/,13X,93HERROR SUM
     $    DELTA METHOD      ANGLE AVGING METH     DELTA METHOD      ANG
     $E AVGING METH  ,//)
      DO 30 NCNT=1,21
C*****INCREMENT ERROR BY .1 RADIANS
      DEL=DEL+.1
C*****INTRODUCE ERRORS OF +,- DEL IN PHI13, PHI32, (RESPECTIVELY)
```

```
      FI13=PHI13+DEL
      FI32=PHI32-DEL
      FI21=PHI21
      TDEL=DEL/3.
      GO TO (31,32,33),JCONT
C*****PUT ERROR ALL INTO PHI13 PHASE
31    FI13=FI13+DEL
      GO TO 34
C*****DIVIDE ERROR AMONG PHI13 AND PHI32
32    FI13=FI13+DEL/2.
      FI32=FI32+DEL/2.
      GO TO 34
C*****DIVIDE ERROR EQUALLY AMONG ALL THREE PHASES
33    FI13=FI13+TDEL
      FI32=FI32+TDEL
      FI21=FI21+TDEL
34    CONTINUE
C*****PERFORM ANGLE AVERAGING METHOD DOA CALCULATION
      CALL AVDIR(FI21,FI13,FI32,DL,AVAZ,AVINC)
      CI21=FI21-TDEL
      CI13=FI13-TDEL
      CI32=FI32-TDEL
C*****PERFORM DELTA METHOD DOA CALCULATION
      CALL AVDIR(CI21,CI13,CI32,DL,DELAZ,DELINC)
      DGDEL=DEL*DEG
30    PRINT 40,DGDEL,DELAZ,AVAZ,DELINC,AVINC
40    FORMAT(5F20.2)
      CALL EXIT
      END
```

COMPARISON OF 2 DOA CALC. TECHNIQUES USING ERRONEOUS PHASE MEASUREMENTS

TRUE AZIMUTH = 200.0 TRUE INCIDENCE = 10.00 BASELINE/WAVELENGTH = 1.00

TRUE PHI21 = -58.74 TRUE PHI13 = 47.89 TRUE PHI32 = 10.85

ERROR SUM CONCENTRATED IN PHI13 PHASE....

(ALSO ASSUMING PHI13, PHI32 HAVE CANCELLING ERRORS OF +,-(SUM OF PHASES))

SUM OF PHASES ERROR SUM	AZIMUTH DELTA METHOD	AZIMUTH ANGLE AVGING METH	INCIDENCE DELTA METHOD	INCIDENCE ANGLE AVGING METH
-57.30	116.99	117.24	14.05	14.72
-51.57	121.45	121.33	12.78	13.37
-45.84	126.84	126.32	11.62	12.13
-40.11	133.34	132.48	10.58	11.01
-34.38	141.09	140.10	9.72	10.06
-28.65	150.14	149.23	9.07	9.32
-22.92	160.28	159.87	8.67	8.84
-17.19	171.01	170.91	8.57	8.67
-11.46	181.60	181.60	8.78	8.82
-5.73	191.40	191.40	9.27	9.28
0.00	200.00	200.00	10.00	10.00
5.73	207.30	207.30	10.93	10.94
11.46	213.39	213.36	12.01	12.04
17.19	218.43	218.38	13.22	13.28
22.92	222.62	222.53	14.51	14.62
28.65	226.11	226.01	15.88	16.03
34.38	229.06	228.94	17.31	17.52
40.11	231.56	231.45	18.80	19.05
45.84	233.70	233.60	20.32	20.64
51.57	235.55	235.47	21.89	22.27
57.30	237.16	237.10	23.50	23.94

COMPARISON OF 2 DOA CALC. TECHNIQUES USING ERRONEOUS PHASE MEASUREMENTS

TRUE AZIMUTH = 200.0 TRUE INCIDENCE = 10.00 BASELINE/WAVELENGTH = 1.00

TRUE PHI21 = -58.74 TRUE PHI13 = 47.89 TRUE PHI32 = 10.85

ERROR SUM DIVIDED EQUALLY AMONG PHI13, PHI32....

(ALSO ASSUMING PHI13, PHI32 HAVE CANCELLING ERRORS OF +,-(SUM OF PHASES))

SUM OF PHASES ERROR SUM	AZIMUTH DELTA METHOD	AZIMUTH ANGLE AVGING METH	INCIDENCE DELTA METHOD	INCIDENCE ANGLE AVGING METH
-57.30	131.52	129.02	9.56	10.50
-51.57	137.44	134.20	9.02	9.83
-45.84	144.03	140.59	8.58	9.25
-40.11	151.21	148.31	8.27	8.81
-34.38	158.83	157.00	8.10	8.50
-28.65	166.62	165.85	8.07	8.36
-22.92	174.32	174.15	8.20	8.38
-17.19	181.66	181.68	8.47	8.57
-11.46	188.44	188.46	8.87	8.91
-5.73	194.56	194.57	9.39	9.40
0.00	200.00	200.00	10.00	10.00
5.73	204.78	204.77	10.69	10.70
11.46	208.95	208.93	11.46	11.49
17.19	212.60	212.53	12.27	12.34
22.92	215.78	215.65	13.14	13.25
28.65	218.57	218.37	14.04	14.21
34.38	221.02	220.75	14.98	15.21
40.11	223.19	222.86	15.95	16.24
45.84	225.11	224.73	16.94	17.31
51.57	226.82	226.41	17.95	18.39
57.30	228.36	227.92	18.99	19.51

COMPARISON OF 2 DOA CALC. TECHNIQUES USING ERRONEOUS PHASE MEASUREMENTS

TRUE AZIMUTH = 200.0 TRUE INCIDENCE = 10.00 BASELINE/WAVELENGTH = 1.00

TRUE PHI21 = -58.74 TRUE PHI13 = 47.89 TRUE PHI32 = 10.85

ERROR SUM DIVIDED EQUALLY AMONG PHI13, PHI21, PHI32....

(ALSO ASSUMING PHI13, PHI32 HAVE CANCELLING ERRORS OF +,-(SUM OF PHASES))

SUM OF PHASES ERROR SUM	AZIMUTH DELTA METHOD	AZIMUTH ANGLE AVGING METH	INCIDENCE DELTA METHOD	INCIDENCE ANGLE AVGING METH
-57.30	142.68	140.13	11.84	12.62
-51.57	146.99	144.58	11.22	11.89
-45.84	151.76	149.72	10.67	11.23
-40.11	157.00	155.51	10.21	10.65
-34.38	162.68	161.79	9.84	10.18
-28.65	168.74	168.34	9.58	9.82
-22.92	175.06	174.96	9.43	9.59
-17.19	181.50	181.51	9.39	9.48
-11.46	187.90	187.92	9.48	9.52
-5.73	194.11	194.11	9.69	9.70
0.00	200.00	200.00	10.00	10.00
5.73	205.48	205.48	10.41	10.42
11.46	210.51	210.48	10.92	10.95
17.19	215.06	214.98	11.50	11.57
22.92	219.16	219.01	12.15	12.27
28.65	222.83	222.60	12.86	13.04
34.38	226.12	225.83	13.61	13.87
40.11	229.05	228.73	14.42	14.74
45.84	231.67	231.36	15.26	15.66
51.57	234.02	233.75	16.13	16.61
57.30	236.14	235.92	17.03	17.60

COMPARISON OF 2 DOA CALC. TECHNIQUES USING ERRONEOUS PHASE MEASUREMENTS

TRUE AZIMUTH = 0.00 TRUE INCIDENCE = 30.00 BASELINE/WAVELENGTH = 1.00

TRUE PHI21 = 180.00 TRUE PHI13 = -90.00 TRUE PHI32 = -90.00

ERROR SUM CONCENTRATED IN PHI13 PHASE....

(ALSO ASSUMING PHI13, PHI32 HAVE CANCELLING ERRORS OF +,-(SUM OF PHASES))

SUM OF PHASES ERROR SUM	AZIMUTH DELTA METHOD	AZIMUTH ANGLE AVGING METH	INCIDENCE DELTA METHOD	INCIDENCE ANGLE AVGING METH
-57.30	26.49	26.39	38.17	38.50
-51.57	24.37	24.29	36.96	37.24
-45.84	22.12	22.06	35.84	36.06
-40.11	19.76	19.72	34.80	34.97
-34.38	17.28	17.25	33.85	33.97
-28.65	14.67	14.66	32.97	33.06
-22.92	11.95	11.94	32.19	32.25
-17.19	9.11	9.10	31.50	31.53
-11.46	6.16	6.16	30.90	30.92
-5.73	3.12	3.12	30.40	30.41
0.00	0.00	0.00	30.00	30.00
5.73	356.81	356.81	29.70	29.70
11.46	353.57	353.57	29.50	29.52
17.19	350.31	350.30	29.41	29.45
22.92	347.03	347.02	29.43	29.49
28.65	343.77	343.75	29.55	29.64
34.38	340.54	340.50	29.77	29.90
40.11	337.37	337.30	30.10	30.28
45.84	334.27	334.17	30.53	30.76
51.57	331.25	331.12	31.05	31.35
57.30	328.34	328.16	31.68	32.04

COMPARISON OF 2 DOA CALC. TECHNIQUES USING ERRONEOUS PHASE MEASUREMENTS

TRUE AZIMUTH = 0.00 TRUE INCIDENCE = 30.00 BASELINE/WAVELENGTH = 1.00

TRUE PHI21 = 180.00 TRUE PHI13 = -90.00 TRUE PHI32 = -90.00

ERROR SUM DIVIDED EQUALLY AMONG PHI13, PHI32....

(ALSO ASSUMING PHI13, PHI32 HAVE CANCELLING ERRORS OF +,-(SUM OF PHASES))

SUM OF PHASES ERROR SUM	AZIMUTH DELTA METHOD	AZIMUTH ANGLE AVGING METH	INCIDENCE DELTA METHOD	INCIDENCE ANGLE AVGING METH
-57.30	18.38	18.28	35.65	35.99
-51.57	16.80	16.73	34.90	35.18
-45.84	15.17	15.11	34.20	34.42
-40.11	13.47	13.44	33.53	33.70
-34.38	11.71	11.69	32.90	33.02
-28.65	9.90	9.89	32.31	32.40
-22.92	8.03	8.02	31.76	31.82
-17.19	6.10	6.10	31.26	31.29
-11.46	4.12	4.12	30.79	30.81
-5.73	2.08	2.08	30.37	30.38
0.00	0.00	0.00	30.00	30.00
5.73	357.87	357.87	29.67	29.68
11.46	355.71	355.71	29.39	29.41
17.19	353.50	353.50	29.16	29.19
22.92	351.27	351.27	28.97	29.03
28.65	349.02	349.00	28.84	28.93
34.38	346.75	346.72	28.75	28.89
40.11	344.47	344.41	28.71	28.90
45.84	342.19	342.09	28.72	28.97
51.57	339.91	339.77	28.79	29.10
57.30	337.65	337.44	28.90	29.28

COMPARISON OF 2 DOA CALC. TECHNIQUES USING ERRONEOUS PHASE MEASUREMENTS

TRUE AZIMUTH = 0.00 TRUE INCIDENCE = 30.00 BASELINE/WAVELENGTH = 1.00

TRUE PHI21 = 180.00 TRUE PHI13 = -90.00 TRUE PHI32 = -90.00

ERROR SUM DIVIDED EQUALLY AMONG PHI13, PHI21, PHI32....

(ALSO ASSUMING PHI13, PHI32 HAVE CANCELLING ERRORS OF +,-(SUM OF PHASES))

SUM OF PHASES ERROR SUM	AZIMUTH DELTA METHOD	AZIMUTH ANGLE AVGING METH	INCIDENCE DELTA METHOD	INCIDENCE ANGLE AVGING METH
-57.30	20.18	20.03	32.19	32.55
-51.57	18.30	18.20	31.78	32.07
-45.84	16.39	16.32	31.41	31.64
-40.11	14.43	14.39	31.08	31.26
-34.38	12.44	12.41	30.80	30.93
-28.65	10.41	10.40	30.56	30.65
-22.92	8.36	8.36	30.36	30.42
-17.19	6.29	6.29	30.20	30.23
-11.46	4.20	4.20	30.09	30.10
-5.73	2.11	2.11	30.02	30.03
0.00	0.00	0.00	30.00	30.00
5.73	357.90	357.90	30.02	30.03
11.46	355.80	355.80	30.09	30.10
17.19	353.71	353.71	30.20	30.23
22.92	351.64	351.63	30.36	30.42
28.65	349.59	349.57	30.56	30.65
34.38	347.56	347.54	30.80	30.93
40.11	345.57	345.53	31.08	31.26
45.84	343.61	343.54	31.41	31.64
51.57	341.70	341.59	31.78	32.07
57.30	339.82	339.67	32.19	32.54

COMPARISON OF 2 DOA CALC. TECHNIQUES USING ERRONEOUS PHASE MEASUREMENTS

TRUE AZIMUTH = 100.0 TRUE INCIDENCE = 60.00 BASELINE/WAVELENGTH = 1.00

TRUE PHI21 = -54.14 TRUE PHI13 = -238.83 TRUE PHI32 = 292.97

ERROR SUM CONCENTRATED IN PHI13 PHASE....

(ALSO ASSUMING PHI13, PHI32 HAVE CANCELLING ERRORS OF +,-(SUM OF PHASES))

SUM OF PHASES ERROR SUM	AZIMUTH DELTA METHOD	AZIMUTH ANGLE AVGING METH	INCIDENCE DELTA METHOD	INCIDENCE ANGLE AVGING METH
-57.30	94.93	94.95	90.00	90.00
-51.57	95.33	95.34	90.00	90.00
-45.84	95.74	95.75	90.00	90.00
-40.11	96.18	96.19	90.00	90.00
-34.38	96.64	96.65	90.00	90.00
-28.65	97.13	97.13	86.77	87.59
-22.92	97.64	97.64	76.35	76.46
-17.19	98.18	98.18	70.94	70.99
-11.46	98.75	98.75	66.74	66.75
-5.73	99.36	99.36	63.16	63.17
0.00	100.00	100.00	60.00	60.00
5.73	100.68	100.68	57.12	57.13
11.46	101.41	101.41	54.47	54.48
17.19	102.19	102.18	51.99	52.02
22.92	103.01	103.01	49.66	49.71
28.65	103.90	103.89	47.44	47.52
34.38	104.85	104.83	45.33	45.45
40.11	105.86	105.85	43.32	43.47
45.84	106.96	106.93	41.38	41.59
51.57	108.14	108.10	39.52	39.79
57.30	109.42	109.36	37.73	38.07

COMPARISON OF 2 DOA CALC. TECHNIQUES USING ERRONEOUS PHASE MEASUREMENTS

TRUE AZIMUTH = 100.0 TRUE INCIDENCE = 60.00 BASELINE/WAVELENGTH = 1.00

TRUE PHI21 = -54.14 TRUE PHI13 = -238.83 TRUE PHI32 = 292.97

ERROR SUM DIVIDED EQUALLY AMONG PHI13, PHI32....

(ALSO ASSUMING PHI13, PHI32 HAVE CANCELLING ERRORS OF +,-(SUM OF PHASES))

SUM OF PHASES ERROR SUM	AZIMUTH DELTA METHOD	AZIMUTH ANGLE AVGING METH	INCIDENCE DELTA METHOD	INCIDENCE ANGLE AVGING METH
-57.30	95.36	95.39	90.00	90.00
-51.57	95.76	95.77	90.00	90.00
-45.84	96.16	96.17	90.00	90.00
-40.11	96.58	96.59	81.12	81.66
-34.38	97.02	97.02	76.02	76.27
-28.65	97.47	97.47	72.33	72.47
-22.92	97.94	97.94	69.28	69.36
-17.19	98.42	98.42	66.62	66.66
-11.46	98.93	98.93	64.23	64.24
-5.73	99.45	99.45	62.04	62.04
0.00	100.00	100.00	60.00	60.00
5.73	100.57	100.57	58.09	58.09
11.46	101.16	101.16	56.29	56.30
17.19	101.78	101.77	54.58	54.61
22.92	102.42	102.42	52.94	53.00
28.65	103.09	103.08	51.38	51.46
34.38	103.79	103.78	49.87	49.99
40.11	104.52	104.50	48.43	48.59
45.84	105.28	105.26	47.03	47.24
51.57	106.08	106.04	45.68	45.94
57.30	106.91	106.86	44.37	44.70

COMPARISON OF 2 DOA CALC. TECHNIQUES USING ERRONEOUS PHASE MEASUREMENTS

TRUE AZIMUTH = 100.0 TRUE INCIDENCE = 60.00 BASELINE/WAVELENGTH = 1.00

TRUE PHI21 = -54.14 TRUE PHI13 = -238.83 TRUE PHI32 = 292.97

ERROR SUM DIVIDED EQUALLY AMONG PHI13, PHI21, PHI32....

(ALSO ASSUMING PHI13, PHI32 HAVE CANCELLING ERRORS OF +,-(SUM OF PHASES))

SUM OF PHASES ERROR SUM	AZIMUTH DELTA METHOD	AZIMUTH ANGLE AVGING METH	INCIDENCE DELTA METHOD	INCIDENCE ANGLE AVGING METH
-57.30	98.25	98.27	90.00	90.00
-51.57	98.40	98.42	90.00	90.00
-45.84	98.55	98.56	90.00	90.00
-40.11	98.71	98.72	83.20	83.91
-34.38	98.87	98.88	77.11	77.38
-28.65	99.04	99.05	73.07	73.21
-22.92	99.22	99.22	69.80	69.88
-17.19	99.40	99.41	66.98	67.02
-11.46	99.59	99.60	64.45	64.47
-5.73	99.79	99.79	62.14	62.15
0.00	100.00	100.00	60.00	60.00
5.73	100.22	100.22	57.99	57.99
11.46	100.44	100.44	56.08	56.10
17.19	100.68	100.67	54.27	54.30
22.92	100.92	100.92	52.54	52.59
28.65	101.18	101.17	50.87	50.95
34.38	101.45	101.44	49.26	49.38
40.11	101.73	101.71	47.70	47.86
45.84	102.03	102.00	46.19	46.40
51.57	102.34	102.30	44.73	44.99
57.30	102.67	102.60	43.30	43.62

APPENDIX M

Herein are listed the various general purpose subroutines called in many of the programs of previous appendices. Their functions are explained within their listings.

```
$      INPUT SOURCE CARDS
$     OUTPUT SUBROUTINE TAPE
$     SENSE SWITCHON,32
$     FORTRAN
H      NAME AVDIR;
H      EQUIP=CARDRE,PRINTE,CARDPU;
H      SINGLEALL;
       SUBROUTINE AVDIR(PHI21,PHI13,PHI32,DL,AZ,VINC)
C*****
C*****THIS SUBROUTINE FINDS THE AVERAGED DOA FROM ALL THREE INTERFEROMETER
C*****PHASES.  IT USES THE ANGLE AVERAGING FORMULA PRESENTED IN CHAPTER VIII,
C*****PHI21, PHI13, PHI32, ARE THE INPUT  INTERFEROMETER PHASES (IN RADIANS),
C*****DL IS THE ARRAY BASELINE/WAVELENGTH, THE ARRAY ANGLE IS ASSUMED TO BE
C*****60 DEGREES. AND THE OUTPUT DOA IS GIVEN BY AZ AND VINC, IN DEGREES.
C*****
       SQRT3=1.7320508076
       DEG=57.29577951
       TPDL=DL*6.2831853072
       SQRH=1.2247448714
C*****CALCULATE 3 VALUES OF ALPHA USING THE 3 DIFFERENT COMBINATIONS
C***** OF 2 ANTENNA PHASE MEASUREMENTS, THEN AVERAGING THEM
       AL2132=ATAN2(2.*PHI32+PHI21,SQRT3*PHI21)
       AL1321=ATAN2(-2.*PHI13-PHI21,SQRT3*PHI21)
       AL1332=ATAN2(PHI32-PHI13,-SQRT3*(PHI32+PHI13))
       X=COS(AL2132)+COS(AL1321)+COS(AL1332)
       Y=SIN(AL2132)+SIN(AL1321)+SIN(AL1332)
       AZ=ATAN2(Y,X)*DEG
       SQRTSM=SQRT(PHI21*PHI21+PHI13*PHI13+PHI32*PHI32)
       STH=SQRTSM/(TPDL*SQRH)
C*****CHECK TO ENSURE STH LESS THAN 1, IF SLIGHTLY GREATER SET = 1.0
       IF(STH-1.)2,2,1
1      STH=1.0
2      CONTINUE
       VINC=ASIN(STH)*DEG
       RETURN
       END
```

```
$     INPUT SOURCE CARDS
$     OUTPUT SUBROUTINE TAPE
$     SENSE SWITCHON,32
$     FORTRAN
H      NAME DIR  ;
H      EQUIP=CARDRE,PRINTE,CARDPU;
       SUBROUTINE DIR(PHI21,PHI32,DL,GAMMA,AZ,VINC)
C*****
C*****THIS IS A DIRECTION FINDING SUBROUTINE FOR GENERAL INTERFEROMETER
C*****ARRAYS.  IT FINDS THE AZIMUTH AND INCIDENCE ANGLE FROM 2 INTERF PHASES,
C*****PHI21 AND PHI32 ARE THE INTERFEROMETER PHASES, DL IS THE BASELINE-TO-
C*****WAVELENGTH RATIO, GAMMA IS THE SPECIFIED ARRAY ANGLE, AZ IS THE
C*****COMPUTED AZIMUTH AND VINC IS THE COMPUTED INCIDENCE ANGLE.
C*****ALL INPUT PHASE DATA ARE IN RADIANS, THE OUTPUT PHASE DATA (AZ AND VINC)
C*****ARE IN DEGREES.
C*****
      DEG=57.29577951
      TPDL=DL*6.2831853072
      ARG1=PHI32*PHI21-PHI21*COS(GAMMA)
      ARG2=PHI21*SIN(GAMMA)
      AZ=ATAN2(ARG1,ARG2)
      SMSQ=PHI21**2+PHI32**2-PHI21*PHI32
      STH=SQRT(SMSQ/(COS(AZ)**2+COS(AZ-GAMMA)**2-COS(AZ)*COS(AZ-GAMMA)))
     $/TPDL
C*****CHECK TO ENSURE STH LESS THAN 1,IF GREATER SET = 1.0
      IF(STH-1.)2,2,1
1     STH=1.0
2     CONTINUE
      VINC=ASIN(STH)*DEG
      AZ=AZ*DEG
      RETURN
      END
```

```
$     INPUT SOURCE CARDS
$     OUTPUT SUBROUTINE TAPE
$     SENSE SWITCHON,32
$     FORTRAN
H      NAME CHOS;
H      EQUIP=CARDRE,PRINTE,CARDPU;
       SUBROUTINE CHOS (XAVBIJ,PHIIJ,TAVBIJ)
C*****
C*****THIS SUBROUTINE CHOSES AVBIJ + OR - N*2*PI THAT COMES CLOSEST TO PHIIJ
C*****THE CHOSEN VALUE IS TAVBIJ.   THIS SUBROUTINE ESSENTIALLY PERFORMS
C*****A PHASE AMBIGUITY RESOLUTION.
C*****ALL PHASES ARE GIVEN IN RADIANS
C*****
       AVBIJ=XAVBIJ
       PI=3.1415926535898
       TUPI=2.*PI
       XPI=PI
       IF(ABSF(PHIIJ-AVBIJ)-PI)10,10,9
9      IF(PHIIJ*AVBIJ)1,1,2
1      IF(PHIIJ)3.3,4
3      AVBIJ=AVBIJ-TUPI
       GO TO 2
4      AVBIJ=AVBIJ+TUPI
2      IF(ABSF(PHIIJ)-ABSF(AVBIJ)-XPI)5,5,8
8      XPI=XPI+TUPI
       GO TO 2
5      TAVBIJ=ABSF(AVBIJ)+XPI-PI
       IF(PHIIJ)6,6,7
6      TAVBIJ=(-TAVBIJ)
       GO TO 7
10     TAVBIJ=AVBIJ
7      RETURN
       END
```

```
$      EXECUTE
$      INPUT SOURCE CARDS
$     OUTPUT SUBROUTINE TAPE
$     SENSE SWITCHON,32
$     FORTRAN
H      NAME PRTPHI;
H      EQUIP=CARDRE,PRINTE,CARDPU;
       SUBROUTINE PRTPHI(ALPHA,THETA,DL,PHAS21,PHAS13,PHAS32,GAMMA)
C*****
C*****THIS SUBROUTINE FINDS THE PHASE DIFFERENCES INDUCED IN THE INTERFEROMETER
C*****ARRAY FOR A GIVEN D/L AND DIR OF ARRIVAL. THE INPUT ARE ALPHA AND THETA,
C*****IN RADIANS--THE SPECIFIED DOA, DL, THE ARRAY BASELINE/WAVELENGTH, AND
C*****GAMMA, THE ARRAY ANGLE IN RADIANS.  THE OUTPUT PHASES ARE PHAS21,
C*****PHAS13, AND PHAS32.
C*****
       TUPI=6.2831853072
       TDLSTH=TUPI*DL*SIN(THETA)
       PHAS21=TDLSTH*COS(ALPHA)
       PHAS13=-TDLSTH*COS(ALPHA-GAMMA)
       PHAS32=TDLSTH*(COS(ALPHA-GAMMA)-COS(ALPHA))
       RETURN
       END
```

```
$       INPUT SOURCE CARDS
$      OUTPUT SUBROUTINE TAPE
$      SENSE SWITCHON,32
$      FORTRAN
H       NAME RANGE;
H       EQUIP=CARDRE,PRINTE,CARDPU;
H       SINGLEALL;
        SUBROUTINE RANGE(AZ,ANG,PHIMX,PHIMN)
C*****
C*****THIS SUBROUTINE FINDS MIN AND MAX VALUES OF FX=COS((AZ-ANG)+ERR) FOR ERR
C*****BETWEEN + OR - 10 DEGREES.   IT IS USED IN CONJUNCTION WITH THE MODIFIED
C*****VERSION OF THE PROGRAM AMBPLT, AS A MEANS OF OBTAINING A MORE STRINGENT
C*****AMBIGUITY REJECTION CRITERION ON THE BASIS OF APPROX AZIMUTH INFORMATION.
C*****PHIMX AND PHIMN DENOTE THE DESIRED MAX AND MIN PHASE VALUES RESPCTIVELY
C*****
        DEG=180./3.1415926535
        DIF=AZ-ANG
        TPDL=1.
C*****KEEP AZ-ANG IN RANGE OF 0-TUPI BY ADDING TUPI IF NOT ALREADY IN RANGE
        IF(DIF)1,2,2
1       DIF=DIF+360.
2       CONTINUE
        IF(DIF-10.)10,10,20
10      PHIMX=TPDL
        PHIMN=0.
        GO TO 170
20      IF(DIF-80.)30,30,40
30      PHIMX=TPDL*COS((DIF-10.)/DEG)
        PHIMN=0.
        GO TO 170
40      IF(DIF-100.)50,50,60
50      PHIMX=TPDL*COS((DIF-10.)/DEG)
        PHIMN=TPDL*COS((DIF+10.)/DEG)
        GO TO 170
60      IF(DIF-170.)70,70,80
70      PHIMX=0.
        PHIMN=TPDL*COS((DIF+10.)/DEG)
        GO TO 170
80      IF(DIF-190.)90,90,100
90      PHIMX=0.
        PHIMN=-TPDL
        GO TO 170
100     IF(DIF-260.)110,110,120
110     PHIMX=0.
        PHIMN=TPDL*COS((DIF-10.)/DEG)
        GO TO 170
120     IF(DIF-280.)130,130,140
130     PHIMX=TPDL*COS((DIF+10.)/DEG)
        PHIMN=TPDL*COS((DIF-10.)/DEG)
        GO TO 170
140      IF(DIF-350.)150,150,160
150     PHIMX=TPDL*COS((DIF+10.)/DEG)
        PHIMN=0.
        GO TO 170
160     PHIMX=TPDL
        PHIMN=0.
C*****ALLOW SLIGHT MARGIN IN PHIMX AND PHIMN (.1 DEGREE) TO ACCOUNT FOR ROUNDOFF
170     PHIMX=PHIMX+.1
        PHIMN=PHIMN-.1

        RETURN
        END
```

```
$     INPUT SOURCE CARDS
$     OUTPUT SUBROUTINE TAPE
$     SENSE SWITCH ON,32
$     FORTRAN
H      NAME REDUCE;
H      EQUIP=CARDRE,PRINTE,CARDPU;
       SUBROUTINE REDUCE(AVBIJ)
C*****
C*****THIS SUBROUTINE REDUCES AVBIJ S BY MULTIPLES OF 2 PI UNTIL BETWEEN - PI
C*****AND + PI.  THE VALUE OF AVBIJ IS PUT WITHIN A BRANCH CUT OF -PI TO + PI
C*****AFTER THIS SUBROUTINE IS CALLED
C*****ALL PHASES MUST BE IN RADIANS.
C*****
       PI=3.1415926535898
       TUPI=2.*PI
       N=AVBIJ/TUPI
       AVBIJ=AVBIJ-N*TUPI
       IF(AVBIJ-PI)2,2,1
1      AVBIJ=AVBIJ-TUPI
       GO TO 6
2      IF(AVBIJ)4,4,3
3      GO TO 6
4      IF(PI+AVBIJ)5,5,6
5      AVBIJ=AVBIJ+TUPI
6      RETURN
       END
```

FOOTNOTES

1. W. Little, "Polar Plot Routines for a CALCOMP Plotter," Unpublished Memorandum, Radiolocation Research Laboratory, University of Illinois, 1972.

2. E. K. Walton, from a private communication at this laboratory.

3. These data were recorded on this laboratory's paper tape number 151.

4. J. Driscoll, from a private communication at this laboratory.

Bibliography

Allen, L. C., "Improved Digital Bearing Computer Techniques," Master's Thesis, University of Illinois, Urbana, Illinois, June 1966. (RRL Publication No. 314.)

Bailey, A. D. and W. C. McClurg, "A Sum- and-Difference Interferometer System for HF Radio Direction Finding," IEEE Transactions on Aerospace and Navigational Electronics, March 1963, pp. 65-72.

Church, J. B., "A Digital Bearing Computer for an Interferometer RDF System," Master's Thesis, University of Illinois, Urbana, Illinois, January 1967. (RRL Publication No. 325.)

Creasy, J., "Digital Techniques for Radio Direction Finding with Interferometer Arrays," Master's Thesis, University of Illinois, June 1966. (RRL Publication No. 309.)

Davies, K., Ionospheric Radio Propagation, Government Printing Office, Washington, D. C., 1965.

Glick, M. I., "Studies in Time Averaging and Wave Interference in Radio Direction Finding," Master's Thesis, University of Illinois, Urbana, Illinois, June 1966. (RRL Publication No. 312.)

Grush, H. L., "An Investigation of a Digital Bearing Computer for a Small Aperture Radio Direction Finding System," Ph.D. Thesis, University of Illinois, Urbana, Illinois, June 1966. (RRL Publication No. 314.)

Hayden, E. C., "Some Basic Problems in the Determination of the Direction of Arrival of Radio Waves," Ph.D. Thesis, University of Illinois, Urbana, Illinois, September 1958. (RRL Publication No. 158.)

Henderson, J. J., "Mismatch Correction Techniques for Twin-Channel Receivers," August 1965. (RRL Publication No. 282.)

Little, W., "Polar Plot Routines for a Calcomp Plotter," Unpublished Memorandum, Radiolocation Research Laboratory, University of Illinois, 1972.

Stenzel, K. D., "An Interferometer RDF System with an On-Line Computer," Master's Thesis, University of Illinois, Urbana, Illinois, September 1971. (RRL Publication No. 400.)

Talbott, C. R., "Aperture Size Effects in a HF Interferometer RDF System," Master's Thesis, University of Illinois, Urbana, Illinois, August 1970. (RRL Publication No. 375.)

Whale, H. A., Effects of Ionospheric Scattering on Very-Long-Distance Radio Communication, Plenum Press, New York, 1969.

DISTRIBUTION LIST

Defense Documentation Center
Cameron Station
Building 5, 5010 Duke Street
Alexandria, Virginia 22314

Electronics Program
Code 427
Office of Naval Research
Department of the Navy
Arlington, Virginia 22217

Commanding Officer
Office of Naval Research Branch Office
Box 39, Fleet Post Office
New York, New York 09510

Director
Naval Research Laboratory
Code 2627
Washington, D. C. 20390

Commanding Officer
Office of Naval Research Branch Office
536 South Clark
Chicago, Illinois 60605

Deputy Director and Chief Scientist
Office of Naval Research Branch Office
1030 East Green Street
Pasadena, California 91106

Chief, Input Section
Clearinghouse for Federal Scientific
and Technical Information, DFSTI
Sills Building
6285 Port Royal Road
Springfield, Virginia 22151

Library
U. S. Naval Observatory
Washington, D. C. 20390

Document Room
Room 26 - 327
Research Laboratory for Electronics
Massachusetts Institute of Technology
Cambridge, Massachusetts 02139

Dr. Samuel Silver
Space Sciences Laboratory
University of California
Berkeley, California 94720

Commanding Officer
ONR Branch Office
346 Broadway
New York, New York 10013

Director
National Security Agency
Ft. George G. Meade, Maryland 20755
Attn: R424

Director
Office of Naval Research
Boston Branch Office
495 Summer Street
Boston, Massachusetts 02210

Library R51 - Technical Reports
National Oceanic and Atmospheric
Administration
Environmental Research Labs.
Boulder, Colorado 80302

Department of the Army
U. S. Army Research Office - Durham
Information Processing Office
Box CM, Duke Station
Durham, North Carolina 27706

Mr. Elias Schutzman
Division of Engineering
National Science Foundation
Washington, D. C. 20550

Commander
Naval Undersea R.& D Center
San Diego, California 92132
Attn: Technical Library, Code 1311

Commanding Officer & Director
U. S. Naval Underwater Sound Laboratory
Fort Trumbell, New London, Connecticut 06320

Librarian
U. S. Navy Post Graduate School
Monterey, California 93940

Commanding Officer
Naval Missile Center
Attn: 5632.2 Tech. Library
Point Mugu, California 93042

Miss Joyce E. Lunde
Assistant Librarian for Reference Services
The Dodge Library
Northeastern University
360 Huntington Avenue
Boston, Massachusetts 02115

Librarian-In-Charge
The University of Auckland
School of Engineering
Ardmore College Post Office
New Zealand

Director U. S. Naval Security Group
Attn: G-N3
3801 Nebraska Avenue
Washington, D. C. 20390

Mr. Wallace C. Olsen
Chief, NAFEC Library
Systems Research & Development Service
Federal Aviation Agency
Atlantic City, New Jersey 08405

Mr. Jerome Fox
Director of Research
Polytechnic Institute of Brooklyn
333 Jay Street
Brooklyn, New York 11363

Commander
Operational Test and Evaluation Force
Naval Station
Norfolk, Virginia 23511

Director, Central Intelligence Agency
OCR/DD/Publications
Washington, D. C. 20505

Director, U. S. Naval Research Laboratory
Attn: Code 5438
Washington, D. C. 20390

Mr. William Fay
Code S 220.2
Naval Electronics Laboratory Center
San Diego, California 92152

Mr. Albert Canal
Naval Security Engineering Facility
3801 Nebraska Avenue
Washington, D. C. 20390

Mr. Leonard M. Posa
Science & Technology Division
Ft. George G. Meade, Maryland 20755

Mr. John Clancy
RADC - OCFL
Griffiss Air Force Base
Rome, New York 13440

Dr. A. D. Morgan
Government Communications Headquarters
Room No. 9/0203
Benhall, Princess Elizabeth Way
Gloucester Road
Cheltenham, Gloucester
ENGLAND

Dr. Thomas Whitaker
Dept. of Electrical Engineering
University of Houston
3801 Cullen
Houston, Texas 77004

Robert Misner
Director, U. S. Naval Research Laboratory
Attn: Code 5470
Washington, D. C. 20390

Augustine A. Strejcek
NSA - Attn: W 62
Ft. George G. Meade, Maryland 20755

Mr. N. C. Gerson
877 Oakdale Circle
Millersville, Maryland 21108

Prof. A. D. Bailey
University of Illinois
Urbana, Illinois 61801

Prof. E. W. Ernst
University of Illinois
Urbana, Illinois 61801

Dr. E. C. Jordan
University of Illinois
Urbana, Illinois 61801

Mr. H. B. Lawler
University of Illinois
Urbana, Illinois 61801

Dr. James Cathey, ONR Res. Rep.
University of Illinois
Urbana, Illinois 61801

Publications Office
Department of Electrical Engineering
University of Illinois
Urbana, Illinois 61801

Prof. J. D. Dyson
University of Illinois
Urbana, Illinois 61801

Mr. W. W. Wood
University of Illinois
Urbana, Illinois 61801

Mr. L. J. Miller
University of Illinois
Urbana, Illinois 61801

Dr. E. Walton
University of Illinois
Urbana, Illinois 61801

Mr. John E. Huff
University of Illinois
Urbana, Illinois 61801

Prof. G. A. Deschamps
University of Illinois
Urbana, Illinois 61801

Prof. S. W. Lee
University of Illinois
Urbana, Illinois 61801

Prof. S. A. Bowhill
University of Illinois
Urbana, Illinois 61801

Prof. N. Narayana Rao
University of Illinois
Urbana, Illinois 61801

Unclassified

Security Classification

DOCUMENT CONTROL DATA - R & D

(Security classification of title, body of abstract and indexing annotation must be entered when the overall report is classified)

1 ORIGINATING ACTIVITY (Corporate author) Department of Electrical Engineering University of Illinois Urbana, Illinois	2a. REPORT SECURITY CLASSIFICATION 2b. GROUP

3 REPORT TITLE

AUTOMATIC TRIPLE INTERFEROMETER DIRECTION OF ARRIVAL CALCULATION TECHNIQUES

4. DESCRIPTIVE NOTES (Type of report and inclusive dates)

Technical Report No. 36

5 AUTHOR(S) (First name, middle initial, last name)

Keith E. Hoover
Edward W. Ernst

6 REPORT DATE September 1972	7a. TOTAL NO. OF PAGES 223	7b. NO OF REFS 13
8a. CONTRACT OR GRANT NO N00014-67-A-0305-0002 b. PROJECT NO c. d.	9a. ORIGINATOR'S REPORT NUMBER(S) RRL Publication No. 414 9b. OTHER REPORT NO(S) (Any other numbers that may be assigned this report) UILU-ENG-72-2551	

10 DISTRIBUTION STATEMENT

EACH TRANSMITTAL OF THIS DOCUMENT OUTSIDE OF THE DEPARTMENT OF DEFENSE MUST HAVE PRIOR APPROVAL OF THE OFFICE OF NAVAL RESEARCH (CODE 427), DEPARTMENT OF THE NAVY, ARLINGTON, VIRGINIA 22217.

11 SUPPLEMENTARY NOTES	12. SPONSORING MILITARY ACTIVITY Office of Naval Research and the Naval Electronics Systems Command

13 ABSTRACT

The work reported here presents the principles of operation of a non-display-oriented triple interferometer RDF system. Particular attention was paid to the ambiguity resolving portion of the system. It was found that phase ambiguity resolution (ambiguity resolution using the differential phase information from a smaller aperture interferometer system) has distinct advantages over direction ambiguity resolution (ambiguity resolution on the basis of knowledge of the approximate direction of arrival). The use of only the approximate azimuthal angle of arrival in the direction ambiguity resolving process appears to be insufficient. Furthermore it was found that the use of averaged values of the small interferometer differential phases appears to be more reliable than the use of instantaneous values of these phases. Finally, a new method of processing erroneous (ideally "redundant") interferometer differential phase data was presented. It was found to be roughly equivalent, and yet much faster, than the old "angle averaging" method.

DD FORM 1 NOV 68 1473

Unclassified

Security Classification

14 KEY WORDS	LINK A		LINK B		LINK C	
	ROLE	WT	ROLE	WT	ROLE	WT
Radio Direction Finding						
Interferometer						
Angle-of-Arrival Calculations						
Ambiguity Resolution						
Phase Measurement Correction						
Wave Interference						